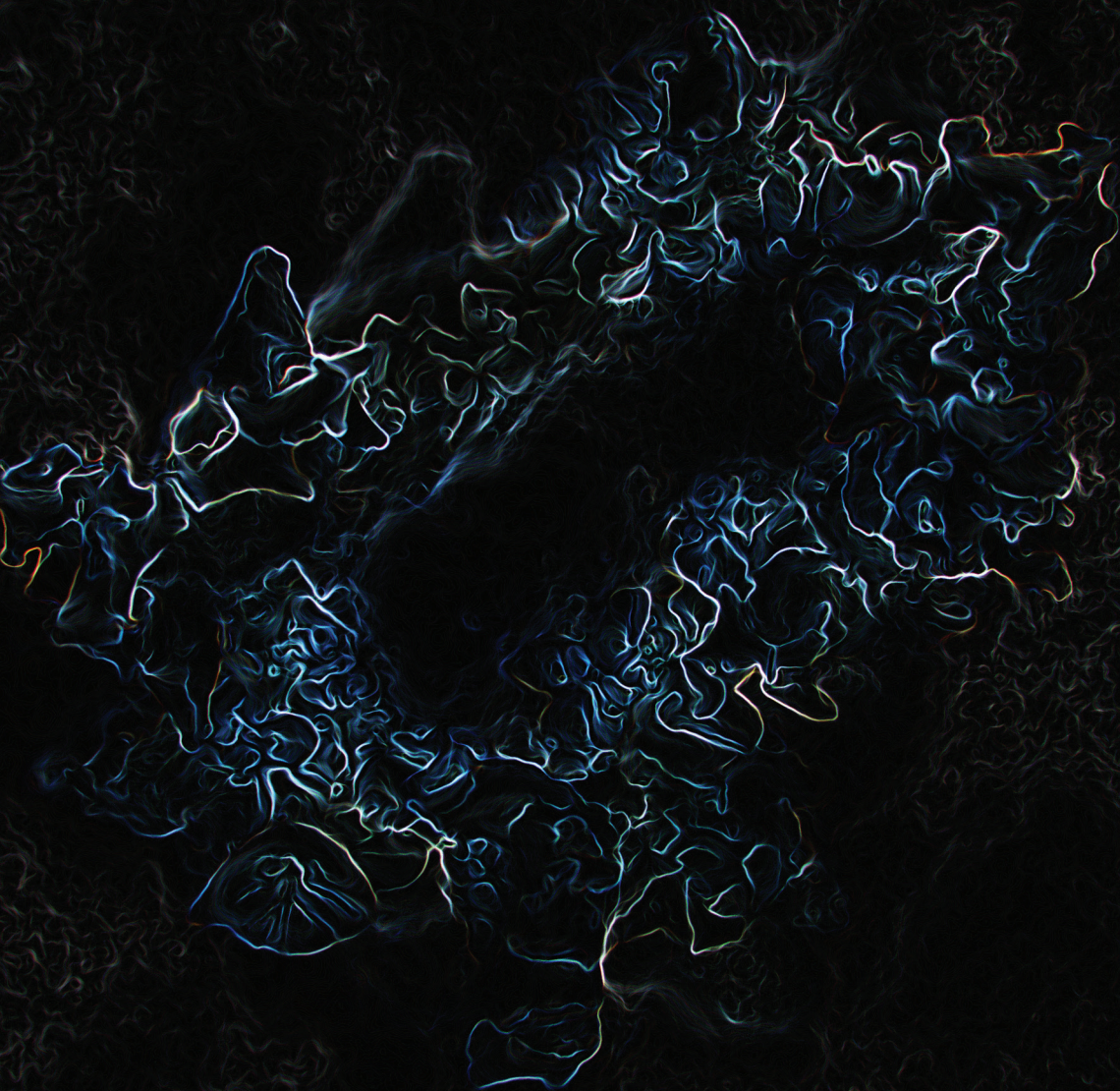


Functional genomics in *Schizophyllum commune*

Peter Jan Vonk



Functional Genomics in
Schizophyllum commune

Peter Jan Vonk

PhD thesis Utrecht University, Utrecht, The Netherlands (2022)

The research described in this Thesis was performed within the Microbiology group of Utrecht University, Padualaan 8, 3584 CH Utrecht, The Netherlands.

Copyright © 2022 by P.J. Vonk. All rights reserved.

Cover design:	Peter Jan Vonk
Printed by:	RidderPrint www.ridderprint.nl
ISBN:	978 90 393 745 66

Functional genomics in *Schizophyllum commune*

Functionele genomica in *Schizophyllum commune*

(met een samenvatting in het Nederlands)

Proefschrift

ter verkrijging van de graad van doctor aan de Universiteit Utrecht op
gezag van de rector magnificus, prof. dr. H.R.B.M. Kummeling, ingevolge
het besluit van het college voor promoties in het openbaar te verdedigen
op maandag 9 mei 2022 des ochtends te 10.15 uur

door

Peter Jan Vonk

geboren op 17 juni 1991
te Giessenlanden

Promotor: Prof. dr. H.A.B. Wösten

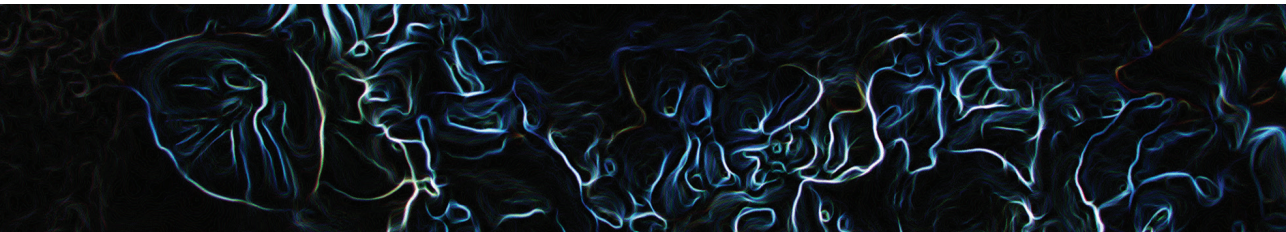
Copromotor: Dr. R.A. Ohm

“Good and evil are names for what people do, not for what they are.”

Philip Pullman

Contents

Chapter 1	General introduction	1
Chapter 2	The role of homeodomain transcription factors in fungal development	23
Chapter 3	High-throughput targeted gene deletion in the model mushroom <i>Schizophyllum commune</i> using pre-assembled Cas9 ribonucleoproteins	37
Chapter 4	H3K4me2 ChIP-Seq reveals the epigenetic landscape during mushroom formation and novel developmental regulators of <i>Schizophyllum commune</i>	49
Chapter 5	The transcription factor Roc1 is a regulator of cellulose degradation in the wood-decaying mushroom <i>Schizophyllum commune</i>	71
Chapter 6	Gene deletion of eight transcription factors reveals new regulators of mushroom development in <i>Schizophyllum commune</i>	97
Chapter 7	Targeted gene knock-in reduces variation between transformants in the mushroom-forming fungus <i>Schizophyllum commune</i>	117
Chapter 8	Summary and General Discussion	127
Appendix		137
	References	
	Nederlandse samenvatting	
	Acknowledgements	
	Curriculum vitae	
	List of publications	



General introduction

Peter Jan Vonk

Parts of this Chapter were included in Nagy, L. G., Vonk, P. J., Künzler, M., Foldi, C., Viragh, M., Ohm, R. A., Hennicke, F., Balint, B., Csernetics, A., Hegedus, B., Hou, Z., Liu, X., Nan, S., Pareek, M., Sahu, N., Szathmari, B., Varga, T., Wu, H., Yang, X., & Merenyi, Z. (2021). Lessons on fruiting body morphogenesis from genomes and transcriptomes of Agaricomycetes (submitted)

The kingdom Fungi is a group of eukaryotic microorganisms. Fungi are separated into two major morphological groups, yeasts and filamentous fungi. While yeasts generally grow as unicellular microorganisms that divide by budding or fission, filamentous fungi grow as a network of branching hyphae called a mycelium. Filamentous fungi propagate by the production of asexual and/or sexual spores. To assist in the dispersion of sexual spores, many filamentous fungi produce fruiting bodies. These fruiting bodies can range from simple structures for spore formation to the highly specialized macroscopic mushrooms in the phylum Basidiomycota. Fungi play an essential ecological role as mutualists, pathogens and in carbon recycling and can be separated into three trophic modes based on their feeding habits (Tedersoo et al. 2014). Mutualistic fungi interact with other organisms in a symbiotic manner. For example, mycorrhizal fungi have a mutualistic relationship with plants and provide water and minerals to plant roots in exchange for access to carbohydrates (Smith and Smith 2011). Pathogenic fungi include many plant, animal and fungal pathogens and are a major source of crop loss and animal infection, but are also important in maintaining plant diversity and ecosystems (Gilbert 2002). Saprotrophic fungi degrade dead biomass and play an important role in carbon recycling of plants and other organisms. Their large arsenal of carbohydrate-active enzymes (CAZymes) allows saprotrophs to depolymerize the recalcitrant lignocellulosic biomass to release simple sugars, which can subsequently be absorbed and used in metabolism (Cantarel et al. 2009). The evolution of fungi has given rise to two major phyla, the Ascomycota and the Basidiomycota, that together form the subkingdom Dikarya (Lutzoni et al. 2004; James et al. 2006; Hibbett et al. 2007). Both groups feature yeasts and filamentous fungi. The Ascomycota are generally characterized by the formation of a sac or ascus in which meiotic spores (ascospores) are formed. On the other hand, the Basidiomycota form meiotic spores on basidia, specialized structures where nuclear fusion and meiosis occur and from which nuclei migrate into basidiospores.

The properties of fungi have been exploited by humans for millennia. The ascomycete yeast *Saccharomyces cerevisiae*, better known as baker's yeast, is famous for its use in alcoholic fermentation and as a leavening agent in baking. Many fungi are now used in the production of alcohols, organic acids, enzymes and other chemicals. For example, the ascomycete *Aspergillus niger* is the primary industrial producer of citric acid (Mattey 1992). More recently, fungi have become increasingly used for their carbohydrate-active enzymes in the conversion of lignocellulosic biomass into added-value chemicals like bioethanol (Sarkar et al. 2012). Fungi also play an important role in the production of pharmaceuticals, most notably in the production of antibiotics, like penicillin, which revolutionized the treatment of bacterial infections (Kardos and Demain 2011). Other drugs include anti-cancer drugs and statins for the reduction of cholesterol levels (Tobert 2003; Patel and Goyal 2012). A novel field of research is the plant microbiome (i.e., rhizosphere), where the composition of the mycorrhiza can improve the yield of crops and promote disease resistance (Parniske 2008). Finally, mushroom-forming fungi of the Basidiomycota are an important food source, either by commercial cultivation or by harvesting from nature. Notable examples of cultivated mushrooms are the white button mushroom *Agaricus bisporus*, the oyster mushroom *Pleurotus ostreatus* and the shiitake *Lentinula edodes* (de Mattos-Shiple et al. 2016).

Despite the uses of fungi, our understanding of these organisms is limited compared to that of plants and animals. The development of mushroom-forming fungi is particularly poorly understood, due to their complex developmental program. Many mushroom-forming fungi



cannot be genetically modified or cultivated under laboratory conditions. Therefore, most of our understanding of mushroom-forming fungi comes from genome and transcriptome sequencing. Functional genomics of these microbes has mostly been limited to two model organisms, *Schizophyllum commune* and *Coprinopsis cinerea*. Both species can be cultivated in the lab and have molecular tools for gene inactivation. Recently there has also been progress in the development of molecular tools in economically important mushroom-forming fungi. Gene knockout by homologous recombination or missense mutations and gene knockdown by RNA interference have been developed for several economically important fungi, including *Pleurotus ostreatus* and *Flammulina velutipes* (Salame et al. 2012; Shi et al. 2017). However, these methods, like the methods developed for *S. commune* and *C. cinerea*, suffer from low efficiency. This necessitates the development of more efficient molecular tools to increase our understanding of mushroom-forming fungi.

Mushroom-forming fungi

Mushroom-forming fungi are a polyphyletic group of fungi that produce macroscopic fruiting bodies for the dispersal of spores. They are found in at least 8 extant fungal lineages (Figure 1) (Nagy et al. 2018). Rather than a single evolutionary origin, mushrooms have developed in several lineages through convergent evolution. In Ascomycetes, the best-known examples are the edible morels of the genus *Morchella* and the subterranean truffles of the genus *Tuber*. However, the most notable mushrooms are found in the basidiomycetes of the subdivision Agaricomycotina, where there is a spectacular diversity in the morphology of mushrooms with a highly complex developmental program (Krizsán et al. 2019; Varga et al. 2019). The mushroom (formally known as a basidiocarp) is classically described as a cap-stipe mushroom that is exemplified by the famous white-spotted, red cap fly agaric *Amanita muscaria*. These mushrooms, called agarics, contain a stipe that raises the mushroom from the substrate and a cap with gills at the bottom from which spores are dispersed. However, many mushrooms do not follow this classical morphology. Mushrooms in the order Agaricales, to which most agarics belong, also include the puffballs of the genus *Bovista* and the split-gill mushroom *S. commune*. Closely related to the Agaricales are the Polyporales, an order which includes many species with pores rather than gills as part of the fruiting body. These species, called polypores, include many of the bracket-shaped mushrooms found on trees. More distantly related are the “jelly fungi”, a heterogenous group of fungi characterized by a jelly-like fruiting body (Millanes et al. 2011).

The primary economic value of mushroom-forming fungi is their use as food. Many mushroom-forming fungi, primarily in the order Agaricales, are edible (de Mattos-Shipley et al. 2016). Mushrooms are a low input food source due to their growth on waste biomass like dead wood and compost. Furthermore, their relatively high dry-weight protein content, as well as high fiber and vitamin composition, make them highly nutritious. Just five genera, *Lentinula*, *Pleurotus*, *Auricularia*, *Agaricus* and *Flammulina*, compose 85 percent of the global production (Royse et al. 2017). This is primarily due to an inability to cultivate many edible species on an industrial scale, due to their complex substrate and environmental requirements (Grimm and Wösten 2018). Therefore, a better understanding of the developmental program of mushroom-formation is necessary.

Mushroom-forming fungi are some of the best degraders of lignocellulose from woody plants. Lignocellulosic biomass consists of cellulose (glucose polymers), hemicellulose

(xylans, mannans, β -glucans and xyloglucans) and lignin (phenolic polymers) (Riley et al. 2014). It is the most abundant renewable waste resource and can play a major role as a feedstock in replacing petroleum-based products (Grimm and Wösten 2018). For example, lignocellulosic biomass can be used to produce biodegradable plastics by converting the simple sugars released during lignocellulose degradation (Kim et al. 2020a). Lignocellulose is very resistant to decay due to the presence of cellulose crosslinked to a lignin backbone (Cragg et al. 2015). Nonetheless, many mushroom-forming saprotrophic fungi can degrade lignin polymers with oxidative enzymes (peroxidases) and break down the sugar polymers to simple sugars with CAZymes. However, the regulation of wood decay in mushroom-forming fungi is poorly characterized and few regulators are characterized (Ohm et al. 2014; Riley et al. 2014).

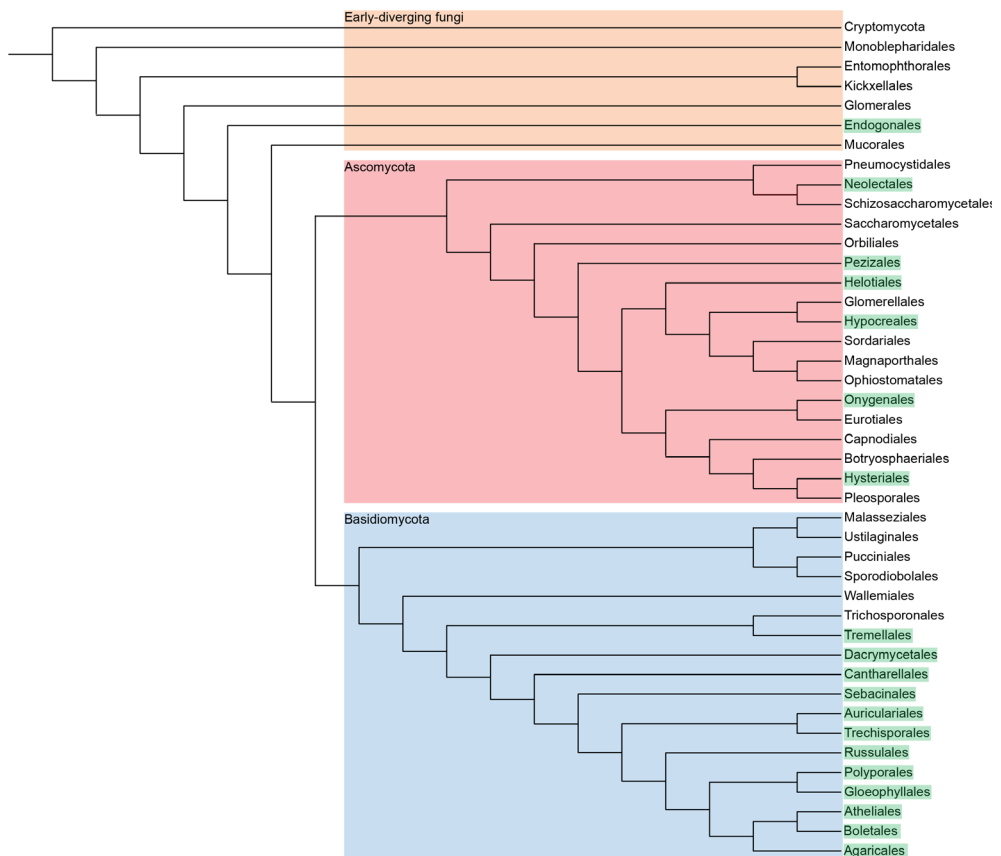


Figure 1. Cladogram of the orders of fungi. Fungi are separated into three major groups. The phyla of Ascomycota and Basidiomycota together comprise the subkingdom Dikarya. The Early-diverging fungi are an evolutionary diverse group of fungi and are not part of a single phylum. Orders highlighted in green produce macroscopic fruiting bodies or mushrooms.

Omics in studying mushroom-forming fungi

The challenges in developing molecular tools for mushroom-forming fungi have caused a shift to omics tools to study the developmental program of mushroom formation and to understand their strategies for wood-degradation. Initially, whole-genome sequencing was limited to model organisms and economically important species, including *A. bisporus*,

C. cinerea, *Laccaria bicolor* and *S. commune* (Morin et al. 2008; 2012; Ohm et al. 2010a; Stajich et al. 2010). With the advent of affordable whole-genome sequencing, over a thousand fungal genomes have been sequenced, including many saprotrophic mushroom-forming species (Floudas et al. 2012; Grigoriev et al. 2014; Riley et al. 2014; Almási et al. 2019; Krizsán et al. 2019; Varga et al. 2019; Sánchez-García et al. 2020). These genomes have resulted in important insights into mushroom-development and wood-degradation strategies. Furthermore, transcriptome profiling of multiple stages of development and growth on different substrates has identified key genes involved in these processes (Plaza et al. 2014; Muraguchi et al. 2015; Pelkmans et al. 2017; Almási et al. 2019; Krizsán et al. 2019; Yan et al. 2019; Kim et al. 2020b). Indeed, comparative genomics and comparative transcriptomics are the primary drivers of our increased understanding of mushroom development and wood-decay. This has been exemplified by comparative genomics of 33 wood-decaying basidiomycetes and comparative transcriptomics of the developmental stages of six mushroom-forming species (Riley et al. 2014; Krizsán et al. 2019). However, these omics approaches lack the functional characterization required to identify the specific functions of genes. The mushroom-forming fungus *S. commune* is an excellent model system for the functional characterization of these genes, due to its genetic accessibility and short life cycle (Ohm et al. 2010a; 2011; Pelkmans et al. 2017).

Schizophyllum commune

Schizophyllum commune is a saprotrophic basidiomycete in the order Agaricales. It is known for its characteristic split-gill fruiting bodies. It has a worldwide distribution and is generally found on decaying wood. While originally characterized as a white-rot fungus, *S. commune* is limited in its ability to degrade lignin, but can effectively release sugars from lignocellulosic biomass (Schmidt and Liese 1980; Floudas et al. 2012; Ohm et al. 2014; Riley et al. 2014; Zhu et al. 2016; Almási et al. 2019). In Southeast Asia, India, Mexico and several African countries *S. commune* is considered an edible mushroom, with a tough, corky structure (Ruán-Soto et al. 2006). However, in Western-Europe and The United States, *S. commune* is considered inedible due to this structure. Presumably the fleshier mushrooms of commonly consumed species like the white-button mushroom are less resistant to rot and therefore less suitable to the warm, humid conditions in countries where *S. commune* is consumed (Van Dijk et al. 2003). While not considered a human pathogen, there are several reports of human infection with *S. commune*. These infections are primarily located in the respiratory tract and occur almost exclusively in immunocompromised patients (Chowdhary et al. 2013).

S. commune is commonly used as a model organism for mushroom development (Horton and Raper 1991; Ohm et al. 2011; Pelkmans et al. 2017). It completes its life cycle in 10 days on defined medium under defined environmental conditions. A high-quality genome assembly is available and multiple genetic tools have been developed, including gene deletion by homologous recombination in a non-homologous end-joining deficient strain (Van Peer et al. 2009; de Jong et al. 2010; Ohm et al. 2010b). Indeed, the majority of gene deletions in mushroom-forming fungi has been performed in *S. commune* (Robertson et al. 1996; Horton et al. 1999; Lengeler and Kothe 1999a; 1999b; Lugones et al. 2004; Schubert et al. 2006; Van Wetter et al. 2006; de Jong et al. 2010; Ohm et al. 2010b; 2011; van Peer et al. 2010; Knabe et al. 2013; Pelkmans et al. 2017).

Fruiting body development in *S. commune*

Mushroom-forming fungi require vegetative growth to sustain the energetically costly development of the highly complex fruiting body. The *S. commune* mycelium starts from the germination of a sexual basidiospore and colonizes a substrate by extension from the hyphal tips. The tips secrete enzymes that degrade the substrate (when grown on a complex substrate) and branch sub-apically (Wessels 1986; 1990). The hyphae consist of haploid, mononucleate compartments that are connected by porous septa (van Peer et al. 2010). All nuclei in the mycelium are identical and therefore it is a monokaryotic and homokaryotic mycelium, also referred to as a monokaryon. On agar the mycelium initially grows submerged, but will start forming aerial hyphae after enough biomass is accumulated (Wösten and Wessels 2006). When the monokaryon encounters a compatible mate, the monokaryotic mycelium of two compatible mates can undergo plasmogamy and exchange nuclei to form a dikaryotic mycelium, also known as a dikaryon. Compatible mating is dependent on genetic differences of the *matA* and *matB* loci (discussed in detail below) (Kües 2015). While the monokaryotic mycelium grows unidirectionally on glucose, once a fertile dikaryon is established, the colony will grow asymmetrically under fruiting conditions (Wessels 1993). When enough biomass has formed and the environmental conditions are suitable, *S. commune* will start fruiting. This process is divided into four stages. In the first stage the branching patterns of aerial hyphae are reprogrammed to create hyphal aggregates. Next, these aggregates form a fruiting-body initial. Subsequently, this primordium develops into a cup-shaped immature fruiting body, covered by a hymenium on the inside. Finally, the cup-shaped fruiting body expands unilaterally and the characteristic split gills of *S. commune* are formed (Figure 2) (Wösten and Wessels 2006). In the basidia of the mushroom, karyogamy takes place, creating the only diploid cells in the lifecycle of *S. commune*. The basidia then undergo meiosis to form four haploid nuclei that migrate into spores.



Figure 2. Developmental stages of fruiting body formation in *S. commune*. The colony first grows as a network of undifferentiated hyphae. After developmental signals the branching of hyphae is reprogrammed and aggregates (A) of hyphae are formed. These aggregates develop into cup shaped primordia (P) that mature and expand in size. Eventually, the primordia expand to form a mushroom (M). Bar indicates 2 mm.

Regulation of fruiting body development

Environmental factors

The best studied environmental cues for mushroom development are light and CO₂ concentration (Kües and Liu 2000). While some species like *A. bisporus* do not require a light signal during fruiting-body development, most species do. In *S. commune* a single short exposure to light has been reported to be sufficient to induce primordia formation (Perkins 1969). In other species, however, multiple stages of light exposure are required for the development of mature mushrooms. For example, five separate exposures to light are required to develop mature, sporulating mushrooms in *C. cinerea* (Kües 2000; Kües and Liu 2000; Lu 2000). Light is needed for the development of fruiting body initials,

cellular differentiation in the fruiting body like the formation of gills, DNA replication and meiosis. These light signals are dose-dependent, and their intensity can promote or inhibit mushroom development (Kües 2000). The light exposure, in the form of blue light, is detected by the white collar complex (Yu and Fischer 2019) and has been extensively studied in the ascomycete *Neurospora crassa* (Corrochano 2011). In *N. crassa*, Wc1 is able to detect light with a specialized PAS domain that binds a flavin adenine dinucleotide chromophore. The detection of light results in a conformational change of Wc1, which then forms a heterodimer with Wc2. Both Wc1 and Wc2 are GATA zinc finger transcription factors (TFs) that can promote transcription after heterodimerization. In *S. commune* Wc1 does not contain a GATA zinc finger domain. It is currently thought that the general mechanism of blue light detection is conserved, but that Wc2 acts as a TF that promotes mushroom development after the detection of light by Wc1. Inactivation of either *wc1* or *wc2* results in blind mutants. In *S. commune* these mutants do not develop fruiting bodies and resemble a monokaryon (Ohm et al. 2013). However, in *C. cinerea*, fruiting-body initials are formed and the primordial shaft is elongated, but the cap and stipe do not develop, resulting in the “dark stipe” phenotype (Terashima et al. 2005; Kamada et al. 2010). Deletion of *dst2* in *C. cinerea* also causes the “dark stipe” phenotype. This gene has a flavin adenine dinucleotide-binding-4 domain that may detect blue light (Kuratani et al. 2010). A mechanism for *dst2* in light detection has not yet been identified.

High CO₂ concentrations repress fruiting body development in many mushroom-forming fungi (Kinugawa 1994, Sakamoto 2018). This can result in an underdeveloped cap and stipe, although the phenotype is species-specific (Kinugawa et al. 1994; Sakamoto 2018). In *S. commune* fruiting is completely abolished under high CO₂ conditions (Raudaskoski and Viitanen 1982; Pelkmans et al. 2017). Based on data from *Candida albicans* and *Cryptococcus neoformans*, it is thought that a high CO₂ concentration is converted to bicarbonate by carbonic anhydrase, which stimulates adenylyl cyclase activity (Klengel et al. 2005; Mogensen et al. 2006). However, this pathway has not yet been identified in *S. commune*.

Temperature has also been implicated in mushroom development. During industrial cultivation of *A. bisporus* the temperature must be lowered before fruiting occurs (Morin et al. 2012; Sakamoto 2018). *C. cinerea* and *S. commune* do not require temperature shifts to induce fruiting (Kües 2000; Wösten and Wessels 2006). However, at higher temperatures (30 °C) the morphology of mushrooms of *S. commune* is altered (Wessels 1965).

Another observation in *S. commune* is the sporadic occurrence of monokaryotic fruiting (Stahl and Esser 1976; Esser et al. 1979). This phenomenon is strain-specific and can in some cases result in the formation of a concentric mushroom ring similar to dikaryotic mushroom formation (Yli-Mattila et al. 1989). It is unclear if this is due to a homothallism, where the mating type genes are compatible within a single strain. Other monokaryotic strains of *S. commune* do not fruit under normal conditions, but only in response to stress. These so-called stress fruiting bodies develop when the mycelium reaches the edge of an agar plate or when nutrients are depleted. A similar response can be induced when a monokaryon of *S. commune* is co-cultivated with *Bacillus subtilis* (Krause et al. 2020). However, there are also strains of *S. commune* that are unable to fruit as a monokaryon under any studied circumstance, suggesting a genetic component in monokaryotic fruiting (Yli-Mattila et al.

1989). Monokaryotic fruiting has also been described in *Agrocybe aegerita* ranging from incomplete mushroom tissue to mature agaric mushrooms (Herzog et al. 2016; 2019).

Regulatory factors

Mating type genes

The mating type genes of basidiomycetes determine the compatibility of strains for mating. They are located on two loci, the *matA* and the *matB* loci (Kües 2015). Compatibility between two strains requires variation in the mating-type genes on both loci, resulting in a tetrapolar mating system, since meiosis leads to spores with one of four possible mating types. However, in some basidiomycetes, like *Cryptococcus neoformans*, the mating type loci are genetically linked (Lengeler et al. 2000; Hull et al. 2002), resulting in a bipolar mating system. In some strains, the mating type loci contain compatible genes within a monokaryon. An example of this is *C. cinerea* #326 (*A43mut B43mut pab1-1*), which has mutations in both mating type loci, resulting in a homothallic *Coprinopsis* strain (Muraguchi et al. 2015).

The *matA* locus encodes homeodomain (HD) TFs that can heterodimerize between compatible mating types to establish a dikaryotic mycelium. Their primary known function is the regulation of formation of clamp connections, which are required for nuclear migration after cell division to maintain the dikaryon (Bistis and Raper 1967). When two *S. commune* strains are incompatible in only their *matA* locus (common *A*), the mycelium still fuses, but the newly formed dikaryotic mycelium grows sickly and is unable to form clamps (Raper et al. 1958). Most fungi contain two HD TFs of different types on the *matA* locus (TALE and non-TALE HD TFs) (Kües et al. 1994), but in several mushroom-forming species, including *C. cinerea* and *S. commune*, the *matA* locus has undergone significant expansion to five and six genes, respectively (Kües 2000; Ohm et al. 2010a; Stajich et al. 2010; Freihorst et al. 2016). In these species, the *matA* locus is separated into two genetically linked loci (*A α* and *A β*). It is predicted that more complex interactions between different HD TFs occur in species with an expanded *matA* locus (Robertson et al. 2002). The structure and function of the *matA* locus is discussed in more detail in **Chapter 2**.

The *matB* locus contains genes encoding pheromones and G-coupled receptors (Raudaskoski and Kothe 2010). In compatible strains, the pheromones expressed from one nucleus can bind the receptors expressed from the other nucleus (Bölker et al. 1992; Specht 1995; Kothe 2001; Kim et al. 2014). Activation of the G-coupled receptor is associated with nuclear migration and fusion of the clamp connection to the receiving cell (Freihorst et al. 2016). Incompatibility of only the *matB* locus (common *B*), causes a clear line of delimitation between two strains (Parag and Raper 1960). Plasmogamy occurs locally, but nuclear migration is limited to the zone of interaction and clamps fail to fuse to the proximal cell.

Transcription factors

TFs are proteins that modulate gene expression by binding to specific DNA sequences, thereby activating or inhibiting transcription. TFs play a major role in the regulation of development across the tree of life, and mushroom-forming fungi are no exception (Shelest 2017). They are involved in many stages of development, ranging from the establishment of a dikaryon to various aspects of mushroom development.



Several TFs that are involved in fruiting body development have been identified. Deletion of the TF genes *hom2*, *tea1* and *wc2* in *S. commune* resulted in strains that do not show dikaryotic development beyond clamp formation in homozygous dikaryons (Figure 3) (Ohm et al. 2011; 2013; Pelkmans et al. 2017). Generally, the resulting colonies remain symmetrical and show no sign of mushroom development under mushroom inducing conditions. Furthermore, homozygous dikaryotic $\Delta hom2$ and $\Delta wc2$ strains accumulate more biomass during vegetative growth (Pelkmans et al. 2017). Hom2 is highly conserved in mushroom-forming fungi and features four putative phosphorylation sites. Disruption of these phosphorylation sites leads to a constitutively active Hom2 and the inhibition of vegetative growth and monokaryotic fruiting, indicating that Hom2 is post-translationally regulated (Pelkmans et al. 2017). Wc2 is part of the blue light sensing white collar complex first identified in *N. crassa*, as discussed above. Orthologs of the white collar complex with the same function have also been reported in *L. edodes* and *P. ostreatus* (Sano et al. 2007; 2009; Qi et al. 2020). Furthermore, their expression has been reported for *F. velutipes* (Liu et al. 2020). A homozygous dikaryotic *tea1* deletion strain, which is down-regulated in homozygous $\Delta wc1$, $\Delta wc2$, $\Delta hom2$, $\Delta bri1$ and $\Delta fst4$ dikaryons, also does not form mushrooms (Figure 3) (Pelkmans et al. 2017). It should be noted that homozygous dikaryotic *tea1* deletion mutants sporadically produce clusters of mushrooms, indicating that Tea1 is not essential for fruiting body formation and may act as a “switch” that can be bypassed. The ARID/BRIGHT DNA binding domain TF Bri1 was initially also thought to play a major role in fruiting development (Ohm et al. 2011). However, later characterization of homozygous *bri1* deletion strains revealed that inactivation of the gene leads to growth defects that result in a delay in fruiting (Pelkmans et al. 2017). The fungal specific TF Fst4 is also involved in mushroom development, and homozygous dikaryotic deletion strains of *fst4* only form asymmetrical colonies under mushroom inducing conditions (Figure 3) (Kües and Liu 2000; Ohm et al. 2010a). Like Hom2 and Wc2, Fst4 is also involved in the inhibition of vegetative growth, as a $\Delta fst4$ strain accumulates more biomass during vegetative growth (Pelkmans et al. 2017). In *Ganoderma lucidum*, silencing of the c_2h_2 -type TF PacC also results in the absence of fruiting bodies, as well as altered mycelial growth (Wu et al. 2016). Interestingly, PacC is conserved across the fungal kingdom and activates genes under alkaline conditions and inhibits genes under acidic conditions (Peñalva et al. 2008). Therefore, it is unclear if the absence of fruiting can be attributed to fruiting-specific transcription or general homeostasis. In *L. edodes*, PriB was described as a primordium up-regulated TF (Endo et al. 1994). Finally, silencing of *hada-1* in *Hypsizygos marmoreus* results in delayed fruiting, as well as multiple growth defects (Zhang et al. 2021).

Downstream in development, homozygous *S. commune c2h2* gene disruption results in arrested fruiting body formation. Its aggregates do not develop into mature fruiting bodies (Figure 3) (Ohm et al. 2011). Interestingly, overexpression of *c2h2* increases the rate of fruiting in *A. bisporus*, indicating that *c2h2* expression is a limiting step in fruiting body development (Pelkmans et al. 2016). Further downstream, the *C. cinerea* high-mobility group TF Exp1 regulates pileus expansion and autolysis to complete fruiting (Muraguchi et al. 2008).

Instead of promoting fruiting body development, several TFs are involved in stimulating vegetative growth or repressing fruiting. These include *Flammulina velutipes* Lfc1 and Hmg1, where silencing increased the rate of fruiting (Wu et al. 2020; Meng et al. 2021). Additional

TFs are *P. ostreatus* Pofst3 and *S. commune* Fst3, Gat1 and Hom1 (Figure 3) (Ohm et al. 2011; Qi et al. 2019). When the genes are deleted (*S. commune*) or silenced (*P. ostreatus*) it results in the formation of more, smaller mushrooms. In *P. ostreatus* a missense mutation in the zinc finger binding domain of *gat1* was reported to prevent fruiting. However, this mutation causes a dominant phenotype and is likely associated with a gain of function of Gat1, as this phenotype is very different from that of a homozygous dikaryotic *S. commune* Δ *gat1* strain. Finally, premature stop codons in *pcc1* in *C. cinerea* (natural variation, truncated from 561 to 210 amino acids, HMG-box not disrupted) and *P. ostreatus* (CRISPR/Cas9-assisted gene mutagenesis, truncated from 471 to 58 amino acids, HMG-box disrupted) result in monokaryotic fruiting and the formation of pseudoclamps (Murata et al. 1998; Boontawon et al. 2021;). In *C. cinerea* these pseudoclamps form during monokaryotic growth, indicating a relation between the *MatA* HD TFs and Pcc1. In *P. ostreatus* however, only dikaryotic strains form pseudoclamps, suggesting a role in clamp formation.

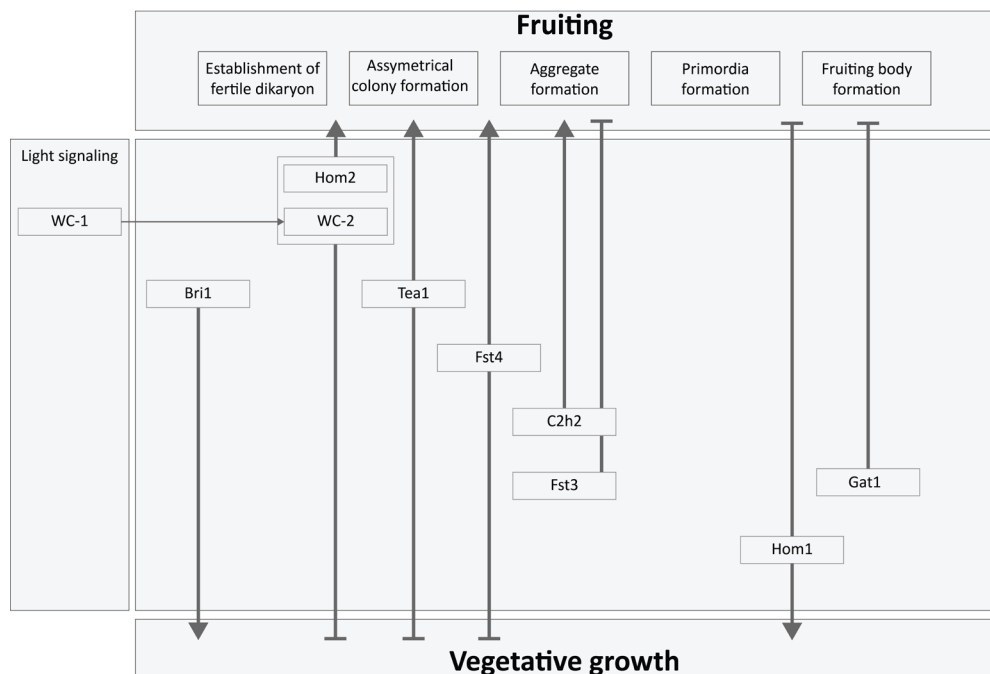


Figure 3. Current schematic overview of the regulation of fruiting body formation and vegetative growth in *S. commune*. Taken from Pelkmans et al. 2017.

Several of the TFs described above are conserved across fungi or specifically in mushroom-forming fungi. For instance, the TFs Hom2, Wc2 and PacC are conserved in both ascomycetes and basidiomycetes. Cag1 and Cc.Top1 of *C. cinerea* are further examples of highly conserved TFs (Masuda et al. 2016). They are homologs of the highly conserved general transcriptional co-repressor Tup1 of *S. cerevisiae*, which can form repressive complexes with a wide range of sequence-specific TFs. Deletion of Cag1 results in a cap-growthless phenotype, which, upon closer inspection turns out to be caused by developmental defects of gills (Masuda et al. 2016). However, the expression patterns are generally not conserved during fruiting body development (Almási et al. 2019; Krizsán et al. 2019). For example, the developmental

stage with the highest expression level of the ortholog can vary greatly between species. This suggests that either transcriptional regulation of fruiting body development is poorly conserved between species, or that TFs are regulated post-translationally. The *matA* mating type genes are an example of post-translational regulation, where the TFs are constitutively expressed, but only become activated when heterodimers are formed between compatible HD TFs (Kües et al. 2002; Kües 2015; Pelkmans et al. 2017). Similarly, in *N. crassa* Wc2 is activated by structural changes in its interaction partner Wc1 when blue light is detected (Corrochano 2019). Furthermore, Hom2 in *S. commune* is constitutively expressed, but post-translationally phosphorylated to become inactive (Pelkmans et al. 2017).

G-protein coupled receptor signaling

G-protein coupled signaling is an important pathway for many processes in eukaryotes. In this signaling pathway, a G-coupled receptor is activated by an external signal. Intracellularly the receptor is associated with a G-protein composed of an α , β and γ subunit ($G_{\alpha\beta\gamma}$) (Komolov and Benovic 2018). Receptor activation causes a conformational change of the receptor and exchanges GDP for GTP on the α subunit of the G-protein, which causes the G protein to dissociate into an α monomer (G_{α}) and β/γ dimer ($G_{\beta\gamma}$) that become activated for downstream signaling. G_{α} has an intrinsic hydrolase activity which is promoted by regulators of G-protein signaling (RGS). Therefore, G_{α} can exist in an active GTP-bound state and an inactive GDP-bound state where G_{α} and $G_{\beta\gamma}$ are recruited back to the G-protein coupled receptor. G-protein coupled receptor signaling is summarized in Figure 4A. Deletion of the RGS *gap1* in *S. commune* results in increased activation of the G_{α} Ras1 (Schubert et al. 2006). Homozygous deletion strains of *gap1* and constitutive activation of Ras1 by inactivation of the GTPase domains have an overlapping phenotype (Knabe et al. 2013). Both strains have a reduced growth rate, increased branching and decreased sexual development. In the case of constitutively active Ras1, the mutant strain does not accept nuclei during mating and fruiting bodies can only be formed at the side of the wild-type mycelium. Furthermore, spores have reduced viability and sometimes do not contain nuclei (Knabe et al. 2013). In homozygous dikaryotic *gap1* deletion strains, development is arrested after karyogamy and no spores are formed. Likely, in a *gap1* deletion mutant Ras1 GTP is still hydrolyzed to GDP due to intrinsic hydrolase activity (Schubert et al. 2006). Both $\Delta gap1$ and constitutively active Ras1 mutant have increased intracellular cyclic AMP (cAMP) concentration, suggesting a link between Ras1 activation and cAMP-signaling. Two other constitutively active G_{α} proteins, ScGP-A and ScGP-C, also increase cAMP levels and repress fruiting and aerial hyphae formation (Yamagishi et al. 2002; 2004). A third G_{α} protein, ScGP-B does not cause a clear phenotype when constitutively activated. A predicted downstream target of activated Ras1 is Cdc42, a small rho-like G-protein with GTPase activity, that also causes growth defects and altered branching patterns when GTPase activity is abolished (Knabe et al. 2013). Cdc42 is conserved in animals and fungi and plays a role in a large variety of cellular processes, including cell-cycle regulation and cytoskeletal assembly (Etienne-Manneville 2004). Indeed, Cdc42 is so highly conserved in animals and fungi, that human *cdc42* can complement a deletion of its ortholog in *S. cerevisiae* (Kachroo et al. 2015).

Another RGS gene, *thn1*, is often inactivated in a naturally occurring mutant caused by a transposon named *scooter* that integrates into this gene (Fowler and Mitton 2000). This mutant cannot form aerial hypha in static liquid cultures and can therefore not produce fruiting bodies in homozygous dikaryons. It is characterized by corkscrew-like hyphal growth

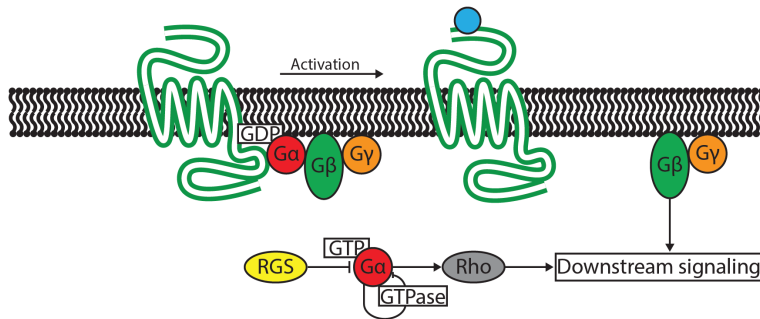
and an unpleasant smell. Similar to $\Delta gap1$ mutants, $\Delta thn1$ mutants have increased cAMP levels and show defects in growth and mating (Wirth et al. 2018). However, $\Delta thn1$ deletion strains also have reduced hydrophobin production and increased volatile organic compound production. Interestingly, the $\Delta thn1$ phenotype can be partially complemented by nearby wild-type mycelium (Schuren 1999; Wirth et al. 2018).

In *F. velutipes* a WD40 protein encoding gene, *Fvcpc2*, is suggested also to be part of G-protein coupled receptor signaling (Wu et al. 2020). *Fvcpc2* is closely related to *cpc2* in the ascomycete *N. crassa*, which encodes a G_β -like protein (Müller et al. 1995). Silencing of *Fvcpc2* reduces the growth rate and completely abolishes fruiting in dikaryons, while overexpression causes fruiting to occur one day earlier. Interestingly, both adenylate cyclase and protein kinase A are down-regulated in *Fvcpc2* silenced strains and the addition of 8-Bromo-cAMP can partially complement the phenotype (Wu et al. 2020). This suggests that activated *Fvcpc2* functions by increasing intracellular cAMP levels.

There are strong indications that fruiting is repressed by intracellular cAMP levels as a result of G-protein coupled receptor signaling (Figure 4B). Constitutive activation of the *S. commune* G_α proteins Ras1, ScGP-A and ScGP-C, as well as the downstream rho-like G-protein Cdc42, leads to increased cAMP levels and a deficiency in aerial hyphae formation and fruiting (Yamagishi et al. 2002; 2004; Schubert et al. 2006; Knabe et al. 2013). Furthermore, inactivation of the RGS proteins Gap1 and Thn1 also increases cAMP in homozygous dikaryons (Wessels et al. 1991; Fowler and Mitton 2000; Schubert et al. 2006; Wirth et al. 2018). Previously, cAMP has also been shown to be involved in mating and morphogenesis in *C. neoformans* and *Ustilago maydis* (D'Souza and Heitman 2001; Huber et al. 2002; Lee et al. 2019). An increase in cAMP has previously also been associated with CO₂-signaling in mushroom development (Eastwood et al. 2013). It is proposed that CO₂ is converted to HCO₃⁻, which stimulates adenylate cyclase to produce cAMP in *C. albicans* and *C. neoformans* (Klengel et al. 2005; Bahn and Mühlischlegel 2006; Mogensen et al. 2006). While the *matB* locus of agaricomycetes also encodes for G-protein coupled receptors, it is currently unclear if mating and an increase in cAMP levels are related. Contradictory, silencing of the G_β subunit FvCPC2 causes a decrease in cAMP levels, but also represses fruiting (Wu et al. 2020). This phenotype can be rescued by the addition of 8-bromo-cAMP. Potentially, a specific range of cAMP levels promotes fruiting, while higher and lower concentrations of this signaling molecule are inhibitory. Besides a shared function it appears that individual components of G-protein coupled receptor signaling have unique functions that are not related to cAMP. Indeed, while there is overlap in the phenotypes of deleted RGS proteins and constitutively activated G_α proteins, they cause diverse phenotypes. For example, Thn1 (directly or indirectly) regulates hydrophobin production and volatile organic compound secretion (Wessels et al. 1991; Wirth et al. 2018). Furthermore, constitutive activation of the G_α protein ScGP-B does not affect fruiting (Yamagishi et al. 2002).



A



B

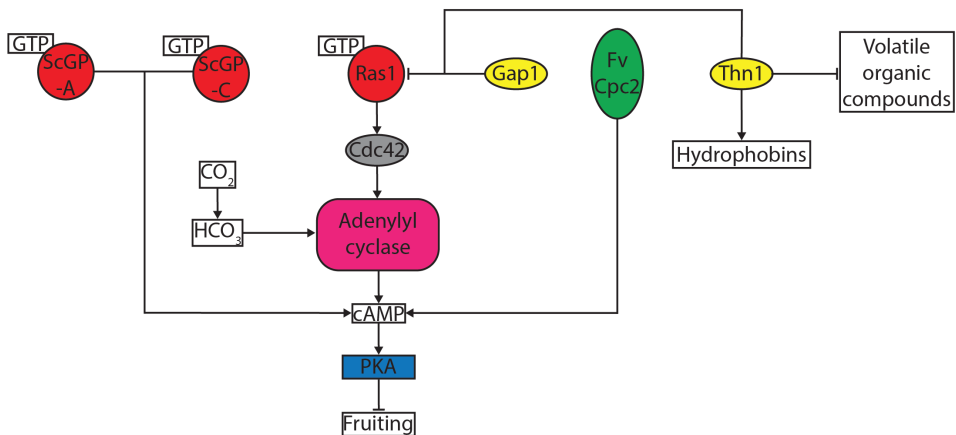


Figure 4. Schematic overview of G-protein coupled receptor signaling (A) and a proposed model for G-protein coupled receptor signaling in mushroom-forming fungi (B). No direct evidence is available for the interactions between components in mushroom-forming fungi.

Other potential regulatory genes

A frameshift mutation in *clp1* of *C. cinerea* and *P. ostreatus* blocks clamp cell formation. It is hypothesized that Clp1 is required to lift the repression of Pcc1 on the *matA* signalling pathway in these fungi (Inada et al. 2001; Boontawon et al. 2021). Clp1 has no predicted protein domains and it is unknown how Clp1 is involved in clamp cell formation. The cytochrome P450 enzyme (CYP502) Elongationless 2 (Eln2) is also involved in fruiting. Truncation of the C-terminus of Eln2 by 18 amino acids causes a dominant short stipe phenotype, where the cap matures normally, but the stipe fails to elongate (Muraguchi and Kamada 2000). In *S. commune*, introduction of a different allele of the RNA exonuclease 4 gene *frt1* can result in monokaryotic fruiting (Horton and Raper 1991). Interestingly, deletion of *frt1* does not result in fruiting defects (Horton et al. 1999). It has therefore been suggested that Frt1 allelic heterogeneity results in the formation of a heterodimer that promotes fruiting-body formation.

The methyltransferase *Ich1* has a role in mushroom development in *C. cinerea* (Muraguchi and Kamada 1998). It is differentially expressed during mushroom development and has a predicted nuclear localization signal as well as a winged-helix DNA binding domain. A mutant strain with a recessive mutation in *ich1* results in barrel-shaped primordia with no cap differentiation. Another methyltransferase, *Cc.Rmt1*, is involved in aerial hyphae development and a mutant strain with an inactive *Cc.rmt1* is unable to form hyphal knots, which are similar to aggregates in *S. commune* (Nakazawa et al. 2010). It is currently not known what the role of methyltransferases is during mushroom development, but it has previously been suggested that *Cc.rmt1* encodes a histone methyltransferase. Indeed, inactivation of gene *Cc.snf5*, part of the SWI/SNF chromatin remodeling complex involved in nucleosome positioning, causes inhibition of fruiting initiation (Ando et al. 2013). This suggests an important, yet unexplored role of chromatin remodeling in mushroom development.

Downstream components

Hydrophobins

Hydrophobins are some of the best-known fungal proteins and an important structural component of aerial structures, including fruiting bodies. They have diverse functions related to the escape of hyphae into the air and conferring their hydrophobicity, which they achieve by self-assembling into an amphipathic layer at the interface of the air and the water or the cell surface. For instance, hydrophobins cover mushrooms making them hydrophobic (Lugones et al. 1996), and line air channels in fruiting bodies preventing them from filling with water due to capillary force (Lugones et al. 1999). In addition, they contribute to water sealing, which is important in fruiting bodies as they are consumers of water transported from the vegetative mycelium (Nehls and Dietz 2014). The family has extensive literature, in general (Wösten 2001; Linder et al. 2005; Bayry et al. 2012), in relation to fruiting body development (Ohm et al. 2010a; Kües and Navarro-González 2015; Kim et al. 2016; Sammer et al. 2016; Tao et al. 2019) or on potential uses in bioengineering (Wösten and Scholtmeijer 2015). Basidiomycota hydrophobins mostly belong to class I hydrophobins (Sammer et al. 2016), that assemble into highly insoluble amphipathic amyloid-like films. In contrast, class II hydrophobins, that are primarily found in ascomycetes, form readily soluble amphipathic films. Moreover, class II hydrophobins show higher homology to each other and have a more precise spacing of the 8 characteristic cysteine residues (Wösten 2001). Class I hydrophobins can be arranged into distinct groups based on expression patterns (Krizsán et al. 2019). Previous studies reported almost no overlap in the hydrophobin genes expressed during vegetative growth and mushroom development, indicating that distinct sets of hydrophobins exist (Ma et al. 2007; Chum et al. 2008; Cheng et al. 2013). Interestingly, hydrophobins are also considered lectins due to their interaction with β -glucans and activity in agglutination assays (Van Wetter et al. 2000; Scholtmeijer et al. 2009). Other lectins are also implicated in mushroom development and are discussed below.

The *S. commune* hydrophobin genes *sc3* and *sc4* have been well studied. While *sc3* is expressed during aerial hyphal growth in all developmental stages, *sc4* is dikaryon-specific (Pelkmans et al. 2017). During vegetative growth, SC3 is secreted into the growth medium and self-assembles when exposed at the water-air interface (van der Vegt et al. 1996; Wösten et al. 1999). The resulting layer strongly decreases the water surface tension and allows *S. commune* hyphae to escape the water and grow into the air. Aerial hyphae also secrete SC3,



which assembles at the cell wall surface to create a hydrophobic layer around the hyphae (Wösten et al. 1994; 1999). This protects the hyphae from rain and dew and prevents re-entry of the aqueous substrate. A homozygous $\Delta sc3$ dikaryon still produces mushrooms but they are not hydrophobic (van Wetter et al. 2006). SC4 is primarily expressed during mushroom development and lines the air channels in the fruiting body. In a homozygous $\Delta sc4$ dikaryon the air channels can fill with water under moist conditions, preventing gas transfer (van Wetter et al. 2000). While both SC3 and SC4 play a role in fruiting body development, deletion of either gene results in mostly normal fruiting-body development. However, when both *sc3* and *sc4* are deleted, no mushrooms are formed by a homozygous dikaryon (van Wetter et al. 2000).

Lectins

Lectins are proteins that specifically recognize and bind carbohydrate moieties, mostly at the cell surface. This ability makes them suitable for multiple biological roles, from cytotoxicity against mushroom grazers (Bleuler-Martínez et al. 2011; Künzler 2015) to roles related to the fungal cell wall (e.g. remodeling), adhesion, cell-to-cell communication, or other functions in the extracellular matrix. However, much is currently unclear about their physiological role in fungi (Bleuler-Martínez et al. 2011). Many lectins are up-regulated during fruiting. For example, *C. cinerea cgl1* and *cgl2* are up-regulated during hyphal knot and primordia development, respectively, and are suggested to play a role in cell-cell adhesion or communication (Boulianne et al. 2000; Bertossa et al. 2004; Walser et al. 2005). In *Agrocybe aegerita* application of the fruiting-specific galectin AAL on mycelia promotes fruiting body production (Luan et al. 2010). However, when AAL is applied prior to inoculation on a solid medium, growth and fruiting are inhibited. Despite the strong relation between the expression of different lectins and mushrooms, no mechanism of action has been proposed to date. As lectins have also been strongly implicated in mushroom defense (see below), it is currently unclear whether lectins are directly involved in facilitating mushroom development, or expressed as a result of mushroom development. Further characterization is required to determine how their expression is related to mushroom development.

Defense

Agaricomycete fruiting bodies are, due to the concentration of biomass, attractive targets of predators, parasites and pathogens. Accordingly, these structures are known to be subject to grazing by slugs, to infestations with larvae of phorid and sciarid flies and to infections by bacteria and molds (Wood et al. 2004; Krivosheina 2008; Hamidzade et al. 2020; Lakkireddy et al. 2020;). Since mushrooms are the sexual reproduction organs and represent a considerable investment in terms of resources and energy, mushroom-forming fungi have evolved several strategies for the protection and defense of these structures (Künzler 2018). Such strategies include physical barriers (Varga et al. 2021) and chemical defense, i.e. the production of molecules (toxins) impairing the growth, development and/or viability of antagonists (Spiteller 2008; Lim and Keller 2014; Stadler and Hoffmeister 2015).

Using saprobic Agaricomycete species, whose sexual cycle can be completed under laboratory conditions, it could be demonstrated that the production of these toxins occurs axenically i.e. in the absence of the antagonist (Plaza et al. 2014; Tayyrov et al. 2019). This axenic toxin production is spatiotemporally regulated in that the toxin-encoding genes are expressed solely during fruiting body formation and in the fruiting body tissue. Some of

these genes belong to the most highly up-regulated genes of the genome during fruiting body formation. This expression pattern presumably results in an efficient, constitutive protection of the fruiting body because at least some toxins are already in place in case the structure is attacked by an antagonist. Antagonist-specific induction of antibacterial and nematotoxic proteins upon challenge with bacteria and fungivorous nematodes, respectively, has recently been reported for the vegetative mycelium of *C. cinerea* (Kombrink et al. 2019; TAYYROV et al. 2019).

Toxins produced in the fruiting bodies of Agaricomycetes include small molecules, defense peptides and proteins. Small molecules are secondary metabolites and often function as agonists of neurotransmitters (Michelot and Melendez-Howell 2003; Tullis 2021). Defense peptides can have a large variety of functions. A well-known member is α -amanitin, an inhibitor of RNA polymerase II with a human lethal dose of 0.1 mg/kg body weight (Liu et al. 2018; Walton 2018). However, the largest group of defense toxins are proteins. These are generally intracellularly stored and get released after ingestion and have a large variety of functions. Defense related lectins can bind and disrupt the epithelial cell membrane of the digestive tract (Stutz et al. 2015). Protease-inhibitors target digestive proteases to reduce growth, development and fertility (Pohleven et al. 2011; Šmid et al. 2015). Pore-forming toxins bind to antagonist cells and recruit more toxins to form a pore, resulting in lysis of the antagonist (Peraro and van der Goot 2016). Ribotoxins function intracellularly as ribonucleases and stop mRNA translation by cleaving a universally conserved site in the 23S or 28S rRNA of prokaryotes and eukaryotes, respectively (Olombrada et al. 2017). Finally, tamavidins sequester biotin to disrupt important metabolic pathways (Bleuler-Martinez et al. 2012).

Fungal cell wall remodeling

A striking observation in recent RNA-seq studies of mushroom development is the high expression of many CAZymes including chitinases, β -glucanases, laccases and mannanases (Krizsán et al. 2019). Many of these enzymes have been shown to degrade the sugar polymers produced by the fruiting body (Sakamoto et al. 2006; Konno and Sakamoto 2011). During mushroom development the immature fruiting body undergoes multiple morphological changes. For example, during late stages of *C. cinerea* mushroom development, stipe elongation and cap expansion occur in quick succession (Kües and Liu 2000). Stipe elongation is the result of lateral extension of stipe cells and requires plasticity of the cell wall. One mechanism for increasing the plasticity of the cell wall to support the rapid stipe elongation is the hydrolysis of chitin-glucan cross-links by chitinase (Liu et al. 2021). Exoglucanases are also expressed in the stipe of the young fruiting body and may also promote stipe elongation (Sakamoto et al. 2005). During mushroom senescence after harvesting, multiple glucanases are expressed in *L. edodes* that degrade the β -1,3-glucan lentinan (Sakamoto et al. 2005; 2006; 2011; Konno and Sakamoto 2011). The function of glucan degradation during senescence is currently unclear, but it is predicted to be involved in spore dispersal. However, transcriptomics suggest that cell wall remodeling is a far more complex process involving many CAZymes that have not yet been characterized (Almásí et al. 2019; Krizsán et al. 2019).

Lignocellulose degradation

Lignocellulose is the most abundant renewable waste material available in the world. It contains many sugar polymers in the form of cellulose and hemicellulose. The material offers many options for renewable energy and chemical production, including bioethanol and plastics (Sarkar et al. 2012; Grimm and Wösten 2018; Kim et al. 2020a). Saprotrophic agaricomycete mushroom-forming fungi are canonically classified as white-rot and brown-rot fungi, based on the method of lignocellulose degradation (Kües and Ruhl 2011; Floudas et al. 2012; Cragg et al. 2015). White-rot fungi can degrade the recalcitrant lignin polymers to access the (hemi)cellulose contained in wood. Furthermore, they are excellent degraders of crystalline cellulose due to the secretion of hydrolases and lytic polysaccharide monoxygenases (LPMOs) (Ohm et al. 2014). The degradation of lignin causes the decaying wood to turn white, hence the name white-rot. Brown-rot fungi on the other hand do not degrade lignin and primarily degrade cellulose through oxidative mechanisms. However, with the increased availability of saprotrophic fungal genomes this paradigm has been challenged. Many species possess the CAZymes to enzymatically degrade crystalline cellulose, but lack the characteristic lignin-degrading peroxidases (PODs) of white-rot fungi (Riley et al. 2014). An example is *S. commune* which was previously characterized as a white-rot fungus, but lacks POD genes (Ohm et al. 2010a). Indeed, *S. commune* uses a chimeric approach to lignocellulose degradation and expresses both CAZymes and enzymes to produce hydroxyl radicals when grown on lignocellulosic biomass (Ohm et al. 2010a; 2014; Floudas et al. 2012; Madhavan et al. 2014; Riley et al. 2014; Pellegrin et al. 2015; Zhu et al. 2016; Almási et al. 2019).

CAZymes are grouped as glycoside hydrolases (GHs), glycosyl transferases (GTs), polysaccharide lyases (PLs), carbohydrate esterases (CEs) and auxiliary activities (AAs) (Levasseur et al. 2013). GHs are the primary degraders of sugar polymers and hydrolyze glycosidic bonds. They may be further subclassified into endohydrolases and exohydrolases, acting on the middle or the end of a carbohydrate polymer, respectively. AAs encode redox enzymes and contain lignin degradation enzymes and LPMOs. Lignin degradation enzymes act by degrading the matrix of lignin polymers to make (hemi)cellulose more accessible (Salame et al. 2012). LPMOs cleave polysaccharides by an oxidative reaction and promote the activity of GHs. It is currently thought that LPMOs primarily act on crystalline carbohydrates, creating new binding sites for GHs (Hemsworth et al. 2015).

The expression of CAZymes is transcriptionally regulated by carbon catabolite repression (CCR) as their expression is energetically expensive and only required when growing on a complex substrate. In the presence of a readily metabolized sugar like glucose, CCR represses CAZyme expression and uses the most efficient substrate available. CCR is regulated by a single zinc-finger TF *creA* (also known as *cre1* and *cre-1*) that represses CAZyme expression (Strauss et al. 1999; Portnoy et al. 2011). Gene *creA* is highly conserved in Ascomycota and Basidiomycota and has been extensively characterized in *A. nidulans*. In *P. ostreatus* the *creA* ortholog *cre1* regulates CCR in the same manner, suggesting that CCR is conserved in fungal evolution (Todd et al. 2014; Yoav et al. 2018).

Several other regulators of CAZyme expression have been identified in ascomycetes. For example, in *Aspergillus* species and *Trichoderma reesei* (hemi)cellulase expression is positively regulated by *xlnR*, which is conserved in most filamentous ascomycetes (van Peij

et al. 1998; Stricker et al. 2008). In *N. crassa* *CLR-1* and *CLR-2* promote cellulase expression (Coradetti et al. 2012). Finally, *ACE1* in *T. reesei* is a repressor of CAZyme expression (Aro et al. 2003). While conserved in many ascomycetes, basidiomycetes lack the orthologs of these regulators (Todd et al. 2014). This suggests an independent regulation mechanism for CAZyme expression in basidiomycetes that is currently not identified. As most wood-decay fungi belong to the phylum Basidiomycota, a better understanding of the regulation of wood-decay in basidiomycetes can improve the utilization of lignocellulosic biomass.

Outline

Given their economic and environmental importance, a better understanding of mushroom development and wood-decay is required. However, this understanding is limited by a lack of efficient molecular genetic tools. These tools are necessary to functionally characterize the candidate genes involved in mushroom development and wood-decay identified in comparative genomics. This thesis includes a comparative genomics analysis to identify candidate TFs in mushroom development. Furthermore, several tools to study TFs and other genes related to fruiting and wood-decay are developed for *S. commune*, including an efficient CRISPR-Cas9 gene-deletion protocol. Finally, these tools are applied to functionally characterize multiple TFs, leading to more insights into the regulation of mushroom development and lignocellulose degradation.

Chapter 2 describes the diversification of HD TFs in fungi based on an analysis of 222 fungal genomes of ascomycetes, basidiomycetes and early-diverging fungi. HD TFs are known to be important developmental TFs in plants and animals. In fungi they are part of the mating type locus, while they can also play a role in later stages of the sexual cycle. We show that in mushroom-forming basidiomycetes, HD TFs have undergone significant expansion and play a potential role in developmental processes.

In **Chapter 3** the first CRISPR-Cas9 gene deletion method is described that can be used to delete any gene of interest in a mushroom-forming fungus. The use of CRISPR-Cas9 ribonucleoproteins during protoplast transformation greatly improves the existing gene deletion method with an average of 10 confirmed gene deletion strains from a single transformation. Furthermore, the method is also applicable in a wild-type background, albeit at a lower efficiency. Therefore, the gene deletion method can also be used in species for which no non-homologous end-joining deficient strain is available.

Chapter 4 describes the changes in the epigenetic landscape during development. The distribution of the activating histone mark H3K4me2 is mapped by ChIP-Seq during early monokaryotic and dikaryotic development. While the genome of *S. commune* carries similar H3K4me2 methylation patterns during both monokaryotic and dikaryotic development (6032 and 5889 sites, respectively), 837 sites carry differential H3K4me2 enrichment. These differential H3K4me2 sites were associated with 965 genes. Surprisingly, the majority of differentially enriched sites were identified during monokaryotic development and associated with 771 genes. Only 194 genes were differentially associated with H3K4me2 during dikaryotic development. To verify the significance of this enrichment, we used the gene deletion method described in **Chapter 3** to delete two TFs, *fst1* and *zfc7*, which both had a similar phenotype with aborted mushroom development after primordia formation in homozygous dikaryons.

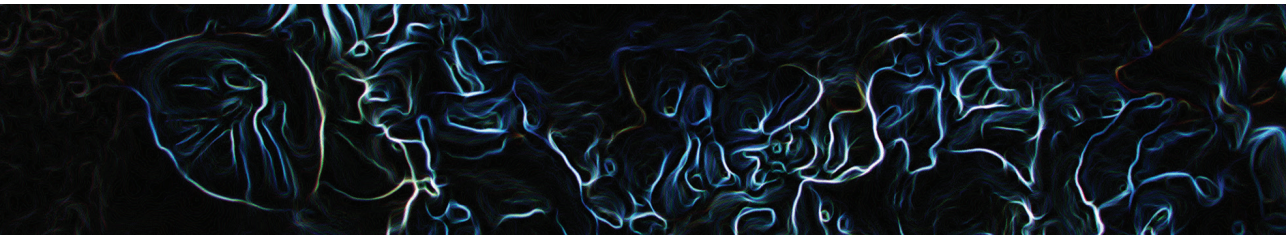
In **Chapter 5** an *S. commune* regulator of cellulase expression, *roc1*, is characterized. This is the only TF gene up-regulated on cellulose and wood when compared to growth on glucose. Deletion of the TF with the CRISPR-Cas9 method described in **Chapter 3** resulted in a strain that did not produce cellulases and could not use cellulose as a substrate. Roc1 was HA-tagged and its DNA-binding locations during growth on glucose and cellulose were identified with the ChIP-Seq protocol described in **Chapter 4**. The promoters of CAZymes were significantly enriched among the binding sites of Roc1. From the ChIP-Seq binding sites a consensus binding motif was identified. When this binding motif was disrupted in the promoter of the LPMO *lpmA*, Roc1 was no longer able to activate the promoter.

In **Chapter 6** eight additional TF gene deletions with CRISPR-Cas9 are reported. Deletion of the fungal-specific TF *ptr1* abolishes fruiting-body formation completely in homozygous dikaryons, similar to the previously reported phenotypes of *bri1*, *hom2*, *wc2* and *tea1*. Deletion of *zfc4* leads to slower and incomplete mushroom development in homozygous dikaryons. Homozygous deletion of *bzt1* resulted in a phenotype with more, but smaller mushrooms. This phenotype is comparable to the previously reported deletions of *gat1* and *hom1*. The deletion of four other TFs did not result in any phenotype during fruiting-body development, despite being developmentally regulated.

Chapter 7 describes the development of a targeted knock-in method. When applied to the integration of a *dTomato* fluorescent reporter gene, fluorescence was stable across all transformants. As a control the same reporter gene was also integrated ectopically, which resulted in a large range of fluorescence intensity. This reduces the necessity of time-consuming screening and characterization of transformants.

The results are summarized and discussed in **Chapter 8**.





The Role of Homeodomain Transcription Factors in Fungal Development

Peter Jan Vonk, Robin A. Ohm

This chapter is based on Vonk, P. J. & Ohm, R. A. (2018). The role of homeodomain transcription factors in fungal development. *Fungal Biology Reviews*, 32(4), 219–230. <https://doi.org/10.1016/j.fbr.2018.04.002>

Abstract

The role of homeodomain transcription factors during development in animals is well established since the identification of the homeobox gene clusters. In the kingdom Fungi homeodomain genes also play a crucial role during multicellular development. They were first identified in mating type loci, which regulate sexual development. Later, other homeodomain genes were shown to be involved in fruiting body development in several members of Ascomycota and Basidiomycota. In this review we describe recent research on homeodomain transcription factors in fungi. An evolutionary framework is provided by reanalyzing 222 previously published fungal genomes to identify potential functions of homeodomain transcription factors in multicellular development and fructification.

Introduction

Fruiting bodies are among the most complex multicellular structures formed by Fungi and have evolved to produce and disperse spores. Although mushrooms of the order Agaricales are generally best known due to their complex macroscopic structure, fruiting bodies are formed by members of many clades of higher fungi (Ascomycota and Basidiomycota). The genetic regulation of fruiting body formation is not well-characterized, despite its potential economic impact. However, several groups of transcription factors (TFs) have been identified as regulators of fructification. In the basidiomycete *Coprinopsis cinerea* the light sensing *dst1*, as well as the high mobility group TF *pcc1* have been shown to be involved in fructification (Murata et al. 1998; Kamada et al. 2010). In *Schizophyllum commune* TFs containing a zinc finger of the fungal-specific Zn(II)2Cys6 domain (*fst3*, *fst4*), the C2H2 domain (*c2h2*) or the GATA domain (*gat1*, *wc-2*) and TFs containing a BRIGHT domain (*bri1*) or a homeodomain (HD)(*hom1*, *hom2*) regulate various aspects of fruiting body formation (Ohm et al. 2011; 2013; Pelkmans et al. 2017). No functional characterization has been done in other Agaricales, although many of the previously mentioned genes are conserved within this order of fungi (Pelkmans et al. 2017).

In the ascomycete *Neurospora crassa* many TF knock-out strains show aberrant perithecium formation: seven Myb-like, seven C2H2, six Zn(II)2Cys6, four GATA, three Zn(II)2Cys6/Fst, two BRIGHT, two bZIP, two HD, two HLH, two HMG, one BRIGHT/Myb-like, one C2H2/Zn(II)2Cys6, one Cbf-NY-Y, one Forkhead, one HTH, KILA-N and one NDT80/PhoG-like TF were shown to have some defect in fructification, ranging from reduced perithecium count to no perithecium formation at all (Degli-Innocenti and Russo 1984; Aramayo et al. 1996; Feng et al. 2000; Li et al. 2005; Colot et al. 2006; Carrillo et al. 2017).

In the ascomycete *Podospora anserina* five HMG and two HD TFs are known to be required for wild-type development of the fruiting body (Coppin et al. 2012; Ait Benkhali et al. 2013). In *Aspergillus nidulans* two C2H2, two Zn(II)2Cys6, one Dopey_N leucine zipper, one GATA and one KILA-N TF have been identified to be involved in successful conidiophore development (Prade and Timberlake 1993; Wu and Miller 1997; Pascon and Miller 2000; Vallim et al. 2000; Han et al. 2001; Vienken et al. 2005; Vienken and Fischer 2006;).

A HD is a conserved DNA-binding domain of 60 amino acids that features a helix-turn-helix structure. HDs are found in TFs in almost all eukaryotic species, except some unicellular species (Derelle et al. 2007). HDs are classified as either TALE (three amino acid length extension) or non-TALE domains, based on the presence of an insertion in the sequence between the two helices. This split occurred before the origin of plants, animals and fungi, as both types are present in each of these kingdoms (Bharathan et al. 1997).

The HD was first identified in homeobox (*hox*) TFs in *Drosophila melanogaster* (Lewis 1978). These *hox* genes are found in several clusters in the genome and control the body plan of an embryo along the anterior-posterior axis (Mallo et al. 2010). For example, a change in the gene order modifies the body plan and leads to the famous antennapedia phenotype, where legs grow in place of the antenna. This is caused by a dominant inversion in the bithorax complex Hox cluster and subsequent *antP* expression in the head (Frischer et al. 1986; Maeda and Karch 2009). Phenotypical changes such as this led to the name HD, after the process of homeosis, where an organ is replaced by another organ. Similar functions are



found in all Bilateria, where spatial expression along the anterior-posterior axis determines segment identity by activating specific expression patterns per segment, leading to the development of these segments. As such the localized activation of hox genes through developmental pathways ultimately regulates the segment identity in Bilateria (Mallo et al. 2010). In plants HD TFs play a similarly important role in development (Hay and Tsiantis 2010). For example, overexpression of the HD TF *kn1* in *Arabidopsis thaliana* leads to lobed leaves, compared to the simple structure in WT plants (Lincoln et al. 1994).

Given their role in developmental processes in a wide range of organisms, it has been suggested that HD TFs are part of the genetic toolkit that allowed organisms to develop multicellularity and cell differentiation (King 2004). In both animals and plants the HD genes expanded to over 100 genes per species (Derelle et al. 2007). In Fungi the diversification happened on a much smaller scale with HD counts ranging from 1 to 51 (Todd et al. 2014; this study). Notably, in Fungi HDs are also associated with regulating (multicellular) development, since they are involved in mating as well as fruiting body development.

This review will focus on the role of HD TFs in multicellular development and fructification in the kingdom Fungi. Recent literature is combined with a re-analysis of 222 previously published fungal genomes to provide a framework for studying the function of HD TFs.

Homeodomain transcription factors in Fungi

Evolutionary framework for homeodomain transcription factors

In recent years hundreds of fungal genomes have been sequenced and published, including those of Ascomycota, Basidiomycota and ‘early diverging fungi’ (i.e. non-Dikarya) (Cherry et al. 2012; Cerqueira et al. 2014; Grigoriev et al. 2014; Hibbett et al. 2016; Nagy et al. 2016; Riley et al. 2016; Skrzypek et al. 2017), resulting in a large number of predicted HD TF genes. These previously published data were reanalyzed and the evolutionary history of fungal HD genes was reconstructed, providing an evolutionary framework for this review (Supplementary Text 1). In the case of Ascomycota and Basidiomycota the number of HD genes generally correlates with the total number of predicted genes (Figure 1). The early diverging fungi are a clear exception to this, however, and generally have much higher counts of HD genes. This increase can be attributed primarily to the Mucoromycotina (Supplementary Table 1). Furthermore, fungi with a predominantly unicellular (yeast) lifestyle generally have fewer HD genes than fungi with a predominantly multicellular (filamentous) lifestyle (Figure 2). This suggests that in Ascomycota and Basidiomycota the HD genes are involved in multicellular development (Derelle et al. 2007), although this effect is less pronounced than in the Metazoa (de Mendoza et al. 2013). Interestingly, it was previously reported that the increase in TF count resulting from genome expansion in fungi can be mostly explained by three TF families, including the HD TFs, which show a higher relative increase compared to the TFome as a whole (van Nimwegen 2003; Shelest 2017). A phylogenetic analysis of all predicted HD genes allowed the identification of 12 groups of HD genes (Figure 3, Supplementary Text 1 and Supplementary Table 1), which were mapped onto the species tree of the 222 fungi (Figure 4, Table 1). This revealed the evolutionary history of each of these 12 groups of HD genes, which will be discussed below.

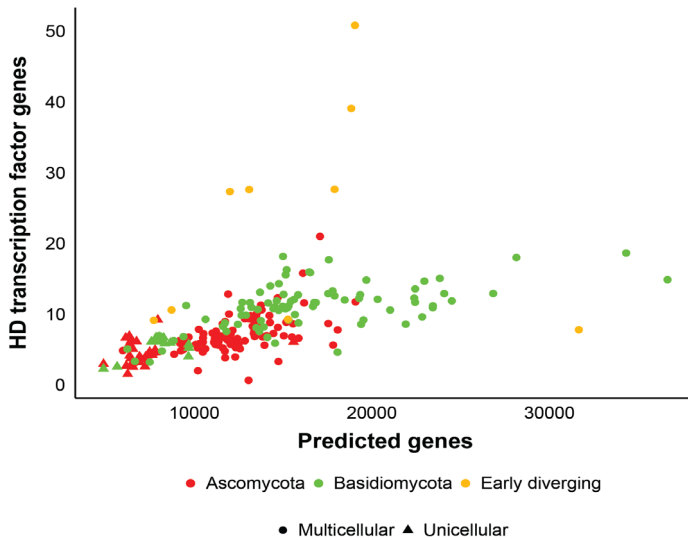


Figure 1. Scatterplot of total predicted genes versus predicted HD TFs in 222 fungal genomes. The colors indicate the clade and the shape indicates lifestyle (unicellular yeasts versus multicellular filamentous fungi). In members of Ascomycota and Basidiomycota the number of HD TFs roughly correlates with the total gene count, but this is not the case for the early diverging fungi. More details can be found in Supplementary Table 1.

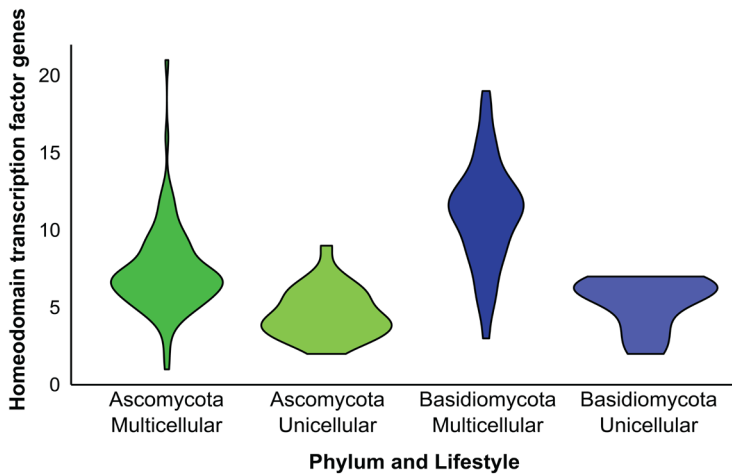


Figure 2. The number of HD TFs per phylum and lifestyle (multicellular/filamentous versus unicellular/yeast-like). Unicellular species encode fewer HD TFs in their genome when compared to multicellular species. More details can be found in Supplementary Table 1.

Mating type homeodomain transcription factors

The best-studied HD TFs in Fungi are those belonging to the mating type locus. In many Fungi this locus is essential for the recognition of (and successful fusion with) a non-self mating partner. This is generally seen as the first step in the initiation of sexual reproduction and (depending on the organism) the associated multicellular differentiation and development (Raudaskoski and Kothe 2010).

In the ascomycete yeast *Saccharomyces cerevisiae* the *mat* locus is either *mat-a* or *mat- α* and transcription of the locus leads to *mat-a* or *mat- α* specific cellular development (Haber 2012). In *mat- α* cells, the HD gene *MAT α 2* is expressed. Together with Mcm1, *MAT α 2* forms a heterotetramer that represses *mat-a* specific genes (Keleher et al. 1988; Passmore et al. 1989; Elble and Tye 1991). This includes *mat-a* specific pheromone signalling to identify the opposing mating type (Johnson 1995). In *mat-a* cells the HD TF *MATa1* is expressed from the *mat* locus. While *MATa1* is expressed it is quickly degraded and has no known functions in haploid cells, indicating that *mat-a* development is the default (Johnson et al. 1998). When compatible mating type cells fuse, they create a diploid cell that expresses both *MATa1* and *MAT α 2*. Expressed together these HD TFs form a heterodimer that prevents degradation and has a specificity distinct from the *MAT α 2* homodimer (Goutte and Johnson 1988; 1993; Keleher et al. 1988). The α 1/ α 2 heterodimer represses a set of genes called haploid-specific genes (Dranginis 1990). These genes include *MAT α 1* (Herskowitz 1989), which regulates the haploid *mat- α* cellular expression and *rme1*, a repressor of meiosis (Covitz et al. 1991). Besides the HD genes, both the *mat-a* and *mat- α* locus carry another gene: *MATa2* is uncharacterized and is dispensable for successful mating (Dranginis 1989), while *MAT α 1* is a HMG box gene responsible for *mat- α* specific transcription (Bender and Sprague 1987). A unique feature of several ascomycete yeasts is the ability to switch mating types (Haber 2012). In *S. cerevisiae*, another mating type locus is located both upstream and downstream, named hidden mat left (*HML*) and hidden mat right (*HMR*). The *HML* locus contains a silenced copy of the *mat- α* genes, while the *HMR* carries an additional silenced *mat-a* copy. During the late G1 phase a specific endonuclease, HO, can replace the *mat* locus with either *HML* or *HMR* (Kostriken et al. 1983).

The role of HD TFs in mating in Basidiomycota is very similar to that found in *S. cerevisiae*. However, in most Basidiomycota the mating type is determined by two unlinked loci, the *matA* locus for HD TFs and the *matB* locus for pheromones and their receptors (Raudaskoski and Kothe 2010). The presence of two loci makes many Basidiomycota tetrapolar, since meiosis leads to spores with one of four possible mating types. However, in some species, including *Cryptococcus neoformans*, the *matA* and *matB* locus are genetically linked and these species are therefore bipolar (Lengeler et al. 2002). In all heterothallic tetrapolar species a fertile dikaryon is only established when both mating loci are compatible. In most species the *matA* locus is composed of two HD genes, one TALE HD1 and one non-TALE HD2 TF (Kües et al. 1994), although in *C. cinerea* and *S. commune* the *matA* locus is composed of five and six HD genes, respectively (Kües 2000; Ohm et al. 2010a; Stajich et al. 2010; Freihorst et al. 2016). Variation in only a single HD gene is necessary for sexual compatibility. Likely, the expansion of the locus increases the chances of finding a compatible mate in nature and increases genetic variation through genetic recombination. The *matA* HD TFs form homodimers or heterodimers (Kües et al. 1994; Asada et al. 1997; Robertson et al. 2002), although heterodimers are necessary for successful mating in *U. maydis* (Gillissen et al. 1992). More complex combinations between homodimerization and heterodimerization have been suggested to occur in Agaricales (Robertson et al. 2002). After dimerization the HD TFs facilitate the establishment of clamp connections in dikaryotic mycelium (Bistis and Raper 1967). No direct targets of a HD1/HD2 heterodimer have been identified, but in *C. cinerea* it has been suggested that targets include *clp1* and *pcc1* (Raudaskoski and Kothe 2010), which are both involved in clamp connection formation .

HD TF genes involved in mating are found in group 7 (mating type genes of *S. cerevisiae*), group 9 (HD2 genes of Basidiomycota) and group 11 (HD1 genes of Basidiomycota) (Figure 3, Table 1 and Supplementary Text 1). None of these groups are closely related, which indicates that these functions have split early during fungal evolution.

Mating type genes tend to be clustered (co-localized) in mating type loci (Raudaskoski and Kothe 2010), which is also reflected in the relatively high percentage of clustered genes in these three groups (Table 1 and Supplementary Text 1), particularly in the case of HD1 and HD2 genes in Basidiomycota. This functional clustering of HD genes is a remarkable parallel with the developmentally important *hox* gene cluster in animals (Maeda and Karch 2009). To our knowledge, similar functional clustering has not been described for any other class of TFs.

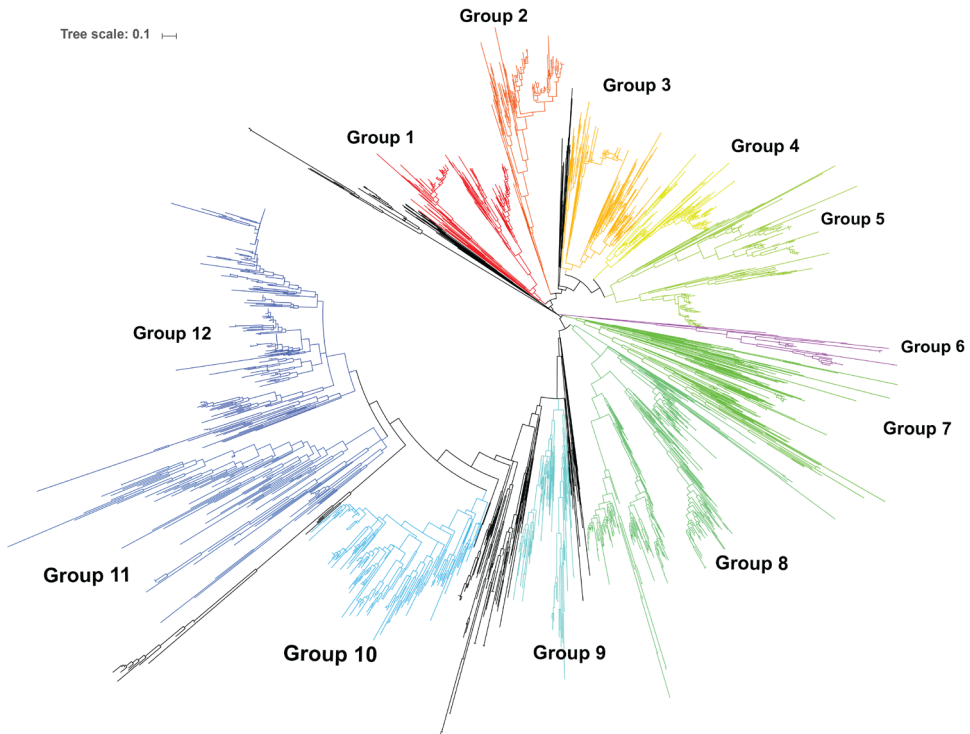


Figure 3. Phylogenetic tree of all 2113 HD genes predicted in 222 fungal genomes. Conserved groups of HD genes are indicated in color. More details can be found in Supplementary Table 1.

Ascomycete HD genes involved in fruiting body development

In the ascomycete *Podospora anserina*, where HD TFs are not part of the mating type locus, seven HD TFs were identified in the genome (Coppin et al. 2012). Initial studies on a single HD gene, *pah1*, showed it represses microconidiation and alters hyphal branching (Arnaise et al. 2001). Knockouts of *pah1*, *pah2*, *pah5* and *pah7* show altered perithecium morphology. Particularly, *pah2* and *pah5* knockouts develop fruiting bodies without a neck, which promotes spore dispersal (Ingold 1933). In both *pah1* and *pah7* knockouts the location of the fruiting bodies on the mycelium is altered and *pah1* knockouts also show more globular perithecia. In double knockouts it was shown that *Pah2* and *Pah5* are

essential for fructification and sexual reproduction, as $\Delta pah2\Delta pah5$ strains do not form any asci and produce only very small fruiting bodies (Coppin et al. 2012). When additional HD gene deletions are introduced, this phenotype becomes more pronounced. The model organism *N. crassa* shows similar phenotypes to *P. anserina*, with *pah1* ortholog *kal1* supporting conidium formation and *pah5* ortholog *bek1* being involved in the formation of the perithecium neck (Colot et al. 2006). In the plant-pathogenic ascomycete *Magnaporthe oryzae*, HD TFs are indispensable for the formation of the appressorium (Kim et al. 2009), a specialized cell used to pierce plant cells upon infection (Liu et al. 2010). Additionally, conidiation is altered or abolished in knock-outs of $\Delta mohox2$. Interestingly, *mohox2* is an ortholog of *pah3* in *P. anserina*, knockouts of which do not show any change in phenotype (Coppin et al. 2012). Gene *mohox7* is the ortholog of *pah5* in *M. oryzae*, but is only involved in the formation of the appressorium and not conidiation (Kim et al. 2009). This suggests that homologous proteins do not necessarily have a similar function in different species. However, perithecium formation was not assessed in *M. oryzae* and *mohox7* expression is increased 12-fold during fructification. Similarly, in *Botrytis cinerea*, *pah1* ortholog *bchox8* is also involved in hyphal growth and conidiation (Antal et al. 2012).

Transcriptome data confirms observations of HD TF involvement in perithecium formation *N. crassa*, as *bek1* is initially down-regulated and later up-regulated during fructification (Wang et al. 2014). Expression of *kal1* increases up to four-fold 48h after initiation of perithecium formation. Several uncharacterized HD genes show similar expression patterns. NCU03070 and NCU05257 are both significantly up-regulated after 48h and both NCU03266 and NCU09556 are highly expressed in the final stages of fructification (after 120 and 72h, respectively). Particularly NCU09556 is of interest as it is an ortholog of the *pah2* in *P. anserina* which has been shown to play a role in fructification (Coppin et al. 2012). NCU03070 was previously knocked out, but had no phenotype in fructification, asexual development or hyphal growth (Colot et al. 2006). In *Fusarium graminearum* several HD genes are differentially expressed during fructification (Sikhakolli et al. 2012). However, orthologs of *pah1* and *pah2* show relatively low expression and mRNA levels actually decrease during fructification. Interestingly, *Fusarium* species have an expansion of *pah6* homologs, almost all of which are up-regulated during fructification, like the *N. crassa* ortholog, while *pah6* knock-outs had no observed phenotype (Coppin et al. 2012; Wang et al. 2014). Together this shows the need for functional identification beyond transcriptome analysis to reliably identify fungal genes involved in fructification

Basidiomycete HD genes involved in fruiting body development

The genome of the basidiomycete *S. commune* encodes 11 non-mating HD proteins, but only two of those have been functionally characterized, *hom1* and *hom2* (Ohm et al. 2011; Pelkmans et al. 2017). The Hom1 TF is involved in mushroom development, maintaining the vegetative state, and biomass formation. A homozygous $\Delta hom1$ dikaryon exhibits lower biomass formation and reduced hyphal thickness (Pelkmans et al. 2017). Moreover, fructification in this strain is increased, but mushrooms are smaller (Ohm et al. 2011). Hom2 is also involved in the fructification process and stimulates fruiting body development (Ohm et al. 2011). A homozygous $\Delta hom2$ dikaryon only produces vegetative mycelium and is incapable of fructification. Hom2 is regulated by protein kinase A, which inactivates Hom2 on four RRXS amino acid motifs by phosphorylation (Pelkmans et al. 2017). Mutation of the RRXS-motifs leads to a constitutively active Hom2 TF, resulting in increased fructification.

A third HD gene of interest is *hom5* (proteinID: 2603970) and although it has not been functionally studied, it is down-regulated during fructification (Pelkmans et al. 2017), suggesting that it plays a role in this process.

No knockouts of HD genes have been reported in other Agaricales, but the *hom1* ortholog in *C. cinerea* (protein ID: 493627) is differentially regulated during fructification, with up-regulation in the stipe and down-regulation in the cap (Muraguchi et al. 2015). The *hom2* ortholog (protein ID: 355616) is increased in stipe elongation and later stages of cap development. Together this suggests that similar regulation patterns can be found in multiple Agaricales species. Especially since other regulatory pathways, like light sensing, are also conserved between *S. commune* and *C. cinerea* (Kamada et al. 2010; Ohm et al. 2013). Additional HD genes with a possible role in development include orthologs of the *S. commune* genes *hom3* (protein ID: 497620), *hom6* (protein ID: 460235) and *hom10* (proteinID: 458752). Expression of *hom3* and *hom10* is down-regulated in late stages of *C. cinerea* development, while *hom6* is differentially regulated depending on developmental stage (Muraguchi et al. 2015).

Yeasts versus multicellular fungi

Yeasts are found in several fungal phyla and include ascomycete species (e.g. *S. cerevisiae*, *Candida albicans*) and basidiomycete species (e.g. *C. neoformans*) (Nagy et al. 2014). Yeasts are generally less complex than filamentous fungi and may lack the genetic toolkit for complex development due to loss of function during unicellular evolution (Nagy 2017). Indeed, the genomes of yeasts generally encode fewer HD genes (Figure 1). Moreover, they have significantly lower HD gene diversification, with one to five groups in Schizosaccharomycotina and Saccharomycotina and two to six groups in Ustilaginomycotina (Figure 4).

The *Saccharomyces* genome database contains 10 HD entries, including four mating type genes (Cherry et al. 2012; Engel et al. 2014). Among these are the *HML* and *HMR* involved in mating type switching that are not expressed. Other genes include *ste12*, involved in invasive growth and mating (Bardwell et al. 1998), and *pho2*, a transcriptional activator of *pho5*, an acid phosphatase (Liu et al. 2000). Finally, it contains two sets of paralogous genes, *yox1*, *yph1*, *tos8* and *cup9*. The former two play a role in cell cycling, repressing early cell-cycle boxes (Horak et al. 2002; Pramila et al. 2002), while *tos8* and *cup9* have diversified in different roles. Gene *tos8* promotes meiosis and polarized growth (Horak et al. 2002), while *cup9* reduces epigenetic modifications during heat shock and prevents copper toxicity (Knight et al. 1994). In the ascomycete yeast *C. albicans*, which can also grow hyphae (Sudbery 2011), *grf10*, a *pho2* ortholog, is important in hyphal growth, with Δ *grf10* strains exhibiting reduced hyphal growth and attenuated virulence (Ghosh et al. 2015). Similar effects have been observed for HD proteins in *C. neoformans*, although they are part of the mating type locus, and therefore are also considered to play additional roles in development through sexual selection (Loftus et al. 2005; Mead et al. 2015). Nevertheless, it shows how closely related the functions of HD TFs can be regardless of evolutionary distance.

Table 1. Annotation of the groups of HD TFs identified in Figure 3 and Figure 4. More details can be found in Supplementary Table 1 and Supplementary Text 1.

Group	Known proteins	Known functions (inferred from known proteins)	Present in	Type	Gene count	Clustered genes (% of total genes in cluster)
1	<i>hom1</i> (<i>S. commune</i> , 257652); <i>hdp1</i> (<i>U. maydis</i> , 5762)	Vegetative growth, filamentous growth	Early diverging fungi; Basidiomycota	Non-TALE	208	3.8
2	<i>yph1/yox1</i> (<i>S. cerevisiae</i> , YDR451C, YML027W); <i>yox1</i> (<i>C. albicans</i> , CaO19.7017.1); <i>pah4</i> (<i>P. anserina</i> , 254); <i>mohox6</i> (<i>M. grisea</i> , 113426)	Cell cycle, filamentous growth	Ascomycota	Non-TALE	123	0
3	<i>hom2</i> (<i>S. commune</i> , 257987); <i>pah2</i> (<i>P. anserina</i> , 3203); <i>mohox5</i> (<i>M. grisea</i> , 114780)	Fructification, perithecia neck	Early diverging fungi; Pezizomycotina; Basidiomycota	Non-TALE	219	0
4	<i>hdp2</i> (<i>U. maydis</i> , 4928)	Pathogenicity	Early diverging fungi; Agaricomycotina	Non-TALE	118	0.8
5	<i>Pho2</i> (<i>S. cerevisiae</i> , YDL106C); <i>Gfr10</i> (<i>C. abicans</i> , CaO19.4000.1); <i>Pah1/3</i> (<i>P. anserina</i> , 3360, 1279); <i>kal1</i> (<i>N. crassa</i> , 7166); <i>mohox1/2</i> (<i>M. grisea</i> , 116399, 116067)	Phosphate metabolism, filamentous growth, conidiation	Mucoromycotina; Ascomycota	Non-TALE	209	3.3
6		Unknown	Agaricomycetes	Non-TALE	35	8.6
7	<i>mata2/alpha2</i> (<i>S. cerevisiae</i> , YCL067C, YCR039C, YCR096C)	Mating in Saccharomyces	Saccharomyces; Basidiomycetes (excluding Ustilaginomycetes and Wallemiomycetes); Dothideomycetes	Non-TALE	127	14.2
8		Unknown	Agaricomycetes	Non-TALE	306	11.8
9	HD2 Genes	Mating in Basidiomycota	Basidiomycota (excluding Tremellomycetes and Pucciniomycetes)	Non-TALE	87	83.9
10	<i>pah6</i> (<i>P. anserina</i> , 4696); <i>mohox3</i> (<i>M. Grisea</i> , 119837)	Unknown	Pezizomycotina	Mixed	175	4
11	HD1 genes	Mating in Basidiomycota	Basidiomycota (excluding Ustilaginomycetes and Pucciniomycotina); Dothideomycetes	TALE	106	67.9
12	<i>Tos8/cup9</i> (<i>S. cerevisiae</i> , YGL096W, YPL177C); <i>cup9</i> (<i>C. albicans</i> , CaO19.6514.1); <i>pah5</i> (<i>P. anserina</i> , 10096); <i>kal1</i> (<i>N. crassa</i> , 4379); <i>mohox7</i> (<i>M. grisea</i> , 111842)	Meiosis, DNA damage, homeostasis, perithecia neck, pathogenicity	Early diverging fungi; Ascomycota (excluding Schizosaccharomycotina and Dothideomycetes); Basidiomycota (excluding Tremellomycetes)	Mixed	229	10.5

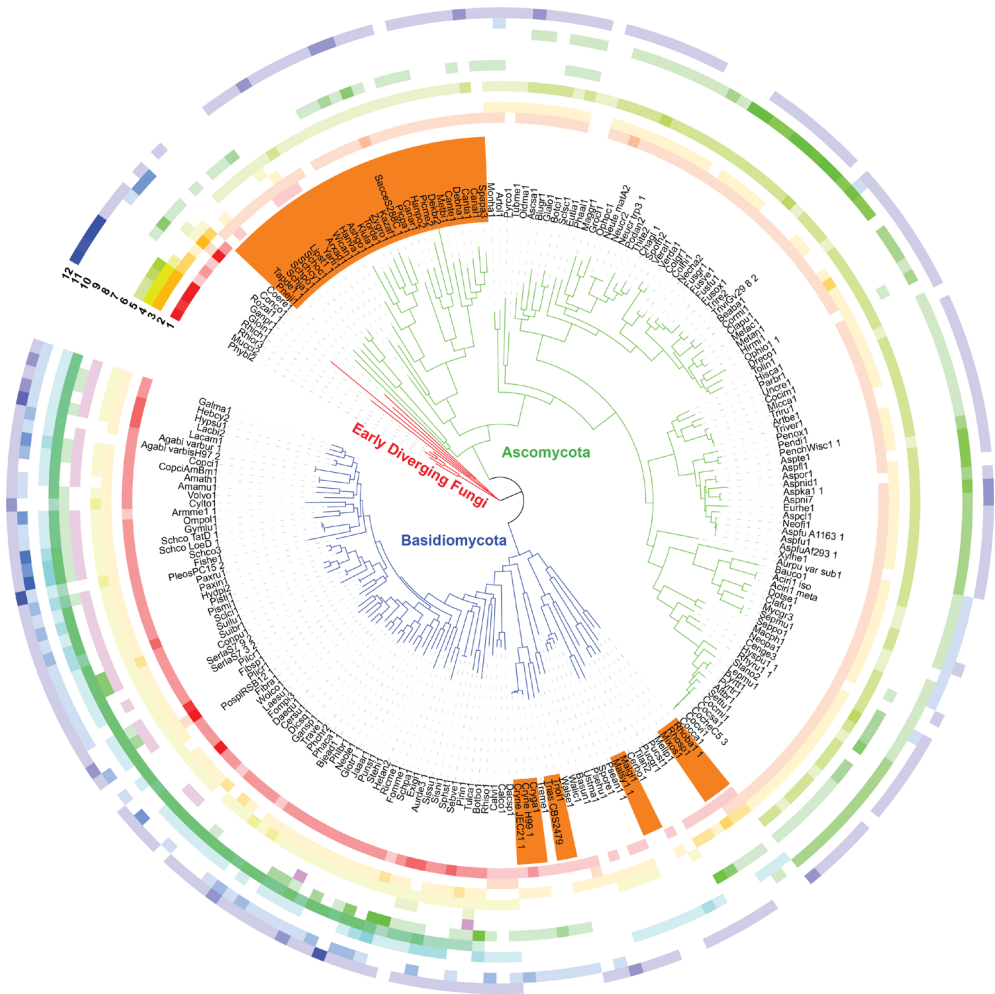


Figure 4. Species tree of 222 fungi reconstructed from 57 highly conserved proteins. Subtree color indicates early diverging Fungi (red), Ascomycota (green) and Basidiomycota (blue). Species names in orange have a (mostly) unicellular lifestyle. The heat maps around the tree indicate the number of HD TFs in each of the groups identified in Figure 3. Group 1 is the innermost ring and group 12 is the outermost ring. The heat map gradient colors range from white for no HD TFs for that species to five (or more) for the maximum color. An annotation of known genes, functions and conservation for each group is given in Table 1. Species names are abbreviated and more detail can be found in Supplementary Table 1. The branch length of *Hanseniaspora valbyensis* (Hanva1_1) is not drawn to scale. The online tree editor iTOL v3 was used for annotation and visualization (Letunic and Bork 2016).

Saccharomycotina lack domains related to *pah2* and *pah6* in the filamentous fungus *P. anserina* (groups 3 and 10 in Figure 4, respectively). Gene *pah2* is implicated in perithecium formation and is related to *hom2* in *S. commune*, which is crucial for fructification, so an absence of these groups in yeasts is not unexpected. The function of *pah6* is currently unknown and the lack of homologs in yeasts may indicate a role in multicellularity, although no phenotype was identified in Δ *pah6* strains (Coppin et al. 2012).

Basidiomycete yeasts notably lack a group conserved in Agaricomycotina (group 8, Figure 4), making these HD genes candidates for regulators of the complex development found in Agaricomycotina (*S. commune* protein IDs: 2565648, 2613044, 2693949). However, neither shows differential expression in *S. commune* and *C. cinerea* orthologs are down-regulated during late stages of fructification (Muraguchi et al. 2015; Pelkmans et al. 2017).

Multicellular ascomycetes have HD genes in four to six groups, while the Agaricomycotina (multicellular basidiomycetes) carry three to ten groups. However, in the latter clade this number varies widely from three to five groups in Tremellales to five to ten groups in Agaricales. Pezizomycotina generally lack HD2 mating genes, Saccharomycotina mating genes and three Basidiomycete-specific HD TF groups. Agaricomycotina lack Saccharomycotina mating genes, and two Ascomycota HD TF groups. Furthermore, the HD domain of *hom2* of *S. commune* is related to *pah2* in *P. anserina*, which is involved in formation of the perithecium neck (Ohm et al. 2011; Coppin et al. 2012). This suggests that there is overlap in the regulatory pathways involved in ascocarp and basidiocarp formation.

In the early diverging Mucoromycotina considerable gene duplication occurred, with HD gene counts ranging from 23 to 51 (Figure 1), which is higher than any other subphylum. However, this expansion is confined to five groups of HD genes (Figure 4). Whole genome duplication has previously been shown in early Mucoromycotina evolution (Ma et al. 2009; Corrochano et al. 2016), but it is currently unknown why the gene count expanded so dramatically.

Conclusions and outlook

Recent sequencing efforts have resulted in large numbers of genomes across the fungal tree of life. As a result, the repertoire of HD TFs can be easily predicted for each of these fungi. Many of these HD TFs play important roles during development in the kingdom Fungi. They are (arguably) best known for their role in mating and subsequent development in both Ascomycota and Basidiomycota. Other HD TFs are involved in regulating fruiting body development in several model systems. Not all HD TFs are involved in multicellular development, however, as exemplified by their presence in yeasts, albeit in lower numbers. The function of the vast majority of HD genes is currently unknown and this is especially the case for the large expansion of HD genes in early diverging fungi.

Further functional characterization is essential to identify the full role and regulatory network of HD TFs. This is hampered by a lack of available molecular tools in many fungi, including protocols for deleting genes. The relatively recent development of CRISPR/Cas9 protocols in several ascomycetes and basidiomycetes may facilitate a more high-throughput approach (Nødvig et al. 2015; Pohl et al. 2016; Ryan et al. 2016; Qin et al. 2017; Sugano et al. 2017).

Regulatory networks involving HD TFs can be elucidated using RNA-Seq and ChIP-Seq. While the former is relatively straightforward with the advent of next generation sequencing techniques, the latter is much more laborious. To our knowledge, no direct targets of HD TFs have been identified in any fungus, which would be an important next step to further elucidate the regulatory network. Moreover, only limited data exists on post-translational modification of HD TFs and their effect on development. The advent of these (and other)

molecular tools may soon improve our knowledge of genetic regulation of development in fungi and this review emphasizes HD genes as important targets.

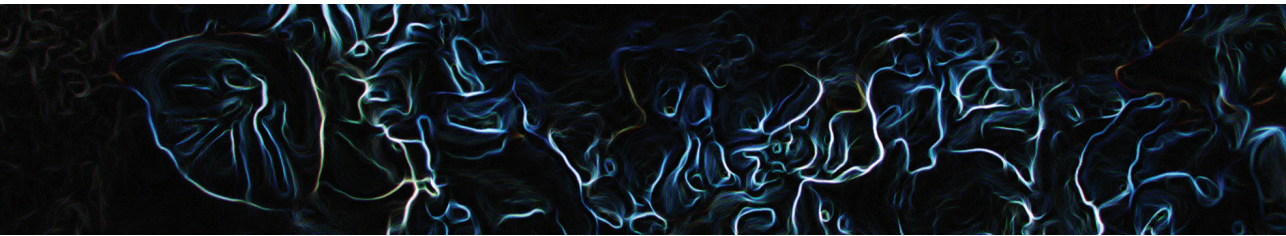
Acknowledgements

This project has received funding from the European Research Council (ERC) under the European Union's Horizon 2020 research and innovation programme (grant agreement number 716123)

Supplementary data

All supplementary data is available at <https://www.sciencedirect.com./science/article/pii/S1749461317300763#appsec1>





High-throughput targeted gene deletion in the model mushroom *Schizophyllum commune* using pre-assembled Cas9 ribonucleoproteins.

Peter Jan Vonk, Natalia Escobar, Han A. B. Wösten, Luis G. Lugones, Robin A. Ohm

This chapter is based on Vonk, P. J. Escobar, N. Wösten, H. A. B. Lugones, L. G. & Ohm, R. A. (2019). High-throughput targeted gene deletion in the model mushroom *Schizophyllum commune* using pre-assembled Cas9 ribonucleoproteins. *Scientific Reports*, 9(1), 1-8.
<https://doi.org/10.1038/s41598-019-44133-2>

Abstract

Efficient gene deletion methods are essential for the high-throughput study of gene function. Compared to most ascomycete model systems, gene deletion is more laborious in mushroom-forming basidiomycetes due to the relatively low incidence of homologous recombination (HR) and relatively high incidence of non-homologous end-joining (NHEJ). Here, we describe the use of pre-assembled Cas9-sgRNA ribonucleoproteins (RNPs) to efficiently delete the homeodomain transcription factor gene *hom2* in the mushroom-forming basidiomycete *Schizophyllum commune* by replacing it with a selectable marker. All components (Cas9 protein, sgRNA, and repair template with selectable marker) were supplied to wild-type protoplasts by PEG-mediated transformation, abolishing the need to optimize the expression of *cas9* and sgRNAs. A $\Delta ku80$ background further increased the efficiency of gene deletion. A repair template with homology arms of 250 bp was sufficient to efficiently induce homologous recombination. This is the first report of the use of pre-assembled Cas9 RNPs in a mushroom-forming basidiomycete and this approach may also improve the genetic accessibility of non-model species.

Introduction

Mushrooms are a nutritious food source that can be cultivated on waste streams, making them important for sustainable food production (Grimm and Wösten 2018). Furthermore, they can produce pharmacological compounds, lignocellulolytic enzymes and have potential as cell factories (de Mattos-Shiple et al. 2016). Their total economic value is estimated at 63 billion USD (Royse et al. 2017). However, the biological mechanisms underlying mushroom formation are poorly understood, primarily due to a lack of efficient genetic tools, which are essential for a deep understanding of these developmental processes (Collins et al. 2010; Ohm et al. 2010b; 2011; Nakazawa et al. 2011; Kües and Navarro-González 2015; Pelkmans et al. 2017). Next-generation sequencing has yielded a vast amount of genome and expression data, but there is a relative lack of functional characterization of gene function in mushroom-forming fungi (Ohm et al. 2010a; Stajich et al. 2010; Morin et al. 2012; Grigoriev et al. 2014; Nagy et al. 2018).

The basidiomycete *Schizophyllum commune* is a model organism for mushroom formation. It completes its lifecycle in the lab in ten days and many genomic and genetic tools are available (de Jong et al. 2010; Ohm et al. 2010a; Pelkmans et al. 2017). Targeted gene deletion has succeeded in four mushroom-forming species to date (Ohm et al. 2010b; Nakazawa et al. 2011; Salame et al. 2012; Qin et al. 2017) and the majority were made in *S. commune*, although even in this organism only 23 gene deletions have been reported (Robertson et al. 1996; Horton et al. 1999; Lengeler and Kothe 1999a; 1999b; Lugones et al. 2004; Schubert et al. 2006; van Wetter et al. 2006; de Jong et al. 2010; Ohm et al. 2010b; 2011; van Peer et al. 2010; Knabe et al. 2013; Pelkmans et al. 2017). The main bottleneck in gene deletion in mushroom-forming fungi is the relatively low incidence of homologous recombination (HR) and relatively high incidence of non-homologous end-joining (NHEJ) (Ohm et al. 2010b). This results in the frequent ectopic integration of plasmids, instead of the desired targeted gene deletion, necessitating the laborious screening of hundreds of transformants to identify a correct gene deletion. This procedure was improved by the development of a $\Delta ku80$ strain in which the incidence of NHEJ is considerably reduced (de Jong et al. 2010), resulting in fewer transformants with an ectopic integration (and therefore fewer colonies to screen). However, the incidence of HR is not markedly increased, which means that the absolute number of transformants with a correct gene deletion does not increase. Therefore, gene deletion in mushroom-forming fungi remains a labor-intensive process. More efficient and high-throughput methods for gene deletion are required to keep up with the genomic data produced.

CRISPR-Cas9 is a powerful genetic tool greatly enhancing the efficiency of genome editing in a large number of species (Jinek et al. 2012). This endonuclease can be programmed by a ~100 bp single guide RNA (sgRNA) to target DNA based on a 20 bp homology sequence, enhancing recombination rates to facilitate insertions, deletions and replacement at the targeted site (Jinek et al. 2012). Currently, the system is primarily used with a plasmid encoding the 4 kb *cas9* gene, an endogenous promoter, a nuclear localization signal and an endogenous terminator (Sugano et al. 2017). The sgRNA can either be expressed using a RNA polymerase III promoter or transcribed *in vitro* and co-transformed into the target cell (Jinek et al. 2012; Hruscha et al. 2013). This method has been applied to several fungi, including the mushrooms *Coprinopsis cinerea* and *Ganoderma lucidum* (Qin et al. 2017; Sugano et al. 2017). However, this procedure requires extensive genetic knowledge of the



target species for codon-optimization, expression and sgRNA delivery. Moreover, methods that allow the efficient deletion of any gene (as opposed to a counter-selectable reporter gene) have not been reported in multicellular basidiomycetes.

An alternative to expressing the *cas9* gene and the sgRNA is to use pre-assembled ribonucleoprotein (RNP) complexes of Cas9 protein and *in vitro* transcribed sgRNAs (Gasiunas et al. 2012; Woo et al. 2015). In fungi this method has been applied to several yeasts and multicellular ascomycetes, including multiple *Aspergillus* species, *Penicillium chrysogenum* and *Cryptococcus neoformans* (Pohl et al. 2016; 2018; Wang et al. 2016; Grahl et al. 2017; Song et al. 2018).

Here, we describe the use of pre-assembled Cas9-sgRNA RNPs to delete the homeodomain transcription factor *hom2* in the basidiomycete *S. commune* with an unprecedented efficiency for mushroom-forming fungi. Although a $\Delta ku80$ background increases the efficiency of gene deletion, it is not required, which improves the genetic accessibility of non-model species. To our knowledge, this is the first report of the use of pre-assembled Cas9-sgRNA RNPs in a mushroom-forming basidiomycete.

Results

Cas9 RNPs are not sufficient for efficient gene disruption without a positive selection marker

The minimal form of gene inactivation using CRISPR-Cas9 is the introduction of errors by NHEJ-mediated repair after the introduction of a double-stranded break (Cong and Zhang 2015). We attempted this approach by disrupting a previously introduced nourseothricin resistance cassette in the genome of strain H4.8A $\Delta hom2$ (Ohm et al. 2011). Two sgRNAs targeting the first 100 bp of the nourseothricin resistance gene were designed and transcribed *in vitro*. The efficacy of these sgRNAs was confirmed by *in vitro* digestion of the nourseothricin gene. The sgRNAs were assembled with Cas9 and introduced in H4.8A $\Delta hom2$ protoplasts using PEG-mediated transformation. After regeneration, the protoplasts were plated on non-selective medium. The resulting colonies were tested for a loss of nourseothricin resistance, which would indicate a disruption of the nourseothricin resistance cassette by the RNPs. However, despite repeated attempts no nourseothricin sensitive colonies were identified among over 100 potential mutants, indicating a lack of gene-inactivating mutations. This means that the efficiency of the procedure is less than 1%, which strongly reduces its use in high-throughput gene deletion.

Co-transformation of Cas9 RNPs with a repair template greatly increases the rate of gene inactivation

Next, we determined whether Cas9-sgRNA RNPs were able to increase the rate of gene deletions when used in combination with a repair template containing a selection marker. We used the previously published *hom2* deletion vector, which is comprised of a nourseothricin antibiotic resistance cassette flanked by approximately 1200 bp flanks of the *hom2* locus (Figure 1). Furthermore, it contains a phleomycin antibiotic resistance cassette, allowing us to distinguish between the desired gene deletion by homologous recombination (nourseothricin resistant and phleomycin sensitive transformants) and the undesired ectopic integration of the full construct (nourseothricin and phleomycin resistant transformants). This approach was used previously to generate a single deletion

strain of the *hom2* gene that grows faster and is not capable of forming mushrooms as a homozygous dikaryon (Ohm et al. 2011). Two sgRNAs were designed that target the *hom2* gene 36 and 57 bp downstream of the translation start site, introducing double-stranded DNA breaks (Figure 1). The efficacy of the sgRNAs was confirmed by *in vitro* digestion of the *hom2* locus. Wild-type H4-8 protoplasts were transformed with the *hom2* deletion vector with or without Cas9-sgRNA RNP complexes. After regeneration, the protoplasts were plated on medium containing nourseothricin and the resulting colonies were screened for phleomycin resistance. Similar numbers of nourseothricin resistant and phleomycin sensitive transformants were found (Table S1). However, seven *hom2* gene deletions were observed with Cas9 RNPs as determined by PCR, while no gene deletions were observed without Cas9 in three replicate experiments (Figure 2; Table S1). Sequencing the genomic locus of these potential gene deletion mutants indeed showed replacement of the *hom2* gene with the nourseothricin resistance cassette in all cases (Figure 3). This indicates that the double-stranded DNA breaks introduced by the Cas9 RNPs increase the rate of gene deletion by homologous recombination. The phenotype of the homozygous dikaryotic *hom2* deletion strains was identical to that previously reported (Figure 4) (Ohm et al. 2011).

A $\Delta ku80$ background further improves gene deletion efficiency

Current gene deletion methods in Basidiomycota often rely on a $\Delta ku80$ background, which inactivates the NHEJ pathway and greatly reduces the number of transformants with ectopic integrations. Therefore, we attempted the same transformation method in *S. commune* $\Delta ku80$. As expected, few nourseothricin resistant transformants were observed without the addition of Cas9 RNPs and no confirmed gene deletions were identified (Figure 2; Table S1). In the $\Delta ku80$ strain co-transformed with Cas9 RNPs, a similar number of nourseothricin resistant transformants was observed as in the wild-type strain with Cas9 (Table S1). However, both the number of phleomycin sensitive transformants and the number of transformants with a confirmed gene deletion were significantly higher (Figure 2; Table S1), with a total of 30 confirmed gene deletions. Sequencing the genomic locus of 10 *hom2* deletion strains confirmed the expected deletion of the *hom2* gene and insertion of the nourseothricin resistance cassette (Figure 3). This indicates that using Cas9 RNPs in a $\Delta ku80$ background increases the rate of homologous recombination and results in a higher rate of gene deletion than in the wild type.

Homology arms of 250 bp are sufficient for consistent recruitment of homology-directed repair

Current gene deletion methods in mushroom-forming Basidiomycota generally rely on repair templates comprised of homology arms of approximately 1000 bp that flank a selectable marker. Indeed, the *hom2* deletion vector described above contains homology arms of 1190 and 1147 bp. We determined whether repair templates with shorter homology arms can also assist in gene deletion when used in combination with Cas9-sgRNA RNPs. To generate the repair templates, PCRs were performed on the *hom2* deletion vector resulting in linear double-stranded DNA fragments with reduced homology arm lengths of approximately 1000, 750, 500, 250 and 100 bp (Figure 1). In all cases deletion mutants were obtained, ranging from 3.6 deletion mutants per 2×10^7 protoplasts with 1000 bp homology arms to 0.3 deletion mutants with 100 bp homology arms (Table S2). For all flank lengths gene deletions were consistently observed in all replicas, except for 100 bp homology arms where only 1 gene deletion was identified after multiple attempts. This indicates that 250



bp of homology is sufficient to efficiently recruit homology-directed repair, resulting in a gene deletion.

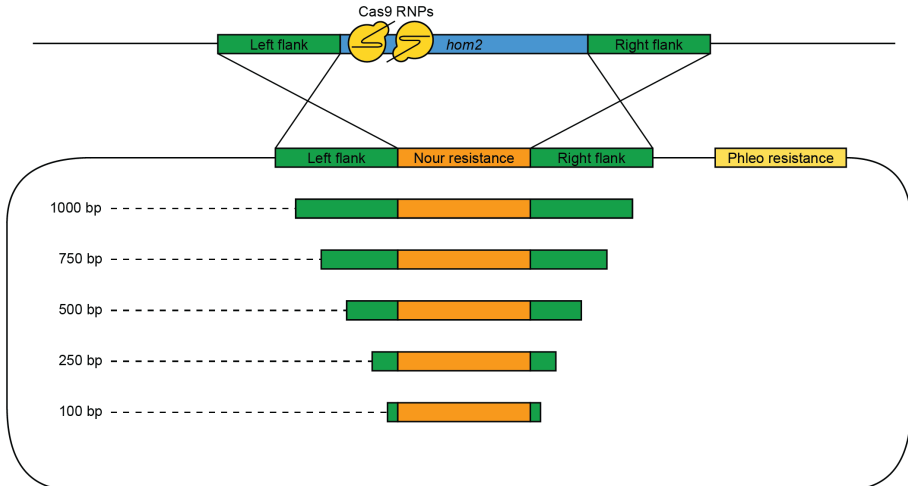


Figure 1. Schematic overview of the approach for targeted deletion of the *hom2* gene. Two single guide RNAs (sgRNAs) were designed that target the 5' region of the *hom2* gene. A circular deletion vector was used as a repair template, comprised of homology arms of approximately 1200 bp flanking a nourseothricin resistance cassette. It also contains a phleomycin resistance cassette that was used to distinguish between the desired gene deletion by homologous recombination (nourseothricin resistant and phleomycin sensitive transformants) and the undesired ectopic integration of the full construct (nourseothricin and phleomycin resistant transformants). Moreover, linear PCR products with shorter homology arms were used as repair template, as indicated. The Cas9 protein, sgRNAs and repair template were introduced into protoplasts by PEG-mediated transformation. All repair templates resulted in confirmed gene deletions.

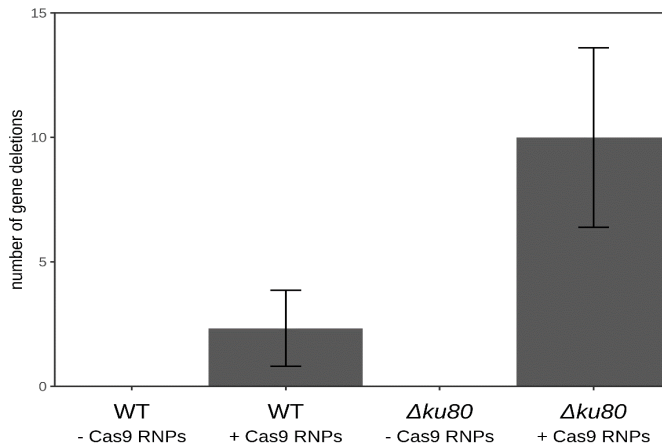


Figure 2. Average number of gene deletions across three replicates. Gene deletions were only obtained when Cas9 RNPs were used to induce double-stranded breaks. This worked in the wild type, but was more efficient in a $\Delta ku80$ background. Error bars indicate the standard deviation

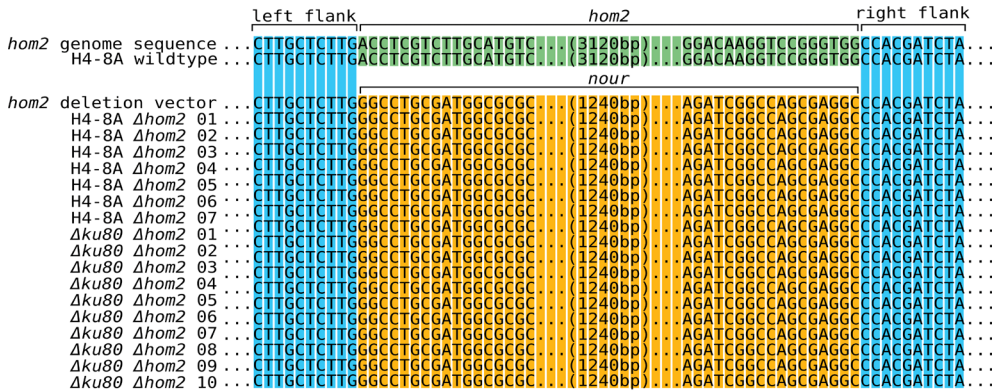


Figure 3. Sanger sequencing confirms the replacement of the *hom2* gene with the nourseothricin resistance cassette for 17 tested deletion strains. The sequence alignments between the left and right homology arms (shaded in blue) are partially shown. As expected, in the wild type the sequence between the homology arms corresponds to the wild-type *hom2* locus (shaded in green). In contrast, in the 17 deletion strains this sequence corresponds to the nourseothricin resistance cassette (shaded in orange) of the repair template, confirming that the *hom2* gene was replaced in these strains.

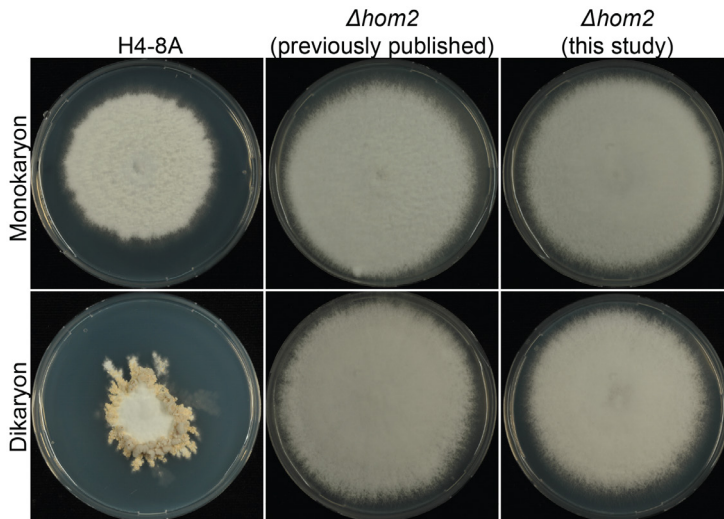


Figure 4. Phenotypes of the H4-8 reference strain (wild type), the previously published $\Delta hom2$ strain (Ohm et al. 2011) and a $\Delta hom2$ strain obtained in this study. The strains were grown as monokaryons and dikaryons (crossed with H4-8B $\Delta hom2$). There was no phenotypic difference between the previously published deletion strain and the one obtained in this study.

Discussion

Efficient gene deletion methods are essential for the high-throughput study of gene function. Here, we described a method based on a pre-assembled ribonucleoprotein (RNP) complex of Cas9 protein and *in vitro* transcribed short guide RNAs. This method was used to create a total of 65 deletion strains of the *hom2* gene by replacing it with a selectable marker. Moreover, we determined that homology arms of 250 bp are sufficient to efficiently

induce homologous recombination. This method yields considerably more gene deletion strains than our previously published methods (de Jong et al. 2010; Ohm et al. 2010b), in which usually only 1 correct deletion strain was obtained and only after repeated attempts.

Various efficient approaches of genome editing using CRISPR/Cas9 have been reported in the model fungus *Saccharomyces cerevisiae*. For example, *cas9* and sgRNAs may be expressed from a plasmid and cause genome edits with such high efficiency that the use of a selectable marker is not necessary (Mans et al. 2015). We have attempted this approach in *S. commune*, but were unsuccessful in producing strains with a targeted gene deletion (data not shown). Nor were we successful with *in vitro* produced Cas9 RNPs without the use of a selectable marker, since no strains with a gene deletion were identified among > 100 colonies. This suggests that the efficiency of the Cas9 RNP approach is much lower in *S. commune* (and possibly other mushroom-forming basidiomycetes) than in ascomycetes. This relatively low efficiency is also observed in *C. cinerea* (Sugano et al. 2017). In contrast, many correct gene deletion strains were obtained when we attempted to replace the target gene with a selectable marker. We hypothesize that the Cas9 RNPs cause double strand breaks in the target gene, after which the DNA repair machinery is recruited to the site and repairs the damage using the provided repair template. Although this is a relatively rare event, positive selection subsequently allows the identification of the (relatively small number of) correct transformants.

Current gene deletion methods in mushroom-forming basidiomycetes generally rely on templates comprised of homology arms of approximately 1000 bp that flank a selectable marker (Ohm et al. 2010b; Salame et al. 2012). The creation of this gene deletion template is currently a bottleneck in high throughput gene deletion, although recent approaches for the assembly of multiple DNA fragments (e.g. Gibson assembly) have considerably improved this (Gibson 2011). Our results show that homology arms as short as 250 bp can efficiently induce homologous recombination when used in combination with RNPs. This relatively short length of the template is well within the range of cost-effective chemical synthesis, which will further facilitate high-throughput gene deletion by allowing *in vitro* construction of this template.

The methods described in this study will remove several bottlenecks for efficient genome editing in non-model mushroom-forming fungi, as well as wild isolate strains of *S. commune*. Firstly, our approach works efficiently not only in a $\Delta ku80$ background, but also in the wild type. This will simplify the gene deletion procedure for non-model system species for which no $\Delta ku80$ strains are available. Secondly, the expression levels of *cas9* and the sgRNAs do not need to be optimized using organism-specific promoters, since both components are supplied externally. Previous studies have shown that the selection markers needed for the repair template are functional in other mushroom-forming fungi (Alves et al. 2004).

In addition to gene deletion, these techniques can be modified to produce other genome edits, including promoter replacement and targeted gene integration (knock-in). Recent efforts in genome and transcriptome sequencing of mushroom-forming species have resulted in a large number of candidate gene families involved in mushroom development and other processes (Grigoriev et al. 2014; Park et al. 2014; Zhang et al. 2015; Sipos et al. 2017; Nagy et al. 2018; Song et al. 2018; Vonk and Ohm 2018; Wu et al. 2018; Krizsán et

al. 2019; **Chapter 2**). The important addition of Cas9 RNP-mediated genome editing to the molecular toolkit of *S. commune* will facilitate the functional characterization of these gene families, leading to important new insights into the biology of this important group of fungi.

Materials & methods

Culture conditions and strains

S. commune was grown from a small agar inoculum in *Schizophyllum commune* minimal medium (SCMM) at 30 °C (van Peer et al. 2009). For solid culture, the medium was supplemented with 1.5% agar. All strains are derived from *S. commune* H4-8 (*matA43matB41*; FGSC 9210) (Ohm et al. 2010a; 2010b). Strain $\Delta ku80$ (de Jong et al. 2010) and strain $\Delta hom2$ (Ohm et al. 2011) were published previously. For selection on nourseothricin (Bio-Connect, Netherlands) or phleomycin (Bio-Connect, Netherlands), SCMM was supplemented with 15 $\mu\text{g ml}^{-1}$ and 25 $\mu\text{g ml}^{-1}$ antibiotic, respectively (Alves et al. 2004). For phenotypical characterization, strains were grown for 7 days at 25 °C in a 16/8 hours day/night cycle.

Cas9 expression and purification

pET-NLS-Cas9-6xHis was a gift from David Liu (Addgene plasmid # 62934; <http://n2t.net/addgene:62934> ; RRID:Addgene_62934) (Zuris et al. 2015) and contains a NLS-Cas9-6xhis fusion sequence under control of the T7 promotor. The plasmid was introduced into *Escherichia coli* BL21 Star (DE3) (Life Technologies, USA). The resulting expression strain was pre-grown for 16 hours in liquid culture at 37 °C in LB supplemented with 50 $\mu\text{g ml}^{-1}$ ampicillin. This pre-culture was diluted 1:100 in fresh LB with ampicillin and grown in liquid culture at 22.5 °C to an OD_{600} of 0.6. Cas9 expression was induced with IPTG at a final concentration of 0.4 mM and incubation was continued for an additional 18 hours. Cells were harvested by centrifugation and resuspended in 80 ml wash buffer (20 mM Tris-HCl pH 8.0, 30 mM imidazole, 500 mM NaCl) supplemented with 1 mM PMFS, 1 mM MgCl_2 and 6.25 U ml^{-1} Dnase I (ThermoFisher Scientific, USA). Cells were lysed three times with a French press (AMINCO, USA) at 500 psi on high setting in a pre-chilled cylinder (4 °C). After lysis, all steps were performed at 4 °C. The lysate was cleared of cellular debris by centrifugation for 30 minutes at 15,000 g. Per liter of culture, 8 ml of bed volume of Ni-NTA resin (Qiagen, Germany) was added and incubated for one hour with gentle agitation. Column purification was performed according to the manufacturer's recommendations and Cas9 was eluted in 24 ml wash buffer with 500 mM imidazole. The protein purity was assessed on SDS-PAGE with colloidal coomassie staining (Dyballa and Metzger 2009) and protein yield was quantified by BCA-assay (ThermoFisher Scientific, USA). Imidazole and salts were removed by three washing steps with 21 ml dialysis buffer (20 mM Tris-HCl pH 8.0, 200 mM KCl, 10 mM MgCl_2) on Amicon 30 kDa filters (Merck Millipore, USA). Cas9 protein was diluted to 10 mg ml^{-1} in dialysis buffer, frozen in liquid nitrogen and stored at -80 °C until use.

Design and synthesis of gene-specific sgRNAs for gene disruption

Candidate protospacers (including PAM site) were identified in the coding region of the nourseothricin resistance cassette (van Peer et al. 2009) and *hom2* (protein ID 257987 in version Schco3 of the genome of *S. commune* (Ohm et al. 2010a)) with Cctop (Stemmer et al. 2015) and checked against the full genome to identify potential off-target regions (defined here as regions with fewer than 5 bp differences with the actual target region as identified by Bowtie2 (Langmead and Salzberg 2012)). Two sgRNAs were selected per gene based on fewest off-targets and the presence of one or more guanines at the start of the sgRNA



as this promotes a high yield of *in vitro* T7 transcription. For the nourseothricin resistance gene, sgRNA 1 and 2 were located 57 and 22 bp downstream of the translation start site, respectively, and for *hom2*, sgRNA 1 and 2 were located 57 and 36 bp downstream of the translation start site of *hom2*, respectively (Figure 1). Oligos were designed (p1_sgRNA and p2_sgRNA; Table 1) and the sgRNAs were synthesized *in vitro* according to the specifications of the GeneArt Precision sgRNA Synthesis Kit (ThermoFisher Scientific, USA).

***In vitro* Cas9 digestion assay**

The efficacy of the RNPs was tested by an *in vitro* digestion of a template containing the target regions. For the nourseothricin resistance cassette, the resistance gene was cut from the pDELcas deletion vector (Ohm et al. 2010b) with EcoRI, resulting in a 3759 bp fragment. *In vitro* digestion by the Cas9 sgRNA RNPs results in two fragments of 2719 bp and 1040 bp for sgRNA 1 and 2684 bp and 1075 bp for sgRNA 2. The template for *hom2* was generated by PCR with primers annealing to the promoter and terminator region of *hom2* (hom2_250_fw and hom2_250_rv). This resulted in a 3656 bp fragment that can be digested by Cas9 with either sgRNA to two fragments of 433 bp and 3223 bp for sgRNA 1 and 412 bp and 3244 bp for sgRNA 2. For digestion, 1 µg of Cas9, 200 ng sgRNA (which is approximately a 1:1 molar ratio) and 1x Cas9 reaction buffer (20 mM HEPES pH 6.5, 100 mM NaCl, 5 mM MgCl₂, 0.1 mM EDTA) were mixed in 25 µl final volume and assembled at 37 °C for 10 minutes. After assembly, 500 ng of template (100 ng µl⁻¹) was added to a final volume of 30 µl and the sample was incubated at 37 °C for 15 minutes. Cas9 was degraded by the addition of 1 U Proteinase K (ThermoFisher Scientific, USA) and incubated at room temperature for 15 minutes, after which DNA digestion was verified on agarose gel.

Design of the repair templates for homologous recombination

The previously described *hom2* deletion vector was used as a template for homologous recombination (Ohm et al. 2011). This plasmid contains a nourseothricin resistance cassette flanked by 1200 bp homology arms outside *hom2*. Moreover, the plasmid harbors a phleomycin resistance cassette that is only integrated if the plasmid integrates through a single cross-over (i.e. ectopically). Linear templates with reduced homology arm lengths (approximately 1000 bp, 750 bp, 500 bp, 250 bp and 100 bp) were made by PCR on the full vector. The primers were designed to bind 1000 bp (hom2_1000_fw and hom2_1000_rv; Table 1), 750 bp (hom2_750_fw and hom2_750_rv; Table 1), 500 bp (hom2_500_fw and hom2_500_rv; Table 1), 250 bp (hom2_250_fw and hom2_250_rv; Table 1) and 100 bp (hom2_100_fw, hom2_100_rv; Table 1) outside of the nourseothricin resistance cassette (Figure 1).

Transformation of S. commune

Protoplasts were prepared as previously described and stored at -80 °C until use (van Peer et al. 2009). 20 µg Cas9 was mixed with the two sgRNAs (2 µg of each sgRNA) targeting the gene of interest (resulting in a 2:1:1 molar ratio of Cas9, sgRNA 1 and sgRNA 2) and 1x Cas9 buffer (20 mM HEPES, 100 mM NaCl, 5 mM MgCl₂, 0.1 mM EDTA, pH 6.5). In the negative controls, Cas9 was replaced with dialysis buffer and sgRNA with MilliQ water. Cas9 and sgRNAs were pre-assembled for 10 minutes at 37 °C. In the case of the nourseothricin gene inactivation, 4 x 10³ protoplasts in 200 µl were added. Subsequent transformation was performed as previously described, but without selection (Ohm et al. 2011). The regenerated protoplasts were plated on non-selective medium and grown for two days. In

the case of *hom2* deletions, the number of protoplasts was changed to 2×10^7 in 200 μ l and 12.5 μ g repair template was added. The regenerated protoplasts were plated on medium supplemented with nourseothricin and grown for 3 days. Next, 48 colonies were randomly selected per transformation after three days and transferred to fresh selection media for a second round of selection. In the case of transformation with a full *hom2* deletion plasmid, nourseothricin-resistant colonies were then transferred to phleomycin selection medium and their resistance was scored. DNA was isolated from agar plugs by microwaving samples for 120 seconds in 50 μ l TE buffer (10 mM Tris pH 8.0, 1 mM EDTA) from candidates that were resistant to nourseothricin and sensitive to phleomycin for PCR verification with primers before the upstream homology arm (*hom2_ChkA*; Table 1) and after the downstream homology arm (*hom2_ChkD*; Table 1) (Ohm et al. 2011; Izumitsu et al. 2012). The size of the DNA band was used to determine whether the gene of interest was replaced with the nourseothricin resistance cassette. Primers *hom2_100_fw* and *hom2_100_rv* (Table 1) were used to sequence the PCR fragment to confirm the correct integration.

Table 1. Primers used in this study

Name	Sequence 5'-3'
<i>p1_sgRNA_nour_1</i>	TAATACGACTCACTATAGGGGTACCGCACCAGTGTCCCG
<i>p2_sgRNA_nour_1</i>	TTCTAGCTCTAAAACCGGGACACTGGTGCGGTACC
<i>p1_sgRNA_nour_2</i>	TAATACGACTCACTATAGGTAAGCCGTGTCGTCAAGAG
<i>p2_sgRNA_nour_2</i>	TTCTAGCTCTAAAACCTCTTGACGACACGGCTTAC
<i>p1_sgRNA_hom2_1</i>	TAATACGACTCACTATAGGGGACCTGTTGCGGATGCGC
<i>p2_sgRNA_hom2_1</i>	TTCTAGCTCTAAAACGCGCATCCGCAACAGGTCCC
<i>p1_sgRNA_hom2_2</i>	TAATACGACTCACTATAGGGGCTGGGAAAGAGCGTGGGT
<i>p2_sgRNA_hom2_2</i>	TTCTAGCTCTAAAACACCCACGCTCTTTCCAGCC
<i>hom2_1000_fw</i>	AGGCCTCAGAGGTAGAGAAGC
<i>hom2_1000_rv</i>	GTACCCCACTGTACCGCCTA
<i>hom2_750_fw</i>	TGTGCGGCGCATCATATC
<i>hom2_750_rv</i>	TCGCTGCTGCATACAGTTTA
<i>hom2_500_fw</i>	CGGATAGGTGCATGGAAGTT
<i>hom2_500_rv</i>	CACCTCTCGCTTATCGGAAG
<i>hom2_250_fw</i>	GCGAAAAGACCGGACTCG
<i>hom2_250_rv</i>	ATCCTAGGAAGCCGGAAGC
<i>hom2_100_fw</i>	ATCGAAGTGAATCGGGAAC
<i>hom2_100_rv</i>	TCGGGCTGCTACTACTGT
<i>hom2_ChkA</i>	AAGAGCCCCATGTTCAAG
<i>hom2_ChkD</i>	CGCGGATAGCAGTTTATCG

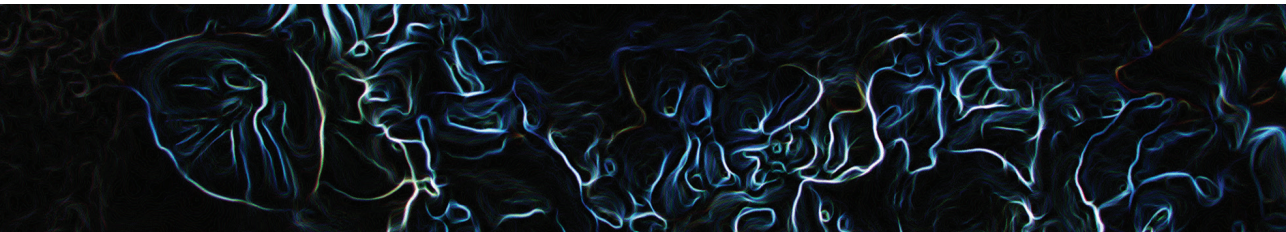
Acknowledgements

This project has received funding from the European Research Council (ERC) under the European Union's Horizon 2020 research and innovation programme (grant agreement number 716132).

Supplementary data

All supplementary data is available at <https://www.nature.com/articles/s41598-019-44133-2#Sec15>





H3K4me2 ChIP-Seq reveals the epigenetic landscape during mushroom formation and novel developmental regulators of *Schizophyllum commune*

Peter Jan Vonk, Robin A. Ohm

This chapter is based on Vonk, P. J. & Ohm, R. A. (2021). H3K4me2 ChIP-Seq reveals the epigenetic landscape during mushroom formation and novel developmental regulators of *Schizophyllum commune*. *Scientific Reports*, 11(1), 1-15. <https://doi.org/10.1038/s41598-021-87635-8>

Abstract

Mushroom formation represents the most complex multicellular development in fungi. In the model mushroom *Schizophyllum commune*, comparative genomics and transcriptomics have previously resulted in a regulatory model of mushroom development. However, little is known about the role of epigenetic regulation. We used chromatin immunoprecipitation sequencing (ChIP-Seq) to determine the distribution of dimethylation of lysine 4 on histone H3 (H3K4me2), a mark for transcriptionally active genes, during monokaryotic and dikaryotic development. We identified a total of 6032 and 5889 sites during monokaryotic and dikaryotic development, respectively. The sites were strongly enriched near translation initiation sites of genes. Although the overall epigenetic landscape was similar between both conditions, we identified 837 sites of differential enrichment during monokaryotic or dikaryotic development, associated with 965 genes. Six transcription factor genes were enriched in H3K4me2 during dikaryotic development, indicating that these are epigenetically regulated during development. Deletion of two of these genes (*fst1* and *zfc7*) resulted in arrested development of fruiting bodies, resulting in immature mushrooms. Together these results indicate that H3K4me2 ChIP-Seq is a powerful new tool to map the restructuring of the epigenetic landscape during mushroom development. Moreover, it can be used to identify novel developmental regulators.

Introduction

Mushroom fruiting bodies are the sexual structures of basidiomycete fungi and produce sexual spores for reproduction (Kües and Liu 2000). Mushrooms are a nutritious food source, produce pharmacological compounds and express a vast array of lignocellulolytic enzymes (de Mattos-Shiple et al. 2016). Their development is regulated by a complex, but largely unknown, developmental program (Kothe 2001; Ohm et al. 2011; 2013; Pelkmans et al. 2017; Vonk and Ohm 2018; **Chapter 2**). Comparative genomics and transcriptomics have recently revealed many genetic elements related to mushroom development, creating a regulatory model of this process (Plaza et al. 2014; Muraguchi et al. 2015; Pelkmans et al. 2017; Wu et al. 2018; Zhang et al. 2018; Almási et al. 2019; Krizsán et al. 2019). However, these methods do not provide a complete overview of the restructuring of chromatin during mushroom development.

During development, the chromatin in eukaryotic genomes is generally heavily restructured to modulate gene expression by making regions of the genome either more or less accessible and by the recruitment of regulatory proteins (Klemm et al. 2019). This process is partially facilitated by modifications on the protruding tails of the histones that form the nucleosomes. These modifications can change the chemical attraction between the tail and DNA and recruit regulatory proteins to the site of modification (Fischle et al. 2003; Bannister and Kouzarides 2011). There is a wide variety of histone modifications, including methylation, acetylation, ubiquitination and phosphorylation (Fischle et al. 2003; Bannister and Kouzarides 2011; Zhao and Garcia 2015). Among the best studied are lysine methylations of the N-terminal tail of histone H3. Methylation of the lysine 4 of histone H3 can occur as mono- (H3K4me1), di- (H3K4me2) or trimethylation (H3K4me3) and is strongly associated with transcription start sites (TSS). Therefore, H3K4 methylation is considered a reliable marker of transcription start sites (Barski et al. 2007), although the exact distribution of mono-, di- and trimethylation around active genes can vary (Orford et al. 2008; Pekowska et al. 2010).

Histones and their epigenetic modifications are highly conserved due to their essential role in eukaryotes (Waterborg 2012). Indeed, antibodies against histone modifications are often shown or predicted to recognize the same modification across many species and even kingdoms, including fungi. However, data on histone modification recognition by antibodies is limited to ascomycetes, including *Saccharomyces cerevisiae*, *Schizosaccharomyces pombe*, *Neurospora crassa*, *Fusarium graminearum* and *Zyoseptoria tritici* (Smith et al. 2011; Maltby et al. 2012; Connolly et al. 2013; Allshire and Ekwall 2015; Schotanus et al. 2015; Soyer et al. 2015). Furthermore, not all histone modifications are present in all fungal clades (Freitag 2017). For example, H3K27 methylation is lost in multiple ascomycete species, including species within the Taprinomycotina, Saccharomycotina, Eurotiomycetes and in the basidiomycete *Ustilago maydis* (Brosch et al. 2008; Veerappan et al. 2008). In Agaricales, the presence of all H3K methyltransferases of these marks is predicted in *Coprinopsis cinerea* (Freitag 2017).

Histone ChIP-Seq (chromatin immunoprecipitation followed by sequencing) is a powerful technique to map the locations of histone modifications across the genome (Johnson et al. 2007; Soyer et al. 2015). With this technique, antibodies against a specific histone modification are used to selectively pull-down fragmented chromatin enriched with the



histone modification of interest. Next, the DNA is extracted from the chromatin, sequenced, and aligned to the reference genome. This reveals the differential enrichment of the histone modification across the genome and, by extension, the genetic accessibility of genomic regions during development.

Schizophyllum commune is a basidiomycete model organism for mushroom development. It has a short, well-defined lifecycle of ten days in the lab and is genetically accessible (de Jong et al. 2010; Ohm et al. 2010b; Pelkmans et al. 2017). Recently, the efficiency of gene deletion was greatly increased with the use of CRISPR-Cas9, enabling more in-depth study of gene function (Vonk et al. 2019; **Chapter 3**).

Here, we developed a method for histone ChIP-Seq in the model mushroom *S. commune* and mapped the distribution of H3K4me2 in the genome during monokaryotic and dikaryotic development. We chose H3K4me2, which is enriched downstream of the TSS of active genes (Pekowska et al. 2010). By assessing the differential enrichment of H3K4me2 between monokaryotic and dikaryotic colonies, we were able to identify potential regulators of mushroom development. We confirmed the role of the transcription factor (TF) genes *fst1* and *zfc7* by gene deletion. This study shows that histone ChIP-Seq is a powerful technique that can further elucidate the complex developmental process of mushroom formation. To our knowledge this is the first report of the use of ChIP-Seq in a mushroom-forming basidiomycete.

Results

Histone H3 conservation in Fungi

While the presence of H3K4, H3K9, H3K27 and H3K36 methylation is predicted in the Agaricales (Freitag 2017), it is currently not known if these are sufficiently conserved for recognition with commercially available mammal-derived antibodies. To assess the conservation of the amino acid sequence surrounding the methylation sites, we aligned the first 50 amino acid residues of histone H3 of several commonly studied species. The N-terminal tail is highly conserved across all the studied species, but immediately downstream of H3K27 there are the substitutions S28T and P30N and the insertion A29_P30insA (i.e., an A was inserted between the A at position 29 and the P at position 30, relative to the human histone H3 sequence.) that are unique to *S. commune* (Figure 1A). Similar changes are observed for the basidiomycete *C. cinerea*, but not for the ascomycetes *S. cerevisiae* and *Aspergillus niger*. This suggests that these changes are unique to basidiomycetes. Indeed, a larger data set of 49 fungal genomes showed variability surrounding H3K27 in basidiomycetes, but not in ascomycetes (Supplemental Figure 1).

A western blot confirmed that an antibody raised against human H3K4me2, but not H3K27me3, was able to detect histone H3 in *S. commune*, while both were able to detect histone H3 in a human protein extract (Figure 1B, Supplemental Figures 2 and 3). This strongly suggests that H3K4me2 is sufficiently conserved between mammals and *S. commune* for the antibody to be used in this fungus. However, this is not the case for H3K27me3, which suggests that either the modification is not present in *S. commune*, or an antibody raised against human H3K27me3 is unable to recognize the region due to significant mutations. Based on these results, we decided to use H3K4me2 to develop a ChIP-Seq protocol in *S. commune*.

Histone ChIP-Seq on H3K4me2 reveals restructuring of euchromatin during development

Chromatin immunoprecipitation sequencing was performed on biological duplicates of 4-day old monokaryotic (haploid) and dikaryotic (haploid) colonies grown at 30 °C in a 16/8 hour day/night cycle. The developmental stage of these cultures was (symmetric and homogenous) vegetative growth and the formation of secondary hyphal knots, respectively (Figure 2A,B). The transition from vegetative monokaryotic growth to secondary hyphal knots is an important stage in the developmental process of mushrooms.

The ChIP pull-down was performed with an anti-H3K4me2 antibody, and the resulting DNA was sequenced and aligned to the genome assembly (a detailed version of the protocol can be found in Supplementary Text 1). Between 9.6 million and 21.3 million (paired-end) 75 bp reads were obtained per sample (Table 1), resulting in an average coverage ranging from 18.7 to 41.6-fold. After removing low quality reads, unaligned reads and optical duplicates, between 9.0 and 19.4 million reads remained, with 6% to 12.5% reads discarded and a coverage ranging from 17.5 to 37.8-fold. The percentage of unaligned reads and optical duplicates was similar between samples and input controls. In general, the input controls (in which no immunoprecipitation was performed) displayed similar read coverage along the genome, whereas the immunoprecipitated samples were concentrated in peaks that represent the binding sites of histone 3 with dimethylation on lysine 4 (Figure 3A). As expected, within input controls and within ChIP-samples there was a high correlation (> 0.93), while the correlation between the input controls and the ChIP-samples was low (< 0.10) (Supplemental Figure 4).

Peaks were called for all samples with MACS2 (Feng et al. 2012), resulting in 6032 and 5889 significant peaks in the monokaryotic and dikaryotic colonies, respectively (Table 2). These peaks were distributed evenly across the genome (Figure 4A,B). The fraction of reads within peaks ranged from 0.85 to 0.9. These peaks tend to locate near the start of genes (Figure 3A). To analyze the location of the peaks with respect to the genes in more detail, each peak was associated with the closest gene (with a maximum of 3 kb from the translation initiation site (TIS)) The coverage depth of the reads was plotted with respect to the TIS of these genes (Figure 4C), showing an enrichment from about 375 bp upstream to 1500 bp downstream of the TIS. This pattern was almost identical in the monokaryon and dikaryon, with a Pearson correlation coefficient of > 0.99.

Next, the peaks between the two conditions were compared, since a difference in the peaks indicates a difference in binding affinity of histone 3 (and therefore the epigenetic regulation) of that locus. A differential peak analysis with DiffBind (Stark and Brown 2011) revealed a correlation of 0.95 and 0.97 within replicates for the monokaryotic and dikaryotic samples and a correlation of 0.79 to 0.81 between the conditions (Figure 4D). This indicates that most of the monokaryotic genome architecture associated with histone 3 methylation (H3K4me2) is maintained in the initial stages of dikaryotic mushroom development. A total of 837 peaks were identified that displayed a difference between the conditions, with 667 enriched in the monokaryotic colonies and 170 in the dikaryotic colonies (Table 2).



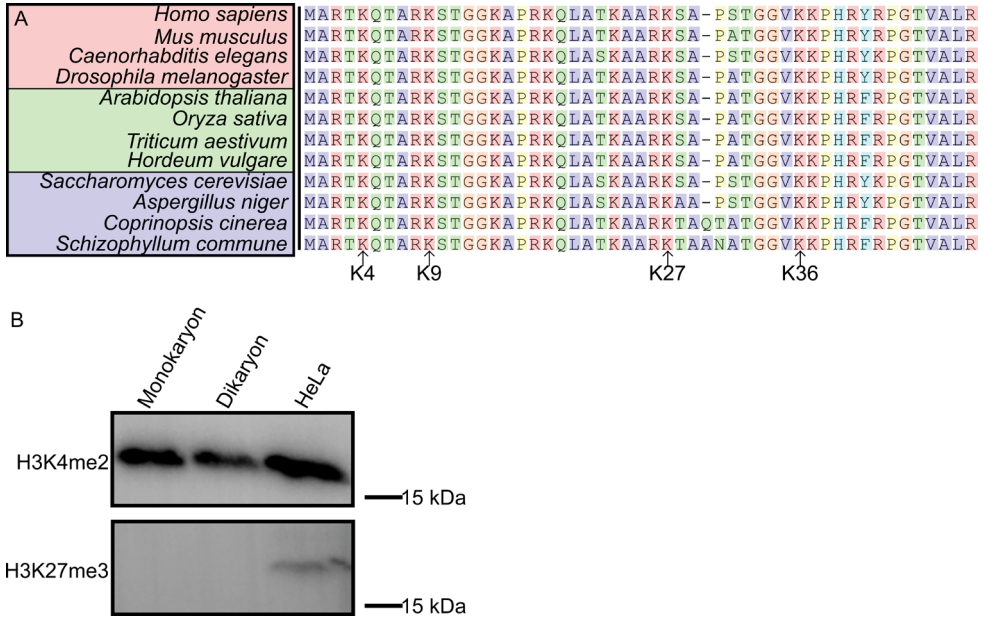


Figure 1. Recognition of methylation on histone H3 by mammalian anti-H3K4me2 and H3K27me3. A: Sequence alignment of the 50 N-terminal amino acids of histone H3 from 12 well-studied species across the kingdoms of animalia (red), plantae (green) and fungi (blue). The four primary lysine methylation sites are indicated. Amino acids are color-coded according to the Clustal X color scheme (Larkin et al. 2007). While the lysines K4, K9, K27 and K36 are conserved across all species, immediately downstream of K27 several substitutions and an insertion have occurred in the basidiomycete fungi (*C. cinerea* and *S. commune*). This is further confirmed in a larger data set of 57 species, including 49 fungi (Supplemental Figure 1). B: Western blot for H3K4me2 and H3K27me3 on a monokaryon and dikaryon of 88 hours old and HeLa whole cell lysate. The presence of the bands indicates that H3K4me2 can be detected by an antibody raised against human histone H3 with lysine 4 dimethylation, while H3K27me3 cannot be detected by an antibody raised against human histone H3 with lysine 27 trimethylation. The full-length blots of H3K4me2 and H3K27me3 are represented in Supplemental Figures 2 and 3, respectively.

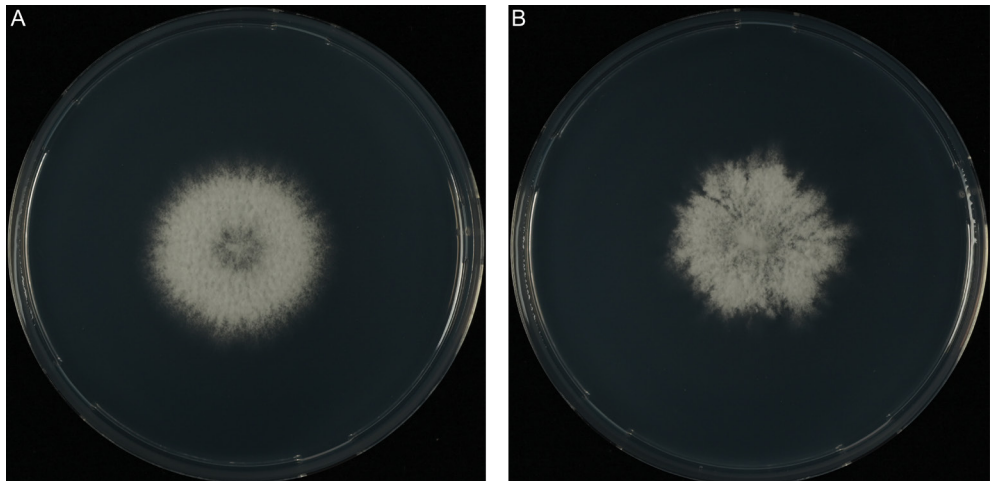


Figure 2. Monokaryotic (A) and dikaryotic (B) growth of *S. commune* H4-8 after 90 hours. The monokaryon grows symmetrically, while the dikaryon is asymmetric and develops hyphal aggregates (the first stage of mushroom development) at the edge of the colony.

Table 1. Sequencing read counts for the samples in this study. Masked reads are after filtering on paired-end aligned reads that are unique and not identified as optical duplicates.

Sample	Raw read count	Average sequencing depth (fold coverage)	Read count after filtering	Kept reads (%)	Average sequencing depth after filtering (fold coverage)
Monokaryon Control 1	13,832,046	26.9	12,104,966	87.5	23.4
Monokaryon Control 2	15,463,640	30.1	14,128,322	91.4	27.5
Dikaryon Control 1	21,339,686	41.6	19,391,294	90.9	37.8
Dikaryon Control 2	17,846,656	34.8	16,264,212	91.1	31.7
Monokaryon Sample 1	9,598,100	18.7	8,973,684	93.5	17.5
Monokaryon Sample 2	1,576,8176	30.7	14,078,416	89.3	27.4
Dikaryon Sample 1	1,454,0244	28.3	13,356,868	91.9	26.0
Dikaryon Sample 2	1,394,7854	27.2	13,115,136	94.0	25.5

These relatively enriched peaks in the monokaryon and dikaryon were associated with the gene(s) they presumably regulate. Based on the general pattern in Figure 4A, we associated a peak with a gene if it was between 375 bp upstream and 1500 bp downstream of the TIS. This resulted in 771 and 194 genes that were specifically enriched in the monokaryotic and dikaryotic developmental stages, respectively (Supplemental Table 1). A functional annotation enrichment analysis of these genes revealed an over-representation of the PFAM domains PF05920 (homeodomain (HD) TFs) and PF13476 (ATPase-related proteins) in genes near peaks that were specific for monokaryotic growth. PF05920-annotated genes are HD TFs and functional annotation revealed 5 of 6 genes were part of the *matA* mating type locus. However, due to the variation in mating type loci between compatible strains, this enrichment is likely an artefact of alignment to the reference genome, which only contains the mating type loci of *matA43* (Ohm et al. 2010a). Therefore, the mating type loci were excluded from the enrichment analysis. No PFAM domains were significantly enriched in the dikaryotic samples.

Table 2. Summary of peaks, differential peaks and associated genes for H3K4me2 ChIP during monokaryotic and dikaryotic development.

Condition	Peaks	Differential peaks	Peak-associated genes
Monokaryon	6032	667	771
Dikaryon	5889	170	194



To verify that H3K4me2 enrichment correlated with gene expression, RT-qPCR was performed on the 10 genes in a 20 kb region on scaffold 2 from 1,742,000 to 1,762,000 (Figure 3A,B). Of these genes, 4 were differentially regulated (2-fold cut-off); Schco3|2610874 and Schco3|2154172 had a 3.3 and 4.3-fold higher expression during monokaryotic development, respectively, while Schco3|2610872 and Schco3|2490027 had a 27.7 and 2-fold higher expression during dikaryotic development, respectively. The two strongest differentially regulated genes, Schco3|2154172 and Schco3|2610872, also had the strongest differential ChIP-Seq peak size of 8.7 and 10.4, respectively (Figure 4C and Supplemental Table 1). Schco3|2675477, which had a stronger enrichment of H3K4me2 during monokaryotic development (0.64) did not have a significant increase in expression during monokaryotic development, suggesting that small differences in H3K4me2 enrichment do not necessarily lead to differential expression.

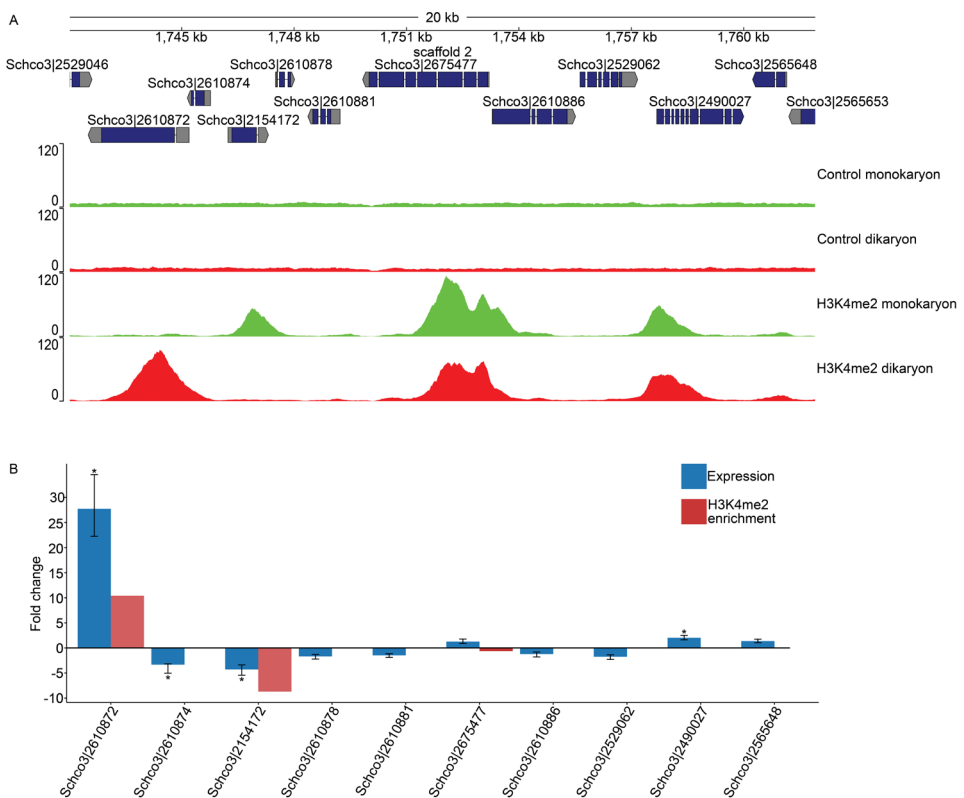


Figure 3. Histone H3 K4 dimethylation distribution and expression during monokaryotic and dikaryotic development on scaffold 2. A: Overview of read depth from both the control samples and the H3K4me2 ChIP samples on a representative part of the genome (scaffold 2: 1,742,000-1,762,000). The controls show a homogenous read depth across the genome, while ChIP resulted in enrichment around the TIS of genes. Most sites of enrichment were found during both monokaryotic and dikaryotic development, while some were unique for each developmental condition. B: Change in expression (blue) and H3K4me2 enrichment (red) of 10 genes on scaffold 2. Positive numbers indicate higher expression and enrichment during dikaryotic growth, while negative numbers indicate higher expression and enrichment during monokaryotic growth. Stars (*) indicate a > 2-fold absolute change in expression.

A total of 25 TFs were associated with enriched peaks in the monokaryon, while six were associated with enriched peaks in the dikaryon (Table 3). Among the TFs identified in the monokaryon was *pri2*, a previously studied zinc-finger TFs with no known function in *S. commune* (de Jong et al. 2010). The six TFs identified in the dikaryon included five fungal specific TF zinc fingers and one C2H2 zinc finger. None of these TFs have previously been studied in a mushroom-forming species.

Table 3. TFs with differential enrichment of H3K4me2 during monokaryotic and dikaryotic development

ProteinId	Condition	TF type
Schco3 1157466	monokaryon	bZIP
Schco3 2645246	monokaryon	bZIP
Schco3 2717189	monokaryon	C2H2 zinc finger
Schco3 2642040	monokaryon	Forkhead
Schco3 2493743	monokaryon	Fungal Specific TF
Schco3 2525437	monokaryon	Fungal Specific TF
Schco3 2611855	monokaryon	Fungal Specific TF
Schco3 2620175	monokaryon	Fungal Specific TF
Schco3 2624428	monokaryon	Fungal Specific TF
Schco3 2628620	monokaryon	Fungal Specific TF
Schco3 2631700	monokaryon	Fungal Specific TF
Schco3 2633058	monokaryon	Fungal Specific TF
Schco3 2635378	monokaryon	Fungal Specific TF
Schco3 82290	monokaryon	Fungal Specific TF
Schco3 2181177	monokaryon	Helix-loop-helix
Schco3 2045557	monokaryon	HMG
Schco3 2467772	monokaryon	HMG
Schco3 2517503	monokaryon	HMG
Schco3 2539542	monokaryon	HMG
Schco3 2662380	monokaryon	HMG
Schco3 2686461	monokaryon	HMG
Schco3 2603970	monokaryon	Homeodomain
Schco3 2613044	monokaryon	Homeodomain
Schco3 2625693	monokaryon	MADS-box
Schco3 2585708	monokaryon	Zinc finger, PARP-type
Schco3 2601101	dikaryon	C2H2 zinc finger
Schco3 2351130	dikaryon	Fungal Specific TF
Schco3 2495705	dikaryon	Fungal Specific TF
Schco3 2502848	dikaryon	Fungal Specific TF
Schco3 2577799	dikaryon	Fungal Specific TF
Schco3 2641534	dikaryon	Fungal Specific TF



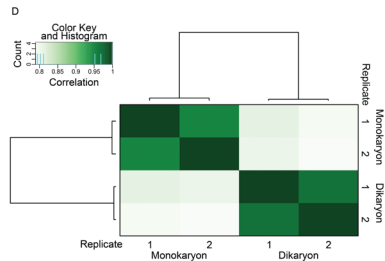
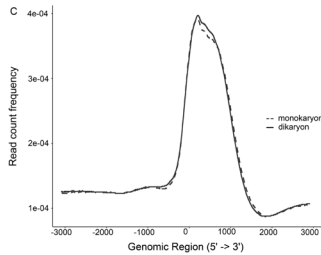
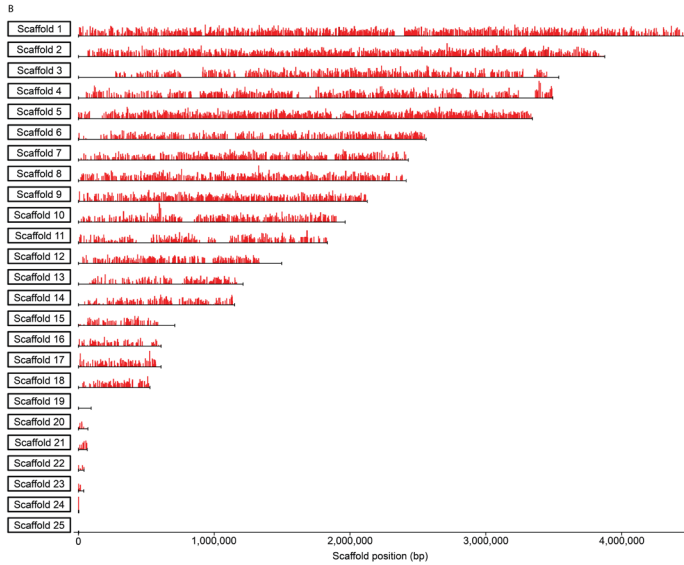
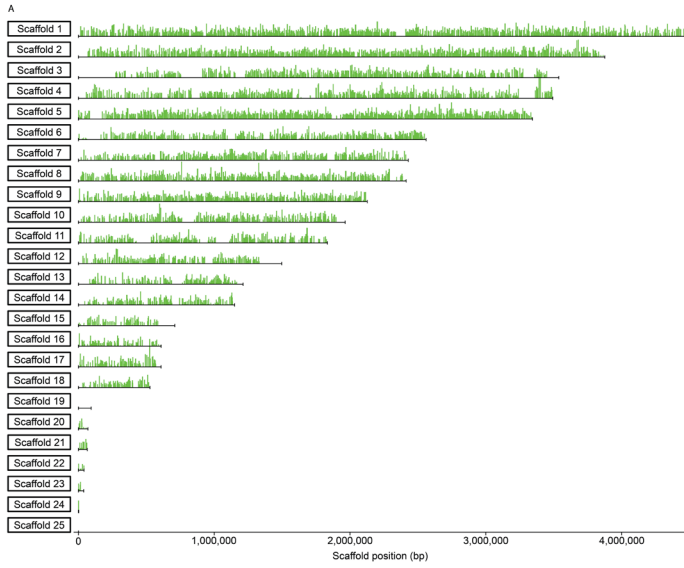


Figure 4. H3K4me2 peak distribution during monokaryotic and dikaryotic development. A: Distribution of H3K4me2 across the *S. commune* genome during monokaryotic development. B: Distribution of H3K4me2 across the *S. commune* genome during dikaryotic development. C: Read count frequency 6000 bp around the translation initiation site (TIS) of genes with a peak in the monokaryon (dotted line) and dikaryon (continuous line) samples. The enrichment ranges from approximately 375 bp upstream to 1500 bp downstream of the TIS, with a summit 100 bp downstream of the TIS. The distribution of both monokaryotic and dikaryotic samples was very similar. D: Correlation between samples and replicates obtained from H3K4me2 ChIP-Seq. The correlation between replicates of the same sample was > 0.95, while the correlation between the monokaryon and dikaryon samples was around 0.8. This indicates considerable conservation of the H3K4me2 landscape across the developmental stages.

Deletion of two dikaryon-specific transcription factors results in incomplete fruiting

TFs *fst1* (ProteinID: 2641534) and *zfc7* (ProteinID: 2601101), named after the fungal-specific TF (PF04082) and zinc finger C2H2 (PF00096) domains, respectively, were selected for gene inactivation. Both genes had nearby peaks that were enriched during dikaryotic growth (specifically, primordia formation) when compared to monokaryotic growth (Figure 5A,B). This profile suggested that their role takes place during primordia formation. Their expression profile also suggested a role in primordia development, as expression increased in the primordia compared to vegetative growth (Figure 5C,D) (Pelkmans et al. 2017)

Furthermore, both *fst1* and *zfc7* had higher expression during dikaryotic development than during monokaryotic development (as determined by quantitative RT-PCR), with a relative expression increase of 2.0 and 14.8-fold, respectively. To study their role, the genes were deleted in a $\Delta ku80$ strain by homologous recombination with a plasmid containing a nourseothricin resistance cassette flanked by 1 kb upstream and downstream flanks of the target gene. To increase efficiency, Cas9 preassembled with two sgRNAs against the gene of interest were co-transformed (Vonk et al. 2019; **Chapter 3**). Candidate gene deletions were selected on nourseothricin and counter-selected on phleomycin. Gene deletions were confirmed by colony PCR (Supplemental Figure 5) and selected knockout strains were crossed with the compatible isogenic H4-8b to obtain compatible monokaryons of the deletion strains with an intact *ku80* gene. To determine if phenotypes could be attributed to the deleted genes, both genes were complemented by ectopic integration of the genes under the control of the endogenous promoter and terminator. Candidate complemented strains were crossed with a compatible deletion strain to assess the recovery of wild-type fruiting body formation (Supplemental Figure 6).

Vegetative growth in monokaryons was not altered by deletion of either *fst1* or *zfc7* after seven days (data not shown). However, both strains showed stunted primordia and mushroom formation (Figure 6A-F) when grown as homozygous dikaryons under mushroom-inducing conditions. While asymmetric growth was established after three days, brown pigmentation and aggregate formation was reduced in the primordia ring. After seven days, wild-type dikaryons formed mature mushrooms with opened gills, while homozygous $\Delta fst1$ dikaryons produced cup-shaped mushrooms covered with aerial hyphae and reduced brown pigmentation. Homozygous $\Delta zfc7$ dikaryons formed some spots of immature fruiting bodies, but most of the primordia halted development after aggregate formation and showed reduced brown pigmentation.



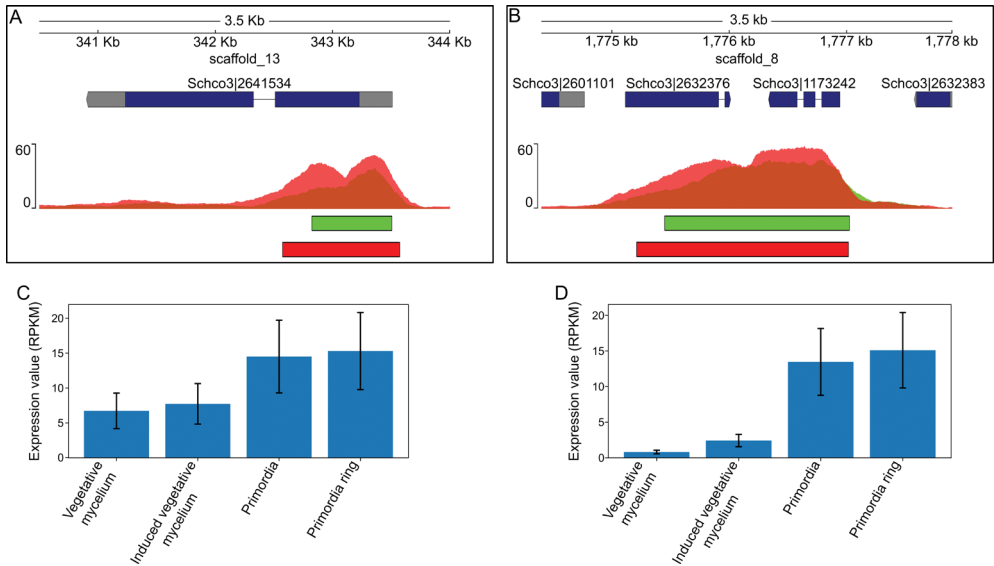


Figure 5. Read depth and expression of the TF genes *fst1* (protein ID Schco3|2601101) and *zfc7* (protein ID Schco3|2601101). A-B: The normalized read depth of H3K4me2 ChIP during monokaryotic (green) and dikaryotic (red) development in the loci of *fst1* (A) and *zfc7* (B). Overlap in read depth is indicated in orange. The identified peaks are indicated below. Both *fst1* and *zfc7* have increased read depth and broader peaks during dikaryotic development. C-D: Expression of *fst1* (C) and *zfc7* (D) during mushroom formation in *S. commune* (Pelkmans et al. 2017). The 95% confidence interval is indicated by black error bars. Both TFs have increased expression during primordia formation.

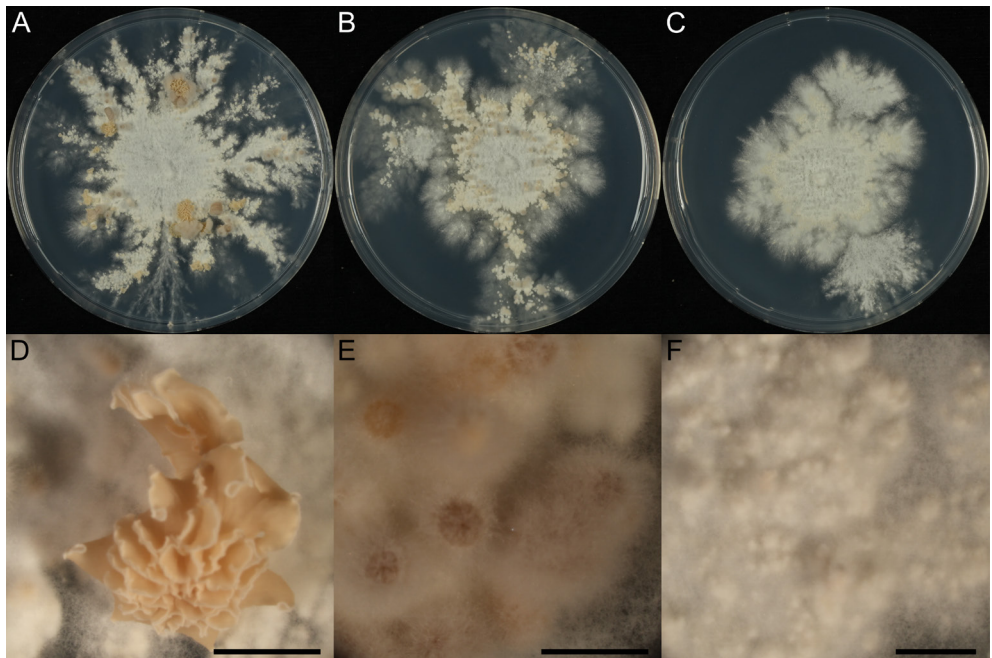


Figure 6. Mushroom development in wild type (A, D), $\Delta fst1$ (B, E) and $\Delta zfc7$ (C, F) dikaryons. A-C represent full colonies and D-F represent magnifications of the fruiting bodies. The scale bars represent 2.5 mm.

Discussion

Comparative genomics and transcriptomics have become commonplace to study the development of mushroom-forming fungi (Ohm et al. 2011; Pelkmans et al. 2017; Wu et al. 2018; Almási et al. 2019; Krizsán et al. 2019). These approaches have provided valuable insight into the developmental plan of fruiting body formation. However, little is known about the underlying epigenetic changes during development. Here, we used ChIP-Seq to fill the gap between the genome of *S. commune* and the transcriptomic changes during development by targeting the conserved activating histone mark H3K4me2 during the initial stages of monokaryotic and dikaryotic development. The H3K4me2 sites were strongly enriched around the TIS. We used the resulting data to identify two genes predicted to play a role in the early stages of primordia formation. Indeed, homozygous deletion strains of either *fst1* or *zfc7* were unable to form mature mushrooms, but instead stopped their development in the primordia stage. This indicates that H3K4me2 enrichment may serve as a marker for the identification of candidate genes involved in processes downstream of the time of sampling.

There are no previous studies on the distribution of H3K4me2 in mushroom-forming fungi, or any other basidiomycete. However, the distribution we observed downstream of the TIS is similar to that observed in ascomycetes, including *Saccharomyces cerevisiae* and *Z. tritici* (Bernstein et al. 2004; Pokholok et al. 2005; Soyer et al. 2015). In some plant-pathogenic species histone modifications can be chromosome-specific due to the presence of accessory chromosomes with low gene content (Wiemann et al. 2013; Schotanus et al. 2015). We did not observe such a distribution in the genome of *S. commune* due to the absence of accessory chromosomes. While in general H3K4me2 is associated with active genes (Pekowska et al. 2010; Wiemann et al. 2013), we did identify genes previously associated with dikaryotic development that were enriched with H3K4me2 during monokaryotic development. This includes *pri2*, which is strongly up-regulated during mushroom-formation and is implicated in dikaryotic development in *Lentinula edodes* (Miyazaki et al. 2004; de Jong et al. 2010; Pelkmans et al. 2017; Krizsán et al. 2019). Recently, H3K4 methylation has also been associated with repression of specific gene clusters in *S. cerevisiae*, which can perhaps explain the methylation profile of *pri2*, although a better understanding of histone modifications in *S. commune* is required to confirm this (Jaiswal et al. 2017).

While epigenetic histone marks are generally strongly conserved across eukaryotes (Waterborg 2012), significant changes in the protein sequence of histones may limit our ability to probe certain histone marks in *S. commune* with commercially available antibodies. Therefore, we were unable to confirm the presence of inhibitory H3K27me3 histone mark in *S. commune*. While this is likely due to amino acid substitutions and insertions surrounding lysine 27 on histone H3, it is also possible that H3K27 methylation is not conserved in *S. commune*. It has previously been shown that H3K27 methylation does not occur in multiple ascomycetes, including several *Aspergillus* species and yeasts, due to the absence of KMT6 homologs (Brosch et al. 2008; Veerappan et al. 2008; Connolly et al. 2013; Allshire and Ekwall 2015; Freitag 2017). In the basidiomycete yeast *Cryptococcus neoformans* H3K27 methylation has previously been detected, and in the mushroom-forming species *C. cinerea* H3K27 methylation is predicted based on presence of a KMT6 ortholog (Dumesic et al. 2015; Freitag 2017). Other basidiomycete species, like *Ustilago maydis*, do not have a KMT6 ortholog, which suggests a loss of function in some species.



With H3K4me2 ChIP-Seq we observed a correlation of 0.95 to 0.97 within replicates and 0.79 to 0.81 between monokaryotic and dikaryotic samples. This indicates that the majority of the H3K4me2 landscape is very similar between these samples. This is in line with the relatively low number of differential peaks that were identified. Additionally, the distribution around the TIS strongly correlated between both developmental stages. In human cell lines, it has previously been described that the distribution and location of H3K4me2 can change drastically during development (Orford et al. 2008; Zhang et al. 2012; Lambrot et al. 2019). Data on more histone modifications during additional stages of development should increase our understanding of the underlying chromatin modifications regulating gene expression in mushroom-forming fungi. Moreover, deletion of histone methyltransferase genes followed by ChIP-Seq may result in more insight into their impact on the epigenetic landscape during development.

Despite the large degree of similarity in the H3K4me2 landscape between monokaryotic and dikaryotic life stages, there were also differences. Surprisingly, more genes had enrichment of H3K4me2 during monokaryotic development than during dikaryotic development, with 771 and 194 genes identified, respectively. Canonically, mushroom development is considered the most complex developmental program of mushroom-forming fungi, but our data suggests that this is not directly reflected in this type of epigenetic regulation (Kües and Liu 2000; Vonk and Ohm 2018; **Chapter 2**). However, in our approach we sampled the entire colonies of a monokaryotic and dikaryotic culture. Likely, the chromatin is constantly remodeled during mushroom development, leading to different patterns of chromatin regulation in various parts of the colony. Therefore, sampling a full dikaryotic colony likely hides some of this complexity by averaging out these differences. Having developed this technique, we can now sample individual developmental stages to accurately determine their epigenetic profile.

We have developed an efficient ChIP-Seq protocol for *S. commune*. Furthermore, we have shown that this approach can be used to identify novel developmental regulators. To our knowledge this is the first report of the use of ChIP-Seq in a mushroom-forming basidiomycete, and it should be straightforward to adapt it to other mushroom-forming fungi. Moreover, it opens the door to performing ChIP-Seq on specific TFs, allowing us to determine their binding dynamics in the genome. Combined, these techniques will further reveal the important layer of epigenetic regulation during mushroom development and other processes. Therefore, the important addition of the study of epigenetic regulation to the molecular toolkit of *S. commune* will facilitate the functional characterization of the genome, leading to important new insights into the biology of this important group of fungi.

Materials & Methods

Culture conditions and strains

S. commune was grown from a small agar inoculum on solid *Schizophyllum commune* minimal medium (SCMM) supplemented with 1.5% agar at 30 °C (van Peer et al. 2009). All strains are derived from *S. commune* H4-8 (*matA43matB41*; FGSC 9210) and the compatible isogenic strain H4-8b (*matA41matB43*) (Ohm et al. 2010a; 2010b). For deletions, a previously published $\Delta ku80$ strain was used (de Jong et al. 2010). For selection on nourseothricin (Bio-Connect, Netherlands) or phleomycin (Bio-Connect, Netherlands), SCMM was supplemented with 15 $\mu\text{g ml}^{-1}$ and 25 $\mu\text{g ml}^{-1}$ antibiotic, respectively (Alves et al. 2004). For phenotypical characterization, strains were grown for 7 days at 25 °C in a 16/8 hours day/night cycle.

Histone H3 alignment

Histone H3 was identified in each organism based on the best blast-hit with *hht1* from *S. cerevisiae*. The sequences were aligned with MAFFT 7.307 and coloured according to the Clustal X colour scheme (Larkin et al. 2007; Katoh and Standley 2013). A species tree was constructed based on 181 highly conserved single copy genes determined by BUSCO v2 (dataset 'fungi_odb9') (Seppey et al. 2019). The sequences were concatenated and aligned with MAFFT 7.307 (Katoh and Standley 2013) and well-aligned positions were selected with Gblocks 0.91b (Castresana 2000). This resulted in 61723 positions per species and from this a tree was calculated with FastTreeMP (Price et al. 2010). Animal and plant species were added manually based on the NCBI taxonomy. The final tree and alignments were visualized with the interactive Tree Of Life v4 (Letunic and Bork 2019). The branch lengths are not drawn to scale.

Western blot

S. commune was grown as a monokaryon or dikaryon for 4 days in a 16/8 hour day/night cycle on porous polycarbonate (PC) membranes (diameter 76 mm; pore size 0.1 μm ; Osmonics; GE Water Technologies, USA). After 90 hours, half colonies were harvested and homogenized in a TissueLyser II (Qiagen, Germany) with 2 grinding beads in 2 mL Eppendorf Safe-Lock tubes (Eppendorf, Germany) at 25 Hz for 2 minutes. The homogenate was dissolved in 500 μL cell lysis buffer (20 mM Tris-HCl pH 8.0, 85 mM KCl, 0.5% IGEPAL CA-630 (Sigma, USA), 1x cOmplete protease inhibitor cocktail (Roche, Switzerland) and incubated for 10 minutes at 4 °C. The samples were centrifuged for 5 minutes at 2500 g at 4 °C and the pellet was resuspended in 250 μL nuclei lysis buffer (10 mM Tris-HCl pH 7.5, 1% IGEPAL CA-630, 0.5% sodium deoxycholate, 0.1% SDS, 1x cOmplete protease inhibitor cocktail). The samples were incubated at 4 °C for 10 minutes and cellular debris was removed by centrifugation for 10 minutes at 15,000 g at 4 °C. As a positive control, 45 μg of HeLa whole cell lysate was used (ab29545, Abcam, UK). All samples were mixed with 250 μL 2x Laemmli sample buffer (4% SDS, 20% glycerol, 10% β -mercaptoethanol, 0.004% bromophenol blue, 125 mM Tris-HCl pH 6.8) and incubated at 100 °C for 10 minutes. The protein extracts were size-separated by SDS-PAGE on Mini-PROTEAN TGX Stain-Free Precast Gels (Bio-Rad, USA) according to the manufacturer's specifications and transferred to polyvinylidene difluoride membrane (ThermoFisher Scientific, USA) according to the manufacturer's specification. The membrane was blocked with 5% bovine serum albumin (Sigma-Aldrich, USA) in phosphate buffered saline supplemented with Tween (PBS-T) (137 mM NaCl, 10 mM Na_2HPO_4 , 1.8 mM KH_2PO_4 , 2.7 mM KCl, 0.1% Tween 20) for 60 minutes, followed by incubation with either Recombinant Rabbit Anti-Histone H3 (di-methyl K4) (ab32356, Abcam, UK) diluted 1:2000



or, rabbit anti-Tri-Methyl-Histone H3 (Lys27) (#9733, Cell Signaling Technology, USA) diluted 1:1000 in PBS-T with blocking buffer for 60 minutes. The membrane was washed 3 times with PBS-T for 5 minutes before incubation with an HRP-linked anti-rabbit IgG (ab205718, Abcam, UK) diluted 1:10,000 in PBS-T for 60 minutes. The membrane was washed 3 times in PBS-T for five minutes and imaged with Clarity ECL Substrate (Bio-Rad, USA) according to manufacturer's specification.

Crosslinking and chromatin isolation

The chromatin immunoprecipitation method was adapted from previous studies in human cell lines and *Z. tritici* (Johnson et al. 2007; Soyer et al. 2015). See also Supplemental Text 1 for a protocol and additional considerations while performing ChIP-Seq. *S. commune* was grown as a monokaryon and dikaryon at 25 °C on porous PC membranes in a 16/8 hour day/night cycle. After 90 hours 5 full colonies were collected per replicate and briefly washed in Tris-buffered saline (TBS) (50 mM Tris-HCl pH 7.6, 150 mM NaCl). Samples were crosslinked by vacuum infiltration in 1% formaldehyde in TBS for 15 minutes and crosslinking was quenched by vacuum infiltration in 0.125 M glycine for 5 minutes. The crosslinked mycelium was briefly dried and frozen in liquid nitrogen. Next, the mycelium was homogenized in stainless steel grinding jars in a TissueLyser II (Qiagen, Germany) at 30 Hz for 2 minutes. The homogenate was dissolved in 10 mL cell lysis buffer (20 mM Tris-HCl pH 8.0, 85 mM KCl, 0.5% IGEPAL CA-630 (Sigma-Aldrich, USA), 1x cComplete protease inhibitor cocktail (Roche, Switzerland) and incubated for 10 minutes at 4 °C. The samples were centrifuged for 5 minutes at 2500 g at 4 °C and the pellet was resuspended in 3 mL nuclei lysis buffer (10 mM Tris-HCl pH 7.5, 1% IGEPAL CA-630, 0.5% sodium deoxycholate, 0.1% SDS, 1x cComplete protease inhibitor cocktail). The soluble chromatin was fragmented by sonication for 8 minutes on ice, using a Branson sonifier 450 with microtip at setting 4 with 35% output. The samples and the tip were cooled every 2 minutes during sonication. After fragmentation, the samples were incubated for 10 minutes at 4 °C and then spun down for 10 minutes at 15,000 g at 4 °C. The supernatant contained the isolated chromatin. 300 µL was stored at -80 °C for input control, while the remaining chromatin was used for ChIP.

Chromatin immunoprecipitation

The entire chromatin immunoprecipitation (ChIP) was performed at 4 °C unless stated otherwise. ChIP dilution buffer (0.01% SDS, 1.1% Triton X-100, 1.2 mM EDTA, 16.7 mM Tris-HCl pH 8.0, 167 mM NaCl, 1x cComplete protease inhibitor cocktail) was added to 3 mL to the chromatin suspension. For pre-clearing, 20 µL Pierce Protein A Magnetic Beads (ThermoFisher Scientific, USA) were incubated with the samples for 1 hour and the supernatant was transferred to a new tube. Next, 5 µL rabbit-anti-histone H3K4me2 (ab32356, Abcam, UK) was incubated with each sample for 18 hours. To each sample 20 µL of Pierce Protein A Magnetic Beads was added and the samples were incubated for an additional hour. The magnetic beads were collected and washed 1 time with low salt washing buffer (0.1% SDS, 1% Triton X-100, 2 mM EDTA, 20 mM Tris-HCl pH 8.0, 150 mM NaCl), 2 times with high salt washing buffer (low salt washing buffer with 500 mM NaCl), 2 times with lithium chloride washing buffer (250 mM LiCl, 1% IGEPAL CA-630, 1% sodium deoxycholate, 1 mM EDTA, 10 mM Tris-HCl pH 8.0) and 2 times TE buffer. During each washing step the samples were incubated for 5 minutes. After the first wash with lithium chloride washing buffer the samples were transferred to room temperature. Chromatin was eluted twice for 10 minutes in 250 µL in fresh elution buffer (1% SDS, 0.1M NaHCO₃). The RNA was degraded

by incubating with 50 mg RNase A (Sigma-Aldrich, USA) for 1 hour at 50 °C and then the samples were de-crosslinked overnight with 75 µL reverse crosslinking buffer (250 mM Tris-HCl pH 6.5, 62.5 mM EDTA, 1.25 M NaCl, 5 mg mL⁻¹ proteinase K (ThermoFisher Scientific, USA)) at 65 °C. The input controls were adjusted to 500 µL with water and de-crosslinked under the same conditions.

DNA isolation

The decrosslinked DNA was purified by phenol-chloroform extraction. Briefly, 1 volume of phenol-chloroform (1:1) was added, mixed thoroughly and the aqueous phase was extracted after centrifugation at 15,000 g for 5 minutes. This step was repeated a total of 3 times. The phenol was removed by repeating extraction with 1 volume of chloroform and 580 µL of the aqueous phase was transferred. The DNA was precipitated with 58 µL 3M NaAc pH 5.6 and 1160 µL ethanol and coprecipitated with 1 µL glycogen (20 mg mL⁻¹) (ThermoFisher Scientific, USA). The sample was mixed thoroughly and then stored at -80 °C for 2 hours. The DNA was collected by centrifugation at 15,000 g for 45 minutes at 4 °C and the DNA pellet was washed with 1 mL 70% ethanol. The pellet was collected by centrifugation at 15,000 g for 15 minutes at 4 °C and resuspended in 30 µL TE buffer. The DNA was further purified with the ChargeSwitch gDNA Plant Kit (ThermoFisher Scientific, USA) according to the manufacturer's specifications and eluted in 50 µL ChargeSwitch elution buffer. The samples were concentrated to 25 µL using a speedvac and sent to the Utrecht Sequencing Facility (USEQ, www.useq.nl) for library preparation and sequencing.

Library preparation and sequencing

For each sample, 80% was used for library prep with the NEXTflex Rapid DNA-Seq Kit Bundle (Bioo Scientific, USA) according to manufacturer's specifications. The resulting libraries were sequenced on the Illumina NextSeq500 2x75 mid output platform.

Sequencing analysis

The sequence reads were mapped to the *S. commune* H4-8 reference genome (version Schco3 (Ohm et al. 2010a)) with bowtie2 (version 2.3.4.1) (Langmead and Salzberg 2012). The aligned reads were filtered on unique, paired-end alignments with a quality score > 1 with samtools (version 1.7) (Li et al. 2009). Duplicated reads were marked with picard (version 2.21.6) (Broad Institute 2009) and removed with samtools. Peak calling was performed by macs2 (version 2.2.3) (Feng et al. 2012) for individual replicates and across all replicates together. The differential peaks were determined with Bioconductor Diffbind (version 2.14.0) (Stark and Brown 2011). The initial peak distribution was determined with ChIPseeker (Wang and He 2015) and genes were correlated to peaks based on this distribution. Final distribution was determined by identifying the closest gene to a peak within 3000 bp upstream and downstream of the TIS (translation initiation site) and calculating the relative read depth of each position around the TIS of these genes (Figure 4A).

Quantitative RT-PCR

S. commune was grown as a monokaryon and dikaryon at 25 °C on porous PC membranes in a 16/8 hour day/night cycle. After 90 hours, half colonies were harvested and homogenized in a TissueLyser II (Qiagen, Germany) with 2 grinding beads in 2 mL Eppendorf Safe-Lock tubes (Eppendorf, Germany) at 25 Hz for 1 minute. The homogenized mycelium was resuspended



in 1 mL TRIzol reagent (ThermoFisher Scientific, USA) and the RNA was isolated according to the manufacturer's specifications and resuspended in 100 μ L nuclease-free water. The RNA was cleaned up with the GeneJET RNA purification kit (ThermoFisher Scientific, USA) according to manufacturer's specification and eluted in 100 μ L nuclease free water. The RNA was then quantified and 1 μ g was used for input in RT-PCR with the Quantitect Reverse Transcription Kit (Qiagen, Germany) according to manufacturer's specification. Primers for qPCR were designed across introns with a product size of 100-150 bp (Table 4). Primer efficiency was determined in duplicate with dilutions of 1:10 to 1:100,000 of cDNA from the monokaryon. All primers had an efficiency between 90% and 110%. SYBR Green chemistry (ThermoFisher Scientific, USA) and an ABI Prism 7900HT SDS (ThermoFisher Scientific, USA) were used for RT-PCR. Data was analyzed with the QuantStudio V1.3 software. As reference genes, *act1*, *tef1* and *ubi1* were used and relative quantification was calculated from an average of these genes (Madhavan et al. 2014).

Gene inactivation

Deletion vectors of *fst1* (ProteinID: 2641534) and *zfc7* (ProteinID: 2601101) were constructed by amplifying the upstream and downstream flanks of each gene and cloned into plasmid pRO402 with a nourseothricin resistance cassette between both flanks. Plasmid pRO402 contains a pUC19 backbone with a phleomycin resistance cassette. For *fst1*, the upstream and downstream flanks were amplified with *fst1_up_fw* + *fst1_up_rv* and *fst1_down_fw* + *fst1_down_rv*, respectively, to create 1087 bp and 1025 bp fragments, respectively (Table 4). For *zfc7*, the upstream and downstream flanks were amplified with *zfc7_up_fw* + *zfc7_up_rv* and *zfc7_down_fw* + *zfc7_down_rv*, respectively, to create 1050 bp and 1007 bp fragments, respectively. All upstream PCR products contained 20 bp overlap with pRO402 and a nourseothricin cassette introduced by the forward and reverse primer respectively, while all downstream PCR products contained 20 bp overlap with a nourseothricin resistance cassette and pRO402, respectively. The upstream flank, nourseothricin resistance cassette and downstream flank were cloned into pRO402 digested with HindIII with gibson assembly (NEBuilder HiFi DNA Assembly Master Mix, New England Biolabs, USA), resulting in deletion constructs pPV021 and pPV023 for *fst1* and *zfc7*, respectively. The transformation with CRISPR-Cas9 was performed as previously described with two sgRNAs per gene close to the upstream and downstream flank respectively (Vonk et al. 2019; **Chapter 3**). The sgRNAs were produced with the GeneArt Precision sgRNA Synthesis Kit (ThermoFisher Scientific, USA) according to manufacturer's specifications with the p1_sgRNA and p2_sgRNA primers listed in Table 4. Gene deletions were verified by PCR. For deletion strains, a primer outside the upstream (*fst1_ChkA* or *zfc7_ChkA*) and downstream (*fst1_ChkD* or *zfc7_ChkD*) and inside the nourseothricin resistance cassette (*nour_ChkB* and *nour_ChkC*) were used. As a negative control, primers inside the gene were used (*fst1_ChkB*, *fst1_ChkC*, *zfc7_ChkB* and *zfc7_ChkC*) (Table 4).

Complementation

To complement the deletion strains, a 1000 bp promoter region and the coding sequence were amplified by PCR for *fst1* (primers *fst1_comp_fw* and *fst1_comp_rv*; Table 4) and *zfc7* (primers *zfc7_comp_fw* and *zfc7_comp_rv*; Table 4). This resulted in DNA fragments of 4207 bp and 2939 bp, respectively. All primers contained 20 bp overhangs to plasmid pPV008. This plasmid contains a pUC19 backbone, phleomycin resistance cassette a promoter and CDS insert flanked by HindIII and BamHI, an intron and a 432 bp *sc3* terminator. The fragments

were assembled with pPV008 digested with HindIII and BamHI with gibson assembly. This resulted in complementation plasmids pPV024 and pPV026 for *fst1* and *zfc7*, respectively. Strains were complemented as described previously and candidate complement strains were selected based on their ability to recover the wild-type fruiting phenotype (Ohm et al. 2011).

Table 4. Primers used in this study. Bold parts are overlapping regions for Gibson assembly. Underlined parts are protospacers for sgRNA

Primer name	Sequence
2610872_qPCR_fw	CCAGGACCAGGACCAGAC
2610872_qPCR_rv	GCACATCGCTAGCACACAAC
2610874_qPCR_fw	GTCGGTGTAGCCGAAAGTG
2610874_qPCR_rv	ATGTACGGCCTTGCGACTT
2154172_qPCR_fw	CTTGGAGCCTTCATACTGC
2154172_qPCR_rv	CGAGGGGAAGATCTTGATGGA
2610878_qPCR_fw	GCGGCTGAGGAAGATAAAT
2610878_qPCR_rv	CGCTAATCGTGTGCAGTCTC
2610881_qPCR_fw	CGACAATCATGTCCGTGTTCC
2610881_qPCR_rv	TCGCCTTCCTTACCCTTTC
2675477_qPCR_fw	AGAGGCCGAGTGAATTTTGA
2675477_qPCR_rv	CGCATCACGGACTCGTCT
2610886_qPCR_fw	CCACCAAAACCAGAGAACGA
2610886_qPCR_rv	GCCAAACAAGCATTCAAAA
2529062_qPCR_fw	ACTCGACGATGGCCAACAC
2529062_qPCR_rv	GCATTGTTGGTCACGGAAAT
2490027_qPCR_fw	ATGCGTATGATCCCCGAGAAG
2490027_qPCR_rv	CATTGCGGTCATAGTTGACG
2565648_qPCR_fw	GATGGGGCATCGCTTCTC
2565648_qPCR_rv	TCATGACCCTCTTCAACTACGA
<i>fst1</i> _qPCR_fw	GGCCCTCCTTCGCGTACT
<i>fst1</i> _qPCR_rv	AGGCGTGCGAGAAGTGTAGA
<i>zfc7</i> _qPCR_fw	ACGACCTCAAGCGACACC
<i>zfc7</i> _qPCR_rv	AGGCTTCATCGATTTTACCG
<i>akt1</i> _qPCR_fw	CTGCTCTTGTTATTGACAATGGTTCC
<i>akt1</i> _qPCR_rv	AGGATACCACGCTTGGACTGAGC
<i>tef1</i> _qPCR_fw	AGCTTGGCAAGGGTTCCTTCA
<i>tef1</i> _qPCR_rv	AACTTCCAGAGGGCGATATCA
<i>ubi1</i> _qPCR_fw	GAAGGAGTACGATGCGAAGG
<i>ubi1</i> _qPCR_rv	TCCTCCTCGCTTCTTGC
<i>fst1</i> _up_fw	CTATGACCATGATTACGCCAAAGACAACAGGACGCGTC
<i>fst1</i> _up_rv	GTCCCCCTCGAGGCGCGCCGTATTGCTTGCTTGCTGCTC



fst1_down_fw	TCCCAGACCACCATGCCGGGTGAGCAGGCAGATGAGATC
fst1_down_rv	GATAACCTTCAGCAGAACGAAGGGAGGGATAGTCCCTCTC
zfc7_up_fw	CTATGACCATGATTACGCCACGCAGATAACTCGAAAGCTG
zfc7_up_rv	GTCCCCCTCGAGGCGCGCCGAGGAGAGACTTTAGAGATCGC
zfc7_down_fw	TCCCAGACCACCATGCCGGGACTCGAGACTTTGAGGTACG
zfc7_down_rv	GATAACCTTCAGCAGAACGAAGGGAGAGTCGAACCTATGG
p1_sgRNA_fst1_left	TAATACGACTCACTATAGGGCAGCGCGACTACTCGCG
p2_sgRNA_fst1_left	TTCTAGCTCTAAAACCGCGAGTACGTCGCGCTGCC
p1_sgRNA_fst1_right	TAATACGACTCACTATAGGAGATGCGTGGTCTGCTGTAG
p2_sgRNA_fst1_right	TTCTAGCTCTAAAACCTACGACGACCACGCATCTC
p1_sgRNA_zfc7_left	TAATACGACTCACTATAGACTGGTCACTGCGCGTATAC
p2_sgRNA_zfc7_left	TTCTAGCTCTAAAACGTATACGCGCACTGACCAGT
p1_sgRNA_zfc7_right	TAATACGACTCACTATAGCGTTAGCTCGTCAAGGGCTG
p2_sgRNA_zfc7_right	TTCTAGCTCTAAAACGAGCCCTTGACGAGCTAACG
fst1_ChkA	CAAACGAGAGCACCAGTATG
fst1_ChkB	AGCTCGTAGTACGTCATTGG
fst1_ChkC	ATCATGGTGGGTTGGGAC
fst1_ChkD	TCCAGCTTGTCCTGAGAAAG
zfc7_ChkA	GTCTTCCTGTACATGCACTG
zfc7_ChkB	TCAGTGCGCGTATACTGG
zfc7_ChkC	CTAAACGAAAGGCTGGTGC
zfc7_ChkD	AGATGAAGATGAGCGAAGGG
nour_ChkB	CCGAAAGATCCGATCGATAC
nour_ChkC	CGTCATGAATGAAGCCTCAG
fst1_comp_fw	GCGTGGCCCCAAGCGTTGGAGACCAAACGAGAGCACCAGT
fst1_comp_rv	AGACTGACGTGCACTCACAGGAGGAGGCATGGTGACATTT
zfc7_comp_fw	GCGTGGCCCCAAGCGTTGGATCTCGCACATCGCAGATAAC
zfc7_comp_rv	AGACTGACGTGCACTCACAGGATCGACCTTGCCATTGACT

Data availability

The sequence reads are available from the Short Read Archive (SRA) of NCBI under accession ID PRJNA702885.

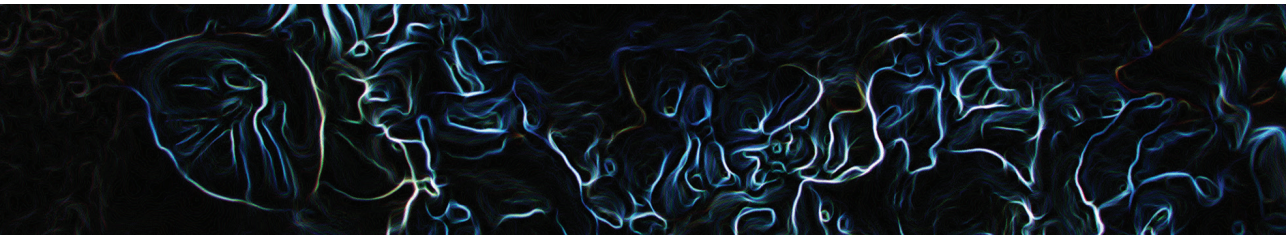
Acknowledgements

This project has received funding from the European Research Council (ERC) under the European Union's Horizon 2020 research and innovation programme (grant agreement number 716132). The authors thank Michal Mokry for helpful discussions about the ChIP-Seq analysis and Noortje van Dungen for technical assistance with the Illumina library preparation. We thank Utrecht Sequencing Facility for providing sequencing service and data. Utrecht Sequencing Facility is subsidized by the University Medical Center Utrecht, Hubrecht Institute, Utrecht University and The Netherlands X-omics Initiative (NWO project 184.034.019).

Supplementary data

All supplementary data is available at <https://www.nature.com/articles/s41598-021-87635-8#Sec19>





The transcription factor Roc1 is a regulator of cellulose degradation in the wood-decaying mushroom *Schizophyllum commune*

Ioana M. Marian*, Peter Jan Vonk*, Ivan D. Valdes, Kerrie Barry, Benedict Bostock, Akiko Carver, Chris Daum, Harry Lerner, Anna Lipzen, Hongjae Park, Margo B. P. Schuller, Martin Tegelaar, Andrew Tritt, Jeremy Schmutz, Jane Grimwood, Luis G. Lugones, In-Geol Choi, Han A. B. Wösten, Igor V. Grigoriev, Robin A. Ohm

* contributed equally to this chapter

This chapter is based on Marian, I. M. Vonk, P. J. Valdes, I. D. Barry, K. Bostock, B. Carver, A. Daum, C. Lerner, H. Lipzen, A. Park, H. Schuller, M. B. P. Tegelaar, M. Tritt, A. Schmutz, J. Grimwood, J. Lugones, L. G. Choi, I. Wösten, H. A. B. Grigoriev, I. V. & Ohm, R. A. (2021). The transcription factor Roc1 is a regulator of cellulose degradation in the wood-decaying mushroom *Schizophyllum commune* (submitted)

Abstract

Wood-decaying fungi of the class Agaricomycetes (phylum Basidiomycota) are saprotrophs that break down lignocellulose and play an important role in the nutrient recycling. They secrete a wide range of extracellular plant cell wall degrading enzymes that break down cellulose, hemicellulose and lignin, the main building blocks of plant biomass. Although the production of these enzymes is regulated mainly at the transcriptional level, no activating regulators have been identified in any wood-decaying fungus in the class Agaricomycetes. We studied the regulation of cellulase expression in the wood-decaying fungus *Schizophyllum commune*. Comparative genomics and transcriptomics on two wild isolates revealed a Zn₂Cys₆-type transcription factor gene (*roc1*) that was highly up-regulated during growth on cellulose, when compared to glucose. It is only conserved in the class Agaricomycetes. A *roc1* knockout strain was unable to grow on medium with cellulose as sole carbon source, and growth on cellobiose and xylan (other components of wood) was inhibited. Growth on non-wood-related carbon sources was not inhibited. Cellulase activity was reduced in the growth medium of the $\Delta roc1$ strain. ChIP-Seq identified 1474 binding sites of the Roc1 transcription factor. Promoters of genes involved in lignocellulose degradation were enriched with these binding sites, especially those of LPMO (lytic polysaccharide monooxygenase) CAZymes, indicating that Roc1 directly regulates these genes. A GC-rich motif was identified as the binding site of Roc1, which was confirmed by a functional promoter analysis. Together, Roc1 is a key regulator of cellulose degradation and the first identified in wood decaying fungi in the phylum Basidiomycota.

Introduction

Plants store a considerable amount of energy in lignocellulose, and for that reason wood has been used as a fuel since prehistoric times. Wood is recalcitrant to decay by most organisms, but fungi have evolved ways to degrade (part of the) lignocellulose. Most wood decay fungi belong to the phylum Basidiomycota, or, more specifically, the class Agaricomycetes. Phylogenetically these are distantly related to the fungi in the phylum Ascomycota such as *Saccharomyces cerevisiae* and *Neurospora crassa*. The last common ancestor of ascomycete and basidiomycete fungi is estimated to have lived over 600 million years ago (Floudas et al. 2012). Although the Ascomycota harbor potent lignocellulose-degrading fungi, the strongest wood-decaying fungi are found in the Basidiomycota.

Lignocellulose consists of a wide range of components, including cellulose, hemicellulose, pectin, and the aromatic polymer lignin. These polymers are found in the plant cell wall. Fungi can generally easily absorb glucose and other monomers from the growth medium, but lignocellulose requires extensive extracellular enzymatic degradation before the breakdown product can be transported into the cells and metabolized. Wood-degrading fungi have evolved a broad range of hydrolytic enzymes that break down the various components of lignocellulose, including cellulases, hemicellulases, pectinases and oxidative enzymes. Collectively, these plant cell wall degrading enzymes are known as carbohydrate-active enzymes (CAZymes) and are classified into families of Glycoside Hydrolases (GHs), Glycosyl Transferases (GTs), Polysaccharide Lyases (PLs), Carbohydrate Esterases (CEs), and Auxiliary Activities (AAs) (Levasseur et al. 2013; Lombard et al. 2014). A typical genome of a wood-degrading fungus encodes hundreds of CAZymes (Ohm et al. 2014; Riley et al. 2014; Almási et al. 2019).

Basidiomycete wood decayers can be broadly divided into white rot fungi, which degrade all components of the plant cell wall, and brown rot fungi, which depolymerize cellulose, but leave lignin largely unmodified. However, fungi that show (genotypic and phenotypic) characteristics of both white rot and brown rot fungi have also been identified (Riley et al. 2014). Neither white rot fungi nor brown rot fungi form monophyletic groups, and the brown rot lifestyle has evolved several times from white rot fungi (Floudas et al. 2012; Riley et al. 2014; Zhang et al. 2019). Genes that encode CAZymes are generally strictly regulated at the transcriptional level, since their production is energetically expensive and not always needed. The primary mechanism of regulation is carbon catabolite repression (CCR). CCR represses the production of ligninolytic enzymes in the presence of an easily metabolizable carbon source, such as glucose, and ensures that the organism pursues the most energy-efficient mode of growth by ideal resource utilization. CCR is regulated by a highly conserved zinc-finger transcription factor (TF) (*CreA/Cre1/Cre-1*) (Strauss et al. 1999; Portnoy et al. 2011; Todd et al. 2014), which functions as a strong inhibitor of gene expression in the presence of simple sugars and has been described in several ascomycetes. The gene is conserved in basidiomycetes (Todd et al. 2014) and it indeed plays the same role in the mushroom-forming white rot *Pleurotus ostreatus* (Yoav et al. 2018).

A wide range of TFs act downstream of CCR (i.e. in the absence of simple sugars). Generally, these TFs activate gene expression of CAZymes involved in the breakdown of specific polysaccharides. Examples include *xlnR*, *CLR-1*, *CLR-2* and *ACE1*. In *Aspergillus* (van Peij et al. 1998) and *Trichoderma* (Stricker et al. 2006) the TF *xlnR* regulates (hemi)cellulose degrading



enzymes and it has an ortholog in almost all filamentous ascomycetes (Benocci et al. 2017). In *N. crassa* the TFs *CLR-1* and *CLR-2* induce the expression of cellulolytic, but not the hemicellulolytic enzymes (Craig et al. 2015). In contrast to the aforementioned regulators, *ACE1* is a repressor of cellulolytic and xylanolytic enzyme production in *Trichoderma reesei* (Aro et al. 2003). It is important to note that these regulators have only been identified in ascomycete fungi, and that there are no orthologs in basidiomycete fungi (Todd et al. 2014). To date, no regulators have been identified in the wood-degrading basidiomycetes that positively regulate CAZymes. In general, very little is known about the regulatory mechanisms involved in plant biomass degradation in the basidiomycetes.

Schizophyllum commune is a model system for mushroom-forming fungi in the class Agaricomycetes. Several molecular tools have been developed for this organism, including an efficient gene deletion protocol (de Jong et al. 2010; Vonk et al. 2019; **Chapter 3**) and a ChIP-Seq protocol for Histone H3 to study the epigenetic landscape (Vonk and Ohm 2021; **Chapter 4**). *S. commune* has a wide geographical distribution and is generally found as white fruiting bodies growing on wood. Its mode of wood decay is atypical, since it is not easily classified as either white rot or brown rot (Riley et al. 2014; Floudas et al. 2015; Almási et al. 2019). *S. commune* lacks lignin-degrading peroxidases, limiting its ability to degrade lignin (Ohm et al. 2010a). Still, *S. commune* degrades all wood components, but leaves the middle lamella of the plant cell wall mostly intact (Floudas et al. 2015). Here, we describe the identification of a regulator of cellulase expression (Roc1) by comparative genomics and comparative transcriptomics. A deletion strain was unable to efficiently utilize cellulose as a carbon source, and growth was inhibited on other components of wood. Moreover, with ChIP-Seq we identified the binding sites of this TF, which were enriched near CAZymes involved in cellulose degradation. This is the first positive regulator of cellulase expression identified in basidiomycetes.

Results

Comparison of growth profile of three strains of S. commune on various carbon sources

The growth profile of *S. commune* was determined on carbon sources associated with wood (including cellulose, hemicellulose, and pectin) and other carbon sources (including glucose, maltose and starch) (Figure 1). The reference strain H4-8 was compared to strains LoenenD and TattoneD. The latter two are haploid (monokaryotic) strains that were obtained (by protoplasting) from the dikaryotic wild isolate strains collected in Loenen aan de Vecht (Netherlands) and Tattone (Corsica, France). Strain LoenenD displayed reduced growth on maltose, starch, xylose, xylan and cellulose, but improved growth on pectin and cellobiose compared to H4-8 (Figure 1). In contrast, the growth profile of strain TattoneD was more similar to that of strain H4-8, with the notable exceptions of cellulose (TattoneD grew slower than H4-8) and pectin (TattoneD grew faster than H4-8). Together, there is considerable phenotypic diversity between the various strains of *S. commune*.

Genome sequences of three strains of S. commune

The genome sequence and annotation of strain H4-8 were previously published (Ohm et al. 2010a) and we here report an updated version (Schco3). Moreover, we sequenced strains TattoneD and LoenenD and generated draft assemblies and annotations (Table S3). The original Sanger-sequenced assembly of strain H4-8 (version Schco1) was improved by extensive targeted gap-sequencing and manual reassembly. This reduced the number of

scaffolds from 36 to 25, and considerably reduced the percentage of assembly gaps from 1.43% to 0.15%. Furthermore, a new set of gene predictions was generated using the RNA-Seq data used for the comparative transcriptomics described below. This raised the gene count from 13181 to 16204. The coding content of the assembly (i.e. the percentage of the assembly consisting of coding sequence) increased from 45.81% to 52.89%, indicating that genes that were missed in the original annotation were added to the new set. All statistics regarding the functional annotation of the predicted genes improved in the new annotation, indicating that the new gene set is more complete (i.e. more predicted genes were assigned a functional annotation) (Table S3). The BUSCO completeness score improved from 98.97% to 99.13%, further showing that the new assembly and gene predictions are of high quality. This new assembly and set of gene predictions will therefore be a valuable tool for functional analysis of this important model system of mushroom-forming fungi.

Draft assemblies and gene predictions were generated for strains TattoneD and LoenenD. Although both are more fragmented than the assembly of reference strain H4-8, the corresponding sets of gene predictions are similarly complete, as determined by BUSCO (98.62% and 99.31%, respectively). Illumina-sequenced genomes are generally more fragmented than Sanger-sequenced genomes, especially regarding repeat-rich regions (Ohm et al. 2012). This is reflected in the lower percentages of repetitive content for strains TattoneD and LoenenD, compared to H4-8. Importantly, the coding content of the assemblies are in a similar range, indicating that the set of gene predictions is reliable.

The three strains displayed a high degree of sequence diversity at the level of the genome (Figure 2A and 2B). Large parts of the genome display less than 95% similarity (over a 1 kb sliding window). In some cases (e.g. scaffolds 12, 15 and 19) the (sub)telomeric regions of strain H4-8 are not found in strains TattoneD or LoenenD. Despite this high degree of sequence diversity among the three strains, the majority of genes are conserved between the strains (Figure S1). The set of predicted carbohydrate-active enzymes (CAZymes) is remarkably similar between the strains (Figure 2C and Table S4). Therefore, the difference in growth profile on the various carbon sources cannot be easily explained by the CAZyme gene counts.



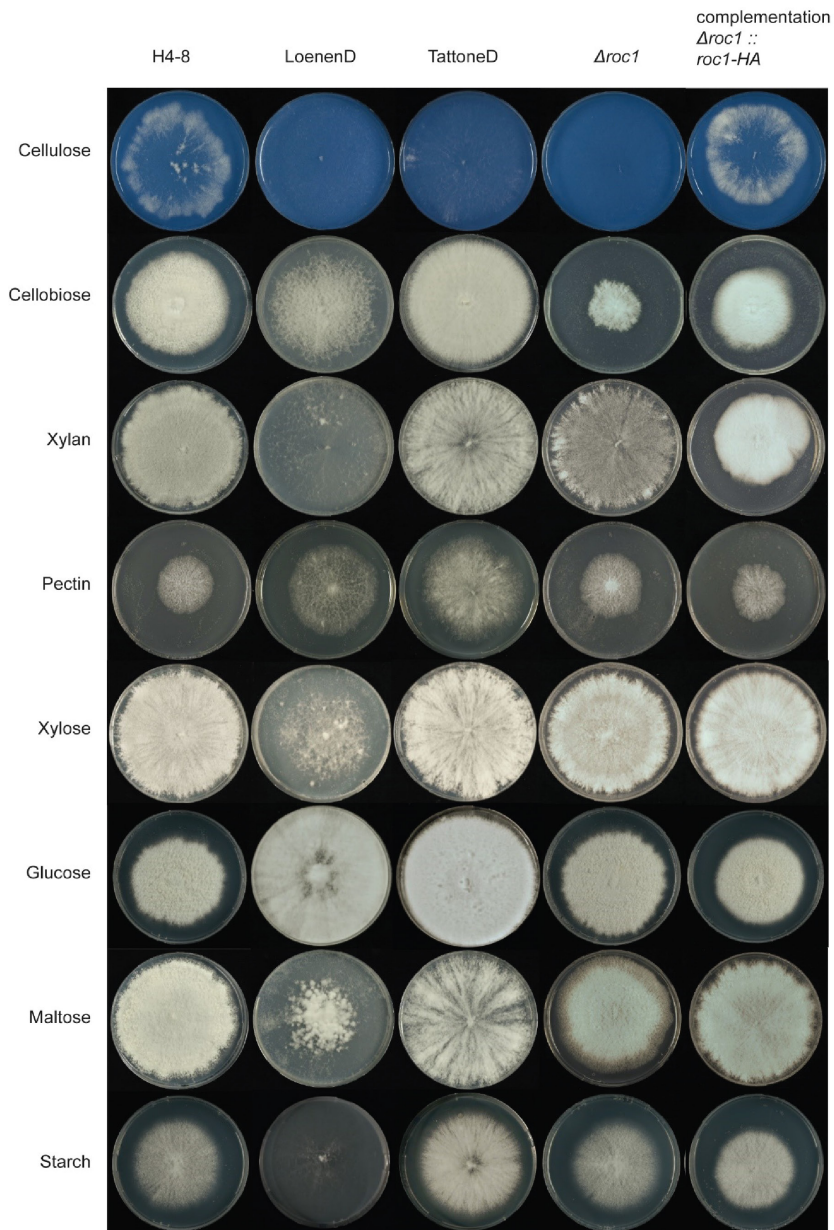


Figure 1. Growth phenotype of *S. commune* strains on various carbon sources. Reference strain H4-8 and wild isolate strains LoenenD and TattoneD displayed high phenotypic plasticity regarding growth on these carbon sources. Strain LoenenD showed reduced growth on maltose, starch, xylose, xylan and cellulose (Avicel), but improved growth on pectin and cellobiose compared to the reference strain H4-8. In contrast, the growth profile of strain TattoneD was more similar to that of strain H4-8, with the notable exceptions of cellulose (TattoneD grew slower than H4-8) and pectin (TattoneD grew faster than H4-8). Deletion strain $\Delta roc1$ showed strongly reduced growth on cellulose and cellobiose, when compared to its parent strain H4-8. This phenotype was rescued when the deletion was complemented. All strains were grown from a point inoculum for 7 days (glucose) and 11 days (other carbon sources) at 30 °C. The cellulose medium was stained blue with Remazol Brilliant Blue R to enhance the visibility of the white mycelium on the white cellulose medium (the dye did not affect growth; data not shown).

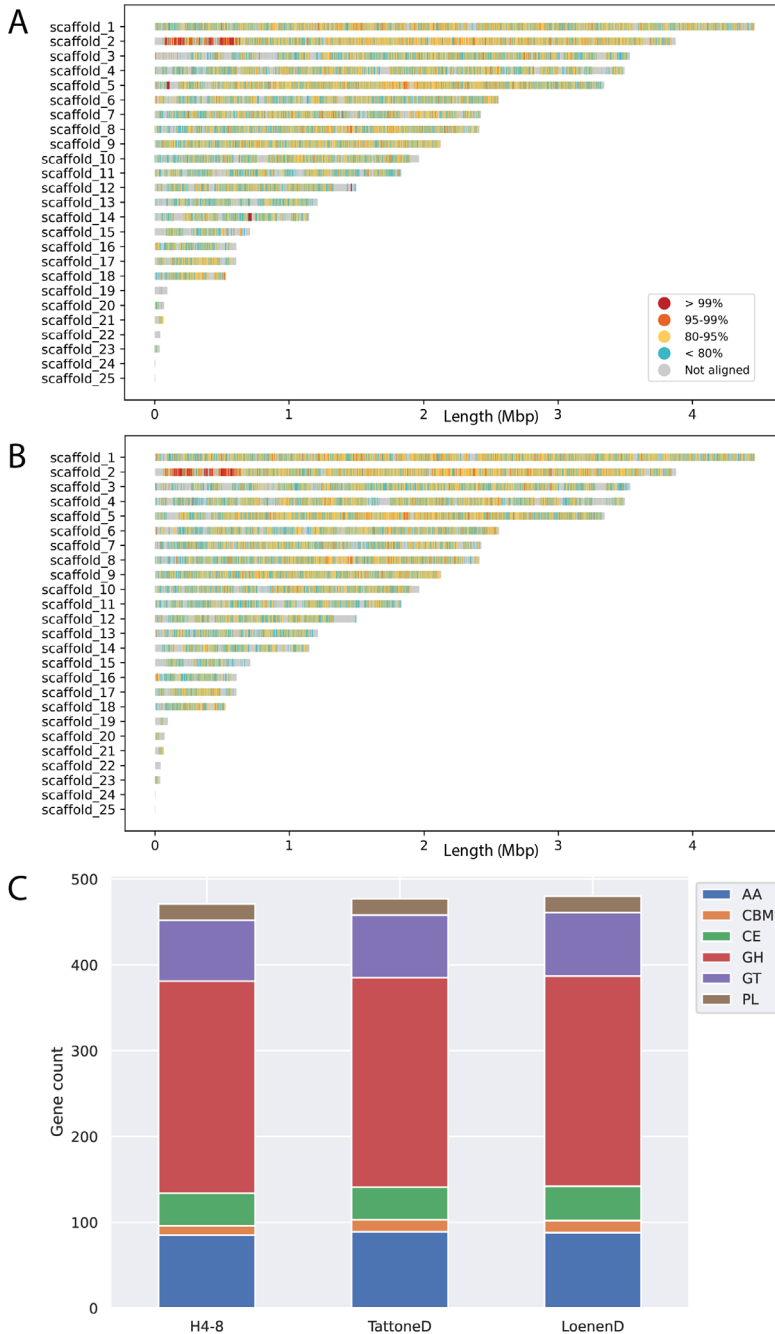


Figure 2. Conservation between the reference assembly of strain H4-8 and those of strains (A) TattoneD and (B) LoenenD. Even though these are strains of the same species, their assemblies display a high degree of variation. C. The number of predicted genes involved with plant cell wall degradation is very similar between the strains. These CAZymes are classified in subfamilies. GH: Glycoside Hydrolases; GT: Glycosyl Transferases; PL: Polysaccharide Lyases; CE: Carbohydrate Esterases; AA: Auxiliary Activities; CBM: carbohydrate-binding modules.



Comparative transcriptomics reveals conserved expression responses to lignocellulosic carbon sources

A comparative transcriptomics analysis was performed to determine whether, despite the high level of phenotypic and sequence diversity, there is a conserved expression response to lignocellulosic carbon sources. Strains H4-8 and Tattoned were pre-grown on minimal medium with glucose as carbon source and after 3 days the colonies were transferred to medium containing either glucose, cellulose (Avicel), or wood. After 3 days of exposure to this carbon source the colonies were harvested, RNA was isolated, and RNA-Seq was performed (Table S5). The heat maps of the expression profiles are depicted in Figure S2.

Glucose does not require extracellular breakdown by CAZymes, in contrast to the polymeric compounds cellulose and wood. Therefore, the most relevant differences in expression profiles were expected between samples grown on glucose and either cellulose or wood. Indeed, 166 and 210 genes of strains H4-8 and Tattoned were up-regulated when growth on cellulose when compared to glucose, respectively. Similarly, 468 and 500 genes of these strains were up-regulated on wood, respectively (Figure S2).

Next, a comparative transcriptomics analysis was performed on the two strains on various carbon sources, in an effort to identify conserved responses. Orthologs were identified between the two strains and their regulation profile was compared (Figure 3). Again, analysis was focused on expression on cellulose when compared to glucose (Figure 3A) and on wood when compared to glucose (Figure 3B). Orthologs in the upper right corner of Figures 3A and 3B displayed a conserved expression profile on the corresponding carbon sources and many of those are predicted CAZymes. The orthologs annotated as CAZymes showed a more conserved response between the strains (Pearson correlation of 0.88 and 0.88, on cellulose and wood, respectively) than for the full set of genes (Pearson correlation of 0.54 and 0.66, on cellulose and wood, respectively). The expression profile of TFs was less conserved between the strains than the CAZymes (Pearson correlation of 0.5 and 0.7, on cellulose and wood, respectively). In fact, only one TF displayed a conserved expression profile in both strains on cellulose and wood.

Orthologs that are up-regulated on complex carbon sources in one strain, but not in the other strain (i.e., the dots above and to the right of the green square in Figures 3A and 3B) do not show a conserved expression response. Therefore, those genes may explain part of the difference in phenotype displayed by these strains on complex carbon sources. Furthermore, orthologs that are up-regulated in both strains during growth on cellulose or wood but that do not have a CAZyme annotation (i.e., the black dots in the upper right corners of Figure 3A and 3B) may represent novel CAZymes, or other genes involved in growth on complex carbon sources.

Next, focus was on the orthologs that displayed a conserved expression response (i.e., in both strains) to complex carbon sources when compared to growth on glucose (Figures 3C and 3D). Orthologs that were up-regulated on cellulose in both strains were largely a subset of the orthologs that were up-regulated on wood, and a considerable number of those were CAZymes (Figure 3C). This indicates that the expression program that is activated during growth on cellulose is also activated during growth on wood. However, on wood a large number of additional genes were also up-regulated and were likely involved in the

degradation of the complex set of polymers present in this substrate. TFs, on the other hand, were not found to a large extent in the conserved changes in gene expression (Figure 3D). In fact, only one TF was up-regulated on both cellulose and on wood (when compared to on glucose) in both strain H4-8 and Tattoned (protein ID Schco3|2615561 and Schco_TatD_1|232687; Figure 3A, 3B and 3D). In strain H4-8 the expression is up-regulated 13-fold and 18-fold on cellulose and wood, respectively, when compared to glucose (Table S5). We hypothesized that this TF (from here on named Roc1 for 'regulator of cellulases') is involved in the regulation of gene expression during growth on lignocellulose.

Regulator Roc1 is only conserved in the class Agaricomycetes

Roc1 is classified as a putative TF based on the presence of a Zn₂Cys₆ DNA binding domain and a fungal-specific TF domain (Pfam domains PF00172 and PF04082, respectively). These domains are frequently found together and in most fungi this is the most common family of TFs (Todd et al. 2014) with many (distant and functionally unrelated) members across the fungal kingdom. Examples include GAL4 in *S. cerevisiae* (Traven et al. 2006) and XlnR in *Aspergillus niger* (van Peij et al. 1998). The reference genome of *S. commune* (strain H4-8) encodes 41 members of this TF family. The genomes of 140 fungi from across the fungal tree were analyzed for orthologs of Roc1 (Table S1). Since the fungal-specific Zn₂Cys₆ TF family is large, numerous homologs of Roc1 are found in each genome. We distinguished between homologs and orthologs using a gene tree-based approach, combined with the location of conserved domains (Figure S3). Roc1 orthologs were only found in members of the class Agaricomycetes in the phylum Basidiomycota (Figure S4). These orthologs clustered closely together in the gene tree (having short branch lengths) and were highly conserved across the length of the protein (Figure S3).

A $\Delta roc1$ strain is incapable of efficiently utilizing cellulose as a carbon source

A $\Delta roc1$ strain was generated in strain H4-8 using our recently published CRISPR/Cas9 genome editing protocol (Vonk et al. 2019; **Chapter 3**) by replacing 2759 bp (including the *roc1* coding sequence) with a nourseothricin resistance cassette.

Growth of $\Delta roc1$ on cellulose (Avicel) was strongly reduced when compared to the reference (Figure 1). Only a very thin mycelium was observed and no aerial hyphae were formed. Moreover, growth on cellobiose and xylan was also reduced, although to a lesser extent than on cellulose. Both these carbon sources are found in lignocellulose. In contrast, $\Delta roc1$ displays no phenotype when grown on glucose, maltose, starch, pectin and xylose when compared to the reference H4-8.

The wild-type phenotype was largely rescued when the $\Delta roc1$ strain was complemented with the *roc1* coding sequence under control of its own promoter (Figure 1), confirming that the phenotype was caused by the deletion of *roc1*. The coding sequence included a C-terminal hemagglutinin (HA) tag, allowing us to use the complementation strain for ChIP-Seq with a commercially available anti-HA antibody (see below).

Total cellulase enzyme activity in the growth medium is strongly reduced in $\Delta roc1$

We assessed whether the strongly reduced growth of the $\Delta roc1$ strain on cellulose coincided with reduced cellulase enzyme activity in the growth medium. Biomass was pre-grown in liquid minimal medium with glucose, washed and subsequently used to inoculate liquid



shaking cultures containing cellulose as carbon source. After 6 days, cellulase activity in the growth medium was determined (Figure 4). Compared to the reference strain H4-8, the $\Delta roc1$ strain had strongly reduced cellulase activity in the growth medium. Moreover, this phenotype was rescued in the complemented $\Delta roc1$ strain. The lack of growth of $\Delta roc1$ on cellulose (Figure 1) can be explained by the low cellulase activity in this strain, since these cellulases are required to break down cellulose. Furthermore, it indicates that Roc1 regulates the expression of cellulose-degrading genes.

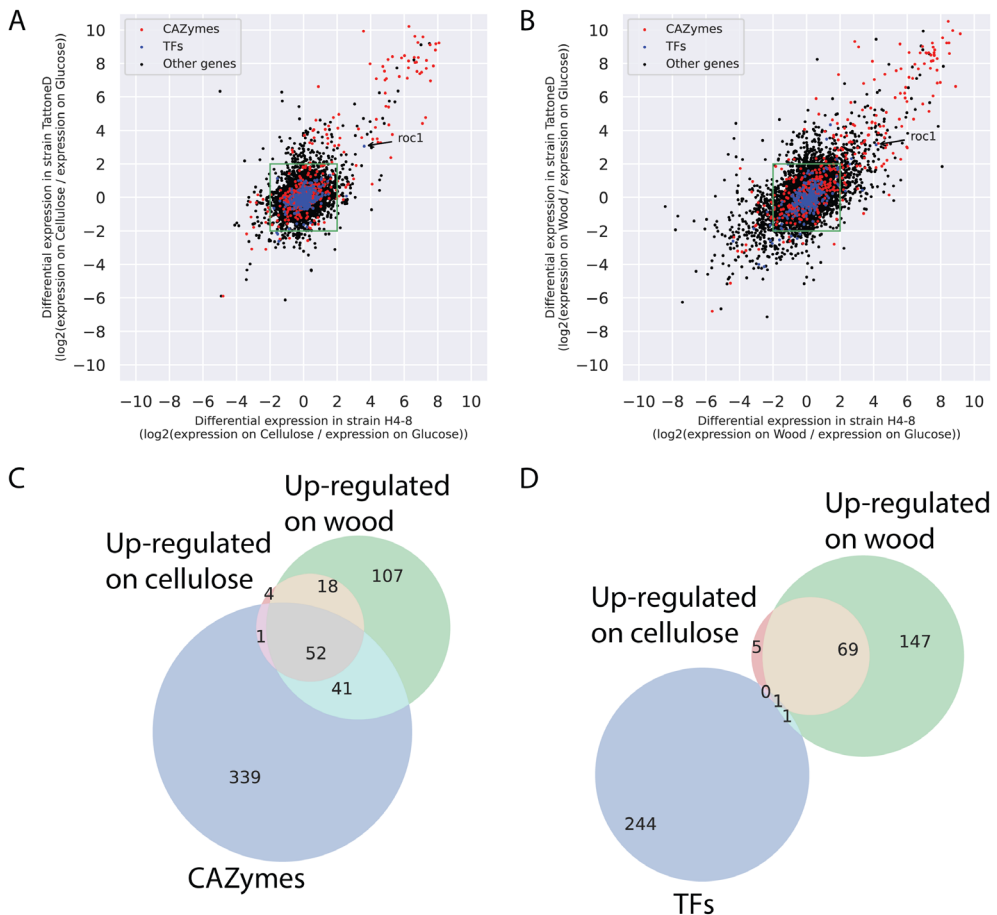


Figure 3. Comparative transcriptomics in strains H4-8 and TattoneD. **A.** Expression of orthologs in the two strains when grown on cellulose, compared to glucose. Orthologs in the green box are not differentially expressed in either strain. Orthologs in the top right quadrant are up-regulated on cellulose in both strains, indicating that they show a conserved response. Many of these orthologs are CAZymes, and only one ortholog is a TF (*roc1*). In general, the response of CAZymes is more conserved than that of other genes **B.** As in (A), but expression on wood when compared to glucose. **C.** VENN diagram of orthologs that are annotated as a CAZyme, are up-regulated on cellulose in both strains, or are up-regulated on wood in both strains (when compared to on glucose). Orthologs that are up-regulated on cellulose in both strains are largely a subset of orthologs up-regulated on wood. Moreover, a considerable number of the up-regulated orthologs are annotated as CAZyme. **D.** As in (C), but for orthologs annotated as TFs. Only one TF gene (*roc1*) was up-regulated in both strains on both cellulose and wood.

ChIP-Seq reveals binding sites of Roc1 in promoters of cellulases

TFs may regulate the expression of genes in a direct (e.g., by binding to their promoter) or indirect manner (e.g., by regulating other TFs that in turn directly regulate these genes). A ChIP-Seq analysis was performed to identify the binding sites of Roc1 in the genome, allowing us to determine whether Roc1 directly binds the promoters of cellulase genes. The Roc1 TF was tagged with a haemagglutinin (HA) tag and expressed in the deletion strain (resulting in strain $\Delta roc1 :: roc1-HA$), allowing the ChIP-Seq to be performed using commercially available antibodies against the HA-tag (Figure S5). Since this tagged version can complement the phenotype of the *roc1* deletion (Figures 1 and 4), it can be concluded that the HA-tag does not interfere with the function of Roc1. The strains H4-8 and $\Delta roc1 :: roc1-HA$ were grown on medium containing cellulose, and the chromatin immunoprecipitation (ChIP) procedure was performed to isolate the DNA to which Roc1 binds. This DNA was subsequently purified and sequenced using Illumina technology. The resulting sequence reads were aligned to the assembly of strain H4-8 and peaks were identified, which may be considered binding sites of Roc1.

A total of 1474 binding sites of Roc1 were identified during growth on cellulose, which were associated with 1125 unique genes (Table S6). CAZyme genes as a group were not enriched among those genes ($p > 0.05$), but, in contrast, specific CAZyme families were strongly enriched (Table S7), as well as genes that were up-regulated on cellulose (Figure 5A). A notable family of genes with binding sites of Roc1 are the lytic polysaccharide monooxygenases (LPMOs), also annotated as CAZyme family AA9 (auxiliary activity 9). This family was previously shown to be involved in cellulose degradation (Villares et al. 2017). Of the 22 LPMO genes encoded in the genome, 12 were associated with a Roc1 binding site. Moreover, 10 of these 12 were up-regulated during growth on cellulose when compared to growth on glucose. This indicates that Roc1 directly binds to the promoters of these genes during growth on cellulose, activating their expression. The GH3 and GH5 CAZyme families were also over-represented among the genes with a Roc1 binding site (Table S7). Both these glycoside hydrolase families comprise a diverse group of enzyme activities, several of which are involved in (hemi)cellulose degradation. GH3 includes members with reported β -glucosidase (involved in cellulose degradation) and xylan 1,4- β -xylosidase (involved in hemicellulose degradation), while GH5 includes members with reported endo- β -1,4-glucanase (involved in cellulose degradation) (Henrissat and Davies 1997; Lombard et al. 2014). Combined, these activities may explain why the $\Delta roc1$ strain can no longer utilize cellulose as a carbon source and displays slower growth on hemicellulose.

Remarkably, gene *roc1* itself is also associated with a Roc1 binding site (Table S6). This indicates that Roc1 regulates its own expression, perhaps in a positive feedback loop. Moreover, TF genes in general are enriched among genes associated with a Roc1 binding site. Of the 296 TF genes encoded in the genome, 52 had a nearby Roc1 binding site (Table S7). Few of these 52 TFs have been described previously, with the exception of C2h2 and Gat1, which play a role in various aspects of mushroom development (Ohm et al. 2011). It should be noted that these two genes were not up-regulated on cellulose or wood, when compared to growth on glucose.



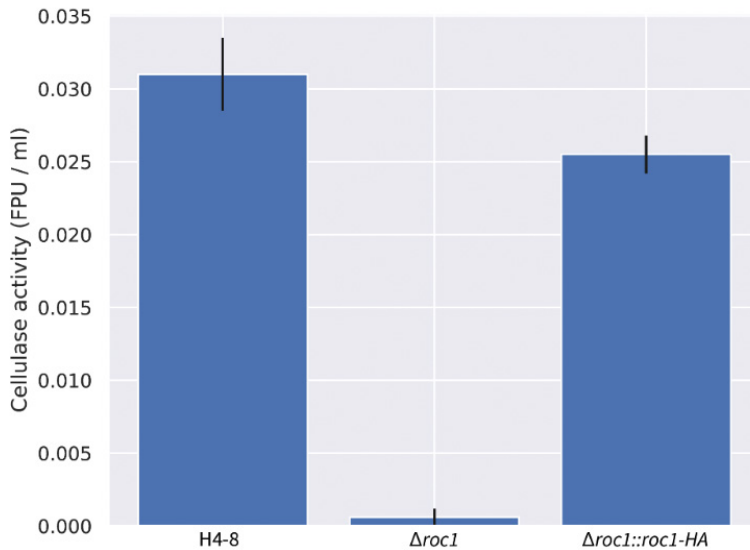


Figure 4. Total cellulase activity of *S. commune* strains in cellulose liquid shaking cultures. There is almost no activity in the $\Delta roc1$ strain when compared to the reference H4-8. This phenotype is largely rescued upon complementation of the gene. All cultures were pre-grown on glucose medium to ensure that sufficient biomass was present, transferred to cellulose medium, and grown for 6 additional days.

Conserved GC-rich motif in the Roc1 ChIP-Seq peaks

The peaks identified in the ChIP-Seq analysis were analyzed to identify a conserved motif that represents the binding site of Roc1. The GC content of the 500 bp sequence around the top of each Roc1 peak was determined (Figure S6). There was a marked increase in GC content near the middle of the peaks, which indicates that the Roc1 binding site is GC-rich. Based on the GC curve, we further limited the search to 200 bp around the top of each Roc1 peak. The sequences were analyzed with STREME, which attempts to find conserved motifs that are over-represented in the peak sequences, compared to a representative negative set (i.e., other genomic sequences). This led to the identification of a GC-rich motif (Figure 5B) that was present in 989 of the 1427 peaks and significantly enriched compared to the negative control sequences ($p = 2.8 \cdot 10^{-8}$ in a Fisher's exact test). Furthermore, this motif was found most frequently in the center of the identified peak (Figure 5C), as would be expected for the binding site.

Functional promoter analysis of a CAZyme of the AA9 family reveals the Roc1 binding site

Twelve out of the 22 members of the lytic polysaccharide monooxygenase family (LPMOs; CAZyme family AA9) were up-regulated during growth on both cellulose and wood when compared to glucose. Moreover, Roc1 had direct binding sites in the promoters of 12 of the 22 LPMO genes, as determined by ChIP-Seq. Ten of the 22 LPMO genes were both up-regulated on cellulose and had a Roc1 ChIP-Seq peak in their promoter, which shows that there is a strong correlation between these. One of these genes, *lpmA* (protein ID 1190128), was strongly up-regulated on cellulose and wood, compared to growth on glucose (246 and 206-fold, respectively; Table S5). The peak from the Roc1 ChIP-Seq was located upstream of the translation start site (Figure 6A).

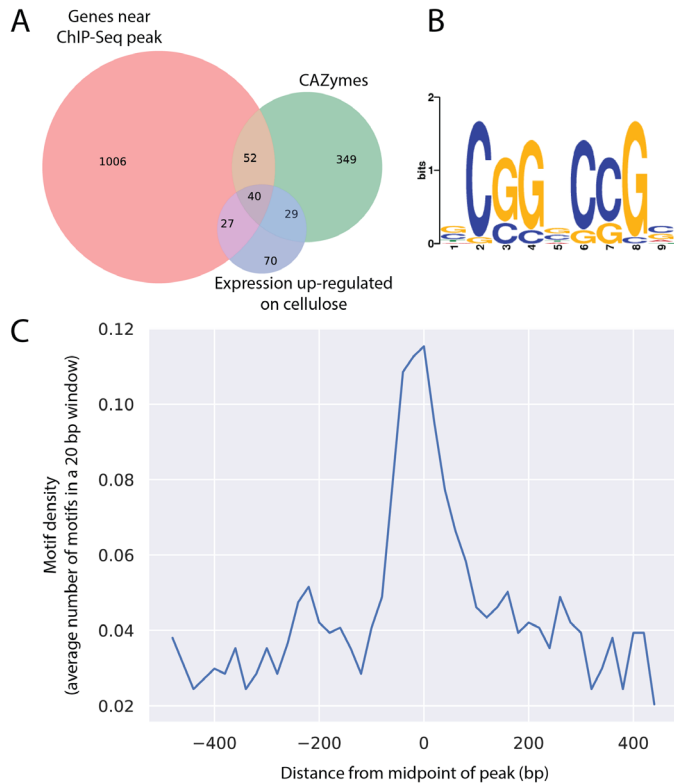


Figure 5. A. Venn diagram depicting the overlap between the sets of genes that are associated with a Roc1 binding site, CAZymes, and genes that are up-regulated on cellulose (when compared to glucose). **B.** Conserved motif identified in the binding sites of Roc1. **C.** The binding site in (B) is enriched in the center of the ChIP-Seq peaks.

A functional promoter analysis was performed to further investigate the expression dynamics and to locate the TF binding sites. The promoter of *lpmA* was used to drive expression of the red fluorescent reporter protein dTomato (Figure 6B). The 700 bp promoter (i.e., the 700 bp upstream of the predicted translation start site) could drive expression of dTomato when growing on cellulose, resulting in red fluorescent mycelium (strain *lpmA*_{prom700}-dTomato; Figures 6C). No fluorescence was observed when grown on glucose or a combination of glucose and cellulose (Figure S7). Next, similar reporter constructs were constructed with promoter lengths of 300, 200 and 100 bp. The promoter of 300 bp could still drive dTomato expression on cellulose, but, in contrast, the promoters of 200 bp and 100 bp could not (Figures 6B and 6C). This indicates that the region between 300 and 200 bp upstream of the translation start site contains an important regulatory element. This region corresponds with the peak in the ChIP-Seq data and therefore a binding site of Roc1. Moreover, the GC-rich conserved motif (Figure 5B) is located in this region (Figure 6A). This motif is also conserved in the promoters of the *lpmA* orthologs TattoneD and LoenenD (data not shown). Removal of this GC-rich motif from the 300 bp promoter of *lpmA* by site-directed mutagenesis resulted in a strong decrease in the ability of the promoter to drive dTomato expression (Figure 6C), since only weak fluorescence was observed. This confirms that the motif is indeed the binding site of Roc1 and that this binding site is required for correct promoter activity.

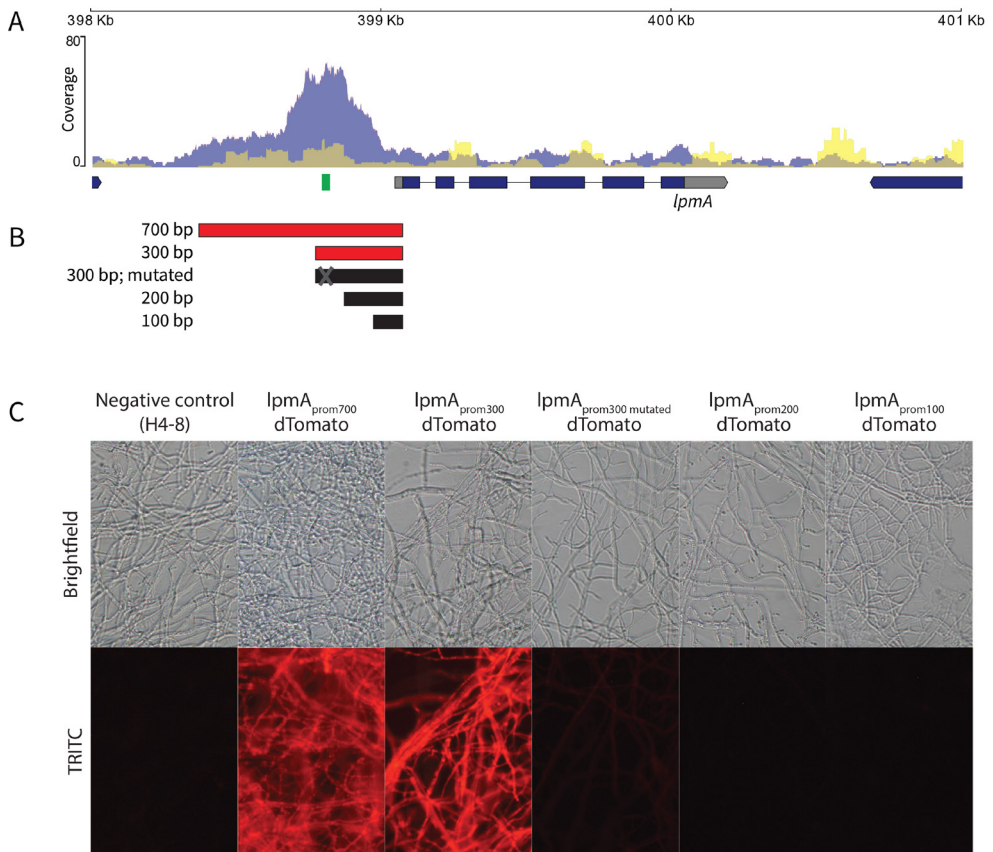


Figure 6. Functional promoter analysis of the lytic polysaccharide monoxygenase *lpmA* gene (protein ID 1190128). **A.** ChIP-Seq read coverage curve in the locus of *lpmA*. The blue curve represents the coverage of the Roc1 ChIP-Seq reads, while the yellow curve represents the negative control. There is a peak in the promoter region up-stream of the *lpmA* coding sequence. The location of the conserved motif (representing the Roc1 binding site; Figure 5B) is indicated in green. **B.** Five regions in the promoter of *lpmA* (5' of the coding sequence) were tested for their ability to drive expression and fluorescence of dTomato. Active promoter fragments are indicated in red, and inactive promoter fragments in black. **C.** Reporter strains with the dTomato gene under control of the promoters in (B), grown on cellulose. The 700 and 300 bp promoters can drive dTomato expression and fluorescence, but the 200 and 100 bp promoters cannot. The 300 bp promoter in which the Roc1 binding motif had been mutated was not able to drive dTomato expression and fluorescence to the same extent, since only weak fluorescence is observed. When grown on glucose, no fluorescence was observed in any of these strains (Figure S7).

Discussion

Fungal deconstruction of lignocellulose in the plant cell requires the complex orchestration of a broad set of enzymes, and the expression of these enzymes is generally tailored to the type of polymers in the substrate by TFs. Several such transcriptional regulators have been identified in the phylum Ascomycota, but to date not in the phylum Basidiomycota. These phyla diverged over 600 million years ago (Riley et al. 2014). Here, we identified the TF Roc1 as a regulator of cellulase expression in the wood-decaying mushroom *S. commune*. A *roc1* deletion strain could not efficiently utilize cellulose (and, to a lesser extent, hemicellulose) as a carbon source. Moreover, ChIP-Seq revealed that Roc1 binds the promoters of various types of cellulase genes (including several lytic polysaccharide monoxygenases) while

growing on cellulose, indicating that Roc1 directly regulates those genes. Furthermore, Roc1 activates its own expression, likely in a positive feedback loop.

S. commune is a highly polymorphic basidiomycete, both phenotypically and genetically. Strains H4-8, TattoneD and LoenenD varied considerably in their growth profiles, and showed a high variation in their genomes. This extraordinary genetic diversity was previously shown for other strains of *S. commune* as well (Baranova et al. 2015). Despite the high level of sequence variation between the strains, the number of CAZyme genes was remarkably similar. Therefore, it is challenging to link the phenotypical differences in growth profiles to a signature in the genome. However, the comparative transcriptomics approach allowed us to detect conserved responses in the expression profile, despite the high strain diversity. Although there is considerable variation between how the strains change their expression profile to the various carbon sources, the expression profile of CAZymes is more conserved. Furthermore, although the response of TFs was generally less conserved than the response of CAZymes, we identified a single TF gene (*roc1*) that was consistently up-regulated under these conditions in both strains.

Cellulose, cellobiose, and xylan are major constituents of lignocellulose in wood. Cellulose is a polysaccharide of β -1,4-linked glucose residues. Cellobiose is a dimer of β -1,4-linked glucose residues and is an intermediate breakdown product of cellulose during enzymatic digestion. Xylan is a group of hemicelluloses consisting of a backbone of β -1,4-linked xylose residues. The observation that growth on these carbon sources is specifically affected, but not on other carbon sources, is a strong indication that Roc1 regulates the process of lignocellulose degradation. Growth on pectin, another constituent of lignocellulose in wood, is not negatively affected in $\Delta roc1$. This indicates that Roc1 is likely not directly involved in pectinase expression.

It was previously shown that TFs involved in the regulation of polysaccharide degradation are generally poorly conserved between ascomycetes and basidiomycetes (Todd et al. 2014) and this is also the case for Roc1. Even within the basidiomycetes, Roc1 is only conserved in the class Agaricomycetes. The majority of fungi in this class are wood-degrading (Ohm et al. 2014), although it also includes mycorrhizal and plant pathogenic fungi (some of which have a partially saprotrophic lifestyle). Inversely, wood-degrading fungi are predominantly found in the class Agaricomycetes. This correlation between lifestyle (lignocellulose-degrading) and the presence of a Roc1 ortholog suggests that the function of Roc1 may be conserved in other members of the Agaricomycetes as well.

Regulators of cellulases were previously identified in the distantly related ascomycete *N. crassa* (Craig et al. 2015). It is important to note that neither these TFs (CLR-1 and CLR-2) are orthologous to Roc1 of *S. commune*, nor are these two genes conserved in *S. commune*. Remarkably, however, the binding motifs of CLR-1 and Roc1 show a large degree of similarity. The binding motif of Roc1 (CCG-N-CGG) is part of the CLR-1 motif (CGG-N₅-CCG-N-CGG). It is tempting to speculate that this is an example of convergent evolution, or that the binding motif predates either Roc1 or CLR-1. In the latter case, one TF could have taken over the role of the other in an ancestor of ascomycetes and basidiomycetes. It should be noted, however, that binding motifs of regulators of the Zn₂Cys₆ TF family frequently contain a CCG triplet, as is also the case for Gal4 of *S. cerevisiae* (Traven et al. 2006).



Orthologs of Roc1 in *Agaricus bisporus* (a litter-degrading, mushroom-forming fungus) and *Dichomitus squalens* (a white rot, mushroom-forming fungus) display an expression profile that is very similar to the profile in *S. commune* when grown on compost and cellulose respectively, compared to growth on glucose. In *A. bisporus* the ortholog of Roc1 is protein ID 224213 (version Agabi_varbis_H97_2 of the genome annotation). Previously, whole-genome microarray expression data was published during growth on (glucose-rich) defined medium as well as on compost (Morin et al. 2012). The expression of *roc1* was more than 10-fold higher when grown on compost (which contains large amounts of complex lignocellulosic carbon sources) than when grown on glucose-rich medium. Similarly, the ortholog of Roc1 in *D. squalens* is protein ID 920001 (version Dicsqu464_1 of the genome annotation). Previously, whole-genome expression data was published during growth on cellulose (avicel) and on cellulose in combination with glucose (Daly et al. 2019). Expression was considerably higher (more than 6-fold) when grown on cellulose alone, when compared to when grown on a combination of glucose and cellulose. Although difficult to directly compare to our study, both these studies show that *roc1* in these fungi is down-regulated in glucose-rich medium, similar to the situation in *S. commune*.

Roc1 not only binds to promoters of cellulases, but also to promoters of several TFs. This suggests that Roc1 not only regulates lignocellulose degradation, but that it is also an important regulator of other downstream processes. While Roc1 ChIP-Seq revealed an enrichment of binding sites near lignocellulolytic CAZymes, the majority of putative binding sites were not in the promoter region of CAZymes or even genes up-regulated during growth on cellulose. It is currently not known what the role of Roc1 is in the regulation of these binding sites. A similar number of peaks has previously been reported for the Zn₂Cys₆ TF PRO1 in *Sordaria macrospora* (Steffens et al. 2016), while fewer peaks were reported for other Zn₂Cys₆ TFs, including AfR in *Aspergillus flavus* (Kong et al. 2020), CrzA in *Aspergillus fumigatus* (de Castro et al. 2014) and FgHtf1 in *Fusarium graminearum* (Fan et al. 2020). Since the consensus sequence of the binding motif is rather short, it seems likely that not every occurrence of the motif results in a change of gene expression after binding by Roc1. Identifying binding sites during growth on additional substrates, in combination with RNA-Seq, may reveal more insights into the role of Roc1 in regulating lignocellulose degradation.

This is the first report of ChIP-Seq with a specific TF in a mushroom-forming fungus. It is a crucial step to mapping the regulatory networks of TFs in this group of fungi, since direct interactions between TFs and promoters can now be revealed in vivo. This will also be useful for studying the direct targets of the TFs involved in mushroom development (Ohm et al. 2010a; 2011; Pelkmans et al. 2017; Vonk and Ohm 2021; **Chapter 4**) and other processes in this important group of fungi.

Materials and methods

Strains, media composition and culture conditions

The reference strains used in this study were *S. commune* H4-8 (*matA43matB41*; FGSC 9210) and the compatible isogenic strain H4-8b (*matA41matB43*) (Ohm et al. 2010a). Strain $\Delta ku80$ was derived from H4-8 and was used for gene deletion (de Jong et al. 2010). The dikaryotic strains *S. commune* Tattone and *S. commune* Loenen were collected in Tattone (Corsica, France) and Loenen aan de Vecht (The Netherlands), respectively. The monokaryotic strains *S. commune* TattoneD and *S. commune* LoenenD were isolated from these strains

by protoplasting. Protoplasting was performed using a *Trichoderma harzianum* Horst lytic enzyme mix as described previously (van Peer et al. 2009).

The strains were grown at 30 °C on a medium comprising (per L) 22 g glucose monohydrate, 1.32 g (NH₄)₂SO₄, 0.5 g MgSO₄·7H₂O, 0.12 g thiamine, 1 g K₂HPO₄, 0.46 g KH₂PO₄, 5 mg FeCl₃·6H₂O, trace elements and with or without 1.5% agar (Dons et al. 1979). For cultures with other carbon sources, glucose was replaced with 1% (w/v) Avicel (cellulose), 1% (w/v) glucose + 1% (w/v) Avicel, 1% (w/v) cellobiose, 1% (w/v) xylan from corncob, 1% (w/v) pectin from apple, 1% (w/v) starch from potato, 2.2% (w/v) xylose, 2.2% (w/v) maltose monohydrate. To improve the visualization of the fungal colonies growing on Avicel, the media was supplemented with 20 µg µl⁻¹ Remazol Brilliant Blue R. Liquid cultures were grown in Erlenmeyer flasks at 30 °C with shaking at 200 rpm. For selection on nourseothricin (Bio-Connect, Netherlands), phleomycin (Bio-Connect, Netherlands) or hygromycin (Bio-Connect, Netherlands), the media was supplemented with 15 µg ml⁻¹, 25 µg ml⁻¹ and 20 µg ml⁻¹ antibiotic, respectively.

Genome sequencing and assembly

To perform genome improvement on assembly version Schco1 of *S. commune* H4-8 (Ohm et al. 2010a), the whole genome shotgun assembly was broken down into scaffolds and each scaffold piece was reassembled with phrap and subsequently improved using our Phred/Phrap/Consed pipeline (Gordon et al. 2001; Gordon 2003). Initially all lowquality regions and gaps were targeted with computationally selected Sanger sequencing reactions completed with 4:1 BigDye terminator: dGTP chemistry (Applied Biosystems). These automated rounds included walking on 3 kb and 8 kb plasmid subclones and fosmid clones using custom primers (400, 3498 and 1183 primers were selected respectively). Following completion of the automated rounds, a trained finisher manually inspected each assembly. Further reactions were then manually selected to improve the genome. Remaining gaps and hairpin structures were resolved by generating small insert shatter libraries of 8 kb-spanning clones. Smaller repeats in the sequence were resolved by transposonhopping and sequencing 8 kb plasmid clones. 136 fosmid clones were shotgun sequenced and finished to fill large gaps and resolve larger repeats. All these sequencing reactions were generated using Sanger long-read technology.

The genomes of *S. commune* TattoneD and LoenenD were sequenced using 270 bp insert standard fragment Illumina libraries in 2x150 format. The resulting reads were filtered for artifact and process contamination and were subsequently assembled with Velvet (Zerbino and Birney 2008). The resulting assembly was used to create *in silico* long mate-pair library with insert 3000 +/- 300 bp, which was then assembled together with the original Illumina library with AllPathsLG release version R42328 (Gnerre et al. 2011).

Gene prediction and functional annotation

The genomes were annotated using the JGI Annotation Pipeline (Grigoriev et al. 2006; 2014), which combines several gene prediction and annotation methods, and integrates the annotated genome into the web-based fungal resource MycoCosm (Grigoriev et al. 2014). Before gene prediction, repetitive sequences in the assemblies were masked using RepeatMasker (Smit et al. 2013), RepBase library (Jurka et al. 2005), and the most frequent (>150 times) repeats were recognized by RepeatScout (Price et al. 2005). The following



combination of gene predictors was run on the masked assembly: ab initio Fgenesh (Salamov and Solovyev 2000) and GeneMark (Ter-Hovhannisyian et al. 2008); homology-based Fgenesh+ (Salamov and Solovyev 2000) and Genewise (Birney et al. 2004) seeded by BLASTx alignments against the NCBI NR database. RNA-Seq data (see below) was used during gene prediction for strains H4-8 and Tattoned, but not for LoenenD. In addition to protein-coding genes, tRNAs were predicted using tRNAscan-SE (Lowe and Eddy 1997).

The predicted proteins of the three assemblies were functionally annotated. PFAM version 32 was used to predict conserved protein domains (El-Gebali et al. 2019) and these were subsequently mapped to their corresponding gene ontology (GO) terms (Ashburner et al. 2000; Hunter et al. 2009). Secretion signals were predicted with Signalp 4.1 (Petersen et al. 2011) and transmembrane domains were predicted with TMHMM 2.0c (Krogh et al. 2001). Proteins were considered small secreted proteins when they had a secretion signal, but no transmembrane domain (except in the first 40 amino acids) and were shorter than 300 amino acids. TFs were identified based on the presence of a PFAM domain with DNA binding properties (Park et al. 2008). Proteases were predicted based on the MEROPS database (Rawlings et al. 2012) using a BlastP E-value cutoff of $1e-5$. A pipeline based on the SMURF method (Khaldi et al. 2010) was used to predict genes and gene clusters involved in secondary metabolism. SMURF parameter d (maximum intergenic distance in base pairs) was set at 3000 bp. SMURF parameter γ (the maximum number of non-secondary metabolism genes upstream or downstream of the backbone gene) was set at 6. CAZymes were annotated with the standalone version of the dbCAN pipeline using HMMdb version 9 (Zhang et al. 2018).

The assemblies of strains Tattoned and LoenenD were aligned to the assembly of H4-8 using PROmer version 3, which is part of the MUMmer package (Kurtz et al. 2004). The setting “mum” was used. Next, a sliding window approach (1 kbp window with 100 bp step size) was taken to determine the percentage of identity across the assemblies of the strains.

Comparative transcriptomics during growth on various carbon sources

Cultures of strain H4-8 and Tattoned were pre-grown on a Whatman CycloPore™ polycarbonate (PC) membrane on top of minimal medium containing glucose at 30 °C in the dark. After 3 days, the PC membranes containing the cultures were carefully transferred to fresh plates containing solid minimal medium with either glucose, cellulose (avicel) or birchwood (ground to a particle size of 1 to 3 mm) as sole carbon source. After 3 days, the cultures were harvested, lyophilized, powdered in liquid nitrogen, and RNA was extracted using the Zymo Direct-zol RNA MiniPrep kit. The quality of the RNA was assessed with an Agilent 2100 Bioanalyzer. All conditions were analyzed with biological triplicates.

Illumina libraries were generated for RNA-Seq and subsequently sequenced on the Illumina HiSeq-2000 platform in 1x50 bp mode. The exceptions to this were the three glucose replicates from strain H4-8, since these were sequenced in 2x100 bp mode. To avoid any biases during mapping and counting between these samples and the others, only the first 50 bp from the left read pair were extracted from these samples using BBduk (part of the BBMap suite (Bushnell 2019)) and used in the subsequent transcriptome analysis.

The sequence reads were aligned to their respective genome assemblies, *S. commune* H4-8 (version Schco3) or *S. commune* TattoneD (version Schco_TatD_1), using the aligner Hisat version 2.1.0 (Kim et al. 2015). Default settings were used, with these exceptions: --min-intronlen 20 --max-intronlen 1000. Expression values were calculated as RPKM values (Reads per Kilobase model per Million mapped reads) using Cuffdiff version 2.2.1, which is part of the Cufflinks package (Trapnell et al. 2010). The bias correction method was used while running Cuffdiff (Roberts et al. 2011). In addition to the cutoff used by Cuffdiff to identify differentially expressed genes, we applied an additional filter of at least a 4-fold change in expression value, as well as at least one condition with an expression value of at least 10 RPKM. Over-representation and underrepresentation of functional annotation terms in sets of differentially expressed genes were calculated using the Fisher Exact test. The Benjamini-Hochberg correction was used to correct for multiple testing and as a cutoff for significance we used a corrected *p*-value of 0.05.

To compare gene expression, we first identified orthologs between the two strains. Here, proteins are considered orthologs if they show strong homology (having a best bidirectional hit in a blastP analysis applying an E-value cutoff of 1e-10) and if they display syntenic gene order conservation (at least 1 of 4 neighbors should be shared between the strains).

The gene expression profiles were visualized with a heat map generated by the seaborn package for python (<https://seaborn.pydata.org>). The genes were clustered using the euclidean distance and average linkage methods. The values were scaled for each gene with a z-transformation, resulting in a z-score.

Conservation of Roc1 in the fungal kingdom

The genome sequences and predicted genes/proteins of 140 previously published fungi were obtained from the publications listed in Table S1. Curating these previously published gene predictions was beyond the scope of this study. Conserved protein domains were identified using PFAM version 32 (El-Gebali et al. 2019). Roc1 is classified as a putative TF based on the presence of a Zn₂Cys₆ DNA binding domain as well as a fungal specific TF domain (Pfam domains PF00172 and PF04082, respectively). We took a multi-step approach to more accurately identify putative Roc1 orthologs. First, we identified TFs of the same broad family by selecting proteins with one Pfam domain PF00172 and one Pfam domain PF04082. Next, the sequences of these domains were concatenated and used to reconstruct an initial gene tree of fungal-specific TFs. The sequences were aligned with MAFFT 7.310 using auto settings (Katoh and Standley 2013). FastTree 2.1 with default settings was used to calculate the gene tree (Price et al. 2010). Manual inspection of the tree revealed a group of proteins from basidiomycetes and ascomycetes that clustered with Roc1, and these were labeled as candidate orthologs. Next, the full proteins of these candidate orthologs were aligned (instead of only the Pfam domains) with MAFFT and FastTree (as described above). Manual inspection of both the tree and the alignments revealed that in the Agaricomycetes the conserved sequence extended along the entire protein, while in the other basidiomycetes as well as the other phyla conservation was largely restricted to the Pfam domains. For this reason, we constructed a custom HMM model using the full protein alignments of only the Roc1 candidates of the Agaricomycetes. This HMM model was made using HMMER version 3.3.2 (hmmer.org) with default settings. The predicted proteins in the genomes of all 140 fungi were scanned with the HMM, using hmmsearch (part of the HMMER package) with



a score cutoff of 500. A new gene tree was calculated as described above, containing the proteins in the previously mentioned tree, as well as any proteins that were additionally identified with the HMM approach. Proteins with this conserved Roc1 HMM domain, Pfam domain PF00172 and Pfam domain PF04082 were considered Roc1 orthologs, while the other candidates were considered distant homologs.

A phylogenetic tree of the 140 species (species tree) was reconstructed using 25 highly conserved proteins identified with BUSCO v2 (dataset 'fungi_odb9') (Simão et al. 2015). Sequences were aligned with MAFFT 7.307 (Katoh and Standley 2013) and well-aligned regions were subsequently identified using Gblocks 0.91b (Talavera and Castresana 2007) resulting in 17196 amino acid positions. FastTree 2.1 was used for phylogenetic tree reconstruction using default settings (Price et al. 2010). The phylogenetic species tree was rooted on 'early-diverging fungi' (i.e. non-Dikarya). Python toolkit ete3 (Huerta-Cepas et al. 2016) was used to visualize the gene tree and species trees.

Deletion of gene *roc1* in strain H4-8

Gene *roc1* (proteinID 2615561 in version Schco3 of the genome of *S. commune*) was deleted using our previously published protocol (Vonk et al. 2019; **Chapter 3**), which uses pre-assembled Cas9-sgRNA ribonucleoproteins and a repair template to replace the target gene with a selectable marker. The repair template was a plasmid comprising a pUC19 backbone, 1068 bp up-flank of *roc1*, a 1326 bp nourseothricin resistance cassette, 1062 bp down-flank of *roc1*, and a phleomycin resistance cassette. The nourseothricin resistance cassette was cut from plasmid pPV010 using the restriction enzyme EcoRI. The 4112 bp pUC19 backbone and phleomycin resistance cassette were cut from plasmid pRO402 using the restriction enzyme HindIII. The up-flank and down-flank were amplified from genomic DNA of strain H4-8 using primer pairs Roc1UpFw / Roc1UpRev and Roc1DownFw / Roc1DownRev, respectively (Table S2). The 5' overhangs of these primers were chosen to facilitate Gibson assembly of the four fragments into a single plasmid (NEBuilder HiFi DNA Assembly Master Mix; New England Biolabs). The resulting plasmid pRO405 was verified by restriction analysis and Sanger sequencing.

The sgRNAs were designed on regions downstream and upstream of the up-flank and downflank of *roc1*, respectively, and one sgRNA was selected for each region as previously described¹⁷. They were synthesized *in vitro* using the GeneArt Precision sgRNA Synthesis Kit (ThermoFisher Scientific) using *roc1*-specific primers Roc1LeftsgRNAp1 / Roc1LeftsgRNAp2 and Roc1RightsgRNAp1 / Roc1RightsgRNAp2 (Table S2).

Protoplasts of strain $\Delta ku80$ were transformed with the pre-assembled ribonucleoproteins and the repair template, as previously described (Vonk et al. 2019; **Chapter 3**). A first selection was done on minimal medium with 15 $\mu\text{g ml}^{-1}$ nourseothricin. The resistant transformants were transferred to a second selection plate with nourseothricin and subsequently screened on minimal medium with 25 $\mu\text{g ml}^{-1}$ phleomycin. Nourseothricin-resistant transformants that are phleomycin-sensitive are candidates for *roc1* deletion strains, whereas those that are phleomycin-resistant are likely the result of an ectopic integration of the plasmid and therefore undesirable. Six transformants were nourseothricin-resistant, of which four were phleomycin-sensitive. The latter were candidates to have the gene deletion and a confirmation PCR was carried out with primers Roc1-Chk-A and Roc1-Chk-D (Table S2)

that amplify the integration locus (resulting in a 5007 bp product in the case of the wild-type situation, or a 3532 bp product in the case of a correct gene deletion). One of these $\Delta roc1\Delta ku80$ strains was selected and crossed with the compatible wild-type H4-8b in order to eliminate the $\Delta ku80$ background. Meiotic basidiospores were collected and the offspring was grown on minimal medium with nourseothricin and 48 out of 72 were resistant. A second selection was done with the 48 nourseothricin-resistant strains on minimal medium with 20 $\mu\text{g ml}^{-1}$ hygromycin and 23 individuals out of 48 were hygromycin-sensitive, indicating that these do not have the $\Delta ku80$ background. A nourseothricin-resistant and hygromycin-sensitive strain with the same mating type as H4-8 was selected.

Complementation of the $\Delta roc1$ deletion

The *roc1* deletion strain was complemented with a plasmid expressing a C-terminally haemagglutinin-tagged version of *roc1*. The promoter and coding sequence of *roc1* were amplified with primers Roc1ChipFw and Roc1ChipRev. Plasmid pPV009 (which contains a C-terminal triple HA tag as well as a phleomycin resistance cassette) was linearized with HindIII. Gibson assembly was used to combine the two fragments into the final complementation plasmid. The protoplasting of *S. commune* $\Delta roc1a$ and the transformation with the complementation plasmid were carried out as previously described (van Peer et al. 2009). A first selection was done on minimal medium with 25 $\mu\text{g ml}^{-1}$ phleomycin. Twenty-three transformants were transferred to a second selection plate with phleomycin. Twenty-one of them showed growth and they were initially screened on cellulose (Avicel) plates together with the wild type. Ten transformants had a similar growth when compared to the wild type. A second screening was done on minimal medium and 7 transformants resembled the wild-type phenotype. These were subjected to a PCR check with primers Roc1ChipCheckFw and Roc1ChipCheckRev (Table S2). Four transformants showed the desired 4330 bp fragment indicating they might be good candidates for $\Delta roc1$ complementation strains. One of these strains was selected and named $\Delta roc1 :: roc1\text{-HA}$. A western blot was done (see below) and this strain showed a 78 kDa band when grown on cellulose, which was absent in the wild type. This indicated that the Roc1 protein was correctly tagged with the HA-tag.

Cellulase activity assay

The *S. commune* strains were pre-cultured on a Poretics™ Polycarbonate Track Etched (PCTE) Membrane (GVS, Italy) placed on top of glucose medium for 5 days at 30 °C. The mycelia of five cultures for each strain were macerated in 100 ml minimal medium with either 1% cellulose (Avicel) or 5% glycerol (as indicated in the Results section) for 1 minute at low speed in a Waring Commercial Blender. The macerate was evenly distributed to 250 ml Erlenmeyers (20 ml each) containing 80 ml minimal medium with either 1% cellulose (Avicel) or 5% glycerol. Four Erlenmeyers for each strain were placed in an Innova incubator shaker for 10 days at 30 °C with shaking at 200 rpm. Samples of the culture medium (1 mL) were collected after 6 days and centrifuged at 9400 g for 10 min. The supernatant was then used for the total cellulase enzyme activity measurement using the filter paper activity (FPase) assay (Xiao et al. 2004). Total cellulase activity was determined by an enzymatic reaction employing circles with a diameter of 7.0 mm of Whatman No. 1 filter paper and 60 μl of supernatant. The reaction was incubated at 50 °C for 72 hours. Next, 120 μL of dinitrosalicylic acid (DNS) was added to the reaction, which was then heated at 95 °C for 5 minutes. Finally, 100 μl of each sample was transferred to the wells of a flatbottom plate and absorbance was read at 540 nm using a BioTek Synergy HTX Microplate Reader. One



enzyme unit (FPU) was defined as the amount of enzyme capable of liberating 1 μmol of reducing sugar per minute (as determined by comparison to a glucose standard curve).

Western blot analysis

A Western blot was performed to confirm that the Roc1 protein was correctly tagged with the haemagglutinin tag. Nine-day old mycelia grown on a Polycarbonate Track Etched (PCTE) Membrane (GVS, Italy) placed on top of 1% Avicel plates were harvested, snap-frozen in liquid nitrogen and ground to a fine powder using a Qiagen Tissue Lyser II (Qiagen, Germany) at 25 Hz for 60 seconds. 120 mg of biomass per sample was boiled in 500 μl of 2x Laemmli sample buffer (4% SDS, 20% glycerol, 10% B-mercaptoethanol, 0.004% bromophenol blue, 0.125M Tris pH 6.8) for 5 minutes, centrifuged for 10 minutes at 10000 g to precipitate cellular debris, and 20 μl of each sample was size separated on a 12% Mini-PROTEAN® TGX Stain-Free™ Precast Gel (Bio-Rad, USA) at 200V for 40 minutes.

After electrophoresis the proteins were transferred to a polyvinylidene difluoride membrane (ThermoFisher Scientific, USA) according to the manufacturer's specification. The membrane was blocked for 1 hour with 5% bovine serum albumin (Sigma-Aldrich, USA) in phosphate buffered saline supplemented with Triton X-100 (PBS-T) (137 mM NaCl, 10 mM Na_2HPO_4 , 1.8 mM KH_2PO_4 , 2.7 mM KCl, 0.1% Triton X-100) and then incubated for one hour with 1:10000 diluted monoclonal mouse anti-HA antibody (#26183, ThermoFisher Scientific, USA) in PBS-T. After incubation, the membrane was washed five times for 15 minutes with PBS-T. The membrane was incubated for one hour with 1:10000 diluted horseradish peroxidase-coupled goat anti-mouse antibody (#62-6520, ThermoFisher Scientific, USA) in PBS-T and washed again five times for 15 minutes with PBS-T. The antibody binding was imaged with Clarity Western ECL Substrate (Bio-Rad, USA).

ChIP-seq analysis

Protein-DNA interaction and binding sites of Roc1 were surveyed by chromatin immunoprecipitation followed by next-generation sequencing (ChIP-Seq). The ChIP was performed with Pierce Anti-HA Magnetic Beads (ThermoFisher Scientific, USA) and was adapted from previous studies in human cell lines and *Zygomycota tritici* (Johnson et al. 2007; Soyer et al. 2015) and our recently developed method for ChIP-Seq on Histone H3 (H3K4me2) in *S. commune* (Vonk and Ohm 2021; **Chapter 3**). Briefly, monokaryons of strains H4-8 or H4-8 $\Delta\text{roc1} :: \text{roc1-HA}$ were grown on medium with Avicel on Poretics™ Polycarbonate Track Etched (PCTE) Membrane (GVS, Italy). After 9 days 10 colonies were collected per replicate and washed twice in Tris-buffered saline (TBS) (50 mM Tris pH 7.5, 150 mM NaCl). The colonies were fixated by vacuum infiltration with 1% formaldehyde in TBS for 10 minutes and the reaction was quenched by vacuum infiltration with 125 mM glycine for 5 minutes. The samples were frozen in liquid nitrogen and homogenized in stainless steel grinding jars in a TissueLyser II (Qiagen) for 2 minutes at 30 Hz. The resulting homogenized mycelium was resuspended in 10 ml cell lysis buffer (20 mM Tris pH 8.0, 85 mM KCl, 0.5% IGEPAL CA-630 (Sigma, USA), 1x cComplete protease inhibitor cocktail (Roche, Switzerland) and incubated on ice for 10 minutes. The samples were centrifuged at 2500 g for 5 minutes at 4 °C and the pellet was resuspended in 3 mL nuclei lysis buffer (10 mM Tris pH 7.5, 1% IGEPAL CA-630, 0.5% sodium deoxycholate, 0.1% SDS, 1x cComplete protease inhibitor cocktail). The released chromatin was fragmented on ice for 8 minutes with sonication, using a branson sonifier 450 (Emerson, USA) with a microtip at setting 4

with 35% output. To prevent sample degradation, the microtip was cooled for 1 minute every 2 minutes. Pure fragmented chromatin was obtained by collecting the supernatant after centrifugation at 15000 g for 10 minutes at 4 °C. As input control, 300 µl of sheared chromatin was stored at -80 °C for subsequent DNA isolation (see below). The volume of the remaining sheared chromatin was adjusted to 3 ml with ChIP dilution buffer (0.01% SDS, 1.1% Triton X-100, 1.2 mM EDTA, 16.7 mM Tris pH 8.0, 167 mM NaCl, 1x cOmplete protease inhibitor cocktail). The chromatin was immunoprecipitated for 16 hours with 50 µl Anti-HA magnetic beads that were equilibrated with ChIP dilution buffer. After incubation, the beads were collected and subsequently washed in low salt washing buffer (0.1% SDS, 1% Triton, 2 mM EDTA, 20 mM Tris pH 8.0, 150 mM NaCl), twice in high salt washing buffer (low salt washing buffer with 500 mM NaCl), twice in lithium chloride washing buffer (250 mM LiCl, 1% IGEPAL CA-630, 1% sodium deoxycholate, 1 mM EDTA, 10 mM Tris pH 8.0) and twice in TE buffer. During all washing steps the samples were incubated for 5 minutes. After addition of the second lithium chloride washing buffer, the samples were transferred from 4 °C to room temperature. The chromatin was eluted from Anti-HA magnetic beads by incubating twice in 250 µl elution buffer (1% SDS, 100 mM NaHCO₃) for 10 minutes. After ChIP, the input controls were adjusted to 500 µl with water. Both samples and input controls were incubated with 50 µg RNase A for 1 hour at 50 °C and decrosslinked overnight at 65 °C with 75 µl reverse crosslinking buffer (250 mM Tris pH 6.5, 62.5 mM EDTA, 1.25 M NaCl, 5 mg ml⁻¹ proteinase K (ThermoFisher Scientific)). DNA was isolated with phenolchloroform extraction. Briefly, samples were mixed with 1 volume of phenol-chloroform (1:1), samples were centrifuged at 15000 g for 5 minutes and the aqueous phase was collected. This step was repeated 2 times. The extraction was repeated with 1 volume of chloroform, to remove residual phenol. The DNA was coprecipitated with 20 mg glycogen (ThermoFisher, USA) by the addition of 58 µl 3M NaAc pH 5.6 and 1160 µl ethanol and stored at -80 °C for 2 hours. The DNA was collected by centrifugation at 15000 g for 45 minutes at 4 °C and washed with 1 mL 70% ethanol. Finally, DNA was dissolved in 30 µl TE buffer. Next, the DNA was purified with the ChargeSwitch gDNA Plant Kit (ThermoFisher Scientific, USA) according to manufacturer's specifications and eluted in 50 µl ChargeSwitch Elution Buffer. The DNA samples were amplified and barcoded with the NEXTFLEX Rapid DNA-Seq library kit (Bioo Scientific, USA) according to manufacturer's specifications without size selection. The DNA concentration was determined with the NEBNext Library Quant Kit for Illumina (New England Biolabs, USA) and pooled in equimolar ratios with unique barcodes for each sample. The libraries were sequenced on an Illumina NextSeq 500 with paired-end mid output of 75 bp by the Utrecht Sequencing Facility (USeq, www.useq.nl).

The paired-end reads of the controls and samples were aligned to the *S. commune* H4-8 reference genome (version Schco3 (Ohm et al. 2010a)) with bowtie2 (version 2.3.4.1) (Langmead and Salzberg 2012). Reads with multiple alignments and a quality score < 2 were removed with samtools (version 1.7) (Li et al. 2009). Optical duplicates were flagged with picard tools (version 2.21.6) (Broad Institute 2009) and removed with samtools. Peaks in both WT H4-8 and H4-8 $\Delta roc1 :: roc1-HA$ were identified with macs2 (version 2.2.3) (Feng et al. 2012). To filter out any non-specific binding, peaks identified in both the WT and $\Delta roc1 :: roc1-HA$ strains were excluded from the analysis. Peaks that overlapped repetitive regions (including transposons) were removed. The peaks were associated with a gene if they were within 1000 bp of the predicted translation start site. The correlation between replicates was determined with the R package DiffBind (version 2.12.0) (Stark and Brown 2011).



Motif discovery

STREME (which is part of the MEME Suite (Bailey et al. 2009)) was used to identify conserved motifs in the ChIP-Seq peaks. STREME looks for ungapped motifs that are relatively enriched in a set of sequences compared to negative control sequences. The 200 bp region around the center of the peak was analyzed for enriched motifs, with 10000 regions of the same length from across the genome as negative sequence set. The minimum motif length was set to 5 bp and the maximum motif length to 25 bp. The location of these motifs in the ChIP-Seq peaks was determined with FIMO (which is part of the MEME Suite (Bailey et al. 2009)). The GC content along the ChIP-Seq peaks was determined with a sliding 25 bp window (step size 5 bp) and averaging the GC content for that window in all ChIP-Seq peaks. To plot the location of the conserved motifs, the peaks were first divided into bins of 20 bp. Next, the density of the motifs along the ChIP-Seq peaks was determined for each bin by dividing the number of motifs in that bin (in all ChIP-Seq peaks) by the total number of ChIP-Seq peaks.

Functional promoter analysis

Several lengths (approximately 100 bp, 200 bp, 300 bp and 700 bp) of the promoter (defined here as the region located 5' of the predicted translation start site) of gene *lpmA* (proteinID 1190128) were amplified from H4-8 genomic DNA with the primers GbGH61Pr700Fw (or the primer corresponding to the length) and GbGH61PrRev. The gene encoding the red fluorescent protein dTomato (Shaner et al. 2004) was amplified from plasmid pRO151 (Ohm et al. 2013) with primers GbdTomatoFw and GbdTomatoRev. The primers used are listed in Table S2. The plasmid backbone (which comprises a nourseothricin resistance cassette) was cut from vector PTUB750_SS3_HC_iT3_Nour_p20 (Scholtmeijer et al. 2014) with restriction enzymes HindIII and BamHI. The components of the construct were joined using the Gibson Assembly method (NEBuilder HiFi DNA Assembly Master Mix, New England Biolabs, USA), resulting in the *dTomato* gene under the control of several lengths of the promoter of *lpmA* (plasmids pRO311, pRO312, pRO313 and pRO305, which contain the promoter length of 100 bp, 200 bp, 300 bp and 700 bp, respectively). A motif in the 300 bp promoter (in plasmid pRO313) was changed from CGGACCG to ATTAAT by site directed mutagenesis using Gibson Assembly (NEBuilder HiFi DNA Assembly Master Mix) and primers GbGH61Pr300MutFw and GbGH61Pr300MutRv (Table S2), resulting in plasmid pPV049. Protoplasts of strain H4-8b were transformed with these dTomato reporter constructs, as previously described (van Peer et al. 2009). Nourseothricin-resistant transformants were selected for further analysis under the fluorescence microscope.

Fluorescence microscopy and sample preparation

Mycelia were grown in triplicate for 72h at 30 °C on a Poretics™ Polycarbonate Track Etched (PCTE) Membrane (GVS, Italy) placed on top of solid minimal medium. Microscopy samples were prepared by carefully scraping mycelium of the colony from the PCTE membrane with a scalpel and placing it on a slide with a drop of water for adherence and a cover slip. The dTomato fluorescence was detected with an Axioskop 2 plus microscope (Zeiss, Germany) equipped with a 100-Watt HBO mercury lamp and a sCMEX-20 Microscope Camera (5440×3648 pixels) using the TRITC (Tetramethyl Rhodamine IsoThiocyanate) filter (excitation at 550 nm and emission at 573nm). The images were taken using ImageFocus Alpha software (24-bit color depth).

Data availability

All genome assemblies and annotations can be interactively accessed through the JGI fungal genome portal MycoCosm (Grigoriev et al. 2014) at <http://mycocosm.jgi.doe.gov>. The RNA Sequencing reads have been deposited in the NCBI Short Read Archive under project IDs SRP048482 (strain H4-8 on various carbon sources) and SRP053470 (strain TattoneD on various carbon sources). The ChIP-Seq reads have been deposited in the NCBI Short Read Archive under bioproject ID PRJNA726034.

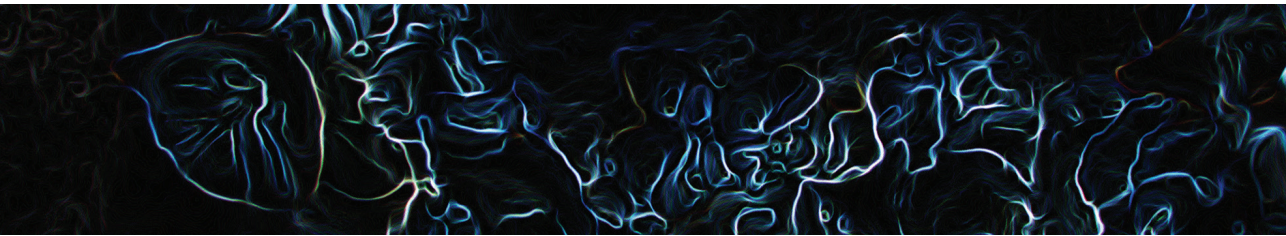
Acknowledgements

The work conducted by the U.S. Department of Energy Joint Genome Institute, a DOE Office of Science User Facility, is supported by the Office of Science of the U.S. Department of Energy under Contract No. DE-AC02-05CH11231. This project has received funding from the European Research Council (ERC) under the European Union's Horizon 2020 research and innovation programme (grant agreement number 716132). We thank Utrecht Sequencing Facility for providing sequencing service and data for the ChIP-Seq analysis. Utrecht Sequencing Facility is subsidized by the University Medical Center Utrecht, Hubrecht Institute, Utrecht University and The Netherlands X-omics Initiative (NWO project 184.034.019). We thank Steven Ahrendt for technical assistance with data submission to GenBank.

Supplementary data

All supplementary data is available at <https://www.biorxiv.org/content/10.1101/2021.06.08.446897v1.supplementary-material>





Gene deletion of eight transcription factors reveals new regulators of mushroom development in *Schizophyllum commune*

Peter Jan Vonk, Esther van den Bergh, Emmeline van Roosmalen, Éva Almási, Han A. B. Wösten, Robin A. Ohm

Abstract

The basidiomycete fungus *Schizophyllum commune* is a model organism for the study of mushroom development. A total of 10 transcriptional regulators with a role in mushroom development have previously been characterized in this basidiomycete. In recent years, transcriptomic datasets of fungal development have become available. Furthermore, a high-throughput gene deletion protocol has been developed. Here, we use this recent information and technology to characterize eight transcription factors. These transcription factors were predicted to have a role in mushroom development based on expression data and/or conservation in mushroom-forming fungi. Three new transcription factors with a role in mushroom development were identified. *Ftr1* and *Zfc4* are important during mushroom development and deletion of these genes resulted in the absence of mushrooms (in the case of *ftr1*) or arrested development during primordia development (in the case of *zfc4*) in homozygous dikaryons. Furthermore, a homozygous dikaryotic *bzt1* deletion strain formed more, but smaller mushrooms. Based on these results, the schematic overview of transcriptional regulation during mushroom development of *S. commune* has been updated. As most of the characterized transcription factors are conserved in mushroom-forming fungi, this knowledge can be used to better understand fruiting body development of economically important species.

Introduction

The mushrooms of basidiomycete fungi are among the most complex multicellular structures found in fungi (de Mattos-Shiple et al. 2016; Nagy et al. 2018). Mushrooms develop from an interconnected network of hyphae and contain basidia that produce sexual spores for propagation (Wessels 1993). Mushroom-forming fungi are primarily used as a food source and for their medicinal compounds (Grimm and Wösten 2018). The edible mushrooms are highly nutritious and can be grown on waste biomass for sustainable food production (Grimm and Wösten 2018). However, the molecular mechanisms of mushroom development are poorly understood due to a lack of functional characterization. Recently, efficient genetic tools have been developed for gene characterization in mushroom-forming fungi (Vonk et al. 2019; Boontawon et al. 2021; Vonk and Ohm 2021; **Chapter 3**; **Chapter 4**). Furthermore, the increased availability of high-resolution -omics data of mushroom development provide genes that are predicted to have a role in fruiting body formation.

Most of what is known about molecular mechanisms of fruiting body formation is based on gene deletion studies in the split-gill mushroom *Schizophyllum commune* (Schubert et al. 2006; van Wetter et al. 2006; van Peer et al. 2009; 2010; de Jong et al. 2010; Ohm et al. 2010a; 2010b; Knabe et al. 2013; Pelkmans et al. 2017; Vonk and Ohm 2021; **Chapter 4**). This basidiomycete completes its lifecycle in 10 days in the lab and an efficient CRISPR-Cas9 gene deletion method is available (de Jong et al. 2010; Ohm et al. 2010b; Vonk et al. 2019; **Chapter 3**). Furthermore, transcriptome datasets and a high-quality genome assembly are available (Ohm et al. 2010a; Pelkmans et al. 2017; Almási et al. 2019; Krizsán et al. 2019; Marian et al. 2021; **Chapter 5**). Previous studies have shown that the transcription factors (TFs) C2H2, Fst1, Fst3, Fst4, Gat1, Hom1, Hom2, Tea1, Wc2 and Zfc7 have a role in mushroom development (Ohm et al. 2010a; 2011; Pelkmans et al. 2017; Vonk and Ohm 2021; **Chapter 4**). Deletions of these genes resulted in the absence of mushroom development (*fst4*, *hom2*, *tea1*, *wc2*), arrested primordia development (*c2h2*, *fst1*, *zfc7*) or the formation of more, smaller mushrooms (*fst3*, *gat1*, *hom1*) in homozygous dikaryons. Bri1 was also thought to have a role in mushroom development (Ohm et al. 2011), but further characterization revealed that it has a role in vegetative growth and that a growth defect prevents fruiting (Pelkmans et al. 2017).

Here, we report the deletion of eight TFs in *S. commune* that were previously reported as developmentally regulated in this fungus (Pelkmans et al. 2017; Almási et al. 2019; Krizsán et al. 2019; Vonk and Ohm 2021; **Chapter 4**). The deleted genes encode proteins with different DNA-binding domains: a bZIP TF domain (Bzt1), a fungal Zn₂Cys₆ binuclear cluster domain (Ftr1, Ftr3, Ftr4), a helix-turn-helix domain (Hth1), a TEA/ATTS domain (Tea3) and a C₂H₂-zinc finger domain (Zfc4, Zfc5). Three genes, *bzt1*, *ftr1* and *zfc4* are shown to be involved in mushroom development. Surprisingly, the other TFs did not show a developmental phenotype during fruiting, despite their developmental regulation. The reporting of these TFs furthers our understanding of the genetic regulation of mushroom development and highlights the limitations of -omics data to establish a complete regulatory network for mushroom development.



Results

Gene selection

Eight predicted TFs were selected that are predicted to be involved in fruiting body development based on transcriptomics data and conservation (see below) in mushroom-forming fungi (Table 1). Gene *ptr3* is down-regulated during mushroom development, which suggests a role in repression of mushroom development. In contrast, TF genes *bzt1*, *ptr1*, *ptr4*, *hth1*, *tea3*, *zfc4* and *zfc5* are all up-regulated during different stages of mushroom development (Almási et al. 2019; Krizsán et al. 2019) (Figure 1). Genes *ptr1* and *hth1* reach their highest expression during early primordia development, while *bzt1* shows the highest expression during late primordia development. Gene *ptr4* has its highest expression during young fruiting body formation, while *tea3*, *zfc4* and *zfc5* are highly expressed during maturation of mushrooms. The TFs *ptr1*, *hth1*, *tea3* and *zfc4* were significantly up-regulated during all stages of mushroom development compared to vegetative mycelium. Genes *ptr1*, *hth1*, *tea3* and *zfc5* are not differentially expressed in time in $\Delta hom2$, $\Delta fst4$, $\Delta wc1$ and $\Delta wc2$ strains, indicating they are (indirectly) regulated by these early developmental regulators (Ohm et al. 2011; Pelkmans et al. 2017). Additionally, the epigenetic landscape suggests that *bzt1* is more transcriptionally accessible during mushroom development, since its locus has increased dimethylation on lysine residue 4 of histone 3 (H3K4) during dikaryotic development (Vonk and Ohm 2021; **Chapter 4**).

Table 1. TF genes studied in this paper

Gene name	Protein ID	PFAM domains
<i>bzt1</i>	Schco3 2624398	bZIP TF (PF00170); Basic region leucine zipper (PF07716); Aft1 HRA domain (PF11786)
<i>ptr1</i>	Schco3 2607375	Fungal Zn(2)-Cys(6) binuclear cluster domain (PF00172)
<i>ptr3</i>	Schco3 2605931	Fungal Zn(2)-Cys(6) binuclear cluster domain (PF00172); Fungal specific TF domain (PF04082)
<i>ptr4</i>	Schco3 2598013	Fungal Zn(2)-Cys(6) binuclear cluster domain (PF00172)
<i>hth1</i>	Schco3 2642179	Helix-turn-helix (PF01381)
<i>tea3</i>	Schco3 2525187	TEA/ATTS domain (PF01285)
<i>zfc4</i>	Schco3 2604883	Zinc finger, C2H2 type (PF00096)
<i>zfc5</i>	Schco3 2667924	Zinc finger, C2H2 type (PF00096)

In a preliminary analysis, the conservation of the selected TFs was assessed with Orthofinder2. To this end, the genomes of 51 species from all major orders of the ascomycetes and basidiomycetes were used (Table 2). *Bzt1* and *Zfc4* are part of large orthologous clusters (which may contain orthologs and paralogs, and for the purpose of this analysis are considered members of the same gene family) encompassing all orders used in the analysis (Figure 2). The orthologous cluster of *Zfc4* has undergone expansion in the mushroom-forming Agaricomycetes. A total of 19 family members of *Zfc4* are found in *S. commune*, including C2H2, a previously characterized regulator of primordia formation in this fungus and *Agaricus bisporus* (Ohm et al. 2011; Pelkmans et al. 2016). *Bzt1* is present as a single copy in mushroom-forming basidiomycetes, but the cluster has undergone significant expansion in multiple ascomycetes. *Ftr1*, *Ftr3*, *Ftr4* and *Hth1* orthologs are primarily found in basidiomycetes. An ortholog of *Ftr1* is found in all basidiomycetes, with the exception of the Mixiales. An ortholog of *Ftr3* is also missing from the Mixiales, as well as the Tremellales.

In contrast, orthologs of *Ftr3* are identified in two ascomycete species. While the cluster for *Ftr3* has undergone expansion, *Ftr1* is almost exclusively identified as a single copy ortholog in all basidiomycetes. Orthologs of *Ftr4* and *Hth1* are only found in mushroom-forming basidiomycetes, although no ortholog could be identified in multiple Agaricales in the case of *Ftr4*. For *Tea3* and *Zfc5*, no clear cluster could be identified and an ortholog is missing in most species included, except for a few mushroom-forming basidiomycetes.

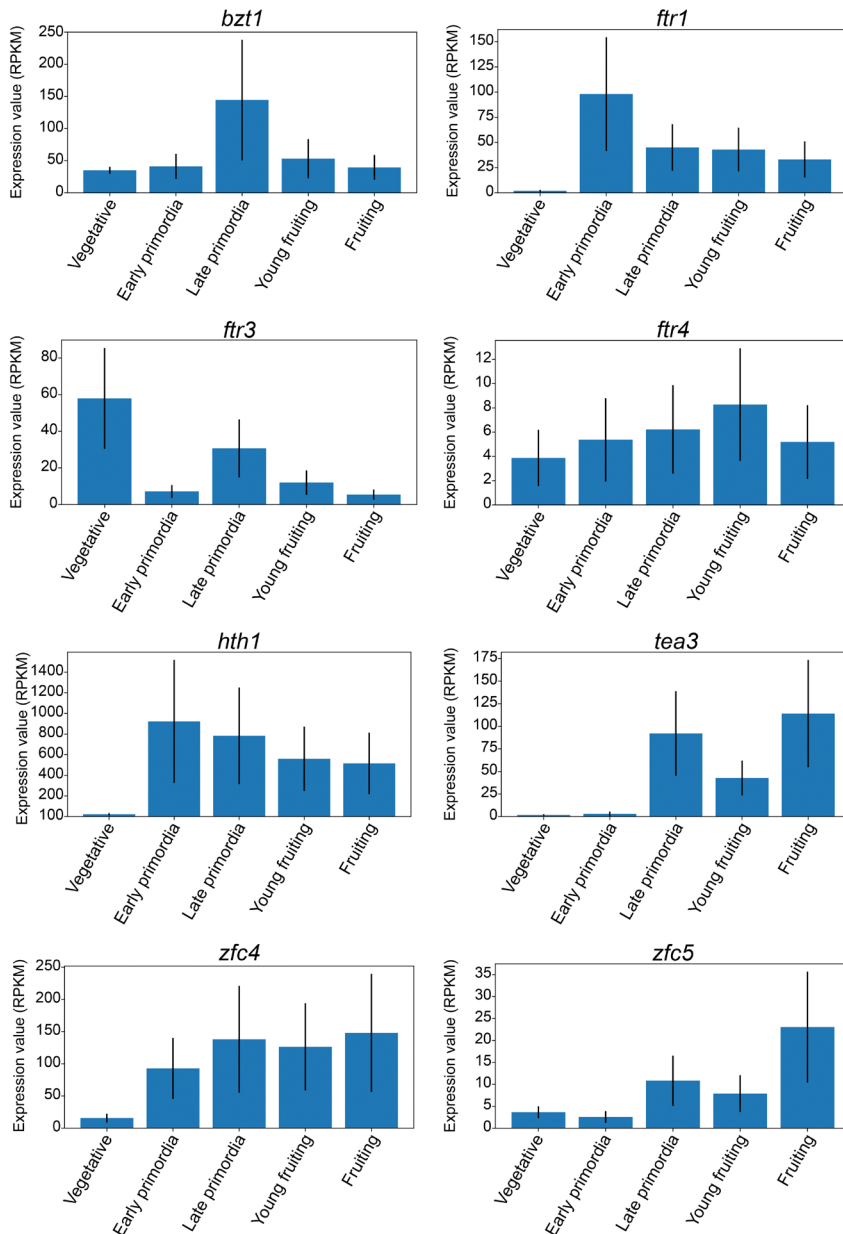


Figure 1. Expression profile of the TF genes during mushroom development. All genes, except for *ftr4*, are significantly regulated during mushroom development. Data obtained from Krizsán et al, 2019.

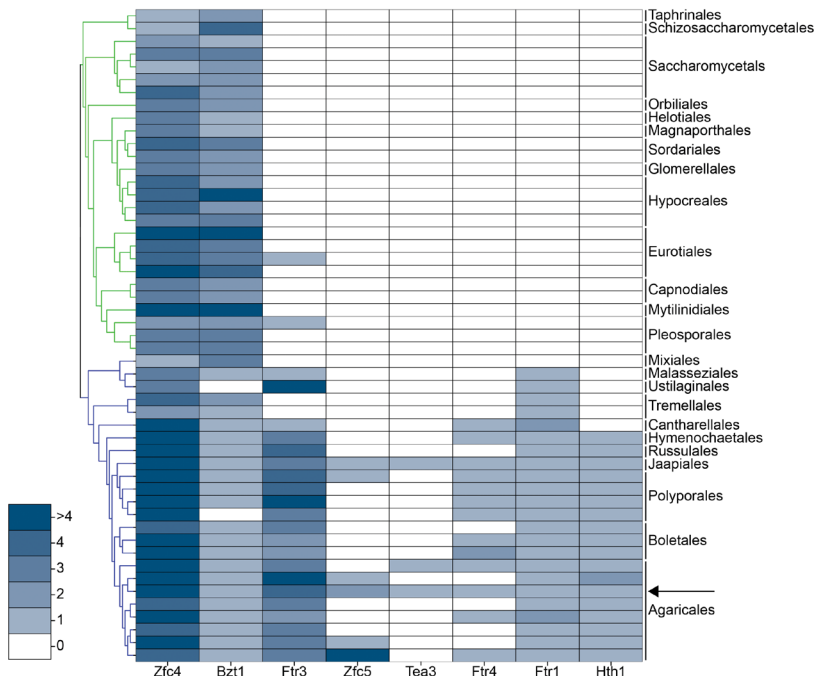


Figure 2. Heatmap of the ortholog counts of the eight selected TFs. The order of species shown is based on a species tree (left of the heatmap). Green branches are ascomycetes and blue branches are basidiomycetes. The arrow indicates *S. commune*. *Zfc4* and *Bzt1* are widely conserved. *Ftr1*, *Ftr3*, *Ftr4* and *Hth1* are primarily conserved in Basidiomycetes. No clear conservation can be identified for *Tea3* and *Zfc5*.

Gene deletion

The selected genes were deleted in a $\Delta ku80$ strain with CRISPR-Cas9 (de Jong et al. 2010; Vonk et al. 2019; **Chapter 3**) and confirmed by PCR (Figure 3). A novel approach was used for template construction to delete *ptr3*, *tea3*, *zfc4* and *zfc5*. We previously determined that 250 bp homology arms were sufficient for gene deletion by homologous recombination (Vonk et al. 2019; **Chapter 3**). We hypothesized that the use of these smaller homology arms could be combined with overlap PCR to assemble a template with selection marker that would not require any cloning. However, only *zfc4* could be deleted with the use of a linear template from overlap PCR (data not shown).

Vegetative monokaryotic growth was not affected in any of the deletion strains (data not shown). A homozygous $\Delta ptr1$ dikaryon did not form any fruiting bodies and was very similar to wild-type vegetative monokaryotic mycelium (Figure 4). This phenotype is very similar to the previously characterized homozygous dikaryotic *hom2*, *tea1* and *wc2* deletion strains. Deletion of *zfc4* resulted in a strain that did form mushrooms in homozygous dikaryons, but development was slowed and mushrooms remained immature (Figure 4). Furthermore, the density of mushrooms was reduced with only small areas of the colony forming fruiting bodies. On the other hand, a homozygous $\Delta bzt1$ dikaryon formed more, but smaller fruiting bodies and had a similar phenotype as the previously described $\Delta gat1$ and $\Delta hom1$ strains (Figure 4). Deletion of *ptr3*, *ptr4*, *hth1*, *tea3* and *zfc5* did not result in altered mushroom development in homozygous dikaryons (Figure 4). With the exception of $\Delta ptr1$ and $\Delta zfc4$, sporulation was not affected in any of the mutants. Complementation of *bzt1* and *zfc4*

resulted in the restoration of wild-type mushroom development in heterozygous dikaryons (Figure 5). However, complementation of *ptr1* did not fully rescue the phenotype. In this strain, no mushroom development took place, but the colony did grow more asymmetrically than the $\Delta ptr1$ strain (data not shown).

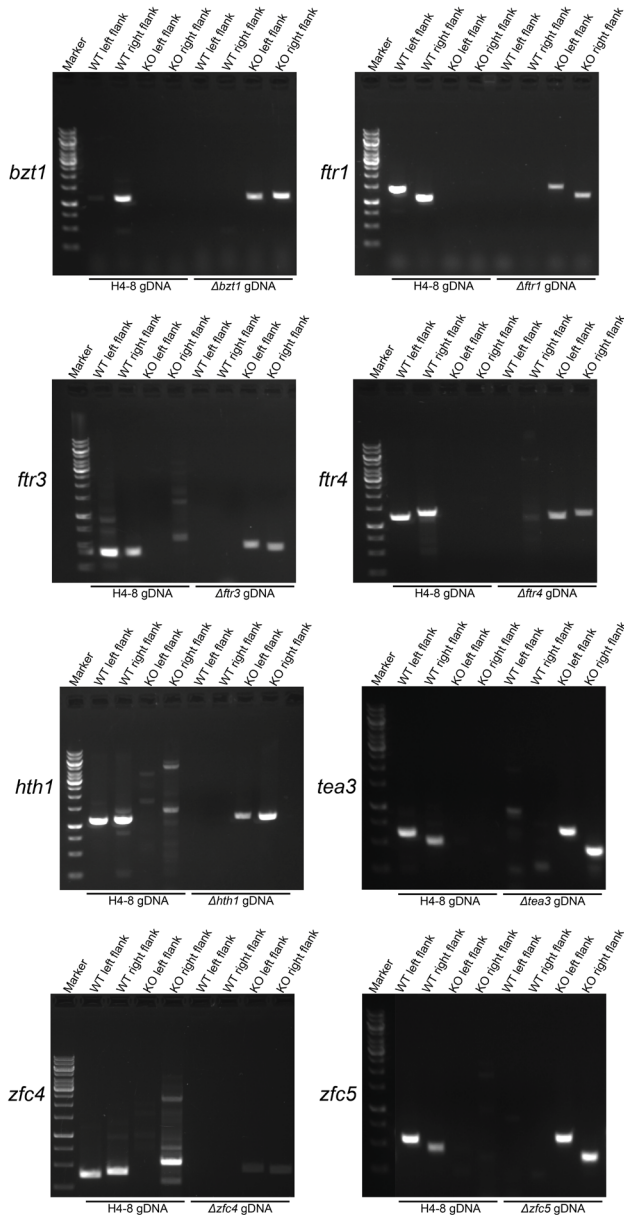


Figure 3. Confirmation of gene deletions using PCR on genomic DNA of the wild-type (strain H4-8) and deletion mutants. Primers used are listed in Table 3. WT primers should give a band in the wild type, while KO primers should give a band in the respective gene deletion strain. The PCRs should yield a band approximately 100 bp larger than the length of the homology arms used in the template. The KO primers of the right flank of *ptr3*, *hth1* and *zfc4* detect a non-specific band in the wild type. The marker used is the GeneRuler 1kb DNA ladder (ThermoFisher Scientific, USA). PCR confirmation is performed as previously described (Vonk and Ohm 2021; **Chapter 4**).

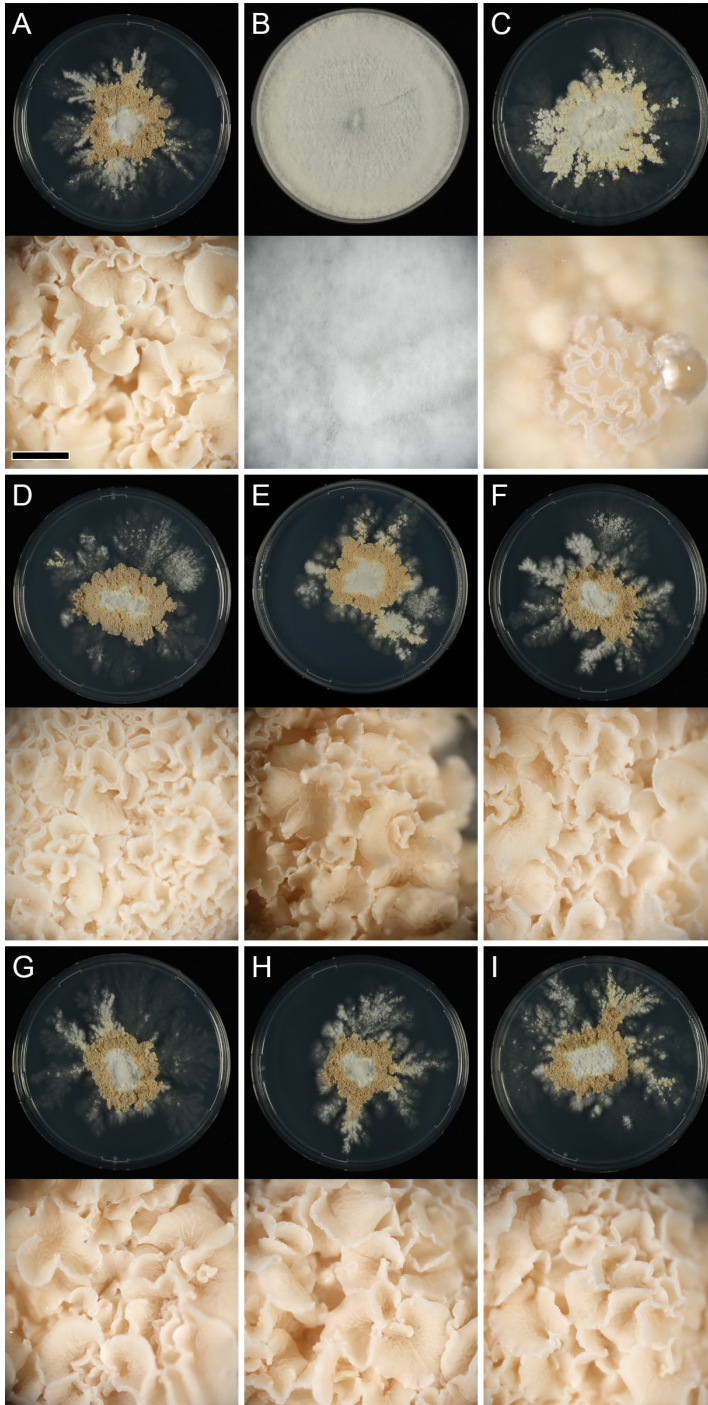


Figure 4. Colony morphology of *S. commune* dikaryotic strains after 10 days. Lower panels are magnifications of the upper panels. Bar represent 1 mm. A. Wild-type dikaryon. B: $\Delta ftr1$ dikaryon. C: $\Delta zfc4$ dikaryon. D: $\Delta bzt1$ dikaryon. E: $\Delta ftr3$ dikaryon. F: $\Delta ftr4$ dikaryon. G: $\Delta hth1$ dikaryon. H: $\Delta tea3$ dikaryon. I: $\Delta zfc5$ dikaryon.

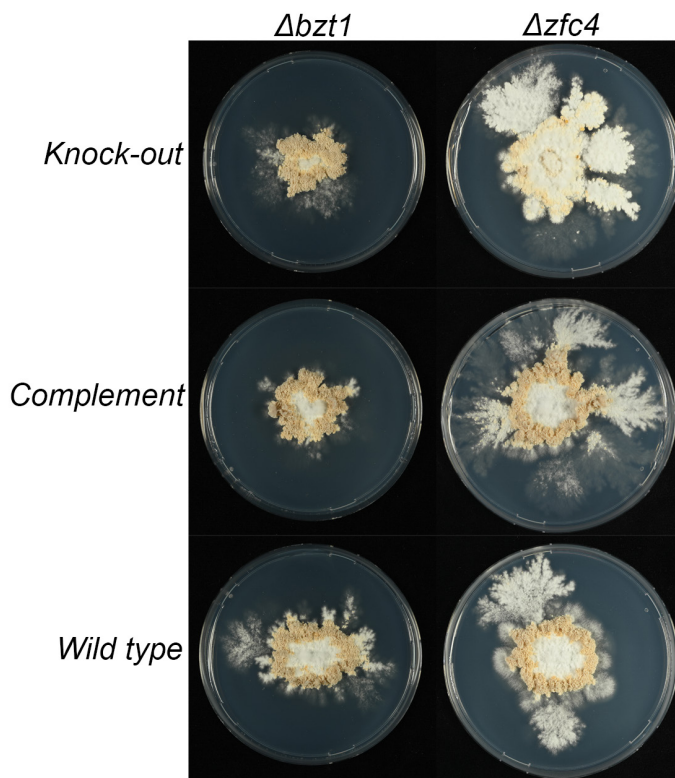


Figure 5. Complementation of $\Delta bzt1$ and $\Delta zfc4$. Upper panels are knock-out dikaryons, middle panels are complemented strains crossed with the knock-out strain, bottom panels are wild-type strains crossed with knock-out strains.

Discussion

The role of 12 TFs has previously been characterized in *S. commune* (de Jong et al. 2010; Ohm et al. 2010a; 2011; 2013; Pelkmans et al. 2017). Together with the increased availability of -omics data, this has improved our understanding of the genetic regulation of mushroom development (Plaza et al. 2014; Pelkmans et al. 2017; Almási et al. 2019; Krizsán et al. 2019; Wang et al. 2019; Yan et al. 2019; Vonk and Ohm 2021; **Chapter 4**). Here, we used functional characterization to identify the role of an additional eight TFs in mushroom development and to improve our understanding of genetic regulation of mushroom development (Figure 6).

We also attempted to improve the construction of the homology template by synthesis of the flanks, combined with overlap PCR. This method would simplify the production of a gene deletion template, since no plasmid assembly and subcloning are required. However, this method drastically reduced the efficiency of gene deletion and only worked for the deletion of *zfc4*. This contrasts our previous results on the deletion of *hom2* in *S. commune*, where 250 bp homology arms of a PCR product were sufficient for gene deletion (Vonk et al. 2019; **Chapter 3**). Previously, it was shown that the efficiency of deletion is gene-specific (Ohm et al. 2011; Vonk et al. 2019; **Chapter 3**), possibly due to differences in chromatin structure.

TF genes *ftr1* and *zfc4* are involved in different stages of fruiting. Gene *ftr1* has a role in early mushroom development and a homozygous deletion strain does not show any development beyond clamp connections. This phenotype is similar to the previously reported phenotypes of $\Delta hom2$, $\Delta tea1$ and $\Delta wc2$ strains, which were shown to have a role in early mushroom development (Ohm et al. 2011; 2013; Pelkmans et al. 2017). In homozygous $\Delta hom2$ and $\Delta wc2$ dikaryons, *ftr1* is not developmentally regulated and we therefore propose that Ftr1 is (indirectly) regulated by Hom2 and Wc2 (Pelkmans et al. 2017). A homozygous $\Delta zfc4$ dikaryon was able to form mushrooms, but development was stalled during maturation of the fruiting body and the density of mushrooms was lower than in wild type. This phenotype has not been identified previously in *S. commune* and is downstream to the phenotypes of TF genes *c2h2*, *fst1* and *zfc7*, in which mushroom development is arrested during primordia development in homozygous dikaryons (Figure 6A) (Ohm et al. 2011; Vonk and Ohm 2021; **Chapter 4**). These results are supported by transcriptomic data, as *ftr1* is up-regulated in young primordia, while *zfc4* is up-regulated in the later stages of development (Pelkmans et al. 2017; Almási et al. 2019; Krizsán et al. 2019). Unlike *ftr1*, *zfc4* expression is only reduced in a homozygous dikaryotic $\Delta wc2$ strain during mushroom development. In contrast, deletion of *bzt1* resulted in the formation of more, smaller mushrooms compared to the wild type in a homozygous dikaryotic deletion strain. The formation of more, smaller mushrooms has also been observed in homozygous $\Delta gat1$, $\Delta fst3$ and $\Delta hom1$ dikaryons (Ohm et al. 2010a; 2011). The consistency of this phenotype suggests that there are multiple regulators involved in preventing increased mushroom development. Gene *bzt1* is up-regulated during mushroom development and may inhibit progression of mushroom development locally (Pelkmans et al. 2017; Almási et al. 2019; Krizsán et al. 2019). Due to the large overlap in phenotypes, we propose that Bzt1 has a similar role as Gat1 (Figure 6A). The expression of *ftr1* is down-regulated in dikaryotic homozygous $\Delta hom2$, $\Delta wc2$ and $\Delta fst4$ strains (Pelkmans et al. 2017), which indicates that *ftr1* is (directly or indirectly) regulated by these TFs (Figure 6B). Similarly, *zfc4* is down-regulated in $\Delta wc2$, which indicates that *zfc4* is (directly or indirectly) regulated by Wc2.

Five candidate TFs did not have an apparent phenotype during mushroom development. This is surprising in particular in the case of *hth1* and *tea3* that are highly up-regulated during mushroom development (41-fold and 63-fold, respectively) (Almási et al. 2019; Krizsán et al. 2019). Furthermore, *hth1* is conserved and differentially regulated in multiple mushroom-forming species, including the close relative *Auriculariopsis ampla*. Possibly, these genes are involved in processes linked to mushroom development such as mushroom defense. These results emphasize the necessity of functional genetics for developing a regulatory model of mushroom development. To increase our understanding of these enigmatic TFs, as well as TFs with a defined role in mushroom development, TF ChIP-Seq can improve our understanding of the regulation of mushroom development (Marian et al. 2021; Vonk and Ohm 2021; **Chapter 4**; **Chapter 5**) by identifying their target genes, thus further revealing the regulatory network of mushroom development.

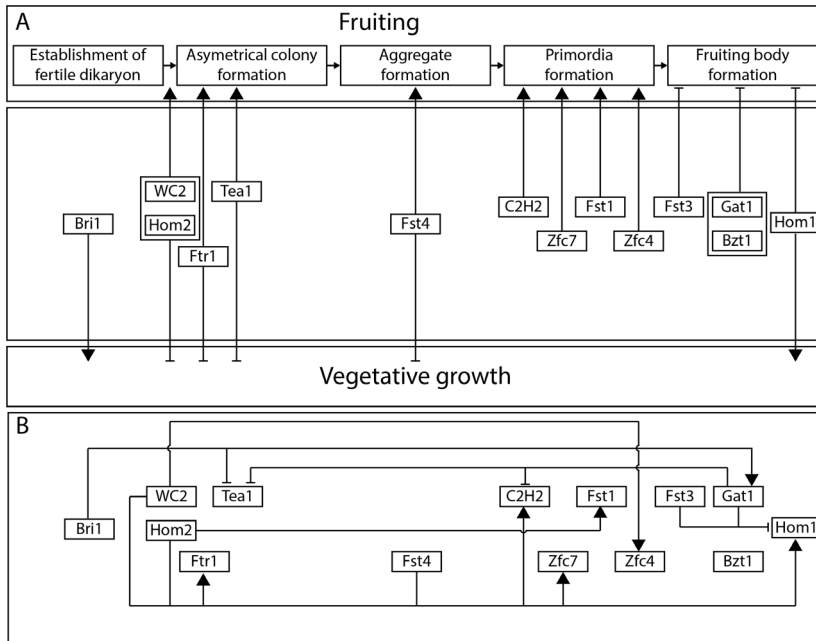


Figure 6. Proposed schematic overview of the genetic regulation of mushroom development in *S. commune* (A) and the proposed (genetic) interactions between TFs based on expression studies (Pelkmans et al. 2017) (B). The figure was adapted from Pelkmans et al. 2017 to also include TFs Ftr1, Zfc7, Fst1, Zfc4 and Bzt1.

Materials and methods

Culture conditions and strains

S. commune was grown on *Schizophyllum commune* minimal medium (SCMM) supplemented with 1.5% agar (van Peer et al. 2009) at 30 °C in the dark. For mushroom development, strains were grown at 25 °C in a 16/8 h day/night cycle for 10 days from point inoculum of compatible monokaryotic strains. For antibiotic selection the medium was supplemented with 15 µg mL⁻¹ nourseothricin (Bio-Connect, Netherlands) or 25 µg mL⁻¹ phleomycin (Bio-Connect, Netherlands) (Alves et al. 2004). All strains that are used in this study are derived from *S. commune* H4-8 (*matA43matB41*; FGSC 9210) (Ohm et al. 2010a). For mushroom development H4-8 was crossed with the compatible isogenic strain H4-8b (*matA41matB43*). Gene deletions were made in a previously published $\Delta ku80$ strain deficient in non-homologous end-joining (de Jong et al. 2010).

Orthofinder analysis

A total of 51 previously published ascomycete and basidiomycete genomes were used to construct ortholog clusters with Orthofinder2 (Table 2) (Emms and Kelly 2015; 2019). An all versus all pairwise blast between the proteins of all genomes was used as input. Orthofinder2 was run with a 4.0 inflation factor. BUSCO v2 (dataset 'fungi_odb9') was used to construct a species tree from 155 highly conserved genes (Seppey et al. 2019). The concatenated sequences were aligned with MAFFT v7.407 (Katoh and Standley 2013) and well-aligned regions were selected with Gblocks 0.91b (Talavera and Castresana 2007). This resulted in 52662 well aligned amino acid positions that were aligned with FastTree 2.1.10 (Price et al. 2010).

Table 2. Species used in the orthofinder conservation analysis

Species	Database name	Reference
<i>Taphrina deformans</i>	Tapde1_1	(Cissé et al. 2013)
<i>Schizosaccharomyces pombe</i>	Schpo1	(Wood et al. 2002)
<i>Yarrowia lipolytica</i>	Yarli1	(Dujon et al. 2004)
<i>Saccharomyces cerevisiae</i>	SacceS288C_1	(Engel et al. 2014)
<i>Torulaspora delbrueckii</i>	Torde1	(Gordon et al. 2011)
<i>Pichia pastoris</i>	Picpa1	(de Schutter et al. 2009)
<i>Candida albicans</i>	Canal1	(Jones et al. 2004)
<i>Monacrosporium haptotylum</i>	Monha1	(Meerupati et al. 2013)
<i>Botrytis cinerea</i>	Botci1	(Amselem et al. 2011)
<i>Magnaporthe grisea</i>	Maggr1	(Dean et al. 2005)
<i>Neurospora crassa</i>	Neucr2	(Galagan et al. 2003)
<i>Podospora anserina</i>	Podan2	(Espagne et al. 2008)
<i>Verticillium dahliae</i>	Verda1	(Klosterman et al. 2011)
<i>Fusarium graminearum</i>	Fusgr1	(Cuomo et al. 2007)
<i>Fusarium oxysporum</i>	Fusox1	(Ma et al. 2010)
<i>Trichoderma reesei</i>	Trire2	(Martinez et al. 2008)
<i>Metarhizium robertsii</i>	Metan1	(Gao et al. 2011)
<i>Penicillium chrysogenum</i>	PenchWisc1_1	(van den Berg et al. 2008)
<i>Aspergillus nidulans</i>	Aspnid1	(Galagan et al. 2005)
<i>Aspergillus niger</i>	Aspni7	(Andersen et al. 2011)
<i>Aspergillus fumigatus</i>	Aspfu1	(Nierman et al. 2005)
<i>Dothistroma septosporum</i>	Dotse1	(Ohm et al. 2012; de Wit et al. 2012)
<i>Mycosphaerella graminicola</i>	Mycgr3	(Goodwin et al. 2011)
<i>Cenococcum geophilum</i>	Cenge3	(Peter et al. 2016)
<i>Leptosphaeria maculans</i>	Lepmu1	(Rouxel et al. 2011)
<i>Cochliobolus heterostrophus</i>	CocheC5_3	(Ohm et al. 2012; Condon et al. 2013)
<i>Cochliobolus carbonum</i>	Cocca1	(Condon et al. 2013)
<i>Mixia osmundae</i>	Mixos1	(Toome et al. 2014)
<i>Malassezia globosa</i>	Malgl1	(Xu et al. 2007)
<i>Ustilago maydis</i>	Ustma1	(Kämper et al. 2006)
<i>Tremella mesenterica</i>	Treme1	(Floudas et al. 2012)
<i>Cryptococcus neoformans</i>	Cryne_JEC21_1	(Loftus et al. 2005)
<i>Botryobasidium botryosum</i>	Botbo1	(Riley et al. 2014)
<i>Fomitiporia mediterranea</i>	Fomme1	(Floudas et al. 2012)
<i>Heterobasidion annosum</i>	Hetan2	(Olson et al. 2012)
<i>Jaapia argillacea</i>	Jaaar1	(Riley et al. 2014)
<i>Phanerochaete chrysosporium</i>	Phchr2	(Ohm et al. 2014)
<i>Trametes versicolor</i>	Trave1	(Floudas et al. 2012)

<i>Fomitopsis pinicola</i>	Fompi3	(Floudas et al. 2012)
<i>Wolfiporia cocos</i>	Wolco1	(Floudas et al. 2012)
<i>Serpula lacrymans</i>	SerlaS7_3_2	(Eastwood et al. 2011)
<i>Coniophora puteana</i>	Conpu1	(Floudas et al. 2012)
<i>Paxillus involutus</i>	Paxin1	(Kohler et al. 2015)
<i>Pleurotus ostreatus</i>	PleosPC15_2	(Riley et al. 2014; Alfaro et al. 2016; Castanera et al. 2016)
<i>Armillaria mellea</i>	Armme1_1	(Collins et al. 2013)
<i>Schizophyllum commune</i>	Schco3	(Ohm et al. 2010a)
<i>Volvariella volvacea</i>	Volvo1	(Bao et al. 2013)
<i>Amanita muscaria</i>	Amamu1	(Kohler et al. 2015)
<i>Agaricus bisporus</i>	Agabi_varbisH97_2	(Morin et al. 2012)
<i>Coprinopsis cinerea</i>	Copci1	(Stajich, et al. 2010)
<i>Laccaria bicolor</i>	Lacbi2	(Martin et al. 2008)

Gene deletion

Homologous recombination plasmids were assembled for *bzt1*, *ptr1*, *ptr4* and *hth1* as previously described (Vonk and Ohm 2021; **Chapter 4**). Briefly, the upstream and downstream flank of the gene were amplified with gene-specific up_fw + up_rv and down_fw + down_rv primers respectively (Table 3). These flanks were cloned into the HindIII sites of pRO402, together with a nourseothricin resistance cassette digested from pPV010 between them (Vonk and Ohm 2021; **Chapter 4**). The upstream flanks contained 20 bp homology arms to the pRO402 backbone on the 5' side and the nourseothricin resistant cassette on the 3' side. The downstream flanks contained 20 bp homology arms to the nourseothricin resistance cassette on the 5' side and the pRO402 backbone on the 3' side. The fragments were assembled by Gibson assembly (NEBuilder HiFi DNA Assembly Master Mix (New England Biolabs, USA) to create homologous recombination plasmids.

Homology arms of *ptr3*, *tea3*, *zfc4* and *zfc5* were synthesized as double stranded DNA (GeneArt Strings DNA Fragments, ThermoFisher Scientific, USA) (Table 4). The upstream flanks contained a 20 bp homology arm to the upstream part of the HindIII site of pRO402 and the M13 Forward (-20) primer sequence at the 5' end and 20 bp homology arms to the 5' end of the nourseothricin resistance cassette on the 3' end. The downstream flanks contained 20 bp homology arms to the 3' end of the nourseothricin resistance cassette on the 5' end and a 20 bp homology arm to the downstream part of the HindIII site of pRO402 and the M13 Reverse primer sequence at the 3' end. For *zfc4*, a deletion template was constructed by overlap PCR of the two fragments and a nourseothricin resistance cassette. This template was amplified by primers M13F Forward (-20) and M13 Reverse and then directly used in transformation. For *ptr3*, *tea3* and *zfc5*, the fragments were assembled into pRO402 together with the nourseothricin resistance cassette as described above to create homologous recombination plasmids. All synthesized DNA fragments are listed in supplementary table 4.

Transformation of *S. commune* $\Delta ku80$ was performed as previously described with 10 μ g of two sgRNAs per gene and 100 μ g Cas9 (Vonk et al. 2019; **Chapter 3**). The sgRNAs were

produced with the p1_sgRNA and p2_sgRNA primers (Table 3) and the GeneArt Precision sgRNA Synthesis Kit (ThermoFisher Scientific, USA). Transformants were selected on nourseothricin and counter selected on phleomycin, except for *zfc4*, as the template for *zfc4* did not contain a phleomycin resistance cassette. Candidate gene deletion transformants were verified by PCR as previously described (Table 3) (Vonk and Ohm 2021; **Chapter 4**).

Complementation

The complementation plasmid of *bzt1* was assembled as previously described (Vonk and Ohm 2021; **Chapter 4**). Briefly, the gene was amplified with gene-specific primers comp_fw and comp_rv, including 1000 bp upstream and downstream to include the promoter and terminator (Table 3). The resulting fragments had 20 bp homology arms with pPV008 digested with HindIII and BamHI and were assembled into this plasmid with Gibson assembly (NEB HiFi DNA Assembly Master Mix, New England Biolabs, USA). For *ftr1* and *zfc4*, the genes were amplified with comp_fw_and comp_rv from 1000 bp upstream until the stop codon (Table 3). These fragments contained 20 bp homology arms to pPV009 digested with HindIII. pPV009 contains a pUC19 backbone, a phleomycin resistance cassette, an artificial intron, a *sc3* terminator and a 3x HA-tag. The fragments were assembled with Gibson assembly (NEB HiFi DNA Assembly Master Mix, New England Biolabs, USA). This resulted in plasmids encoding *ftr1* and *zfc4*, followed by an in-frame 3x HA-tag, as previously described (Marian et al. 2021; **Chapter 5**). Plasmids were introduced into protoplasts of the knock-out strains as previously described and complementation strains were selected based on the ability to recover the wild-type phenotype (Ohm et al. 2011).

Table 3. Primers used in this study. Underlined sequences indicate homology arms for Gibson assembly.

Primer name	Sequence
bzt1_up_fw	CTATGACCATGATTACGCCATGACGATCTACTTCCAAGCC
bzt1_up_rv	GTCCCCCTCGAGGCGCGCCGGTCTGTTGCTTCTCTTC
bzt1_down_fw	TCCCAGACCACCATGCCGGGTGCTGCAATGACGAAG
bzt1_down_rv	GATAACCTTCAGCAGAACGAGTGAAGGAGAGCAATAACG
ftr1_up_fw	CTATGACCATGATTACGCCACCGTGTGTTGGGAACTC
ftr1_up_rv	GTCCCCCTCGAGGCGCGCCGCTGAACTAAGCCAGGGTC
ftr1_down_fw	TCCCAGACCACCATGCCGGGTATCTTGCAATGTTGACCGC
ftr1_down_rv	GATAACCTTCAGCAGAACGACCTTCCATCTTCGTCTTTCC
ftr4_up_fw	CTATGACCATGATTACGCCAAGATACATCGACTCCAACGC
ftr4_up_rv	GTCCCCCTCGAGGCGCGCCCAATTATTAGGGCGCACC
ftr4_down_fw	TCCCAGACCACCATGCCGGGACGTTGGGAAAGCGTAAG
ftr4_down_rv	GATAACCTTCAGCAGAACGACTTCGTGCGATGCTGTAAGGG
hth1_up_fw	CTATGACCATGATTACGCCACTTCGACGACCTTCTCCTC
hth1_up_rv	GTCCCCCTCGAGGCGCGCCGCTGGAACCATGTATTCTGC
hth1_down_fw	TCCCAGACCACCATGCCGGGTGAGCGTAGGAAGGAAGAAG
hth1_down_rv	GATAACCTTCAGCAGAACGAATATCTTTGTCGTGGGCTC
hth1_down_rv	GATAACCTTCAGCAGAACGAACGTGTAATAGGCGGTCCAC
M13 Forward (-20)	GTAAAACGACGGCCAG

M13 Reverse	CAGGAAACAGCTATGAC
bzt1_p1_sgRNA_up	TAATACGACTCACTATAGCCGCGCTCCTTGATGCCAAC
bzt1_p2_sgRNA_up	TTCTAGCTCTAAAACGTTGGCATCAAGGAGCGCGG
bzt1_p1_sgRNA_down	TAATACGACTCACTATAGCTGCGACCATTGTTTCCTG
bzt1_p2_sgRNA_down	TTCTAGCTCTAAAACCAGGAAAACAATGGTCGCAG
ftr1_p1_sgRNA_up	TAATACGACTCACTATAGGGCACACGATGAGCTATGTTA
ftr1_p2_sgRNA_up	TTCTAGCTCTAAAACATAGCTCATCGTGTGC
ftr1_p1_sgRNA_down	TAATACGACTCACTATAGGGGACTATGGGCCCTCGCC
ftr1_p2_sgRNA_down	TTCTAGCTCTAAAACGCGAGGGGCCATAGTCCC
ftr3_p1_sgRNA_up	TAATACGACTCACTATAGGGCGGAACGCGTCCGGGGTA
ftr3_p2_sgRNA_up	TTCTAGCTCTAAAACACCCCGACGCGTTCCGCG
ftr3_p1_sgRNA_down	TAATACGACTCACTATAGGGACCCCAATCCCCGACCAG
ftr3_p2_sgRNA_down	TTCTAGCTCTAAAACCTGGTCGGGGATTGGGGTC
ftr4_p1_sgRNA_up	TAATACGACTCACTATAGGCTGCTCGCATAGCGGCCCG
ftr4_p2_sgRNA_up	TTCTAGCTCTAAAACCGGGCCGCTATGGCGAGCAG
ftr4_p1_sgRNA_down	TAATACGACTCACTATAGGGGTCTGCTGGGGTCCATGG
ftr4_p2_sgRNA_down	TTCTAGCTCTAAAACCATGGACCCAGCAGACCC
hth1_p1_sgRNA_up	TAATACGACTCACTATAGGGAGCGCTGCACTGGGGGTG
hth1_p2_sgRNA_up	TTCTAGCTCTAAAACCGACCCCAAGTGCAGCGCTC
hth1_p1_sgRNA_down	TAATACGACTCACTATAGGGTGGAGTGCACGCCAGTAT
hth1_p2_sgRNA_down	TTCTAGCTCTAAAACATACTGGCGTCACTCCACC
tea3_p1_sgRNA_up	TAATACGACTCACTATAGGCACATTCGCTGTTTCTGAAG
tea3_p2_sgRNA_up	TTCTAGCTCTAAAACCTTCAGAAACAGCGAATGTG
tea3_p1_sgRNA_down	TAATACGACTCACTATAGGCAGGTTGGCCGGTAGCATGG
tea3_p2_sgRNA_down	TTCTAGCTCTAAAACCATGCTACCGGCCAACCTG
zfc4_p1_sgRNA_up	TAATACGACTCACTATAGGGACCGCGCTTGGGCTGATG
zfc4_p2_sgRNA_up	TTCTAGCTCTAAAACCATAGCCCAAGCGCCGGTC
zfc4_p1_sgRNA_down	TAATACGACTCACTATAGGGTCCCGATGTCGGGTTCTG
zfc4_p2_sgRNA_down	TTCTAGCTCTAAAACAGAACCCGACATCGGGGAGC
zfc5_p1_sgRNA_up	TAATACGACTCACTATAGGGTTGTAACCCCGTTGCACC
zfc5_p2_sgRNA_up	TTCTAGCTCTAAAACGGTGCAACGGGAGTTACAAC
zfc5_p1_sgRNA_down	TAATACGACTCACTATAGGGTTGTAACCCCGTTGCACC
zfc5_p2_sgRNA_down	TTCTAGCTCTAAAACGTGTATGCAATGGACTGCGC
bzt1_ChkA	GGACTATCCTGCATGCATTG
bzt1_ChkB	GGTATTAGCCCGATGTTGTC
bzt1_ChkC	GTCGACGACATGATCTCGG
bzt1_ChkD	AAAGAACCCCTCAACGAGCTC
ftr1_ChkA	GCCAGCGATGCTGGTAGAT
ftr1_ChkB	GGATATGCCGTACCTCTCA
ftr1_ChkC	ACCACGGTTTCTATCATCAC



ftr1_ChkD	CGGAGAATGGATCTGTTCTC
ftr3_ChkA	TGACGGGCCTTAAGAATCCG
ftr3_ChkB	TTGACATCCTCCTCGGT
ftr3_ChkC	GGGGATTGGGGTCTATCGGA
ftr3_ChkD	GTCAGATGTGTCCCCGATG
ftr4_ChkA	TGAACGTGCTACAAACCC
ftr4_ChkB	TCCTGTCAACGCTTACGG
ftr4_ChkC	GTTGAGGAAAGGGTGGAGG
ftr4_ChkD	GGCAGAACATTCAGAAGGC
hth1_ChkA	GAACTTGC GCGAGAAGAG
hth1_ChkB	CACTCCACCGCTTGATTATAC
hth1_ChkC	GGCCATTGCAGTAAGTTGAG
hth1_ChkD	GAGCATTACGAGGACTGACC
tea3_ChkA	GTCCAGTCCTCTGCAAAGCT
tea3_ChkB	AACCTCTCGCGTCACCTCTA
tea3_ChkC	GATGGAGTTTGCTGGAAGGA
tea3_ChkD	CCGGCCAGGATGTCTTTCTT
zfc4_ChkA	AACGTCAGCGCAAGAGAGAA
zfc4_ChkB	GCGTGGGATGAGATGACGAA
zfc4_ChkC	GGGTCTGTGGGGATGTCTG
zfc4_ChkD	AGGAAAAAGCGAGCTCCTGG
zfc5_ChkA	CGAGATGAAGCGAGAAAACC
zfc5_ChkB	GTCAACGTGCAGTGGATGAC
zfc5_ChkC	AGTTCAAGATTGCGCCTGT
zfc5_ChkD	CTTCAAGCGGATGTGAAAT
nour_ChkB	CCGAAAGATCCGATCGATAC
nour_ChkC	CGTCATGAATGAAGCCTCAG
bzt1_comp_fw	<u>GC</u> GTGGCCCAAGCGTTGGACTCTGACAACGTCCCATT
bzt1_comp_rv	<u>AG</u> ACTGACGTGCACTCACAGAGGAAAAGTTGGATGGCTCA
ftr1_comp_fw	<u>GC</u> GTGGCCCAAGCGTTGGACCGTGAATTGGAGGCGTAT
ftr1_comp_rv	<u>TC</u> AGGGACGTCGTAGGGGTAGTGATGATAGAAACCGTGGTC
zfc4_comp_fw	<u>GC</u> GTGGCCCAAGCGTTGGAGTATAGACTGGCGGAGGAG
zfc4_comp_rv	<u>TC</u> AGGGACGTCGTAGGGGTAAGCCTTAGACTCGGTTACATCC

Table 4. Synthesized double-stranded DNA fragments used in this study

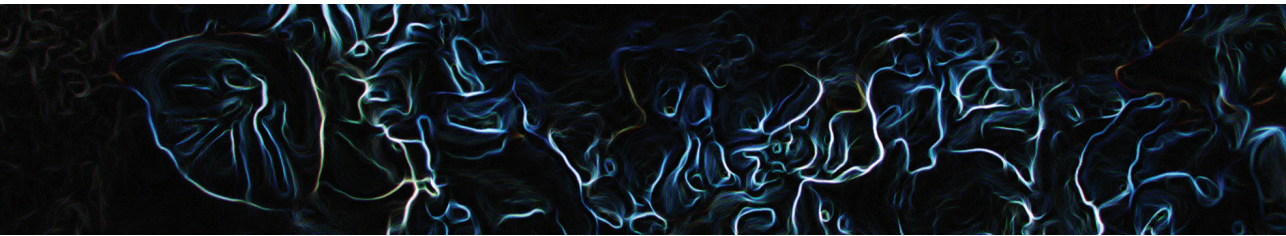
Fragment name	Sequence
<i>ptr3</i> upstream flank	CTATGACCATGATTACGCCAGTAAAACGACGGCCAGAGCTACCTGTCTATCCAGGTTTTGCGCGAC- CAACCCACAGCTATTACCGTGCCTCTCTGAGGCCCTGACGATCCTTGTGTACGGGTAAGCTG- CACGCGTCTTCTTAATGATGGACACTAACAGCATCCTCTATGATGTGCATTACTACGGGTACATCCCAT- GTTGGTTCGAACATCGGGCACCATGTCATCTCCGTCTCTCTCTCCGAGCAGTCACGACGAGTGTAT- TCTTCTCCAATTCGGCGCCCTCGAGGGGACTCGACCAGGGCTGGTG
<i>ptr3</i> downstream flank	TTACCATCCTTCCACCTCCCAGACCACCATGCCGGGAATTGGACTGCCTACAAAAAGAAAGAAATC- GCTGGCGATTATCCGGATATCTATGTAGCTTGCTTCTTCGGGTGTAGCTTACTACTGTGCCCTTGTGA- ATTTGTGTTCTCCATCCAATTCGTCCGACCGATGTACTTTACATACCACCCTACCTTACTTACTTGTCT- GCTCGGATGTTATCGCCGCGGATGTCTACTGTAGTACTTCTGTATGATCTTGGATTATGCATGGTG- CGGTTCCGTGTATCATAGCTGTTTCTGTCTGTTCTGCTGAAGGTTATC
<i>tea3</i> upstream flank	CTATGACCATGATTACGCCAGTAAAACGACGGCCAGATTACCTGCCTAGTCGGCTACTGTGCGCACCG- GGAAGCCGCCCCGCCAGTCTCTGCTTGCGCCACATCGGATTCTCCGAAAGACATGCATTACCATC- GTAGCTCGTGAGCCCGAAAATACATCTGACCAGAAGAAAAGACCGCAACCAAGACAGTGGATTG- TACAGTATGCTGGAGACACTACACTAAGGTACAGGGGTGATACACAGTCGAGCAGGTAGGTCACA- CAAAACCTACGTACTTGTACATATTATACTTACGAGGCAGGAAGCTATATATCGCAACGAGACACGGAG- CAGGGAGCGTCTCAAAAAGAGCGTGGTATAAGAGCAGGGCAGTCCAAGTTTGTCCAAGCGCAAGA- TAAGGTGACGCGAACAGTGTCAATCGGAAATCGTAGTCTCTAATTCGGCGCCCTCGAGGGGGACTC- GACCAGGGCTGGTG
<i>tea3</i> downstream flank	TTACCATCCTTCCACCTCCCAGACCACCATGCCGGGAATTGCCGGCGAGAGATACCGAGTCTTGAC- GAAGGCATGAGGGTCTTGAGGGAAGGTTGAGCTTGAAGGAGGGGATTCGCGAGGCCGGCTGGAT- GGAAGTGCAGGAAGAGAGCAATGCGCAATCAACAACAACAACGCGTCAATGCGCCGCTCGAC- CCCCTGACCAACCGTTCATGATCGCGTCCAATGCGGGCAAAACGCGACTCGTCAACAACGTC- CAGCTTCAAGTTTCCAACAGTCGCGCTCATAGCTGTTTCTGTCTGTTCTGCTGAAGGTTATC
<i>zfc4</i> upstream flank	CTATGACCATGATTACGCCAGTAAAACGACGGCCAGTGCCTGTATCATCATGTGATGTCACAGTTC- GACTTTGACGTGACACGGAGAAAAGACCTACACCTCGTCTATAAAAGGATACGCGCTCTTGCCATGAC- CCTCCGTGCGGGGGCATTACATCATGAATTCGATCCATATATTCAAAGACTTCATAAAGACATCACTATC- CAGCTACGCTAAGTAAGTCAGAGGGTATCACAAGAACAGACAGACCAAGATGGATAAGTAGCCG- TATCGACAGTCCATTCAATTCGGCGCCCTCGAGGGGACTCGACCAGGGCTGGTG
<i>zfc4</i> downstream flank	TTACCATCCTTCCACCTCCCAGACCACCATGCCGGGAATTGGTTGACGGGAAGGGGAGGGCGGC- CAAAGACGAAAGGGCTTCTGATCGTACCGCTCGCTTATATTCGTCTCTACCGTGGAGGAAAGCGAAG- CCGGGCCCGCTGTTGAAGGCCCGCTTCTAGCCGATACACATCATTAACCCCGCTTTACGTC- TACCTGCCATCACGGGCTGACCCGCGTCACTTCCGCTCTCGCTCCCTCATGCCAAACCATGTT- CATCGCCGCTGAGGCTATCGCCTGTATAGCTGTTTCTGTCTGCTGAAAGTTATC
<i>zfc5</i> upstream flank	CTATGACCATGATTACGCCAGTAAAACGACGGCCAGATATCAAGCAACGATACAAGTTGATCGATATC- CCCGACGCCAACCGACGACGTTGAACGGATGGCGCAAATACGAGCGCTCTACAAAGACGATCAG- CAAAGGACGAAGACGACGACCCGTACGCGCAAGCGCAAAATTGGAAGGACATACTGAGATGTG- CAATACAGAAAGAGGAGAGAAGAGGCACTGCGGACAAAAGAAGAAGCAGCAGTACAATGAGG- GAGGAGGCAAGAACAGCAGCGTGAGACGATGAAGGGTGACACGTGACAAAAAGTACTATGACGAC- GCAGGAGCGGAGCATCGGCCGAATCGGATCAATCCCGTTCACCCGAAAGTCTTGTAAAAATCTCCG- CAAAACGATACCACAAGAAGCGGTGAGATAGTAACTTGAAGTCACTACCCCAACCAACCTATACCTATCGTAT- GACCAGCGTCATAGGCCACACCTCCCTCTCCCATCAAACGCTATCGTTCGCATCTCTAATTCGGCG- CGCCTCGAGGGGGACTCGACCAGGGCTGGTG
<i>zfc5</i> downstream flank	TTACCATCCTTCCACCTCCCAGACCACCATGCCGGGAATTACATCTCTGTTGGCTGGCTAAATGGGT- GTGGAAGTTGCAGATCAGCCGTCCAGTAGCCGCACAGCAGAGGCCGGGACATTAGAGCCCAACCTTC- GATCCTGTCTCGTGACTTACCGGCCCGGGTGTGCTACGGGCATGCGACCTTCTGTGTACGACAG- GAATACGGCAAGAGTCTGTAATCTTGAGAGGGGCGAGGTGCGTGGAGATTCTGCCGCTAGATGGA- GAGCTTGGCCCAAGATTTGGGGTAGTGCATATCAGCCGACGACCTACGAATCTTCGAGCTGTCTGT- GTGTCTCGGTCGCCCTTTCGATGACACTTCAGATTCTGTTCTTTGGGACTAGTTCATCCAGGCCCTCT- TATTGGACTGGCGAGTTGTCTACGATGTCAAGGCTACCGACAAGCGTCTTACGCTCCTGAACG- CAATTCAGTACGAAAGCCCGAGCGCGTTCGTAGACAGAGTCTGTACGAAAACGACGGAGGGT- CATAGCTGTTCTGTCTGTTCTGCTGAAGGTTATC



Acknowledgements

This project has received funding from the European Research Council (ERC) under the European Union's Horizon 2020 research and innovation programme (grant agreement number 716132).





**Targeted gene knock-in
reduces variation between
transformants in the
mushroom-forming fungus
*Schizophyllum commune***

Peter Jan Vonk, Robin A. Ohm

This chapter is based on Vonk, P. J. & Ohm, R. A. (2021). Targeted gene knock-in reduces variation between transformants in the mushroom-forming fungus *Schizophyllum commune* (manuscript under review)

Abstract

Gene integration in mushroom-forming fungi currently occurs by the ectopic integration of a plasmid. The locus of integration is unpredictable and, problematically, this generally results in a high variability in gene expression and phenotypes between the transformants. Here, we developed an approach for targeted gene integration (knock-in) in the basidiomycete *Schizophyllum commune* by replacing a 75 bp non-coding region of the genome with a selection marker and an arbitrary gene of interest using CRISPR-Cas9 ribonucleoproteins. To assess the suitability of our method, we compared targeted integration and ectopic integration of the gene encoding the red fluorescent protein dTomato. Targeted integration resulted in a higher average fluorescence intensity and less variability between the transformants. This method may be applied to any gene construct and may therefore greatly increase the efficiency of functional gene analysis in *Schizophyllum commune*.

Introduction

Mushrooms are primarily used as a sustainable food source, but they also produce many pharmacological compounds and carbohydrate-active enzymes (de Mattos-Shiple et al. 2016). *Schizophyllum commune* is a mushroom-forming basidiomycete in the order Agaricales and serves as a model for fruiting body development due to its short life cycle and genetic accessibility (Ohm et al. 2010a). Unlike most mushroom-forming fungi, high transformation efficiency can be achieved in *S. commune* with PEG-mediated transformation of protoplasts (de Jong et al. 2010; Ohm et al. 2010b; Vonk et al. 2019; **Chapter 3**). Additionally, an efficient gene deletion (knock-out) method is available (Vonk et al. 2019; **Chapter 3**). These methods provide quick and efficient genome editing tools to study the function of genes *S. commune*.

The study of gene function often requires the complementation of gene deletions, over-expression of genes, the expression of recombinant genes, or the heterologous expression of genes encoding fluorescent markers (Ohm et al. 2011; 2013; Pelkmans et al. 2017; Vonk and Ohm 2021; **Chapter 4**). The current gene integration method relies on random integration of a plasmid that comprises the gene of interest and a selectable marker (Schuren and Wessels 1994). This method reliably creates transformant strains, but expression of the gene can vary considerably between these strains with some not even showing expression of the integrated gene (van Peer et al. 2009). This can likely be attributed to variations in copy number, to partial integration of the plasmid into the genome (which may result in an incomplete gene), and the epigenetic state of the locus of integration. Moreover, some strains show phenotypes that are not caused by the integrated gene but by the interruption of a gene at the integration site. It is often difficult to distinguish between these two, which complicates the study of gene function. Fungal genomes generally have a high gene density. The 38.67 Mbp genome assembly of *S. commune* encodes 16,204 predicted genes, resulting in 419.03 genes per Mbp and a coding content of 52.89% (Ohm et al. 2010a; Marian et al. 2021; **Chapter 5**). Including regulatory elements of the genome, such as promoters, enhancers, terminators and non-coding RNA transcripts, this results in a very dense genome where random integrations are likely to affect genetic elements at the site of integration.

High variation of phenotypes between transformants complicates the study of gene function, especially since the observed phenotype may not even be caused by the gene of interest. For this reason, generally several transformants are phenotyped in an effort to identify the actual phenotype of the gene integration. Instead, it would be beneficial to predictably target the gene of interest to a predetermined locus, leading to consistent expression dependent only on the selected promoter. This approach has already been applied in other fungal model species, including *Saccharomyces cerevisiae* and *Neurospora crassa* (Matsura et al. 2015; Ronda et al. 2015), but not in any mushroom-forming fungus. Previously, homologous recombination (which is required for targeted integration) was not efficient enough in *S. commune* to make this a feasible strategy. Furthermore, transformation in *S. commune* always requires a selection marker, making the method used in *S. cerevisiae* (which does not require a selection marker) unfeasible. However, we recently developed a CRISPR-Cas9-based method that considerably increases the occurrence of homologous recombination (Vonk et al. 2019; **Chapter 3**). Here, we modified this method to efficiently target a gene of interest and a nourseothricin selection marker to a non-coding locus by homologous recombination. We show that this greatly enhances the reproducibility of integration and gene expression compared to ectopic integrations.



Results

A suitable locus for targeted integration was selected using the following criteria: the neighboring genes (i) should be convergently transcribed and (ii) should be spaced at least 2 Kbp apart, to minimize the odds of disrupting regulatory elements in a promoter. The neighboring genes (iii) should have stable expression during development and (iv) active histone 3 lysine 4 dimethylation (H3K4me2) during development (which indicates that the chromatin structure facilitates transcription), to increase the odds of stable expression solely under control of the selected promoter. Based on these criteria, a 2723 bp area on scaffold 6 from 2367903-2370626 was selected (Figure 1A). This region is flanked by a putative vacuolar transporter chaperone (protein ID Schco3|2627341, 57% amino acid identity match to *S. cerevisiae* VTC4) and a fungal-specific TF (protein ID Schco3|2543274) that both have stable expression at approximately 40 FPKM during development (Almási et al. 2019). Furthermore, we previously determined that this region has high H3K4 dimethylation that does not change during development (Vonk and Ohm 2021; **Chapter 4**).

We created a plasmid to facilitate targeted integration, comprising a nourseothricin resistance cassette flanked by 1.1 kbp upstream and downstream homology flanks. A promoter, gene of interest and terminator can be subcloned into an NcoI restriction site between the upstream flank and nourseothricin resistance cassette. Moreover, a phleomycin resistance cassette is located outside the homology flanks, allowing for counter-selection of transformants that do not originate from a double cross-over. Upon successful integration into the genome, this would result in the deletion of 75 bp at the integration site, replacing it with the nourseothricin resistance cassette and the gene of interest (Figure 1). Homologous recombination during the transformation is further induced by a CRISPR-Cas9 ribonucleoprotein programmed to cut in the integration site.

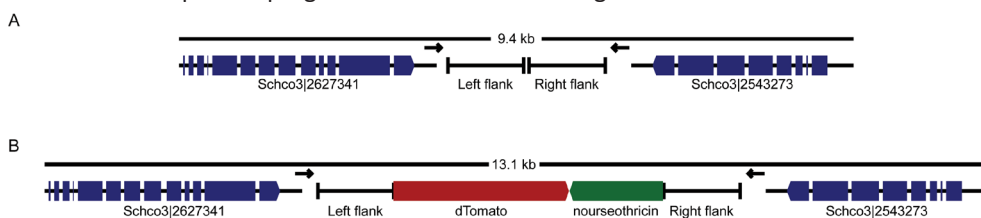


Figure 1. Genomic region of scaffold 6 (2,364,297 – 2,373,735 bp) before (A) and after (B) integration of the targeted insertion. Arrows indicate the location of PCR primers to verify successful targeted knock-in transformants.

We determined the efficacy of our method by comparing transformants generated by the traditional ectopic integration approach with transformants generated with our novel targeted integration approach. As a marker gene we used dTomato under control of the tubulin promoter (Figure 1B), which allowed us to efficiently determine the variation between the transformants by measuring the colony-wide intensity of red fluorescence as well as its distribution pattern across the colony. We first transformed wild-type *S. commune* with our plasmid but without Cas9-RNPs, which resulted in random integration, as verified by PCR (Figure 2A). Twelve nourseothricin-resistant transformants, named E1-E12 were screened for dTomato fluorescence (Figure 2B). The fluorescence intensity varied greatly between the transformants with a spread of 115.4 arbitrary units of fluorescence (AU) between the strain with the lowest and highest fluorescence (0.6 AU and 116 AU, respectively) (Table 1). Strain E11 showed very little fluorescence, while strain E1 had the highest fluorescence (Figure 2D).

Next, we created targeted knock-in transformants by introducing the plasmid in a $\Delta ku80$ strain (which is deficient in non-homologous end-joining) assisted by Cas9-RNPs. This resulted in 6 nourseothricin-resistant, phleomycin-sensitive strains, named TI1-TI6, that were all red fluorescent (Figure 2C). With PCR it was confirmed that all targeted knock-in transformants integrated the dTomato gene and nourseothricin resistance cassette at the targeted locus (Figure 2A). Compared to the ectopic integration transformants, the spread in fluorescence intensity between the lowest and highest fluorescent strain was much lower at 44.2 AU (69.3 AU and 113.2 AU, respectively) (Table 1). Furthermore, the variance was markedly lower. Additionally, the average intensity was 40.1 AU higher in the targeted integration transformants. While no strain showed more intense fluorescence than ectopic integration strain E1 (possibly due to several integrations of the plasmid), only three of the twelve ectopic integration strains had a higher fluorescence than the lowest fluorescence intensity measured in the targeted knock-in transformants (Figure 2D).

Discussion

We developed a method for targeted gene integration (knock-in) in *S. commune*. This method greatly reduced the variation in fluorescence intensity between the transformants from 115.4 AU to 44.2 AU (in transformants resulting from ectopic integration and targeted integration, respectively). Average dTomato fluorescence was also stronger during targeted integration, indicating that the selected region for targeted integration is suitable for expression of genes. Unlike a similar method applied in *S. cerevisiae*, our method does not rely on the integration of a selection marker (Ronda et al. 2015). It was previously shown that homologous recombination and transformation efficiency are not sufficient for transformation without a selection marker in *S. commune* and therefore a selection marker is still required (Vonk et al. 2019; **Chapter 3**). Although the transformation efficiency with targeted integration is still markedly lower than with ectopic integrations, it is comparable to the efficiency of Cas9-RNP-mediated gene deletion and therefore sufficient for gene integration. Although the size of the integration was considerably larger (3.8 kbp) than in the case of a gene deletion (1.3 kbp), the transformation efficiency did not appear to be negatively affected. Together, this method expands on the toolkit available for functional genomics in *S. commune* with reliable and consistent expression of integrated genes. This can be used for the complementation of previously deleted genes, but also the integration of genes modified in their active sites. An example of this is the mutation of the phosphorylation sites of the homeodomain TF *hom2* (Pelkmans et al. 2017). Furthermore, combined with our previously developed CHIP-Seq protocol, it enables efficient integration and expression of epitope-tagged TFs to identify their binding sites (Vonk and Ohm 2021; **Chapter 4**).



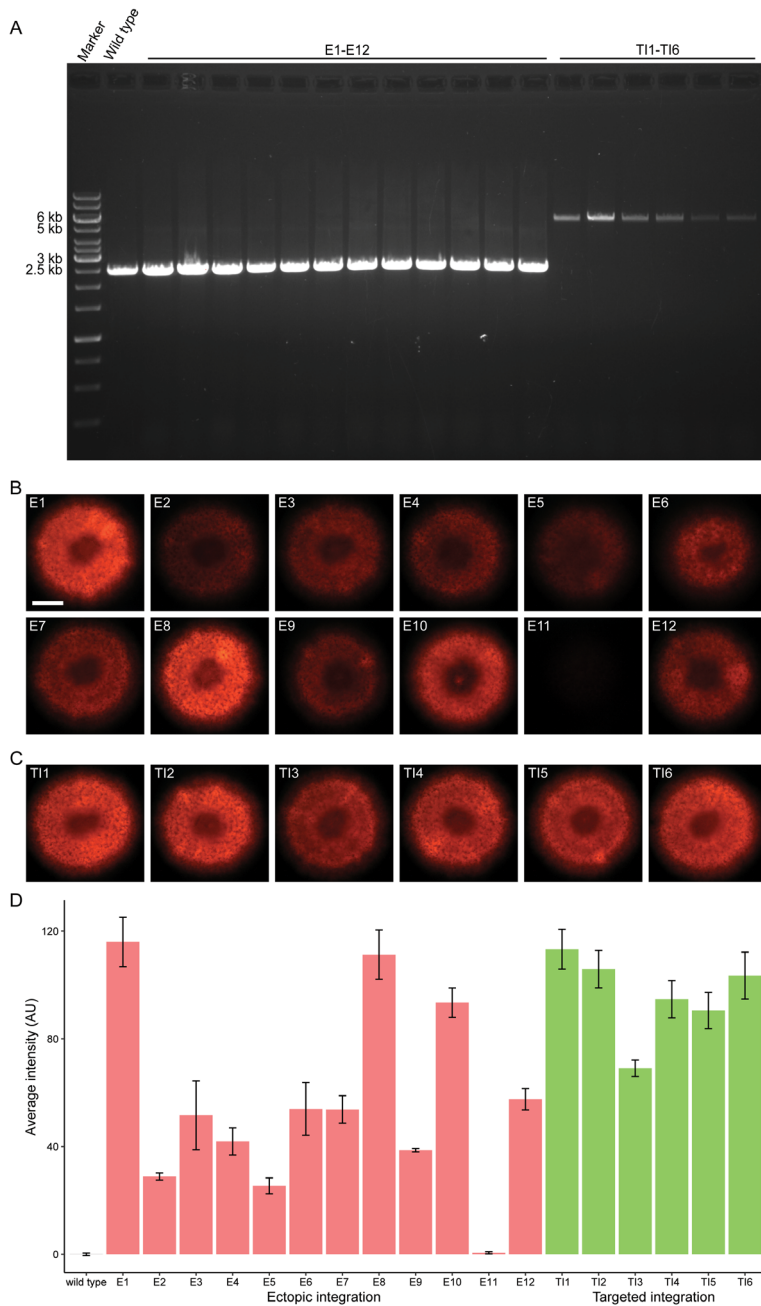


Figure 2. Genotyping and phenotyping the strains transformed with the dTomato targeted insertion plasmid. **A:** PCR on the targeted integration locus. Integration of the dTomato expression cassette and nourseothricin cassette results in an increase in band size from 2473 bp to 6178 bp. All ectopic integration strains show the wild-type band, while all targeted knock-in strains show the larger band that indicates successful integration. **B:** Strains with ectopic integration of dTomato. The white bar indicates 1 cm. **C:** Strains with targeted integration of dTomato. **D:** Quantification of fluorescence intensity in arbitrary units. On average, fluorescence is more consistent in strains generated by targeted integration, compared to ectopic integration. The fluorescence was measured in three biological replicates.

Table 1. Statistics on dTomato fluorescence after ectopic and targeted integration.

Strain	Average fluorescence intensity	Minimal fluorescence intensity	Maximum fluorescence intensity	Spread	Variance
Ectopic integration	56.1	0.6	116	115.4	1110.96
Targeted integration	96.2	69.1	113.3	44.2	201.2

Materials and methods

Culture conditions and strains

S. commune was grown from a small agar inoculum on solid *Schizophyllum commune* minimal medium (SCMM) supplemented with 1.5% agar at 30 °C (van Peer et al. 2009). All strains are derived from *S. commune* H4-8 (*matA43matB41*; FGSC 9210) (Ohm et al. 2010a). For targeted integration, a previously published $\Delta ku80$ strain in a H4-8 background was used (de Jong et al. 2010). For selection on nourseothricin (Bio-Connect, Netherlands) or phleomycin (Bio-Connect, Netherlands), SCMM was supplemented with 15 $\mu\text{g mL}^{-1}$ and 25 $\mu\text{g mL}^{-1}$ antibiotic, respectively (Alves et al. 2004).

Plasmid construction

The locus selected for targeted integration was on scaffold 6: 2369122-2369196. Flanks upstream and downstream of this region were amplified with *spi_up_fw* + *spi_up_NcoI_rv* and *spi_down_fw* + *spi_down_rv* respectively (Table 2), resulting in 1106 bp and 1107 bp fragments. The primer *spi_up_NcoI_rv* introduced an NcoI site into the 3' end of the upstream fragment for future cloning. The targeted integration plasmid was constructed as previously described for gene deletion plasmids (Vonk and Ohm 2021; **Chapter 4**), resulting in plasmid pPV033 (Addgene plasmid # 178359). To construct the dTomato targeted integration plasmid, the tubulin promoter and dTomato were amplified from pPV040 with primers *ptub_dtom_fw* + *ptub_dTom_rv* resulting in a 1475 fragment (Table 2). The *hom2* terminator was amplified from the *S. commune* H4-8 genome with primers *hom2_term_fw* and *hom2_term_rv*, resulting in a 1021 bp fragment (Table 2). Primers *ptub_dtom_fw* and *hom2_term_rv* contained 20 bp overhangs with pPV033 at the NcoI site. The tubulin promoter with dTomato and *hom2* terminator were integrated in pPV033 digested with NcoI using NEB HiFi DNA Assembly Master Mix (New England Biolabs, USA) resulting in plasmid pPV048.

Transformation of S. commune

Ectopic integration was performed as previously described (van Peer et al. 2009). Targeted integration (knock-in) was performed using a similar approach as previously described for gene deletions (knock-out) (Vonk and Ohm 2021; **Chapter 4**). A sgRNA was designed on the 75 bp and produced with the primers *spi_sgRNA_fw* + *spi_sgRNA_rv* (Table 2) with the GeneArt Precision sgRNA Synthesis Kit (ThermoFisher Scientific, USA) according to manufacturer's specifications (Vonk et al. 2019; **Chapter 3**). The plasmid pPV048 was linearized with Anza NdeI (ThermoFisher Scientific, USA). Integration of the plasmid in the candidate transformants was verified by PCR with two primers (*spi_chk_fw* + *spi_chk_rv*, Table 2), binding outside the upstream and downstream flanks site of integration. In the case of successful integration, this results in the insertion of 3780 bp at the 75 bp region inside the selected upstream and downstream flanks. For the check PCR this results in a

change of band size from 2473 bp in the wild type to 6177 bp in transformants with a successful targeted integration.

Table 2. Primers used in this study. Underlined sequences indicate homologous sequences for Gibson assembly.

Primer name	Sequence
spi_up_fw	<u>CTATGACCATGATTACGCCAGCCAACAATCAGATCCGCTAGC</u>
spi_up_NcoI_rv	<u>TCCCAGACCACCATGCCGGGCCATGGAGCAACCTCGGTGCTTATGACT</u>
spi_down_fw	<u>GTCCCCCTCGAGGCGCGCCGGGTCCTTCTGACGATGACCA</u>
spi_down_rv	<u>GATAACCTTCAGCAGAACGACGTGACTTTTCGCCGTCTGTAC</u>
ptub_dtom_fw	<u>CATAAGCACCCGAGGTTGCTCAAGCTTTGGAACCGGGCCTCAA</u>
ptub_dtom_rv	CTTGACAGCTCGTCCATGC
hom2_term_fw	<u>GCATGGACGAGCTGTACAAGTAGCCCTGGCAATCATTGTC</u>
hom2_term_rv	<u>CCCAGACCACCATGCCGGGCTGACCTTGGGGAAAATCAAG</u>
spi_sgRNA_fw	TAATACGACTCACTATAGTCTCCAGAGCTCCGCGCCA
spi_sgRNA_rv	TTCTAGCTCTAAAAGTGGCGGGAGCTCTGGAGGA
spi_chk_fw	GCAGATGCTGGATAGGCTTC
spi_chk_rv	GGGACATGGTGGTAGAGAGC

Fluorescent imaging and analysis

Transformants and wild-type H4-8 were grown for 5 days in triplicate at 25 °C with a 16-hour light, 8-hour dark cycle. Imaging was done with an Euromex sCMED-20 camera on a Leica MZ16FA with a Leica Planapo 0.63x with fluorescent light from a Leica EL6000 at 1 second exposure and 10x digital gain. Pictures were converted to 8-bit grey-scale and the average fluorescence of pixels with an intensity >14 in a range from 0 to 255 was determined in ImageJ and used as an arbitrary unit of measurement of dTomato fluorescence (AU). Fluorescence intensity was normalized by subtracting measured autofluorescence of wild-type H4-8.

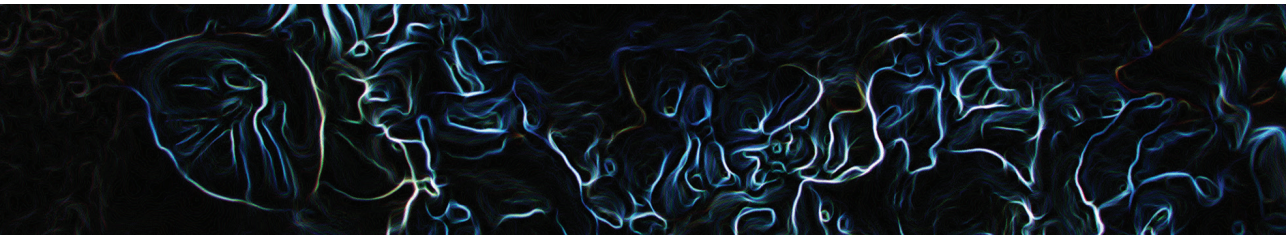
Acknowledgements

This project has received funding from the European Research Council (ERC) under the European Union's Horizon 2020 research and innovation programme (grant agreement number 716132).

Data and software availability

All supplementary data is available at <https://doi.org/10.5281/zenodo.5644994>





Summary and general discussion

Peter Jan Vonk

The fungal kingdom is a diverse group of micro-organisms ranging from unicellular yeast to highly complex mushroom-forming species. They are used for the large-scale production of enzymes and chemicals (Mattey 1992; Sarkar et al. 2012). Furthermore, fungi can produce pharmacological compounds, including antibiotics of the class of penicillins, which revolutionized medical treatment (Kardos and Demain 2011). They are also a component of the plant rhizosphere and can promote the yield of crops (Smith and Smith 2011). The fact that mushroom-forming species produce highly nutritious fruiting bodies on agricultural waste streams (de Mattos-Shipley et al. 2016) also illustrates the importance of fungi for global food security. Additionally, fungi are efficient degraders of plant biomass and their carbohydrate-active enzymes can be used to release simple sugars from the recalcitrant lignocellulosic biomass produced by plants (Levasseur et al. 2013; Grimm and Wösten 2018) that in turn can be used to produce biofuels and other chemicals. Despite their economic importance, many fungi remain poorly characterized. The complex multicellular development of mushroom-forming fungi is particularly poorly understood, due to challenges in cultivation, their slow development and a lack of genetic tools. The mushroom-forming fungi *Schizophyllum commune* and *Coprinopsis cinerea* are exceptions to these limitations as they have a short life-cycle and can develop mushrooms under laboratory conditions (Ohm et al. 2010a; Kües and Navarro-González 2015). Furthermore, several genetic tools are available for functional characterization of genes in these species. Particularly in *S. commune*, multiple regulators of different stages in mushroom development have been identified, leading to a schematic model of mushroom development in this species (Ohm et al. 2011; Pelkmans et al. 2017). However, this model is incomplete and the role of the identified developmental regulators is not yet fully understood. The majority of recent progress in the understanding of mushroom-forming fungi has been derived from -omics approaches rather than functional genetic characterization (Floudas et al. 2012; Ohm et al. 2014; Riley et al. 2014; Pelkmans et al. 2017; Almási et al. 2019; Krizsán et al. 2019; Varga et al. 2019; Ohm 2020). These -omics datasets provide a good overview of the studied process, but functional characterization of individual genes is essential to validate the role of these genes in processes such as wood-degradation and mushroom development. In this thesis, comparative genomics was used to identify *S. commune* transcription factors (TFs) that are predicted to be involved in mushroom-development and wood decay, while functional genetics was used to study the role of part of these regulators. To this end, new, more efficient, genetic tools were developed.

Comparative genomics of homeodomain transcription factors

The rise of genomics in studying mushroom development started with the genome sequence of *Laccaria bicolor* (Martin et al. 2008). Sequencing the genome of this mycorrhizal fungus was followed by whole-genome sequencing of other important mushroom-forming species, including *Agaricus bisporus*, *S. commune* and *C. cinerea* (Stajich et al. 2010; Ohm et al. 2010a; Morin et al. 2012). The rapidly decreasing costs of whole genome sequencing resulted in the availability of a large number of fungal genomes in the last decade, including more than 400 mushroom-forming species (Floudas et al. 2012; Grigoriev et al. 2014; Ohm et al. 2014; Riley et al. 2014; Almási et al. 2019; Krizsán et al. 2019; Park et al. 2019; Miyauchi et al. 2020; Ohm 2020). These data enable large scale comparative genomics in studying growth and mushroom development. In **Chapter 2**, 222 previously published genomes from multiple fungal clades were used to construct a gene tree of fungal homeodomain (HD) TFs. These TFs are important in many developmental processes in eukaryotes (Pearson et al. 2005).



Notably, the higher number of TF genes in fungi with a larger gene count is largely limited to an expansion of Zn₂Cys₆, C2H2 and HD TFs (Shelest 2017). This suggests that more complex developmental processes are primarily regulated by these TF families. This is supported by the fact that the HD TF count is expanded in multicellular fungi compared to unicellular fungi (**Chapter 2**). Based on sequence similarity and branch lengths in a gene tree, 12 groups of HD TFs could be distinguished in fungi (**Chapter 2**). While the largest number of HD TFs was found in early-diverging filamentous fungi, multicellular basidiomycetes had the largest diversity of HD TF types. Mating type loci generally contain HD TFs. For instance, the *matA* locus of *Saccharomyces cerevisiae* contains one HD TF, while that of *S. commune* even contains eight such genes. Few HD TFs that are not part of a mating type locus have been characterized in multicellular fungi with the exception of *S. commune* and some ascomycete model species (Kim et al. 2009; Coppin et al. 2012; Kües 2015; Carrillo et al. 2017). Multiple HD TFs have a role in perithecia development in the ascomycetes. For example, perithecia formation is affected in deletion strains of three HD TFs in *Podospora anserina*. Similarly, the HD TF genes *hom1* and *hom2* are involved in mushroom development in *S. commune* (Ohm et al. 2011). A homozygous $\Delta hom1$ dikaryon forms more, but smaller mushrooms with an enlarged hymenium. On the other hand, deletion of *hom2* results in absence of mushroom development and homozygous dikaryotic colonies of this deletion mutant resemble monokaryons. Furthermore, the $\Delta hom2$ strain forms more biomass, indicative of a role in vegetative growth inhibition (Pelkmans et al. 2017). *S. commune* contains another eight HD TFs that are not part of the mating type locus. These TFs, together with *hom1* and *hom2*, belong to 8 different groups. The HD TF PID: Schco3|2702236 belongs to the same phylogenetic group as *hom1* and could have a similar role to *hom1* in mushroom development (Ohm et al. 2011). Most HD TFs are not differentially regulated during mushroom development in *S. commune* except for *hom1* and Schco3|2493745 (Krizsán et al. 2019). This suggests that post-translational modification has a major role in the regulation of HD TFs, as was shown for *hom2* (Pelkmans et al. 2017).

Tools in studying the genetics of mushroom-forming fungi

Early genetic studies in mushroom-forming fungi were primarily limited to the mating type loci, as these DNA regions have a very clear effect on the compatibility of strains and their offspring (Bistis and Raper 1967). The availability of selectable markers and transformation methods made the study of specific genes in mushroom-forming species viable. Nowadays, gene integration methods are available in many mushroom-forming fungi, including *A. bisporus*, *C. cinerea*, *Flammulina velutipes*, *Pleurotus ostreatus* and *S. commune* (Binninger et al. 1987; van Peer et al. 2009; Pelkmans et al. 2016; Jiao et al. 2018). Gene deletion methods are less developed and have only been reported in *C. cinerea*, *Ganoderma lucidum*, *P. ostreatus* and *S. commune* (de Jong et al. 2010; Ohm et al. 2010b; Nakazawa et al. 2011; Boontawon et al. 2021). As an alternative, gene silencing has been developed to study gene function in *F. velutipes*, *L. bicolor*, *Phanerochaete chrysosporium* and *S. commune* (de Jong et al. 2006; Matityahu et al. 2008; Kemppainen et al. 2009; Shi et al. 2017). Despite efforts to improve the genetic tools available for mushroom-forming fungi, they are limited by low efficiency and a lack of genetic markers (de Jong et al. 2010; Ohm et al. 2010b; Nakazawa et al. 2011). On top of this, the low rate of homologous recombination in mushroom-forming fungi requires a $\Delta ku80$ background to reduce the number of transformants that must be screened for gene deletion (de Jong et al. 2010).

To facilitate a more effective study of gene function in *S. commune*, a CRISPR-Cas9 method for gene deletion was developed (**Chapter 3**). CRISPR (Clustered Regularly Interspaced Short Palindromic Repeats) is an important component of the prokaryotic antiviral immune system (Barrangou et al. 2007). Short DNA sequences of previous viral infections are stored in the prokaryote genome and provide adaptive immunity. The repeats are transcribed as RNA and are used to recognize reinfection in coordination with CRISPR associated proteins (Cas). When recognition occurs, viral DNA is cleaved to prevent infection. This system was adapted for genome editing with Cas9 from *Streptococcus pyogenes* to create CRISPR-Cas9 genome editing. This protein can cleave DNA based on homology to a single guide RNA. Imperfect repair of the double-stranded break may cause insertions or deletions (indels) in the target locus and thereby can disrupt gene function. Moreover, CRISPR-Cas9 can increase the rate of homologous recombination by the introduction of double-stranded breaks at the site of integration (Jinek et al. 2012). Cas9 can be expressed in target cells constitutively or under the control of an inducible promoter (Dicarlo et al. 2013; Fuller et al. 2015). It can also be expressed transiently by transformation with a selectable plasmid that is maintained inside the nucleus (van Leeuwe et al. 2019). While the expression of Cas9 in target cells is cheap, the expression of a bacterial protein often requires species-specific codon optimization (Gustafsson et al. 2012). Indeed, Cas9 optimized for the ascomycete yeast *Candida albicans* was unable to introduce indels in a target gene in *C. cinerea*, whereas expression of a basidiomycete optimized Cas9 did result in indels (Sugano et al. 2017). It is currently unclear if this Cas9 is active in other mushroom-forming basidiomycetes. As an alternative, Cas9 can be purified from a bacterial expression system and directly introduced into target cells (Al Abdallah et al. 2017). This method is more laborious, but is not species-specific and ensures that Cas9 is only active for a short period. The sgRNA can be expressed in the host, which requires the use of RNA polymerase III promoters. These promoters have not been identified in most mushroom-forming fungi and are species-specific (Miyagishi and Taira 2002; Friedland et al. 2013; Sugano et al. 2017). Alternatively, sgRNA can be introduced as transcribed RNA. In **Chapter 3**, sgRNA was pre-assembled with Cas9. Introduction of the resulting ribonucleoprotein (RNP) in protoplasts greatly improved the rate of gene deletion, even to such an extent that a $\Delta ku80$ background is not required (**Chapter 3**). Moreover, the use of the RNP allowed for a reduction of the size of homology arms from 1,000 bp to 250 bp, which enables high-throughput gene deletion in *S. commune*.

Despite the vastly increased rate of gene deletion observed with the use of Cas9 RNPs, efficiency is still markedly lower than gene deletion methods with Cas9 in model ascomycetes like *S. cerevisiae* (Mans et al. 2015). This reduced efficiency is likely caused by a lower rate of homologous recombination and less optimized transformation methods (Ohm et al. 2010b). Indeed, homologous recombination is the dominant mode of DNA repair in *S. cerevisiae* and a gene deletion efficiency of over 50% with 100 bp homology arms is generally reported (Hegemann et al. 2006). In filamentous fungi, non-homologous end-joining is the preferred DNA repair pathway and gene deletion efficiency is much lower. For *Neurospora crassa*, a gene deletion efficiency of 21% has been reported in the wild type with the use of 1000 bp homology arms. Inactivation of the genes encoding Ku70 or Ku80 increased the efficiency to 100% (Ninomiya et al. 2004). Similarly, the efficiency of gene deletion in *Aspergillus fumigatus* was raised from 5-10% to 96% when a $\Delta ku70$ background was used. Similar improvements have been reported in other species (Krappmann 2007) including *S. commune* where the rate of gene deletion increased from 3.25% to 70% by using a $\Delta ku80$ background (de Jong

et al. 2010). However, this increased gene deletion efficiency was accompanied by an up to 100-fold reduction in transformants, as homologous recombination was not up-regulated in the $\Delta ku80$ strain. In contrast, such a reduction was not reported in *N. crassa* (Ninomiya et al. 2004). While the efficiency of gene deletion is lower than previously reported in a $\Delta ku80$ background, the total number of gene deletion events is strongly increased. This suggests that Cas9-induced double-stranded breaks can effectively recruit DNA repair by homologous recombination to the site of integration. The effectiveness of the RNP-mediated gene deletion is illustrated by the fact that 11 gene deletions were created with this method in **Chapters 4-6**, which is 32% of all reported gene deletions in *S. commune* (Robertson et al. 1996; Horton et al. 1999; Lengeler and Kothe 1999a; 1999b; Lugones et al. 2004; Schubert et al. 2006; van Wetter et al. 2006; de Jong et al. 2010; Ohm et al. 2010b; 2011; van Peer et al. 2010; Knabe et al. 2013; Pelkmans et al. 2017). Together, the method developed in **Chapter 3** is versatile and may also be used in other mushroom-forming species, for which fewer genetic tools are available. Moreover, the method enables other genome edits, like promoter replacement or targeted gene-integration (**Chapter 7**).

To further study the function of genes and their regulatory network, a chromatin immunoprecipitation sequencing (ChIP-Seq) method for *S. commune* was developed (**Chapter 4**). ChIP-Seq enables the identification of protein-DNA interactions by chromatin immunoprecipitation of DNA-associated proteins followed by high-throughput sequencing (Johnson et al. 2007). Chromatin in eukaryotes is generally highly plastic and constantly remodeled based on developmental cues (Fischle et al. 2003; Bannister and Kouzarides 2011; Klemm et al. 2019). The local structure of chromatin affects the accessibility of genes and can be altered by DNA methylation and histone modifications. The presence of methylation and histone modifications can be assessed with ChIP-Seq. The technique can also be used to identify TF binding sites. To validate the method, ChIP-Seq was used to identify the distribution of dimethylation on lysine at position 4 of Histone 3 (H3K4me2) during early monokaryotic and dikaryotic development in *S. commune* (**Chapter 4**). H3K4me2 is an activating histone mark that improves the accessibility of chromatin and increases transcription (Orford et al. 2008; Pekowska et al. 2010; Zhang et al. 2012; Wang et al. 2014; Lambrot et al. 2019). It is generally associated with actively transcribed genes. Surprisingly, more genes were differentially enriched in H3K4me2 during monokaryotic development. Generally, dikaryotic development is considered more complex due to increased cell differentiation and the development of complex structures (Kües and Liu 2000). Potentially, chromatin is restructured many times during development, with unique H3K4me2 distribution patterns for each developmental stage. This chromatin restructuring may have been missed in **Chapter 4** since H3K4me2 distribution was only determined for two developmental stages. Moreover, the whole culture was used for determining the H3K4me2 distribution patterns. Therefore, identifying H3K4me2 distribution during additional stages of mushroom development as well as by specific parts of the colony (e.g. vegetative hyphae vs aerial structures) may reveal more insight in the role of genomic plasticity during development.

The relevance of differential H3K4me2 enrichment during development was assessed by the deletion of the TF genes *fst1* and *zfc7* that were enriched in H3K4me2 during dikaryotic development. Deletion of both genes led to arrested development during primordia development, which is immediately downstream of the sampled dikaryotic developmental

stage. This suggests that H3K4me2 is used to restructure the chromatin to promote development. ChIP-Seq was further used in the identification of binding sites of the TF Roc1 (see below; **Chapter 5**). This enabled the identification of its target genes, as well as the DNA binding site of this TF. Together, ChIP-Seq is a powerful tool in the study of genetic regulation in *S. commune*.

Finally, a method for targeted integration (knock-in) was developed in *S. commune* (**Chapter 7**). In multiple chapters of this thesis, complementation strains of gene deletions are created (**Chapter 4-6**). Furthermore, Roc1 tagged with an HA epitope tag was expressed in *S. commune* for TF ChIP-Seq. The introduction of these genes relied on ectopic integration mediated by non-homologous end-joining (Ohm et al. 2011; 2013; Pelkmans et al. 2017). Ectopic integrations introduce a large variability in the phenotype of transformant strains and require extensive screening (Schuren and Wessels 1994; van Peer et al. 2009). The method for more efficient targeted gene deletion (**Chapter 3**) was modified into a targeted knock-in protocol. As a target locus, a genomic region was selected without important regulatory elements, stable gene expression and H3K4 dimethylation (**Chapter 4**) (Krizsán et al. 2019). Targeted knock-in greatly improved the reproducibility of gene integration and resulted in stable more uniform production of the reporter dTomato in transformants. This technique can greatly improve functional gene characterization in *S. commune* by gene complementation. Furthermore, it can be used for the expression of modified genes and epitope-tagged genes.

Genetic regulation of lignocellulose degradation in *S. commune*

The best degraders of lignocellulosic biomass belong to the class of Agaricomycetes to which *S. commune* belongs (Floudas et al. 2012; Ohm et al. 2014). However, the genetic regulation of biomass degradation by these fungi is poorly understood compared to that of ascomycetes. Transcriptomics of *S. commune* grown on different substrates was used to identify potential regulators of wood-degradation in *S. commune*. Surprisingly, only a single TF gene, *roc1*, was up-regulated during growth on cellulose and wood. This regulator is conserved in basidiomycetes, but is not found in ascomycetes. This is expected as regulators of carbohydrate degradation are generally poorly conserved between these phyla (Todd et al. 2014). Deletion mutants of *roc1* were unable to grow on cellulose as sole carbon source and did not secrete cellulases. A HA-epitope-tagged Roc1 combined with the ChIP-Seq technique (**Chapter 4**) was used to identify the DNA binding sites of this regulator. CAZymes of the GH3, GH5 and AA9 families were overrepresented in genes regulated by Roc1. It is known that these families contain enzymes involved in the degradation of (hemi)cellulose (Levasseur et al. 2013). However, many of the binding sites of Roc1 are in the promoters of genes that are neither related to cellulose degradation nor up-regulated when grown on lignocellulose. It is currently unknown if Roc1 regulates these genes. ChIP-Seq revealed the binding motif CCG-N-CGG. Roc1 was unable to activate a promoter when this motif was mutated. The Roc1 motif is similar to that of the CAZyme regulator CLR-1 in *N. crassa* (CGG-N₅-CCG-N-CGG) (Craig et al. 2015). It is currently not known if this is the result of convergent evolution. The CCG triplet is a common motif in the binding sites of Zn₂Cys₆ TFs, like Gal4 in *S. cerevisiae* (Traven et al. 2006). This may explain the high number of binding sites identified by Roc1 ChIP-Seq. Indeed, the number of binding sites can vary greatly in Zn₂Cys₆ TFs. AflR in *Aspergillus flavus*, CrzA in *Aspergillus fumigatus* and FgHtf1 in *Fusarium graminearum* have fewer binding sites, while PRO1 of *Sordaria macrospora* has a similar



number of binding sites as Roc1 (de Castro et al. 2014; Steffens et al. 2016; Fan et al. 2020; Kong et al. 2020).

Genetic regulation of mushroom development in *S. commune*

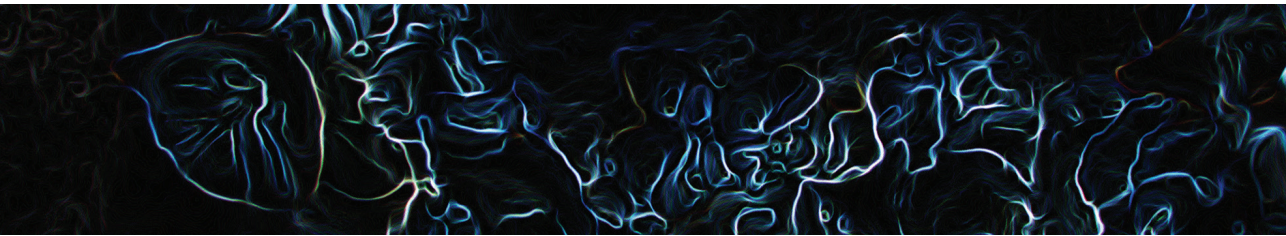
In **Chapter 4** and **Chapter 6**, the role of 10 TFs in mushroom development was assessed, resulting in an updated and expanded model of mushroom formation of *S. commune* (**Chapter 6**). The TFs were selected based on expression profiles during mushroom formation (**Chapter 6**) and H3K4me2 enrichment during dikaryotic development (**Chapter 4**). Five out of the 10 TFs were shown to have a role in mushroom development. *Ftr1* is involved in the early establishment of a dikaryotic mycelium and a homozygous $\Delta ftr1$ dikaryon resembles monokaryotic mycelium during fruiting conditions. A similar phenotype was previously reported for homozygous $\Delta hom2$, $\Delta tea1$ and $\Delta wc2$ dikaryons and suggests a role in early mushroom development (Ohm et al. 2011; Pelkmans et al. 2017). In homozygous dikaryotic deletion strains of *hom2*, *fst4*, *wc1* and *wc2* the expression of *ftr1* is reduced and not developmentally regulated (Pelkmans et al. 2017). It is surprising that deletion of *fst4* influences *ftr1* expression, as a homozygous $\Delta fst4$ dikaryon establishes an asymmetrical colony, which is downstream in development of the phenotype of a homozygous $\Delta ftr1$ dikaryon (Ohm et al. 2010a). This suggests that *Fst4* has a developmental role prior to asymmetric colony formation. *Fst1*, *Zfc4* and *Zfc7* have a role in primordia formation and homozygous dikaryotic deletion strains are unable to form mature fruiting bodies. Homozygous dikaryotic $\Delta fst1$ and $\Delta zfc7$ strains form primordia, but further development is arrested. *Zfc4* also has a role in primordia development and a homozygous $\Delta zfc4$ dikaryon is unable to form a mushroom ring. While most of the ring consists of aggregates and immature primordia, gilled mushrooms are formed in some parts of the ring. However, these gills are underdeveloped and the mushrooms are malformed. Gene *zfc7*, but not *fst1* and *zfc4*, is regulated (directly or indirectly) by *Hom2* and *Wc2* (Pelkmans et al. 2017). This indicates that multiple regulatory pathways are required for the maturation of primordia in *S. commune*. *Bzt1* is also involved in fruiting. Homozygous dikaryotic deletion strains of either of these TFs caused the formation of more, but smaller mushrooms. The formation of more, smaller mushrooms in a homozygous $\Delta bzt1$ dikaryon is very similar to the previously identified phenotype of homozygous dikaryotic *gat1* and *hom1* deletion mutants (Ohm et al. 2011). *Bzt1* is highly expressed during late primordia development and may inhibit the formation of new primordia to provide sufficient space to maturing mushrooms (Ohm et al. 2011; Almási et al. 2019; Krizsán et al. 2019). RNA-Seq of the deletion strains described in this Thesis during different developmental stages will give more insight into the roles of these TFs. Furthermore, the CHIP-Seq protocol developed in **Chapter 4** and used in **Chapter 5** can give more insight into function of TFs involved in fruiting.

Outlook

This thesis describes new tools for studying the genetics of mushroom-forming fungi and were used to study the transcriptional regulation of fruiting body development and lignocellulose degradation. This has increased our understanding of regulation in mushroom-forming fungi. However, transcriptional regulation is only a part of the complex regulatory network. Signaling pathways like G-protein coupled receptor signaling are known to have a major role in mushroom development, but have not been characterized in detail. Furthermore, while many TFs with a role in mushroom development have been characterized, their putative role is primarily hypothesized from their deletion phenotype during fruiting. Due to the

complex nature of mushroom development this characterization is insufficient to fully establish the role of these regulatory genes. The high-throughput gene deletion method, targeted integration method and ChIP-Seq protocol can be used to further establish the role of TFs in *S. commune* and potentially other mushroom-forming fungi. They will enable the identification of a complete regulatory network by combining multiple -omics tools with detailed functional characterization. In particular, the identification of TF binding sites can reveal the function of TFs in more detail. The study of protein interactions is an important future avenue to further the understanding of mushroom-forming fungi. For example, not all binding sites of Roc1 (**Chapter 4**) can be attributed to the regulation of cellulase expression and the putative binding motif is not complex enough to independently control Roc1 specificity. Therefore, the association of other TFs, or co-factors is likely important in the function of Roc1. Protein interaction studies are needed to identify putative interaction partners of Roc1 and other TFs.





Appendix

References

Nederlandse samenvatting

Acknowledgements

Curriculum vitae

List of publications

References

- Ait Benkhali, J., Coppin, E., Brun, S., Peraza-Reyes, L., Martin, T., Dixelius, C., Lazar, N., van Tilbeurgh, H., & Debuchy, R. (2013). A Network of HMG-box Transcription Factors Regulates Sexual Cycle in the Fungus *Podospora anserina*. *PLoS Genetics*, *9*(7), e1003642. <https://doi.org/10.1371/journal.pgen.1003642>
- Al Abdallah, Q., Ge, W., & Fortwendel, J. R. (2017). A Simple and Universal System for Gene Manipulation in *Aspergillus fumigatus*: In Vitro-Assembled Cas9-Guide RNA Ribonucleoproteins Coupled with Microhomology Repair Templates. *MSphere*, *2*(6), e00446-17. <https://doi.org/10.1128/msphere.00446-17>
- Alfaro, M., Castanera, R., Lavín, J. L., Grigoriev, I. V., Oguiza, J. A., Ramírez, L., & Pisabarro, A. G. (2016). Comparative and transcriptional analysis of the predicted secretome in the lignocellulose-degrading basidiomycete fungus *Pleurotus ostreatus*. *Environmental Microbiology*, *18*(12), 4710–4726. <https://doi.org/10.1111/1462-2920.13360>
- Allshire, R. C., & Ekwall, K. (2015). Epigenetic regulation of chromatin states in *Schizosaccharomyces pombe*. *Cold Spring Harbor Perspectives in Biology*, *7*(7), a018770. <https://doi.org/10.1101/cshperspect.a018770>
- Almási, É., Sahu, N., Krizsán, K., Bálint, B., Kovács, G. M., Kiss, B., Cseklye, J., Drula, E., Henrissat, B., Nagy, I., Chovatia, M., Adam, C., LaButti, K., Lipzen, A., Riley, R., Grigoriev, I. V., & Nagy, L. G. (2019). Comparative genomics reveals unique wood-decay strategies and fruiting body development in the Schizophyllaceae. *New Phytologist*, *224*(2), 902–915. <https://doi.org/10.1111/nph.16032>
- Alves, A. M. C. R., Record, E., Lomascolo, A., Scholtmeijer, K., Asther, M., Wessels, J. G. H., & Wösten, H. A. B. (2004). Highly efficient production of laccase by the basidiomycete *Pycnoporus cinnabarinus*. *Applied and Environmental Microbiology*, *70*(11), 6379–6384. <https://doi.org/10.1128/AEM.70.11.6379-6384.2004>
- Amselem, J., Cuomo, C. A., van Kan, J. A. L., Viaud, M., Benito, E. P., Couloux, A., Coutinho, P. M., de Vries, R. P., Dyer, P. S., Fillinger, S., Fournier, E., Gout, L., Hahn, M., Kohn, L., Lapalu, N., Plummer, K. M., Pradier, J. M., Quévillon, E., Sharon, A., ... Dickman, M. (2011). Genomic analysis of the necrotrophic fungal pathogens sclerotinia sclerotiorum and botrytis cinerea. *PLoS Genetics*, *7*(8), e1002230. <https://doi.org/10.1371/journal.pgen.1002230>
- Andersen, M. R., Salazar, M. P., Schaap, P. J., van de Vondervoort, P. J. I., Culley, D., Thykaer, J., Frisvad, J. C., Nielsen, K. F., Albang, R., Albermann, K., Berka, R. M., Braus, G. H., Braus-Stromeyer, S. A., Corrochano, L. M., Dai, Z., van Dijk, P. W. M., Hofmann, G., Lasure, L. L., Magnuson, J. K., ... Baker, S. E. (2011). Comparative genomics of citric-acid-producing *Aspergillus niger* ATCC 1015 versus enzyme-producing CBS 513.88. *Genome Research*, *21*(6), 885–897. <https://doi.org/10.1101/gr.112169.110>
- Ando, Y., Nakazawa, T., Oka, K., Nakahori, K., & Kamada, T. (2013). *Cc.snf5*, a gene encoding a putative component of the SWI/SNF chromatin remodeling complex, is essential for sexual development in the agaricomycete *Coprinopsis cinerea*. *Fungal Genetics and Biology*, *50*, 82–89. <https://doi.org/10.1016/j.fgb.2012.09.010>
- Antal, Z., Rasche, C., Cimerman, A., Viaud, M., Billon-Grand, G., Choquer, M., & Bruel, C. (2012). The Homeobox *BcHOX8* Gene in *Botrytis Cinerea* Regulates Vegetative Growth and Morphology. *PLoS ONE*, *7*(10), e48134. <https://doi.org/10.1371/journal.pone.0048134>
- Aramayo, R., Peleg, Y., Addison, R., & Metzberg, R. (1996). *Asm-1+*, a *Neurospora crassa* gene related to transcriptional regulators of fungal development. *Genetics*, *144*(3), 991–1003. <https://doi.org/10.1093/genetics/144.3.991>
- Arnaise, S., Zickler, D., Poisier, C., & Debuchy, R. (2001). PAH1: A homeobox gene involved in hyphal morphology and microconidiogenesis in the filamentous ascomycete *Podospora anserina*. *Molecular Microbiology*, *39*(1), 54–64. <https://doi.org/10.1046/j.1365-2958.2001.02163.x>
- Aro, N., Ilmén, M., Saloheimo, A., & Penttilä, M. (2003). ACE1 of *Trichoderma reesei* is a repressor of cellulase and xylanase expression. *Applied and Environmental Microbiology*, *69*(1), 56–65. <https://doi.org/10.1128/AEM.69.1.56-65.2003>
- Asada, Y., Yue, C., Wu, J., Shen, G. P., Novotny, C. P., & Ullrich, R. C. (1997). Schizophyllum commune $A\alpha$ mating-type proteins, Y and Z, form complexes in all combinations in vitro. *Genetics*, *147*(1), 117–123. <https://doi.org/10.1093/genetics/147.1.117>
- Ashburner, M., Ball, C. A., Blake, J. A., Botstein, D., Butler, H., Cherry, J. M., Davis, A. P., Dolinski, K., Dwight, S. S., Eppig, J. T., Harris, M. A., Hill, D. P., Issel-Tarver, L., Kasarskis, A., Lewis, S., Matese, J. C., Richardson, J. E., Ringwald, M., Rubin, G. M., & Sherlock, G. (2000). Gene ontology: Tool for the unification of biology. *Nature Genetics*, *25*(1), 25–29. <https://doi.org/10.1038/75556>
- Bahn, Y. S., & Mühlischlegel, F. A. (2006). CO₂ sensing in fungi and beyond. *Current Opinion in Microbiology*, *9*(6), 572–578. <https://doi.org/10.1016/j.mib.2006.09.003>
- Bailey, T. L., Boden, M., Buske, F. A., Frith, M., Grant, C. E., Clementi, L., Ren, J., Li, W. W., & Noble, W. S. (2009). MEME Suite: Tools for motif discovery and searching. *Nucleic Acids Research*, *37*(suppl_2), 202–208. <https://doi.org/10.1093/nar/gkn338>

- doi.org/10.1093/nar/gkp335
- Bannister, A. J., & Kouzarides, T. (2011). Regulation of chromatin by histone modifications. *Cell Research*, 21(3), 381–395. <https://doi.org/10.1038/cr.2011.22>
- Bao, D., Gong, M., Zheng, H., Chen, M., Zhang, L., Wang, H., Jiang, J., Wu, L., Zhu, Y., Zhu, G., Zhou, Y., Li, C., Wang, S., Zhao, Y., Zhao, G., & Tan, Q. (2013). Sequencing and Comparative Analysis of the Straw Mushroom (*Volvariella volvacea*) Genome. *PLoS ONE*, 8(3), e58294. <https://doi.org/10.1371/journal.pone.0058294>
- Baranova, M. A., Logacheva, M. D., Penin, A. A., Seplyarskiy, V. B., Safonova, Y. Y., Naumenko, S. A., Klepikova, A. V., Gerasimov, E. S., Bazykin, G. A., James, T. Y., & Kondrashov, A. S. (2015). Extraordinary genetic diversity in a wood decay mushroom. *Molecular Biology and Evolution*, 32(10), 2775–2783. <https://doi.org/10.1093/molbev/msv153>
- Bardwell, L., Cook, J. G., Voora, D., Baggott, D. M., Martinez, A. R., & Thorner, J. (1998). Repression of yeast Ste12 transcription factor by direct binding of unphosphorylated Kss1 MAPK and its regulation by the Ste7 MEK. *Genes and Development*, 12(18), 2887–2898. <https://doi.org/10.1101/gad.12.18.2887>
- Barrangou, R., Fremaux, C., Deveau, H., Richards, M., Boyaval, P., Moineau, S., Romero, D. A., & Horvath, P. (2007). CRISPR provides acquired resistance against viruses in prokaryotes. *Science*, 315(5819), 1709–1712. <https://doi.org/10.1126/science.1138140>
- Barski, A., Cuddapah, S., Cui, K., Roh, T. Y., Schones, D. E., Wang, Z., Wei, G., Chepelev, I., & Zhao, K. (2007). High-Resolution Profiling of Histone Methylations in the Human Genome. *Cell*, 129(4), 823–837. <https://doi.org/10.1016/j.cell.2007.05.009>
- Bayry, J., Aïmanianda, V., Guïjarro, J. I., Sunde, M., & Latgé, J. P. (2012). Hydrophobins-unique fungal proteins. *PLoS Pathogens*, 8(5), e1002700. <https://doi.org/10.1371/journal.ppat.1002700>
- Bender, A., & Sprague, G. F. (1987). MAT α 1 protein, a yeast transcription activator, binds synergistically with a second protein to a set of cell-type-specific genes. *Cell*, 50(5), 681–691. [https://doi.org/10.1016/0092-8674\(87\)90326-6](https://doi.org/10.1016/0092-8674(87)90326-6)
- Benocci, T., Aguilar-Pontes, M. V., Zhou, M., Seiboth, B., & de Vries, R. P. (2017). Regulators of plant biomass degradation in ascomycetous fungi. *Biotechnology for Biofuels*, 10(1), 1-25. <https://doi.org/10.1186/s13068-017-0841-x>
- Bernstein, B. E., Liu, C. L., Humphrey, E. L., Perlstein, E. O., & Schreiber, S. L. (2004). Global nucleosome occupancy in yeast. *Genome Biology*, 5(9), 1-11. <https://doi.org/10.1186/gb-2004-5-9-r62>
- Bertossa, R. C., Kües, U., Aebi, M., & Künzler, M. (2004). Promoter analysis of *cgl2*, a galectin encoding gene transcribed during fruiting body formation in *Coprinopsis cinerea* (*Coprinus cinereus*). *Fungal Genetics and Biology*, 41(12), 1120–1131. <https://doi.org/10.1016/j.fgb.2004.09.001>
- Bharathan, G., Janssen, B. J., Kellogg, E. A., & Sinha, N. (1997). Did homeodomain proteins duplicate before the origin of angiosperms, fungi, and metazoa? *Proceedings of the National Academy of Sciences of the United States of America*, 94(25), 13749–13753. <https://doi.org/10.1073/pnas.94.25.13749>
- Binnering, D. M., Skrzynia, C., Pukkila, P. J., & Casselton, L. A. (1987). DNA-mediated transformation of the basidiomycete *Coprinus cinereus*. *The EMBO Journal*, 6(4), 835–840. <https://doi.org/10.1002/j.1460-2075.1987.tb04828.x>
- Birney, E., Clamp, M., & Durbin, R. (2004). GeneWise and Genomewise. *Genome Research*, 14(5), 988–995. <https://doi.org/10.1101/gr.1865504>
- Bistis, G. N., & Raper, J. R. (1967). Genetics of Sexuality in Higher Fungi. *Mycologia*, 59(2), 384. <https://doi.org/10.2307/3756816>
- Bleuler-Martínez, S., Buttschi, A., Garbani, M., Wilti, M. A., Wohlschlager, T., Potthoff, E., Sabotia, J., Pohleven, J., Lüthy, P., Hengartner, M. O., Aebi, M., & Künzler, M. (2011). A lectin-mediated resistance of higher fungi against predators and parasites. *Molecular Ecology*, 20(14), 3056–3070. <https://doi.org/10.1111/j.1365-294X.2011.05093.x>
- Bleuler-Martínez, S., Schmieder, S., Aebi, M., & Künzler, M. (2012). Biotin-binding proteins in the defense of mushrooms against predators and parasites. *Applied and Environmental Microbiology*, 78(23), 8485–8487. <https://doi.org/10.1128/AEM.02286-12>
- Bölker, M., Urban, M., & Kahmann, R. (1992). The a mating type locus of *U. maydis* specifies cell signaling components. *Cell*, 68(3), 441–450. [https://doi.org/10.1016/0092-8674\(92\)90182-C](https://doi.org/10.1016/0092-8674(92)90182-C)
- Boontawon, T., Nakazawa, T., Horii, M., Tsuzuki, M., Kawauchi, M., Sakamoto, M., & Honda, Y. (2021). Functional analyses of *Pleurotus ostreatus* *pcc1* and *clp1* using CRISPR/Cas9. *Fungal Genetics and Biology*, 154, 103599. <https://doi.org/10.1016/j.fgb.2021.103599>
- Boulianne, R. P., Liu, Y., Aebi, M., Lu, B. C., & Kües, U. (2000). Fruiting body development in *Coprinus cinereus*: Regulated expression of two galectins secreted by a non-classical pathway. *Microbiology*, 146(8), 1841–1853. <https://doi.org/10.1099/00221287-146-8-1841>
- Broad Institute. (2009). *Picard Tools - By Broad Institute*. Github. <http://broadinstitute.github.io/picard/>
- Brosch, G., Loidl, P., & Graessle, S. (2008). Histone modifications and chromatin dynamics: A focus on filamentous fungi. *FEMS Microbiology Reviews*, 32(3), 409–439. <https://doi.org/10.1111/j.1574-6976.2007.00100.x>



- Bushnell, B. (2019). BMAP. <https://Sourceforge.Net/Projects/Bbmap/>.
- Cantarel, B. I., Coutinho, P. M., Rancurel, C., Bernard, T., Lombard, V., & Henrissat, B. (2009). The Carbohydrate-Active EnZymes database (CAZy): An expert resource for glycogenomics. *Nucleic Acids Research*, *37*(suppl_1), 233–238. <https://doi.org/10.1093/nar/gkn663>
- Carrillo, A. J., Schacht, P., Cabrera, I. E., Blahut, J., Prudhomme, L., Dietrich, S., Bekman, T., Mei, J., Carrera, C., Chen, V., Clark, I., Fierro, G., Ganzen, L., Orellana, J., Wise, S., Yang, K., Zhong, H., & Borkovich, K. A. (2017). Functional profiling of transcription factor genes in *Neurospora crassa*. *G3: Genes, Genomes, Genetics*, *7*(9), 2945–2956. <https://doi.org/10.1534/g3.117.043331>
- Castanera, R., López-Varas, L., Borgognone, A., LaButti, K., Lapidus, A., Schmutz, J., Grimwood, J., Pérez, G., Pisabarro, A. G., Grigoriev, I. V., Stajich, J. E., & Ramírez, L. (2016). Transposable Elements versus the Fungal Genome: Impact on Whole-Genome Architecture and Transcriptional Profiles. *PLoS Genetics*, *12*(6), e1006108. <https://doi.org/10.1371/journal.pgen.1006108>
- Castresana, J. (2000). Selection of conserved blocks from multiple alignments for their use in phylogenetic analysis. *Molecular Biology and Evolution*, *17*(4), 540–552. <https://doi.org/10.1093/oxfordjournals.molbev.a026334>
- Cerqueira, G. C., Arnaud, M. B., Inglis, D. O., Skrzypek, M. S., Binkley, G., Simison, M., Miyasato, S. R., Binkley, J., Orvis, J., Shah, P., Wymore, F., Sherlock, G., & Wortman, J. R. (2014). The *Aspergillus* Genome Database: Multispecies curation and incorporation of RNA-Seq data to improve structural gene annotations. *Nucleic Acids Research*, *42*(D1), 705–10. <https://doi.org/10.1093/nar/gkt1029>
- Cheng, C. K., Au, C. H., Wilke, S. K., Stajich, J. E., Zolan, M. E., Pukkila, P. J., & Kwan, H. S. (2013). 5'-Serial Analysis of Gene Expression studies reveal a transcriptomic switch during fruiting body development in *Coprinopsis cinerea*. *BMC Genomics*, *14*(1), 195. <https://doi.org/10.1186/1471-2164-14-195>
- Cherry, J. M., Hong, E. L., Amundsen, C., Balakrishnan, R., Binkley, G., Chan, E. T., Christie, K. R., Costanzo, M. C., Dwight, S. S., Engel, S. R., Fisk, D. G., Hirschman, J. E., Hitz, B. C., Karra, K., Krieger, C. J., Miyasato, S. R., Nash, R. S., Park, J., Skrzypek, M. S., ... Wong, E. D. (2012). *Saccharomyces* Genome Database: The genomics resource of budding yeast. *Nucleic Acids Research*, *40*(D1). <https://doi.org/10.1093/nar/gkr1029>
- Chowdhary, A., Randhawa, H. S., Gaur, S. N., Agarwal, K., Kathuria, S., Roy, P., Klaassen, C. H., & Meis, J. F. (2013). *Schizophyllum commune* as an emerging fungal pathogen: A review and report of two cases. *Mycoses*, *56*(1), 1–10. <https://doi.org/10.1111/j.1439-0507.2012.02190.x>
- Chum, W. W. Y., Ng, K. T. P., Shih, R. S. M., Au, C. H., & Kwan, H. S. (2008). Gene expression studies of the dikaryotic mycelium and primordium of *Lentinula edodes* by serial analysis of gene expression. *Mycological Research*, *112*(8), 950–964. <https://doi.org/10.1016/j.mycres.2008.01.028>
- Cissé, O. H., Almeida, J. M. G. C. F., Fonseca, Á., Kumar, A. A., Salojärvi, J., Overmyer, K., Hauser, P. M., & Pagni, M. (2013). Genome sequencing of the plant pathogen *Taphrina deformans*, the causal agent of peach leaf curl. *MBio*, *4*(3), e00055–13. <https://doi.org/10.1128/mBio.00055-13>
- Collins, C., Keane, T. M., Turner, D. J., O'Keefe, G., Fitzpatrick, D. A., & Doyle, S. (2013). Genomic and proteomic dissection of the ubiquitous plant pathogen, *armillaria mellea*: Toward a new infection model system. *Journal of Proteome Research*, *12*(6), 2552–2570. <https://doi.org/10.1021/pr301131t>
- Collins, C. M., Heneghan, M. N., Kilaru, S., Bailey, A. M., & Foster, G. D. (2010). Improvement of the *Coprinopsis cinerea* molecular toolkit using new construct design and additional marker genes. *Journal of Microbiological Methods*, *82*(2), 156–162. <https://doi.org/10.1016/j.mimet.2010.05.007>
- Colot, H. V., Park, G., Turner, G. E., Ringelberg, C., Crew, C. M., Litvinkova, L., Weiss, R. L., Borkovich, K. A., & Dunlap, J. C. (2006). A high-throughput gene knockout procedure for *Neurospora* reveals functions for multiple transcription factors. *Proceedings of the National Academy of Sciences of the United States of America*, *103*(27), 10352–10357. <https://doi.org/10.1073/pnas.0601456103>
- Condon, B. J., Leng, Y., Wu, D., Bushley, K. E., Ohm, R. A., Otilar, R., Martin, J., Schackwitz, W., Grimwood, J., MohdZainudin, N. A. I., Xue, C., Wang, R., Manning, V. A., Dhillon, B., Tu, Z. J., Steffenson, B. J., Salamov, A., Sun, H., Lowry, S., ... Turgeon, B. G. (2013). Comparative Genome Structure, Secondary Metabolite, and Effector Coding Capacity across *Cochliobolus* Pathogens. *PLoS Genetics*, *9*(1), e1003233. <https://doi.org/10.1371/journal.pgen.1003233>
- Cong, L., & Zhang, F. (2015). Genome engineering using CRISPR-Cas9 system. *Methods in Molecular Biology*, *1239*(11), 197–217. https://doi.org/10.1007/978-1-4939-1862-1_10
- Connolly, L. R., Smith, K. M., & Freitag, M. (2013). The *Fusarium graminearum* Histone H3 K27 Methyltransferase KMT6 Regulates Development and Expression of Secondary Metabolite Gene Clusters. *PLoS Genetics*, *9*(10), e1003916. <https://doi.org/10.1371/journal.pgen.1003916>
- Coppin, E., Berteaux-Lecellier, V., Bidard, F., Brun, S., Ruprich-Robert, G., Espagne, E., Ait-Benkhalil, J., Goarin, A., Nesseir, A., Planamente, S., Debuchy, R., & Silar, P. (2012). Systematic deletion of homeobox genes in *Podospora anserina* uncovers their roles in shaping the fruiting body. *PLoS ONE*, *7*(5), e37488. <https://doi.org/10.1371/journal.pone.0037488>
- Coradetti, S. T., Craig, J. P., Xiong, Y., Shock, T., Tian, C., & Glass, N. L. (2012). Conserved and essential transcription

- factors for cellulase gene expression in ascomycete fungi. *Proceedings of the National Academy of Sciences of the United States of America*, 109(19), 7397–7402. <https://doi.org/10.1073/pnas.1200785109>
- Corrochano, L. M. (2011). Fungal photobiology: A synopsis. *IMA Fungus*, 2(1), 25–28. <https://doi.org/10.5598/ima fungus.2011.02.01.04>
- Corrochano, L. M. (2019). Light in the Fungal World: From Photoreception to Gene Transcription and beyond. *Annual Review of Genetics*, 53, 149–170. <https://doi.org/10.1146/annurev-genet-120417-031415>
- Corrochano, L. M., Kuo, A., Marcet-Houben, M., Polaino, S., Salamov, A., Villalobos-Escobedo, J. M., Grimwood, J., Álvarez, M. I., Avalos, J., Bauer, D., Benito, E. P., Benoit, I., Burger, G., Camino, L. P., Cánovas, D., Cerdá-Olmedo, E., Cheng, J. F., Domínguez, A., Eliáš, M., ... Grigoriev, I. V. (2016). Expansion of Signal Transduction Pathways in Fungi by Extensive Genome Duplication. *Current Biology*, 26(12), 1577–1584. <https://doi.org/10.1016/j.cub.2016.04.038>
- Covitz, P. A., Herskowitz, I., & Mitchell, A. P. (1991). The yeast RME1 gene encodes a putative zinc finger protein that is directly repressed by a1- α 2. *Genes and Development*, 5(11), 1982–1989. <https://doi.org/10.1101/gad.5.11.1982>
- Cragg, S. M., Beckham, G. T., Bruce, N. C., Bugg, T. D. H., Distel, D. L., Dupree, P., Etxabe, A. G., Goodell, B. S., Jellison, J., McGeehan, J. E., McQueen-Mason, S. J., Schnorr, K., Walton, P. H., Watts, J. E. M., & Zimmer, M. (2015). Lignocellulose degradation mechanisms across the Tree of Life. *Current Opinion in Chemical Biology*, 29, 108–119. <https://doi.org/10.1016/j.cbpa.2015.10.018>
- Craig, J. P., Coradetti, S. T., Starr, T. L., & Louise Glass, N. (2015). Direct target network of the neurospora crassa plant cell wall deconstruction regulators clr-1, clr-2, and xlr-1. *MBio*, 6(5), e01452–15. <https://doi.org/10.1128/mBio.01452-15>
- Cuomo, C. A., Güldener, U., Xu, J. R., Trail, F., Turgeon, B. G., Di Pietro, A., Walton, J. D., Ma, L. J., Baker, S. E., Rep, M., Adam, G., Antoniw, J., Baldwin, T., Calvo, S., Chang, Y. L., DeCaprio, D., Gale, L. R., Gnerre, S., Goswami, R. S., ... Kistler, H. C. (2007). The *Fusarium graminearum* genome reveals a link between localized polymorphism and pathogen specialization. *Science*, 317(5843), 1400–1402. <https://doi.org/10.1126/science.1143708>
- D'Souza, C. A., & Heitman, J. (2001). Conserved cAMP signaling cascades regulate fungal development and virulence. *FEMS Microbiology Reviews*, 25(3), 349–364. <https://doi.org/10.1111/j.1574-6976.2001.tb00582.x>
- Daly, P., Peng, M., Falco, M. Di, Lipzen, A., Wang, M., Ng, V., Grigoriev, I. V., Tsang, A., Mäkelä, M. R., & de Vries, R. P. (2019). Glucose-mediated repression of plant biomass utilization in the white-rot fungus *dichomitus squalens*. *Applied and Environmental Microbiology*, 85(23), e01828–19. <https://doi.org/10.1128/AEM.01828-19>
- de Castro, P. A., Chen, C., de Almeida, R. S. C., Freitas, F. Z., Bertolini, M. C., Morais, E. R., Brown, N. A., Ramalho, L. N. Z., Hagiwara, D., Mitchell, T. K., & Goldman, G. H. (2014). ChIP-seq reveals a role for CrzA in the *Aspergillus fumigatus* high-osmolarity glycerol response (HOG) signalling pathway. *Molecular Microbiology*, 94(3), 655–674. <https://doi.org/10.1111/mmi.12785>
- de Jong, J. F., Deelstra, H. J., Wösten, H. A. B., & Lugones, L. G. (2006). RNA-mediated gene silencing in monokaryons and dikaryons of *Schizophyllum commune*. *Applied and Environmental Microbiology*, 72(2), 1267–1269. <https://doi.org/10.1128/AEM.72.2.1267-1269.2006>
- de Jong, J. F., Ohm, R. A., de Bekker, C., Wösten, H. A. B., & Lugones, L. G. (2010). Inactivation of ku80 in the mushroom-forming fungus *Schizophyllum commune* increases the relative incidence of homologous recombination. *FEMS Microbiology Letters*, 310(1), 91–95. <https://doi.org/10.1111/j.1574-6968.2010.02052.x>
- de Mattos-Shipley, K. M. J., Ford, K. L., Alberti, F., Banks, A. M., Bailey, A. M., & Foster, G. D. (2016). The good, the bad and the tasty: The many roles of mushrooms. *Studies in Mycology*, 85, 125–157. <https://doi.org/10.1016/j.simyco.2016.11.002>
- de Mendoza, A., Sebé-Pedrós, A., Šestak, M. S., Matejčić, M., Torruella, G., Domazet-Lošo, T., & Ruiz-Trillo, I. (2013). Transcription factor evolution in eukaryotes and the assembly of the regulatory toolkit in multicellular lineages. *Proceedings of the National Academy of Sciences of the United States of America*, 110(50), 4858–4866. <https://doi.org/10.1073/pnas.1311818110>
- de Schutter, K., Lin, Y. C., Tiels, P., van Hecke, A., Glinka, S., Weber-Lehmann, J., Rouzé, P., van de Peer, Y., & Callewaert, N. (2009). Genome sequence of the recombinant protein production host *Pichia pastoris*. *Nature Biotechnology*, 27(6), 561–566. <https://doi.org/10.1038/nbt.1544>
- de Wit, P. J. G. M., van der Burgt, A., Ökmen, B., Stergiopoulos, I., Abd-El salam, K. A., Aerts, A. L., Bahkali, A. H., Beenen, H. G., Chettri, P., Cox, M. P., Datema, E., de Vries, R. P., Dhilon, B., Ganley, A. R., Griffiths, S. A., Guo, Y., Hamelin, R. C., Henrissat, B., Kabir, M. S., ... Bradshaw, R. E. (2012). The Genomes of the Fungal Plant Pathogens *Cladosporium fulvum* and *Dothistroma septosporium* Reveal Adaptation to Different Hosts and Lifestyles But Also Signatures of Common Ancestry. *PLoS Genetics*, 8(11), e1003088. <https://doi.org/10.1371/journal.pgen.1003088>
- Dean, R. A., Talbot, N. J., Ebbole, D. J., Farman, M. L., Mitchell, T. K., Orbach, M. J., Thon, M., Kulkarni, R., Xu, J. R., Pan, H., Read, N. D., Lee, Y. I., Carbone, I., Brown, D., Yeon, Y. O., Donofrio, N., Jun, S. J., Soanes, D. M.,



- Djonovic, S., ... Dirren, B. W. (2005). The genome sequence of the rice blast fungus *Magnaporthe grisea*. *Nature*, 434(7036), 980–986. <https://doi.org/10.1038/nature03449>
- Degli-Innocenti, F., & Russo, F. E. A. (1984). Isolation of new white collar mutants of *Neurospora crassa* and studies of their behavior in the blue light-induced formation of protoperithecia. *Journal of Bacteriology*, 159(2), 757–761. <https://doi.org/10.1128/jb.159.2.757-761.1984>
- Derelle, R., Lopez, P., Guyader, H. Le, & Manuel, M. (2007). Homeodomain proteins belong to the ancestral molecular toolkit of eukaryotes. *Evolution and Development*, 9(3), 212–219. <https://doi.org/10.1111/j.1525-142X.2007.00153.x>
- Dicarlo, J. E., Norville, J. E., Mali, P., Rios, X., Aach, J., & Church, G. M. (2013). Genome engineering in *Saccharomyces cerevisiae* using CRISPR-Cas systems. *Nucleic Acids Research*, 41(7), 4336–4343. <https://doi.org/10.1093/nar/gkt135>
- Dons, J. J. M., de Vries, O. M. H., & Wessels, J. G. H. (1979). Characterization of the genome of the basidiomycete *Schizophyllum commune*. *Biochimica et Biophysica Acta (BBA)-Nucleic Acids and Protein Synthesis*, 563(1), 100–112. [https://doi.org/10.1016/0005-2787\(79\)90011-X](https://doi.org/10.1016/0005-2787(79)90011-X)
- Dranginis, A. M. (1989). Regulation of STA1 gene expression by MAT during the life cycle of *Saccharomyces cerevisiae*. *Molecular and Cellular Biology*, 9(9), 3992–3998. <https://doi.org/10.1128/mcb.9.9.3992>
- Dranginis, A. M. (1990). Binding of yeast $\alpha 1$ and $\alpha 2$ as a heterodimer to the operator DNA of a haploid-specific gene. *Nature*, 347(6294), 682–685. <https://doi.org/10.1038/347682a0>
- Dujon, B., Sherman, D., Fischer, G., Durrens, P., Casaregola, S., Lafontaine, I., de Montigny, J., Marck, C., Neuvéglise, C., Talla, E., Goffard, N., Frangeul, L., Algie, M., Anthouard, V., Babour, A., Barbe, V., Barnay, S., Blanchin, S., Beckerich, J. M., ... Souciet, J. L. (2004). Genome evolution in yeasts. *Nature*, 430(6995), 35–44. <https://doi.org/10.1038/nature02579>
- Dumesic, P. A., Homer, C. M., Moresco, J. J., Pack, L. R., Shanle, E. K., Coyle, S. M., Strahl, B. D., Fujimori, D. G., Yates, J. R., & Madhani, H. D. (2015). Product binding enforces the genomic specificity of a yeast Polycomb repressive complex. *Cell*, 160(1–2), 204–218. <https://doi.org/10.1016/j.cell.2014.11.039>
- Dyballa, N., & Metzger, S. (2009). Fast and sensitive colloidal Coomassie G-250 staining for proteins in polyacrylamide gels. *Journal of Visualized Experiments*, 30, e1431. <https://doi.org/10.3791/1431>
- Eastwood, D. C., Floudas, D., Binder, M., Majcherzyk, A., Schneider, P., Aerts, A., Asiegbu, F. O., Baker, S. E., Barry, K., Bendiksby, M., Blumentritt, M., Coutinho, P. M., Cullen, D., de Vries, R. P., Gathman, A., Goodell, B., Henriissat, B., Ihrmark, K., Kausserud, H., ... Watkinson, S. C. (2011). The plant cell wall-decomposing machinery underlies the functional diversity of forest fungi. *Science*, 333(6043), 762–765. <https://doi.org/10.1126/science.1205411>
- Eastwood, D. C., Herman, B., Noble, R., Dobrovin-Pennington, A., Sreenivasaprasad, S., & Burton, K. S. (2013). Environmental regulation of reproductive phase change in *Agaricus bisporus* by 1-octen-3-ol, temperature and CO₂. *Fungal Genetics and Biology*, 55, 54–66. <https://doi.org/10.1016/j.fgb.2013.01.001>
- El-Gebali, S., Mistry, J., Bateman, A., Eddy, S. R., Luciani, A., Potter, S. C., Qureshi, M., Richardson, L. J., Salazar, G. A., Smart, A., Sonnhammer, E. L. L., Hirsh, L., Paladin, L., Piovesan, D., Tosatto, S. C. E., & Finn, R. D. (2019). The Pfam protein families database in 2019. *Nucleic Acids Research*, 47(D1), D427–D432. <https://doi.org/10.1093/nar/gky995>
- Elble, R., & Tye, B. K. (1991). Both activation and repression of α -mating-type-specific genes in yeast require transcription factor Mcm1. *Proceedings of the National Academy of Sciences of the United States of America*, 88(23), 10966–10970. <https://doi.org/10.1073/pnas.88.23.10966>
- Emms, D. M., & Kelly, S. (2015). OrthoFinder: solving fundamental biases in whole genome comparisons dramatically improves orthogroup inference accuracy. *Genome Biology*, 16(1), 157. <https://doi.org/10.1186/s13059-015-0721-2>
- Emms, D. M., & Kelly, S. (2019). OrthoFinder: Phylogenetic orthology inference for comparative genomics. *Genome Biology*, 20(1), 1–14. <https://doi.org/10.1186/s13059-019-1832-y>
- Endo, H., Kajiwara, S., Tsunoka, O., & Shishido, K. (1994). A novel cDNA, priBc, encoding a protein with a Zn(II)2Cys6 zinc cluster DNA-binding motif, derived from the basidiomycete *Lentinus edodes*. *Gene*, 139(1), 117–121. [https://doi.org/10.1016/0378-1119\(94\)90533-9](https://doi.org/10.1016/0378-1119(94)90533-9)
- Engel, S. R., Dietrich, F. S., Fisk, D. G., Binkley, G., Balakrishnan, R., Costanzo, M. C., Dwight, S. S., Hitz, B. C., Karra, K., Nash, R. S., Weng, S., Wong, E. D., Lloyd, P., Skrzypek, M. S., Miyasato, S. R., Simison, M., & Cherry, J. M. (2014). The Reference Genome Sequence of *Saccharomyces cerevisiae*: Then and Now. *G3: Genes, Genomes, Genetics*, 4(3), 389–398. <https://doi.org/10.1534/g3.113.008995>
- Espagne, E., Lespinet, O., Malagnac, F., Da Silva, C., Jaillon, O., Porcel, B. M., Couloux, A., Aury, J. M., Séguens, B., Poulain, J., Anthouard, V., Grossetete, S., Khalili, H., Coppin, E., Déquard-Chablat, M., Picard, M., Contamine, V., Arnais, S., Bourdais, A., ... Silar, P. (2008). The genome sequence of the model ascomycete fungus *Podospora anserina*. *Genome Biology*, 9(5), 1–22. <https://doi.org/10.1186/gb-2008-9-5-r77>
- Esser, K., Saleh, F., & Meinhardt, F. (1979). Genetics of fruit body production in higher basidiomycetes II.

- Monokaryotic and dikaryotic fruiting in schizophyllum commune. *Current Genetics*, 1(1), 85–88. <https://doi.org/10.1007/BF00413309>
- Etienne-Manneville, S. (2004). Cdc42 - The centre of polarity. *Journal of Cell Science*, 117(8), 1291–1300. <https://doi.org/10.1242/jcs.01115>
- Fan, G., Zheng, H., Zhang, K., Ganeshan, V. D., Opiyo, S. O., Liu, D., Li, M., Li, G., Mitchell, T. K., Yun, Y., Wang, Z., & Lu, G. D. (2020). FgHtf1 regulates global gene expression towards aerial mycelium and conidiophore formation in the cereal fungal pathogen fusarium graminearum. *Applied and Environmental Microbiology*, 86(9), e03024-19. <https://doi.org/10.1128/AEM.03024-19>
- Feng, B., Haas, H., & Marzluf, G. A. (2000). ASD4, a new GATA factor of Neurospora crassa, displays sequence-specific DNA binding and functions in ascus and ascospore development. *Biochemistry*, 39(36), 11065–11073. <https://doi.org/10.1021/bi000886j>
- Feng, J., Liu, T., Qin, B., Zhang, Y., & Liu, X. S. (2012). Identifying ChIP-seq enrichment using MACS. *Nature Protocols*, 7(9), 1728–1740. <https://doi.org/10.1038/nprot.2012.101>
- Fischle, W., Wang, Y., & Allis, C. D. (2003). Histone and chromatin cross-talk. *Current Opinion in Cell Biology*, 15(2), 172–183. [https://doi.org/10.1016/S0955-0674\(03\)00013-9](https://doi.org/10.1016/S0955-0674(03)00013-9)
- Floudas, D., Binder, M., Riley, R., Barry, K., Blanchette, R. A., Henrissat, B., Martínez, A. T., Otilar, R., Spatafora, J. W., Yadav, J. S., Aerts, A., Benoit, I., Boyd, A., Carlson, A., Copeland, A., Coutinho, P. M., de Vries, R. P., Ferreira, P., Findley, K., ... Hibbett, D. S. (2012). The paleozoic origin of enzymatic lignin decomposition reconstructed from 31 fungal genomes. *Science*, 336(6089), 1715–1719. <https://doi.org/10.1126/science.1221748>
- Floudas, D., Held, B. W., Riley, R., Nagy, L. G., Koehler, G., Ransdell, A. S., Younus, H., Chow, J., Chiniquy, J., Lipzen, A., Tritt, A., Sun, H., Haridas, S., LaButti, K., Ohm, R. A., Kües, U., Blanchette, R. A., Grigoriev, I. V., Minto, R. E., & Hibbett, D. S. (2015). Evolution of novel wood decay mechanisms in Agaricales revealed by the genome sequences of *Fistulina hepatica* and *Cylindrobasidium torrendii*. *Fungal Genetics and Biology*, 76, 78–92. <https://doi.org/10.1016/j.fgb.2015.02.002>
- Fowler, T. J., & Mitton, M. F. (2000). Scooter, a new active transposon in *Schizophyllum commune*, has disrupted two genes regulating signal transduction. *Genetics*, 156(4), 1585–1594. <https://doi.org/10.1093/genetics/156.4.1585>
- Freiherst, D., Fowler, T. J., Bartholomew, K., Raudaskoski, M., Horton, J. S., & Kothe, E. (2016). 13 The Mating-Type Genes of the Basidiomycetes. *Growth, Differentiation and Sexuality*, 329–349. https://doi.org/10.1007/978-3-319-25844-7_13
- Freitag, M. (2017). Histone Methylation by SET Domain Proteins in Fungi. *Annual Review of Microbiology*, 71(1), 413–439. <https://doi.org/10.1146/annurev-micro-102215-095757>
- Friedland, A. E., Tzur, Y. B., Esvelt, K. M., Colaiácovo, M. P., Church, G. M., & Calarco, J. A. (2013). Heritable genome editing in *C. elegans* via a CRISPR-Cas9 system. *Nature Methods*, 10(8), 741–743. <https://doi.org/10.1038/nmeth.2532>
- Frischer, L. E., Hagen, F. S., & Garber, R. L. (1986). An inversion that disrupts the *Antennapedia* gene causes abnormal structure and localization of RNAs. *Cell*, 47(6), 1017–1023. [https://doi.org/10.1016/0092-8674\(86\)90816-0](https://doi.org/10.1016/0092-8674(86)90816-0)
- Fuller, K. K., Chen, S., Loros, J. J., & Dunlap, J. C. (2015). Development of the CRISPR/Cas9 system for targeted gene disruption in *Aspergillus fumigatus*. *Eukaryotic Cell*, 14(11), 1073–1080. <https://doi.org/10.1128/EC.00107-15>
- Galagan, J. E., Calvo, S. E., Borkovich, K. A., Selker, E. U., Read, N. O., Jaffe, D., FitzHugh, W., Ma, L. J., Smirnov, S., Purcell, S., Rehman, B., Elkins, T., Engels, R., Wang, S., Nielsen, C. B., Butler, J., Endrizzi, M., Qui, D., Ianakiev, P., ... Birren, B. (2003). The genome sequence of the filamentous fungus *Neurospora crassa*. *Nature*, 422(6934), 859–868. <https://doi.org/10.1038/nature01554>
- Galagan, J. E., Calvo, S. E., Cuomo, C., Ma, L. J., Wortman, J. R., Batzoglou, S., Lee, S. I., Baştürkmen, M., Spevak, C. C., Clutterbuck, J., Kapitonov, V., Jurka, J., Scazzocchio, C., Farman, M., Butler, J., Purcell, S., Harris, S., Braus, G. H., Draht, O., ... Birren, B. W. (2005). Sequencing of *Aspergillus nidulans* and comparative analysis with *A. fumigatus* and *A. oryzae*. *Nature*, 438(7071), 1105–1115. <https://doi.org/10.1038/nature04341>
- Gao, Q., Jin, K., Ying, S. H., Zhang, Y., Xiao, G., Shang, Y., Duan, Z., Hu, X., Xie, X. Q., Zhou, G., Peng, G., Luo, Z., Huang, W., Wang, B., Fang, W., Wang, S., Zhong, Y., Ma, L. J., St. Leger, R. J., ... Wang, C. (2011). Genome sequencing and comparative transcriptomics of the model entomopathogenic fungi *Metarhizium anisopliae* and *M. acridum*. *PLoS Genetics*, 7(1), e1001264. <https://doi.org/10.1371/journal.pgen.1001264>
- Gasiunas, G., Barrangou, R., Horvath, P., & Siksnys, V. (2012). Cas9-crRNA ribonucleoprotein complex mediates specific DNA cleavage for adaptive immunity in bacteria. *Proceedings of the National Academy of Sciences of the United States of America*, 109(39), E2579–E2586. <https://doi.org/10.1073/pnas.1208507109>
- Ghosh, A. K., Wangsanut, T., Fonzi, W. A., & Rolfes, R. J. (2015). The GRF10 homeobox gene regulates filamentous growth in the human fungal pathogen *Candida albicans*. *FEMS Yeast Research*, 15(8), fov093. <https://doi.org/10.1093/femsyr/fov093>
- Gibson, D. G. (2011). Enzymatic assembly of overlapping DNA fragments. *Methods in Enzymology*, 498, 349–361.

- <https://doi.org/10.1016/B978-0-12-385120-8.00015-2>
- Gilbert, G. S. (2002). Evolutionary ecology of plant diseases in natural ecosystems. *Annual Review of Phytopathology*, 40, 13–43. <https://doi.org/10.1146/annurev.phyto.40.021202.110417>
- Gillissen, B., Bergemann, J., Sandmann, C., Schroerer, B., Bölker, M., & Kahmann, R. (1992). A two-component regulatory system for self/non-self recognition in *Ustilago maydis*. *Cell*, 68(4), 647–657. [https://doi.org/10.1016/0092-8674\(92\)90141-X](https://doi.org/10.1016/0092-8674(92)90141-X)
- Gnerre, S., MacCallum, I., Przybylski, D., Ribeiro, F. J., Burton, J. N., Walker, B. J., Sharpe, T., Hall, G., Shea, T. P., Sykes, S., Berlin, A. M., Aird, D., Costello, M., Daza, R., Williams, L., Nicol, R., Gnirke, A., Nusbaum, C., Lander, E. S., & Jaffe, D. B. (2011). High-quality draft assemblies of mammalian genomes from massively parallel sequence data. *Proceedings of the National Academy of Sciences of the United States of America*, 108(4), 1513–1518. <https://doi.org/10.1073/pnas.1017351108>
- Goodwin, S. B., M'Barek, S. Ben, Dhillon, B., Wittenberg, A. H. J., Crane, C. F., Hane, J. K., Foster, A. J., van der Lee, T. A. J., Grimwood, J., Aerts, A., Antoniw, J., Bailey, A., Bluhm, B., Bowler, J., Bristow, J., van der Burgt, A., Canto-Canché, B., Churchill, A. C. L., Conde-Ferràez, L., ... Kema, G. H. J. (2011). Finished genome of the fungal wheat pathogen *Mycosphaerella graminicola* reveals dispensome structure, chromosome plasticity, and stealth pathogenesis. *PLoS Genetics*, 7(6), e1002070. <https://doi.org/10.1371/journal.pgen.1002070>
- Gordon, D. (2003). Viewing and editing assembled sequences using Consed. *Current Protocols in Bioinformatics*, 2(1), 11-2. <https://doi.org/10.1002/0471250953.bi1102s02>
- Gordon, D., Desmarais, C., & Green, P. (2001). Automated finishing with autofinish. *Genome Research*, 11(4), 614–625. <https://doi.org/10.1101/gr.171401>
- Gordon, J. L., Armisen, D., Proux-Weřa, E., O'Éigeartaigh, S. S., Byrne, K. P., & Wolfe, K. H. (2011). Evolutionary erosion of yeast sex chromosomes by mating-type switching accidents. *Proceedings of the National Academy of Sciences of the United States of America*, 108(50), 20024–20029. <https://doi.org/10.1073/pnas.1112808108>
- Goutte, C., & Johnson, A. D. (1988). a1 Protein alters the dna binding specificity of $\alpha 2$ repressor. *Cell*, 52(6), 875–882. [https://doi.org/10.1016/0092-8674\(88\)90429-1](https://doi.org/10.1016/0092-8674(88)90429-1)
- Goutte, C., & Johnson, A. D. (1993). Yeast a1 and $\alpha 2$ homeodomain proteins form a DNA-binding activity with properties distinct from those of either protein. *Journal of Molecular Biology*, 233(3), 359–371. <https://doi.org/10.1006/jmbi.1993.1517>
- Grahl, N., Demers, E. G., Crocker, A. W., & Hogan, D. A. (2017). Use of RNA-Protein Complexes for Genome Editing in Non- albicans Candida Species. *MSphere*, 2(3), e00218-17. <https://doi.org/10.1128/msphere.00218-17>
- Grigoriev, I. V., Martinez, D. A., & Salamov, A. A. (2006). Fungal genomic annotation. In *Applied Mycology and Biotechnology* (Vol. 6, Issue C, pp. 123–142). [https://doi.org/10.1016/S1874-5334\(06\)80008-0](https://doi.org/10.1016/S1874-5334(06)80008-0)
- Grigoriev, I. V., Nikitin, R., Haridas, S., Kuo, A., Ohm, R., O'tillar, R., Riley, R., Salamov, A., Zhao, X., Korzeniewski, F., Smirnova, T., Nordberg, H., Dubchak, I., & Shabalov, I. (2014). MycoCosm portal: Gearing up for 1000 fungal genomes. *Nucleic Acids Research*, 42(D1), D699–D704. <https://doi.org/10.1093/nar/gkt1183>
- Grimm, D., & Wösten, H. A. B. (2018). Mushroom cultivation in the circular economy. In *Applied Microbiology and Biotechnology* (Vol. 102, Issue 18, pp. 7795–7803). Springer Verlag. <https://doi.org/10.1007/s00253-018-9226-8>
- Gustafsson, C., Minshull, J., Govindarajan, S., Ness, J., Villalobos, A., & Welch, M. (2012). Engineering genes for predictable protein expression. *Protein Expression and Purification*, 83(1), 37–46. <https://doi.org/10.1016/j.pep.2012.02.013>
- Haber, J. E. (2012). Mating-type genes and MAT switching in *Saccharomyces cerevisiae*. *Genetics*, 191(1), 33–64. <https://doi.org/10.1534/genetics.111.134577>
- Hamidzade, M., Taghavi, S. M., Martins, S. J., Herschlag, R. A., Hockett, K. L., Bull, C. T., & Osdaghi, E. (2020). Bacterial brown pit, a new disease of edible mushrooms caused by *mycetocola* sp. *Plant Disease*, 104(5), 1445–1454. <https://doi.org/10.1094/PDIS-10-19-2176-RE>
- Han, K. H., Han, K. Y., Yu, J. H., Chae, K. S., Jahng, K. Y., & Han, D. M. (2001). The nsdD gene encodes a putative GATA-type transcription factor necessary for sexual development of *Aspergillus nidulans*. *Molecular Microbiology*, 41(2), 299–309. <https://doi.org/10.1046/j.1365-2958.2001.02472.x>
- Hay, A., & Tsiantis, M. (2010). KNOX genes: Versatile regulators of plant development and diversity. *Development*, 137(9), 3153–3165. <https://doi.org/10.1242/dev.030049>
- Hegemann, J. H., Goldener, U., & Köhler, G. J. (2006). Gene disruption in the budding yeast *Saccharomyces cerevisiae*. In *Yeast Protocol* (pp. 129–144). Humana Press, Totowa, NJ. <https://doi.org/10.1385/1-59259-958-3:129>
- Hemsworth, G. R., Johnston, E. M., Davies, G. J., & Walton, P. H. (2015). Lytic Polysaccharide Monooxygenases in Biomass Conversion. *Trends in Biotechnology*, 33(12), 747–761. <https://doi.org/10.1016/j.tibtech.2015.09.006>
- Henrissat, B., & Davies, G. (1997). Structural and sequence-based classification of glycoside hydrolases. *Current Opinion in Structural Biology*, 7(5), 637–644. [https://doi.org/10.1016/S0959-440X\(97\)80072-3](https://doi.org/10.1016/S0959-440X(97)80072-3)

- Herskowitz, I. (1989). A regulatory hierarchy for cell specialization in yeast. *Nature*, *342*(6251), 749–757. <https://doi.org/10.1038/342749a0>
- Herzog, R., Solovyeva, I., Böcker, M., Lugones, L. G., & Hennicke, F. (2019). Exploring molecular tools for transformation and gene expression in the cultivated edible mushroom *Agrocybe aegerita*. *Molecular Genetics and Genomics*, *294*(3), 663–677. <https://doi.org/10.1007/s00438-018-01528-6>
- Herzog, R., Solovyeva, I., Rühl, M., Thines, M., & Hennicke, F. (2016). Dikaryotic fruiting body development in a single dikaryon of *Agrocybe aegerita* and the spectrum of monokaryotic fruiting types in its monokaryotic progeny. *Mycological Progress*, *15*(9), 947–957. <https://doi.org/10.1007/s11557-016-1221-9>
- Hibbett, D., Abarenkov, K., Kõljalg, U., Öpik, M., Chai, B., Cole, J., Wang, Q., Crous, P., Robert, V., Helgason, T., Herr, J. R., Kirk, P., Lueschow, S., O'Donnell, K., Nilsson, R. H., Oono, R., Schoch, C., Smyth, C., Walker, D. M., ... Geiser, D. M. (2016). Sequence-based classification and identification of Fungi. *Mycologia*, *108*(6), 1049–1068. <https://doi.org/10.3852/16-130>
- Hibbett, D. S., Binder, M., Bischoff, J. F., Blackwell, M., Cannon, P. F., Eriksson, O. E., Huhndorf, S., James, T., Kirk, P. M., Lücking, R., Thorsten Lumbsch, H., Lutzoni, F., Matheny, P. B., McLaughlin, D. J., Powell, M. J., Redhead, S., Schoch, C. L., Spatafora, J. W., Stalpers, J. A., ... Zhang, N. (2007). A higher-level phylogenetic classification of the Fungi. *Mycological Research*, *111*(5), 509–547. <https://doi.org/10.1016/j.mycres.2007.03.004>
- Horak, C. E., Luscombe, N. M., Qian, J., Bertone, P., Piccirillo, S., Gerstein, M., & Snyder, M. (2002). Complex transcriptional circuitry at the G1/S transition in *Saccharomyces cerevisiae*. *Genes and Development*, *16*(23), 3017–3033. <https://doi.org/10.1101/gad.1039602>
- Horton, J. S. & Raper, C. A. (1991). A mushroom-inducing DNA sequence isolated from the basidiomycete, *Schizophyllum commune*. *Genetics*, *129*(3), 707–716. <https://doi.org/10.1093/genetics/129.3.707>
- Horton, J. Stephen, Palmer, G. E., & Smith, W. J. (1999). Regulation of dikaryon-expressed genes by FRT1 in the basidiomycete *Schizophyllum commune*. *Fungal Genetics and Biology*, *26*(1), 33–47. <https://doi.org/10.1006/fgbi.1998.1104>
- Hruscha, A., Krawitz, P., Rechenberg, A., Heinrich, V., Hecht, J., Haass, C., & Schmid, B. (2013). Efficient CRISPR/Cas9 genome editing with low off-target effects in zebrafish. *Development*, *140*(24), 4982–4987. <https://doi.org/10.1242/dev.099085>
- Huber, S., Lottspeich, F., & Kämper, J. (2002). A gene that encodes a product with similarity to dioxygenases is highly expressed in teliospores of *Ustilago maydis*. *Molecular Genetics and Genomics*, *267*(6), 757–771. <https://doi.org/10.1007/s00438-002-0717-y>
- Huerta-Cepas, J., Serra, F., & Bork, P. (2016). ETE 3: Reconstruction, Analysis, and Visualization of Phylogenomic Data. *Molecular Biology and Evolution*, *33*(6), 1635–1638. <https://doi.org/10.1093/molbev/msw046>
- Hull, C. M., Davidson, R. C., & Heitman, J. (2002). Cell identity and sexual development in *Cryptococcus neoformans* are controlled by the mating-type-specific homeodomain protein SX1 α . *Genes and Development*, *16*(23), 3046–3060. <https://doi.org/10.1101/gad.1041402>
- Hunter, S., Apweiler, R., Attwood, T. K., Bairoch, A., Bateman, A., Binns, D., Bork, P., Das, U., Daugherty, L., Duquenne, L., Finn, R. D., Gough, J., Haft, D., Hulo, N., Kahn, D., Kelly, E., Laugraud, A., Letunic, I., Lonsdale, D., ... Yeats, C. (2009). InterPro: The integrative protein signature database. *Nucleic Acids Research*, *37*(suppl_1), D211–D215. <https://doi.org/10.1093/nar/gkn785>
- Ian Robertson, C., Kende, A. M. M., Toenjes, K., Novotny, C. P., & Ullrich, R. C. (2002). Evidence for interaction of *Schizophyllum commune* Y mating-type proteins in vivo. *Genetics*, *160*(4), 1461–1467. <https://doi.org/10.1093/genetics/160.4.1461>
- Inada, K., Morimoto, Y., Arima, T., Murata, Y., & Kamada, T. (2001). The *clp1* gene of the mushroom *Coprinus cinereus* is essential for A-regulated sexual development. *Genetics*, *157*(1), 133–140. <https://doi.org/10.1093/genetics/157.1.133>
- Ingold, C. T. (1933). Spore discharge in the ascomycetes: I. pyrenomyces. *New Phytologist*, *32*(3), 175–196. <https://doi.org/10.1111/j.1469-8137.1933.tb07006.x>
- Izumitsu, K., Hatoh, K., Sumita, T., Kitade, Y., Morita, A., Gafur, A., Ohta, A., Kawai, M., Yamanaka, T., Neda, H., Ota, Y., & Tanaka, C. (2012). Rapid and simple preparation of mushroom DNA directly from colonies and fruiting bodies for PCR. *Mycoscience*, *53*(5), 396–401. <https://doi.org/10.1007/s10267-012-0182-3>
- Jaiswal, D., Jezek, M., Quijote, J., Lum, J., Choi, G., Kulkarni, R., Park, D. H., & Green, E. M. (2017). Repression of middle sporulation genes in *Saccharomyces cerevisiae* by the Sum1-Rfm1-Hst1 complex is maintained by Set1 and H3K4 methylation. *G3: Genes, Genomes, Genetics*, *7*(12), 3971–3982. <https://doi.org/10.1534/g3.117.300150>
- James, T. Y., Kauff, F., Schoch, C. L., Matheny, P. B., Hofstetter, V., Cox, C. J., Celio, G., Gueidan, C., Fraker, E., Miadlikowska, J., Lumbsch, H. T., Rauhut, A., Reeb, V., Arnold, A. E., Amtoft, A., Stajich, J. E., Hosaka, K., Sung, G. H., Johnson, D., ... Vilgalys, R. (2006). Reconstructing the early evolution of Fungi using a six-gene phylogeny. *Nature*, *443*(7113), 818–822. <https://doi.org/10.1038/nature05110>
- Jiao, X., Li, G., Wang, Y., Nie, F., Cheng, X., Abdullah, M., Lin, Y., & Cai, Y. (2018). Systematic analysis of the pleurotus

- ostreatus lacase gene (PoLac) Family and functional characterization of PoLac2 involved in the degradation of cotton-straw lignin. *Molecules*, 23(4), 880. <https://doi.org/10.3390/molecules23040880>
- Jinek, M., Chylinski, K., Fonfara, I., Hauer, M., Doudna, J. A., & Charpentier, E. (2012). A programmable dual-RNA-guided DNA endonuclease in adaptive bacterial immunity. *Science*, 337(6096), 816–821. <https://doi.org/10.1126/science.1225829>
- Johnson, A. D. (1995). Molecular mechanisms of cell-type determination in budding yeast. *Current Opinion in Genetics and Development*, 5(5), 552–558. [https://doi.org/10.1016/0959-437X\(95\)80022-0](https://doi.org/10.1016/0959-437X(95)80022-0)
- Johnson, D. S., Mortazavi, A., Myers, R. M., & Wold, B. (2007). Genome-wide mapping of in vivo protein-DNA interactions. *Science*, 316(5830), 1497–1502. <https://doi.org/10.1126/science.1141319>
- Johnson, P. R., Swanson, R., Rakhilina, L., & Hochstrasser, M. (1998). Degradation signal masking by heterodimerization of MAT α 2 and MAT α 1 blocks their mutual destruction by the ubiquitin-proteasome pathway. *Cell*, 94(2), 217–227. [https://doi.org/10.1016/S0092-8674\(00\)81421-X](https://doi.org/10.1016/S0092-8674(00)81421-X)
- Jones, T., Federspiel, N. A., Chibana, H., Dungan, J., Kalman, S., Magee, B. B., Newport, G., Thorstenson, Y. R., Agabian, N., Magee, P. T., Davis, R. W., & Scherer, S. (2004). The diploid genome sequence of *Candida albicans*. *Proceedings of the National Academy of Sciences of the United States of America*, 101(19), 7329–7334. <https://doi.org/10.1073/pnas.0401648101>
- Jurka, J., Kapitonov, V. V., Pavlicek, A., Klonowski, P., Kohany, O., & Walichiewicz, J. (2005). Repbase Update, a database of eukaryotic repetitive elements. *Cytogenetic and Genome Research*, 110(1–4), 462–467. <https://doi.org/10.1159/000084979>
- Kachroo, A. H., Laurent, J. M., Yellman, C. M., Meyer, A. G., Wilke, C. O., & Marcotte, E. M. (2015). Systematic humanization of yeast genes reveals conserved functions and genetic modularity. *Science*, 348(6237), 921–925. <https://doi.org/10.1126/science.aaa0769>
- Kamada, T., Sano, H., Nakazawa, T., & Nakahori, K. (2010). Regulation of fruiting body photomorphogenesis in *Coprinopsis cinerea*. *Fungal Genetics and Biology* 47(11), 917–921. <https://doi.org/10.1016/j.fgb.2010.05.003>
- Kämper, J., Kahmann, R., Bölker, M., Ma, L. J., Brefort, T., Saville, B. J., Banuett, F., Kronstad, J. W., Gold, S. E., Müller, O., Perlin, M. H., Wösten, H. A. B., de Vries, R., Ruiz-Herrera, J., Reynaga-Peña, C. G., Snetselaar, K., McCann, M., Pérez-Martín, J., Feldbrügge, M., ... Birren, B. W. (2006). Insights from the genome of the biotrophic fungal plant pathogen *Ustilago maydis*. *Nature*, 444(7115), 97–101. <https://doi.org/10.1038/nature05248>
- Kardos, N., & Demain, A. L. (2011). Penicillin: The medicine with the greatest impact on therapeutic outcomes. *Applied Microbiology and Biotechnology* 92(4), 677–687. <https://doi.org/10.1007/s00253-011-3587-6>
- Katoh, K., & Standley, D. M. (2013). MAFFT multiple sequence alignment software version 7: Improvements in performance and usability. *Molecular Biology and Evolution*, 30(4), 772–780. <https://doi.org/10.1093/molbev/mst010>
- Keleher, C. A., Goutte, C., & Johnson, A. D. (1988). The yeast cell-type-specific repressor α 2 acts cooperatively with a non-cell-type-specific protein. *Cell*, 53(6), 927–936. [https://doi.org/10.1016/S0092-8674\(88\)90449-7](https://doi.org/10.1016/S0092-8674(88)90449-7)
- Kemppainen, M., Duplessis, S., Martin, F., & Pardo, A. G. (2009). RNA silencing in the model mycorrhizal fungus *Laccaria bicolor*: Gene knock-down of nitrate reductase results in inhibition of symbiosis with *Populus*. *Environmental Microbiology*, 11(7), 1878–1896. <https://doi.org/10.1111/j.1462-2920.2009.01912.x>
- Khalidi, N., Seifuddin, F. T., Turner, G., Haft, D., Nierman, W. C., Wolfe, K. H., & Fedorova, N. D. (2010). SMURF: Genomic mapping of fungal secondary metabolite clusters. *Fungal Genetics and Biology*, 47(9), 736–741. <https://doi.org/10.1016/j.fgb.2010.06.003>
- Kim, D., Langmead, B., & Salzberg, S. L. (2015). HISAT: A fast spliced aligner with low memory requirements. *Nature Methods*, 12(4), 357–360. <https://doi.org/10.1038/nmeth.3317>
- Kim, H., Lee, S., Ahn, Y., Lee, J., & Won, W. (2020). Sustainable Production of Bioplastics from Lignocellulosic Biomass: Technoeconomic Analysis and Life-Cycle Assessment. *ACS Sustainable Chemistry and Engineering*, 8(33), 12419–12429. <https://doi.org/10.1021/acssuschemeng.0c02872>
- Kim, H. I., Lee, C. S., & Park, Y. J. (2016). Further characterization of hydrophobin genes in genome of *Flammulina velutipes*. *Mycoscience*, 57(5), 320–325. <https://doi.org/10.1016/j.myc.2016.04.004>
- Kim, J. Y., Kim, D. Y., Park, Y. J., & Jang, M. J. (2020). Transcriptome analysis of the edible mushroom *Lentinula edodes* in response to blue light. *PLoS ONE*, 15(3), e0230680. <https://doi.org/10.1371/journal.pone.0230680>
- Kim, K. H., Kang, Y. M., Im, C. H., Ali, A., Kim, S. Y., Je, H. J., Kim, M. K., Rho, H. S., Lee, H. S., Kong, W. S., & Ryu, J. S. (2014). Identification and functional analysis of pheromone and receptor genes in the B3 mating locus of *Pleurotus eryngii*. *PLoS ONE*, 9(8), e104693. <https://doi.org/10.1371/journal.pone.0104693>
- Kim, S., Park, S. Y., Kim, K. S., Rho, H. S., Chi, M. H., Choi, J., Park, J., Kong, S., Park, J., Goh, J., & Lee, Y. H. (2009). Homeobox transcription factors are required for conidiation and appressorium development in the rice blast fungus *Magnaporthe oryzae*. *PLoS Genetics*, 5(12), e1000757. <https://doi.org/10.1371/journal.pgen.1000757>
- King, N. (2004). The unicellular ancestry of animal development. *Developmental Cell* 7(3), 313–325. <https://doi.org/10.1016/j.devcel.2004.02.003>

- org/10.1016/j.devcel.2004.08.010
- Kinugawa, K., Suzuki, A., Takamatsu, Y., Kato, M., & Tanaka, K. (1994). Effects of concentrated carbon dioxide on the fruiting of several cultivated basidiomycetes (II). *Mycoscience*, *35*(4), 345–352. <https://doi.org/10.1007/BF02268504>
- Klemm, S. L., Shipony, Z., & Greenleaf, W. J. (2019). Chromatin accessibility and the regulatory epigenome. In *Nature Reviews Genetics* *20*(4), 207–220. <https://doi.org/10.1038/s41576-018-0089-8>
- Klengel, T., Liang, W. J., Chaloupka, J., Ruoff, C., Schröppel, K., Naglik, J. R., Eckert, S. E., Mogensen, E. G., Haynes, K., Tuite, M. F., Levin, L. R., Buck, J., & Mühlischlegel, F. A. (2005). Fungal adenyllyl cyclase integrates CO₂ sensing with cAMP signaling and virulence. *Current Biology*, *15*(22), 2021–2026. <https://doi.org/10.1016/j.cub.2005.10.040>
- Klosterman, S. J., Subbarao, K. V., Kang, S., Veronese, P., Gold, S. E., Thomma, B. P. H. J., Chen, Z., Henrissat, B., Lee, Y. H., Park, J., Garcia-Pedrajas, M. D., Barbara, D. J., Anchieta, A., de Jonge, R., Santhanam, P., Maruthachalam, K., Atallah, Z., Amyotte, S. G., Paz, Z., ... Ma, L. J. (2011). Comparative genomics yields insights into niche adaptation of plant vascular wilt pathogens. *PLoS Pathogens*, *7*(7), e1002137. <https://doi.org/10.1371/journal.ppat.1002137>
- Knabe, N., Jung, E. M., Freihorst, D., Hennicke, F., Horton, J. S., & Kothe, E. (2013). A central role for ras1 in morphogenesis of the basidiomycete *Schizophyllum commune*. *Eukaryotic Cell*, *12*(6), 941–952. <https://doi.org/10.1128/EC.00355-12>
- Knight, S. A., Tamai, K. T., Kosman, D. J., & Thiele, D. J. (1994). Identification and analysis of a *Saccharomyces cerevisiae* copper homeostasis gene encoding a homeodomain protein. *Molecular and Cellular Biology*, *14*(12), 7792–7804. <https://doi.org/10.1128/mcb.14.12.7792>
- Kohler, A., Kuo, A., Nagy, L. G., Morin, E., Barry, K. W., Buscot, F., Canbäck, B., Choi, C., Cichocki, N., Clum, A., Colpaert, J., Copeland, A., Costa, M. D., Doré, J., Floudas, D., Gay, G., Girlanda, M., Henrissat, B., Herrmann, S., ... Martin, F. (2015). Convergent losses of decay mechanisms and rapid turnover of symbiosis genes in mycorrhizal mutualists. *Nature Genetics*, *47*(4), 410–415. <https://doi.org/10.1038/ng.3223>
- Kombrink, A., Tayyrov, A., Essig, A., Stöckli, M., Micheller, S., Hintze, J., van Heuvel, Y., Dürig, N., Lin, C. wei, Kallio, P. T., Aebi, M., & Künzler, M. (2019). Induction of antibacterial proteins and peptides in the coprophilous mushroom *Coprinopsis cinerea* in response to bacteria. *ISME Journal*, *13*(3), 588–602. <https://doi.org/10.1038/s41396-018-0293-8>
- Komolov, K. E., & Benovic, J. L. (2018). G protein-coupled receptor kinases: Past, present and future. *Cellular Signalling* *41*, 17–24. Elsevier Inc. <https://doi.org/10.1016/j.cellsig.2017.07.004>
- Kong, Q., Chang, P. K., Li, C., Hu, Z., Zheng, M., Sun, Q., & Shan, S. (2020). Identification of AfIR binding sites in the genome of *Aspergillus flavus* by ChIP-Seq. *Journal of Fungi*, *6*(2), 52. <https://doi.org/10.3390/jof6020052>
- Konno, N., & Sakamoto, Y. (2011). An endo- β -1,6-glucanase involved in *Lentinula edodes* fruiting body autolysis. *Applied Microbiology and Biotechnology*, *91*(5), 1365–1373. <https://doi.org/10.1007/s00253-011-3295-2>
- Kostriken, R., Strathern, J. N., Klar, A. J. S., Hicks, J. B., & Heffron, F. (1983). A site-specific endonuclease essential for mating-type switching in *Saccharomyces cerevisiae*. *Cell*, *35*(1), 167–174. [https://doi.org/10.1016/0092-8674\(83\)90219-2](https://doi.org/10.1016/0092-8674(83)90219-2)
- Kothe, E. (2001). Mating-type genes for basidiomycete strain improvement in mushroom farming. In *Applied Microbiology and Biotechnology* *56*(5–6), 602–612. <https://doi.org/10.1007/s002530100763>
- Krappmann, S. (2007). Gene targeting in filamentous fungi: the benefits of impaired repair. *Fungal Biology Reviews* *21*(1), 25–29. <https://doi.org/10.1016/j.fbr.2007.02.004>
- Krause, K., Jung, E. M., Lindner, J., Hardiman, I., Poetschner, J., Madhavan, S., Matthäus, C., Kai, M., Menezes, R. C., Popp, J., Svatoš, A., & Kothe, E. (2020). Response of the wood-decay fungus *Schizophyllum commune* to co-occurring microorganisms. *PLoS ONE*, *15*(4), e0232145. <https://doi.org/10.1371/journal.pone.0232145>
- Krivoshchina, N. P. (2008). Macromycete fruit bodies as a habitat for dipterans (Insecta, Diptera). *Entomological Review*, *88*(7), 778–792. <https://doi.org/10.1134/S0013873808070038>
- Krizsán, K., Almási, É., Merényi, Z., Sahu, N., Virágh, M., Kószó, T., Mondo, S., Kiss, B., Bálint, B., Kües, U., Barry, K., Cseklye, J., Hegedüs, B., Henrissat, B., Johnson, J., Lipzen, A., Ohm, R. A., Nagy, I., Pangilinan, J., ... Nagy, L. G. (2019). Transcriptomic atlas of mushroom development reveals conserved genes behind complex multicellularity in fungi. *Proceedings of the National Academy of Sciences of the United States of America*, *116*(15), 7409–7418. <https://doi.org/10.1073/pnas.1817822116>
- Krogh, A., Larsson, B., Von Heijne, G., & Sonnhammer, E. L. L. (2001). Predicting transmembrane protein topology with a hidden Markov model: Application to complete genomes. *Journal of Molecular Biology*, *305*(3), 567–580. <https://doi.org/10.1006/jmbi.2000.4315>
- Kües, U., & Liu, Y. (2000). Fruiting body production in basidiomycetes. *Applied Microbiology and Biotechnology* *54*(2), 141–152. <https://doi.org/10.1007/s002530000396>
- Kües, U., Walsler, P. J., Klaus, M. J., & Aebi, M. (2002). Influence of activated A and B mating-type pathways on developmental processes in the basidiomycete *Coprinus cinereus*. *Molecular Genetics and Genomics*,



- 268(2), 262–271. <https://doi.org/10.1007/s00438-002-0745-7>
- Kües, U. (2000). Life History and Developmental Processes in the Basidiomycete *Coprinus cinereus*. *Microbiology and Molecular Biology Reviews*, 64(2), 316–353. <https://doi.org/10.1128/mmbr.64.2.316-353.2000>
- Kües, U. (2015). From two to many: Multiple mating types in Basidiomycetes. *Fungal Biology Reviews*, 29(3–4), 126–166. <https://doi.org/10.1016/j.fbr.2015.11.001>
- Kües, U., Asante-Owusu, R. N., Mutasa, E. S., Tymon, A. M., Pardo, E. H., O’Shea, S. F., Göttgens, B., & Casselton, L. A. (1994). Two classes of homeodomain proteins specify the multiple A mating types of the mushroom *Coprinus cinereus*. *Plant Cell*, 6(10), 1467–1475. <https://doi.org/10.2307/3869982>
- Kües, U., & Navarro-González, M. (2015). How do Agaricomycetes shape their fruiting bodies? 1. Morphological aspects of development. *Fungal Biology Reviews* 29(2), 63–97. <https://doi.org/10.1016/j.fbr.2015.05.001>
- Kües, U., & Ruhl, M. (2011). Multiple Multi-Copper Oxidase Gene Families in Basidiomycetes – What for? *Current Genomics*, 12(2), 72–94. <https://doi.org/10.2174/138920211795564377>
- Künzler, M. (2015). Hitting the sweet spot-glycans as targets of fungal defense effector proteins. *Molecules* 20(5), 8144–8167. <https://doi.org/10.3390/molecules20058144>
- Künzler, M. (2018). How fungi defend themselves against microbial competitors and animal predators. *PLoS Pathogens* 14(9), e1007184. <https://doi.org/10.1371/journal.ppat.1007184>
- Kuratani, M., Tanaka, K., Terashima, K., Muraguchi, H., Nakazawa, T., Nakahori, K., & Kamada, T. (2010). The dst2 gene essential for photomorphogenesis of *Coprinopsis cinerea* encodes a protein with a putative FAD-binding-4 domain. *Fungal Genetics and Biology*, 47(2), 152–158. <https://doi.org/10.1016/j.fgb.2009.10.006>
- Kurtz, S., Phillippy, A., Delcher, A. L., Smoot, M., Shumway, M., Antonescu, C., & Salzberg, S. L. (2004). Versatile and open software for comparing large genomes. *Genome Biology*, 5(2), 1–9. <https://doi.org/10.1186/gb-2004-5-2-r12>
- Lakkireddy, K., Khonsuntia, W., & Kües, U. (2020). Mycoparasite *Hypomyces odoratus* infests *Agaricus xanthodermus* fruiting bodies in nature. *AMB Express*, 10(1), 1–22. <https://doi.org/10.1186/s13568-020-01085-5>
- Lambrot, R., Siklenka, K., Lafleur, C., & Kimmins, S. (2019). The genomic distribution of histone H3K4me2 in spermatogonia is highly conserved in sperm. *Biology of Reproduction*, 100(6), 1661–1672. <https://doi.org/10.1093/biolre/iz055>
- Langmead, B., & Salzberg, S. L. (2012). Fast gapped-read alignment with Bowtie 2. *Nature Methods*, 9(4), 357–359. <https://doi.org/10.1038/nmeth.1923>
- Larkin, M. A., Blackshields, G., Brown, N. P., Chenna, R., Mcgettigan, P. A., McWilliam, H., Valentin, F., Wallace, I. M., Wilm, A., Lopez, R., Thompson, J. D., Gibson, T. J., & Higgins, D. G. (2007). Clustal W and Clustal X version 2.0. *Bioinformatics*, 23(21), 2947–2948. <https://doi.org/10.1093/bioinformatics/btm404>
- Lee, D., Jang, E. H., Lee, M., Kim, S. W., Lee, Y., Lee, K. T., & Bahna, Y. S. (2019). Unraveling melanin biosynthesis and signaling networks in *Cryptococcus neoformans*. *MBio*, 10(5), e02267-19. <https://doi.org/10.1128/mBio.02267-19>
- Lengeler, K. B., Fox, D. S., Fraser, J. A., Allen, A., Forrester, K., Dietrich, F. S., & Heitman, J. (2002). Mating-type locus of *Cryptococcus neoformans*: A step in the evolution of sex chromosomes. *Eukaryotic Cell*, 1(5), 704–718. <https://doi.org/10.1128/EC.1.5.704-718.2002>
- Lengeler, K. B., & Kothe, E. (1999a). Identification and characterization of *brt1*, a gene down-regulated during B-regulated development in *Schizophyllum commune*. *Current Genetics*, 35(5), 551–556. <https://doi.org/10.1007/s002940050452>
- Lengeler, K. B., & Kothe, E. (1999b). Mated: A putative peptide transporter of *Schizophyllum commune* expressed in dikaryons. *Current Genetics*, 36(3), 159–164. <https://doi.org/10.1007/s002940050486>
- Lengeler, K. B., Wang, P., Cox, G. M., Perfect, J. R., & Heitman, J. (2000). Identification of the MATa mating-type locus of *Cryptococcus neoformans* reveals a serotype A MATa strain thought to have been extinct. *Proceedings of the National Academy of Sciences of the United States of America*, 97(26), 14455–14460. <https://doi.org/10.1073/pnas.97.26.14455>
- Letunic, I., & Bork, P. (2016). Interactive tree of life (iTOL) v3: an online tool for the display and annotation of phylogenetic and other trees. *Nucleic Acids Research*, 44(W1), W242–W245. <https://doi.org/10.1093/nar/gkw290>
- Letunic, I., & Bork, P. (2019). Interactive Tree Of Life (iTOL) v4: recent updates and new developments. *Nucleic Acids Research* 47(W1), W256–259. <https://doi.org/10.1093/nar/gkz239>
- Levasseur, A., Drula, E., Lombard, V., Coutinho, P. M., & Henrissat, B. (2013). Expansion of the enzymatic repertoire of the CAZy database to integrate auxiliary redox enzymes. *Biotechnology for Biofuels*, 6(1), 1–14. <https://doi.org/10.1186/1754-6834-6-41>
- Lewis, E. B. (1978). A gene complex controlling segmentation in *Drosophila*. *Nature*, 276(5688), 565–570. <https://doi.org/10.1126/AAC.03728-14>
- Li, D., Bobrowicz, P., Wilkinson, H. H., & Ebbole, D. J. (2005). A mitogen-activated protein kinase pathway essential for mating and contributing to vegetative growth in *Neurospora crassa*. *Genetics*, 170(3), 1091–1104.

- <https://doi.org/10.1534/genetics.104.036772>
- Li, H., Handsaker, B., Wysoker, A., Fennell, T., Ruan, J., Homer, N., Marth, G., Abecasis, G., & Durbin, R. (2009). The Sequence Alignment/Map format and SAMtools. *Bioinformatics*, 25(16), 2078–2079. <https://doi.org/10.1093/bioinformatics/btp352>
- Lim, F. Y., & Keller, N. P. (2014). Spatial and temporal control of fungal natural product synthesis. *Natural Product Reports*, 31(10), 1277–1286. <https://doi.org/10.1039/c4np00083h>
- Lincoln, C., Long, J., Yamaguchi, J., Serikawa, K., & Hake, S. (1994). A knotted1-like homeobox gene in Arabidopsis is expressed in the vegetative meristem and dramatically alters leaf morphology when overexpressed in transgenic plants. *Plant Cell*, 6(12), 1859–1876. <https://doi.org/10.2307/3869913>
- Linder, M. B., Szilvay, G. R., Nakari-Setälä, T., & Penttilä, M. E. (2005). Hydrophobins: The protein-amphiphiles of filamentous fungi. *FEMS Microbiology Reviews* 29(5), 877–896. Oxford Academic. <https://doi.org/10.1016/j.femsre.2005.01.004>
- Liu, X. B., Xia, E. H., Li, M., Cui, Y. Y., Wang, P. M., Zhang, J. X., Xie, B. G., Xu, J. P., Yan, J. J., Li, J., Nagy, L. G., & Yang, Z. L. (2020). Transcriptome data reveal conserved patterns of fruiting body development and response to heat stress in the mushroomforming fungus *Flammulina filiformis*. *PLoS ONE*, 15(10), e0239890. <https://doi.org/10.1371/journal.pone.0239890>
- Liu, C, Yang, Z., Yang, J., Xia, Z., & Ao, S. (2000). Regulation of the yeast transcriptional factor PHO2 activity by phosphorylation. *Journal of Biological Chemistry*, 275(41), 31972–31978. <https://doi.org/10.1074/jbc.M003055200>
- Liu, Cuicui, Bi, J., Kang, L., Zhou, J., Liu, X., Liu, Z., & Yuan, S. (2021). The molecular mechanism of stipe cell wall extension for mushroom stipe elongation growth. *Fungal Biology Reviews* 35, 14–26. <https://doi.org/10.1016/j.fbr.2020.11.001>
- Liu, W., Xie, S., Zhao, X., Chen, X., Zheng, W., Lu, G., Xu, J. R., & Wang, Z. (2010). A homeobox gene is essential for conidiogenesis of the rice blast fungus *magnaporthe oryzae*. *Molecular Plant-Microbe Interactions*, 23(4), 366–375. <https://doi.org/10.1094/MPMI-23-4-0366>
- Liu, X., Farnung, L., Wigge, C., & Cramer, P. (2018). Cryo-EM structure of a mammalian RNA polymerase II elongation complex inhibited by α -amanitin. *Journal of Biological Chemistry*, 293(19), 7189–7194. <https://doi.org/10.1074/jbc.RA118.002545>
- Loftus, B. J., Fung, E., Roncaglia, P., Rowley, D., Amedeo, P., Bruno, D., Vamathevan, J., Miranda, M., Anderson, I. J., Fraser, J. A., Allen, J. E., Bosdet, I. E., Brent, M. R., Chiu, R., Doering, T. L., Donlin, M. J., D’Souza, C. A., Fox, D. S., Grinberg, V., ... Hyman, R. W. (2005). The genome of the basidiomycetous yeast and human pathogen *Cryptococcus neoformans*. *Science*, 307(5713), 1321–1324. <https://doi.org/10.1126/science.1103773>
- Lombard, V., Golaconda Ramulu, H., Drula, E., Coutinho, P. M., & Henrissat, B. (2014). The carbohydrate-active enzymes database (CAZy) in 2013. *Nucleic Acids Research*, 42(D1), D490–D495. <https://doi.org/10.1093/nar/gkt1178>
- Lowe, T. M., & Eddy, S. R. (1997). tRNAscan-SE: A Program for Improved Detection of Transfer RNA Genes in Genomic Sequence. *Nucleic Acids Research*, 25(5), 955–964. <https://doi.org/10.1093/nar/25.5.955>
- Lu, B. C. (2000). The control of meiosis progression in the fungus *Coprinus cinereus* by light/dark cycles. *Fungal Genetics and Biology*, 31(1), 33–41. <https://doi.org/10.1006/fgbi.2000.1229>
- Luan, R., Liang, Y., Chen, Y., Liu, H., Jiang, S., Che, T., Wong, B., & Sun Hui, H. (2010). Opposing developmental functions of *Agrocybe aegerita* galectin (AAL) during mycelia differentiation. *Fungal Biology*, 114(8), 599–608. <https://doi.org/10.1016/j.funbio.2010.05.001>
- Lugones, L. G., de Jong, J. F., de Vries, O. M. H., Jalving, R., Dijksterhuis, J., & Wösten, H. A. B. (2004). The SC15 protein of *Schizophyllum commune* mediates formation of aerial hyphae and attachment in the absence of the SC3 hydrophobin. *Molecular Microbiology*, 53(2), 707–716. <https://doi.org/10.1111/j.1365-2958.2004.04187.x>
- Lugones, L. G., Bosscher, J. S., Scholtmeyer, K., de Vries, O. M. H., & Wessels, J. G. H. (1996). An abundant hydrophobin (ABH1) forms hydrophobic rodlet layers in *Agaricus bisporus* fruiting bodies. *Microbiology*, 142(5), 1321–1329. <https://doi.org/10.1099/13500872-142-5-1321>
- Lugones, L. G., Wösten, H. A. B., Birkenkamp, K. U., Sjollem, K. A., Zagers, J., & Wessels, J. G. H. (1999). Hydrophobins line air channels in fruiting bodies of *Schizophyllum commune* and *Agaricus bisporus*. *Mycological Research*, 103(5), 635–640. <https://doi.org/10.1017/S0953756298007552>
- Lutzoni, F., Kauff, F., Cox, C. J., McLaughlin, D., Celio, G., Dentinger, B., Padamsee, M., Hibbett, D., James, T. Y., Baloch, E., Grube, M., Reeb, V., Hofstetter, V., Schoch, C., Arnold, A. E., Miadlikowska, J., Spatafora, J., Johnson, D., Hambleton, S., ... Vilgalys, R. (2004). Assembling the fungal tree of life: progress, classification, and evolution of subcellular traits. *American Journal of Botany*, 91(10), 1446–1480. <https://doi.org/10.3732/ajb.91.10.1446>
- Ma, A., Shan, L., Wang, N., Zheng, L., Chen, L., & Xie, B. (2007). Characterization of a *Pleurotus ostreatus* fruiting body-specific hydrophobin gene, *Po.hyd*. *Journal of Basic Microbiology*, 47(4), 317–324. <https://doi.org/10.1002/jobm.200710317>



- Ma, L. J., Ibrahim, A. S., Skory, C., Grabherr, M. G., Burger, G., Butler, M., Elias, M., Idrum, A., Lang, B. F., Sone, T., Abe, A., Calvo, S. E., Corrochano, L. M., Engels, R., Fu, J., Hansberg, W., Kim, J. M., Kodira, C. D., Koehrsen, M. J., ... Wickes, B. L. (2009). Genomic analysis of the basal lineage fungus *Rhizopus oryzae* reveals a whole-genome duplication. *PLoS Genetics*, *5*(7), e1000549. <https://doi.org/10.1371/journal.pgen.1000549>
- Ma, L. J., van der Does, H. C., Borkovich, K. A., Coleman, J. J., Daboussi, M. J., Di Pietro, A., Dufresne, M., Freitag, M., Grabherr, M., Henrissat, B., Houterman, P. M., Kang, S., Shim, W. B., Woloshuk, C., Xie, X., Xu, J. R., Antoniw, J., Baker, S. E., Bluhm, B. H., ... Rep, M. (2010). Comparative genomics reveals mobile pathogenicity chromosomes in *Fusarium*. *Nature*, *464*(7287), 367–373. <https://doi.org/10.1038/nature08850>
- Madhavan, S., Krause, K., Jung, E. M., & Kothe, E. (2014). Differential regulation of multi-copper oxidases in *Schizophyllum commune* during sexual development. *Mycological Progress*, *13*(4), 1199–1206. <https://doi.org/10.1007/s11557-014-1009-8>
- Maeda, R. K., & Karch, F. (2009). Chapter 1 The Bithorax Complex of *Drosophila*. An Exceptional Hox Cluster. *Current Topics in Developmental Biology* *88*, 1–33. [https://doi.org/10.1016/S0070-2153\(09\)88001-0](https://doi.org/10.1016/S0070-2153(09)88001-0)
- Mallo, M., Wellik, D. M., & Deschamps, J. (2010). Hox genes and regional patterning of the vertebrate body plan. *Developmental Biology* *344*(1), 7–15. <https://doi.org/10.1016/j.ydbio.2010.04.024>
- Maltby, V. E., Martin, B. J. E., Brind'Amour, J., Chruscicki, A. T., McBurney, K. L., Schulze, J. M., Johnson, I. J., Hills, M., Hentrich, T., Kobor, M. S., Lorincz, M. C., & Howe, L. A. J. (2012). Histone H3K4 demethylation is negatively regulated by histone H3 acetylation in *Saccharomyces cerevisiae*. *Proceedings of the National Academy of Sciences of the United States of America*, *109*(45), 18505–18510. <https://doi.org/10.1073/pnas.1202070109>
- Mans, R., van Rossum, H. M., Wijsman, M., Backx, A., Kuijpers, N. G. A., van den Broek, M., Daran-Lapujade, P., Pronk, J. T., van Maris, A. J. A., & Daran, J. M. G. (2015). CRISPR/Cas9: A molecular Swiss army knife for simultaneous introduction of multiple genetic modifications in *Saccharomyces cerevisiae*. *FEMS Yeast Research*, *15*(2), 1–15. <https://doi.org/10.1093/femsyr/fov004>
- Marian, I. M., Vonk, P. J., Valdes, I. D., Barry, K., Bostock, B., Carver, A., Daum, C., Lerner, H., Lipzen, A., Park, H., Schuller, M. B. P., Tegelaar, M., Tritt, A., Schmutz, J., Grimwood, J., Lugones, L. G., Choi, I.-G., Wösten, H. A. B., Grigoriev, I. V., & Ohm, R. A. (2021). The transcription factor Roc1 is a regulator of cellulose degradation in the wood-decaying mushroom *Schizophyllum commune*. *BioRxiv*, 2021.06.08.446897. <https://doi.org/10.1101/2021.06.08.446897>
- Martin, F., Aerts, A., Ahrén, D., Brun, A., Danchin, E. G. J., Duchaussoy, F., Gibon, J., Kohler, A., Lindquist, E., Pereda, V., Salamov, A., Shapiro, H. J., Wuyts, J., Blaudez, D., Buée, M., Brokstein, P., Canbäck, B., Cohen, D., Courty, P. E., ... Grigoriev, I. V. (2008). The genome of *Laccaria bicolor* provides insights into mycorrhizal symbiosis. *Nature*, *452*(7183), 88–92. <https://doi.org/10.1038/nature06556>
- Martinez, D., Berka, R. M., Henrissat, B., Saloheimo, M., Arvas, M., Baker, S. E., Chapman, J., Chertkov, O., Coutinho, P. M., Cullen, D., Danchin, E. G. J., Grigoriev, I. V., Harris, P., Jackson, M., Kubicek, C. P., Han, C. S., Ho, I., Larrondo, L. F., de Leon, A. L., ... Brettin, T. S. (2008). Genome sequencing and analysis of the biomass-degrading fungus *Trichoderma reesei* (syn. *Hypocrea jecorina*). *Nature Biotechnology*, *26*(5), 553–560. <https://doi.org/10.1038/nbt1403>
- Masuda, R., Iguchi, N., Tukuta, K., Nagoshi, T., Kemuriyama, K., & Muraguchi, H. (2016). The coprinopsis cinerea *Tup1* homologue *cag1* is required for gill formation during fruiting body morphogenesis. *Biology Open*, *5*(12), 1844–1852. <https://doi.org/10.1242/bio.021246>
- Matyiyahu, A., Hadar, Y., Dosoretz, C. G., & Belinky, P. A. (2008). Gene silencing by RNA interference in the white rot fungus *Phanerochaete chrysosporium*. *Applied and Environmental Microbiology*, *74*(17), 5359–5365. <https://doi.org/10.1128/AEM.02433-07>
- Matsu-ura, T., Baek, M., Kwon, J., & Hong, C. (2015). Efficient gene editing in *Neurospora crassa* with CRISPR technology. *Fungal Biology and Biotechnology*, *2*(1), 4. <https://doi.org/10.1186/s40694-015-0015-1>
- Mattey, M. (1992). The production of organic acids. *Critical Reviews in Biotechnology*, *12*(1–2), 87–132. <https://doi.org/10.3109/07388559209069189>
- Mead, M. E., Stanton, B. C., Kruzal, E. K., & Hull, C. M. (2015). Targets of the Sex Inducer homeodomain proteins are required for fungal development and virulence in *Cryptococcus neoformans*. *Molecular Microbiology*, *95*(5), 804–818. <https://doi.org/10.1111/mmi.12898>
- Meerupati, T., Andersson, K. M., Friman, E., Kumar, D., Tunlid, A., & Ahrén, D. (2013). Genomic Mechanisms Accounting for the Adaptation to Parasitism in Nematode-Trapping Fungi. *PLoS Genetics*, *9*(11), e1003909. <https://doi.org/10.1371/journal.pgen.1003909>
- Meng, L., Lyu, X., Shi, L., Wang, Q., Wang, L., Zhu, M., Mukhtar, I., Xie, B., & Wang, W. (2021). The transcription factor FvHmg1 negatively regulates fruiting body development in Winter Mushroom *Flammulina velutipes*. *Gene*, *785*, 145618. <https://doi.org/10.1016/j.gene.2021.145618>
- Michelot, D., & Melendez-Howell, L. M. (2003). *Amanita muscaria*: chemistry, biology, toxicology, and ethnomycolgy. *Mycological Research*, *107*(2), 131–146. <https://doi.org/10.1017/S0953756203007305>

- Millanes, A. M., Diederich, P., Ekman, S., & Wedin, M. (2011). Phylogeny and character evolution in the jelly fungi (Tremellomycetes, Basidiomycota, Fungi). *Molecular Phylogenetics and Evolution*, *61*(1), 12–28. <https://doi.org/10.1016/j.ympev.2011.05.014>
- Miyagishi, M., & Taira, K. (2002). U6 promoter-driven siRNAs with four uridine 3' overhangs efficiently suppress targeted gene expression in mammalian cells. *Nature Biotechnology*, *20*(5), 497–500. <https://doi.org/10.1038/nbt0502-497>
- Miyauchi, S., Kiss, E., Kuo, A., Drula, E., Kohler, A., Sánchez-García, M., Morin, E., Andreopoulos, B., Barry, K. W., Bonito, G., Buée, M., Carver, A., Chen, C., Cichocki, N., Clum, A., Culley, D., Crous, P. W., Fauchery, L., Girlanda, M., ... Martin, F. M. (2020). Large-scale genome sequencing of mycorrhizal fungi provides insights into the early evolution of symbiotic traits. *Nature Communications*, *11*(1). <https://doi.org/10.1038/s41467-020-18795-w>
- Miyazaki, Y., Sakuragi, Y., Yamazaki, T., & Shishido, K. (2004). Target genes of the developmental regulator PRIB of the mushroom *Lentinula edodes*. *Bioscience, Biotechnology and Biochemistry*, *68*(9), 1898–1905. <https://doi.org/10.1271/bbb.68.1898>
- Mogensen, E. G., Janbon, G., Chaloupka, J., Steegborn, C., Man, S. F., Moyrand, F., Klengel, T., Pearson, D. S., Geeves, M. A., Buck, J., Levin, L. R., & Mühlischlegel, F. A. (2006). *Cryptococcus neoformans* senses CO₂ through the carbonic anhydrase Can2 and the adenyllyl cyclase Cac1. *Eukaryotic Cell*, *5*(1), 103–111. <https://doi.org/10.1128/EC.5.1.103-111.2006>
- Morin, E., Kohler, A., Baker, A. R., Foulongne-Oriol, M., Lombard, V., Nagy, L. G., Ohm, R. A., Patyshakuliyeva, A., Brun, A., Aerts, A. L., Bailey, A. M., Billette, C., Coutinho, P. M., Deakin, G., Doddapaneni, H., Floudas, D., Grimwood, J., Hildén, K., Kües, U., ... Martin, F. (2012). Genome sequence of the button mushroom *Agaricus bisporus* reveals mechanisms governing adaptation to a humic-rich ecological niche. *Proceedings of the National Academy of Sciences of the United States of America*, *109*(43), 17501–17506. <https://doi.org/10.1073/pnas.1206847109>
- Müller, F., Krüger, D., Sattlegger, E., Hoffmann, B., Ballario, P., Kanaan, M., & Barthelmess, I. B. (1995). The *cpc-2* gene of *Neurospora crassa* encodes a protein entirely composed of WD-repeat segments that is involved in general amino acid control and female fertility. *MGG Molecular & General Genetics*, *248*(2), 162–173. <https://doi.org/10.1007/BF02190797>
- Muraguchi, H., Fujita, T., Kishibe, Y., Konno, K., Ueda, N., Nakahori, K., Yanagi, S. O., Kamada, T. (2008). The *exp1* gene essential for pileus expansion and autolysis of the inky cap mushroom *Coprinopsis cinerea* (*Coprinus cinereus*) encodes an HMG protein. *Fungal Genetics and Biology*, *45*(6), 890–896. <https://doi.org/10.1016/j.fgb.2007.11.004>
- Muraguchi, H., & Kamada, T. (1998). The *ich1* gene of the mushroom *Coprinus cinereus* is essential for pileus formation in fruiting. *Development*, *125*(16), 3133–3141. <https://doi.org/10.1242/dev.125.16.3133>
- Muraguchi, H., & Kamada, T. (2000). A mutation in the *eln2* gene encoding a cytochrome P450 of *Coprinus cinereus* affects mushroom morphogenesis. *Fungal Genetics and Biology*, *29*(1), 49–59. <https://doi.org/10.1006/fgbi.2000.1184>
- Muraguchi, H., Umezawa, K., Niihara, M., Yoshida, M., Kozaki, T., Ishii, K., Sakai, K., Shimizu, M., Nakahori, K., Sakamoto, Y., Choi, C., Ngan, C. Y., Lindquist, E., Lipzen, A., Tritt, A., Haridas, S., Barry, K., Grigoriev, I. V., & Pukkila, P. J. (2015). Strand-specific RNA-seq analyses of fruiting body development in *Coprinopsis cinerea*. *PLoS ONE*, *10*(10), e0141586. <https://doi.org/10.1371/journal.pone.0141586>
- Murata, Y., Fujii, M., Zolan, M. E., & Kamada, T. (1998). Molecular analysis of *pcc1*, a gene that leads to A-regulated sexual morphogenesis in *Coprinus cinereus*. *Genetics*, *149*(4), 1753–1761. <https://doi.org/10.1093/genetics/149.4.1753>
- Nagy, L. G. (2017). Evolution: Complex Multicellular Life with 5,500 Genes. *Current Biology*, *27*(12), R609–R612. <https://doi.org/10.1016/j.cub.2017.04.032>
- Nagy, L. G., Riley, R., Tritt, A., Adam, C., Daum, C., Floudas, D., Sun, H., Yadav, J. S., Pangilinan, J., Larsson, K. H., Matsuura, K., Barry, K., Labutti, K., Kuo, R., Ohm, R. A., Bhattacharya, S. S., Shirouzu, T., Yoshinaga, Y., Martin, F. M., ... Hibbett, D. S. (2016). Comparative genomics of early-diverging mushroom-forming fungi provides insights into the origins of lignocellulose decay capabilities. *Molecular Biology and Evolution*, *33*(4), 959–970. <https://doi.org/10.1093/molbev/msv337>
- Nagy, L. G., Kovács, G. M., & Krizsán, K. (2018). Complex multicellularity in fungi: evolutionary convergence, single origin, or both? *Biological Reviews*, *93*(4), 1778–1794. <https://doi.org/10.1111/brv.12418>
- Nagy, L. G., Ohm, R. A., Kovács, G. M., Floudas, D., Riley, R., Gácsér, A., Sipiczki, M., Davis, J. M., Doty, S. L., de Hoog, G. S., Lang, B. F., Spatafora, J. W., Martin, F. M., Grigoriev, I. V., & Hibbett, D. S. (2014). Latent homology and convergent regulatory evolution underlies the repeated emergence of yeasts. *Nature Communications*, *5*(1), 1–8. <https://doi.org/10.1038/ncomms5471>
- Nakazawa, T., Ando, Y., Kitaaki, K., Nakahori, K., & Kamada, T. (2011). Efficient gene targeting in Δ Cc.ku70 or Δ Cc.lig4 mutants of the agaricomycete *Coprinopsis cinerea*. *Fungal Genetics and Biology*, *48*(10), 939–946. <https://doi.org/10.1016/j.fgb.2011.07.004>



- doi.org/10.1016/J.FGB.2011.06.003
- Nakazawa, T., Tatsuta, Y., Fujita, T., Nakahori, K., & Kamada, T. (2010). Mutations in the Cc.rmt1 gene encoding a putative protein arginine methyltransferase alter developmental programs in the basidiomycete *Coprinopsis cinerea*. *Current Genetics*, *56*(4), 361–367. <https://doi.org/10.1007/s00294-010-0307-1>
- Nehls, U., & Dietz, S. (2014). Fungal aquaporins: cellular functions and ecophysiological perspectives. *Applied Microbiology and Biotechnology* *98*(21), 8835–8851. <https://doi.org/10.1007/s00253-014-6049-0>
- Nierman, W. C., Pain, A., Anderson, M. J., Wortman, J. R., Kim, H. S., Arroyo, J., Berriman, M., Abe, K., Archer, D. B., Bermejo, C., Bennett, J., Bowyer, P., Chen, D., Collins, M., Coulsen, R., Davies, R., Dyer, P. S., Farman, M., Fedorova, N., ... Denning, D. W. (2005). Genomic sequence of the pathogenic and allergenic filamentous fungus *Aspergillus fumigatus*. *Nature*, *438*(7071), 1151–1156. <https://doi.org/10.1038/nature04332>
- Ninomiya, Y., Suzuki, K., Ishii, C., & Inoue, H. (2004). Highly efficient gene replacements in *Neurospora* strains deficient for nonhomologous end-joining. *Proceedings of the National Academy of Sciences of the United States of America*, *101*(33), 12248–12253. <https://doi.org/10.1073/pnas.0402780101>
- Nødvig, C. S., Nielsen, J. B., Kogle, M. E., & Mortensen, U. H. (2015). A CRISPR-Cas9 system for genetic engineering of filamentous fungi. *PLoS ONE*, *10*(7), e0133085. <https://doi.org/10.1371/journal.pone.0133085>
- Ohm, R. A. (2020). Fungal Genomics. In *Genetics and Biotechnology. The Mycota*, (Vol. 2, pp. 207–224). Springer, Cham. https://doi.org/10.1007/978-3-030-49924-2_9
- Ohm, R. A., Aerts, D., Wösten, H. A. B., & Lugones, L. G. (2013). The blue light receptor complex WC-1/2 of *Schizophyllum commune* is involved in mushroom formation and protection against phototoxicity. *Environmental Microbiology*, *15*(3), 943–955. <https://doi.org/10.1111/j.1462-2920.2012.02878.x>
- Ohm, R. A., de Jong, J. F., Berends, E., Wang, F., Wösten, H. A. B., & Lugones, L. G. (2010). An efficient gene deletion procedure for the mushroom-forming basidiomycete *Schizophyllum commune*. *World Journal of Microbiology and Biotechnology*, *26*(10), 1919–1923. <https://doi.org/10.1007/s11274-010-0356-0>
- Ohm, R. A., de Jong, J. F., de Bekker, C., Wösten, H. A. B., & Lugones, L. G. (2011). Transcription factor genes of *Schizophyllum commune* involved in regulation of mushroom formation. *Molecular Microbiology*, *81*(6), 1433–1445. <https://doi.org/10.1111/j.1365-2958.2011.07776.x>
- Ohm, R. A., de Jong, J. F., Lugones, L. G., Aerts, A., Kothe, E., Stajich, J. E., de Vries, R. P., Record, E., Levasseur, A., Baker, S. E., Bartholomew, K. A., Coutinho, P. M., Erdmann, S., Fowler, T. J., Gathman, A. C., Lombard, V., Henrissat, B., Knabe, N., Kües, U., ... Wösten, H. A. B. (2010). Genome sequence of the model mushroom *Schizophyllum commune*. *Nature Biotechnology*, *28*(9), 957–963. <https://doi.org/10.1038/nbt.1643>
- Ohm, R. A., Feau, N., Henrissat, B., Schoch, C. L., Horwitz, B. A., Barry, K. W., Condon, B. J., Copeland, A. C., Dhillon, B., Glaser, F., Hesse, C. N., Kosti, I., LaButti, K., Lindquist, E. A., Lucas, S., Salamov, A. A., Bradshaw, R. E., Ciuffetti, L., Hamelin, R. C., ... Grigoriev, I. V. (2012). Diverse Lifestyles and Strategies of Plant Pathogenesis Encoded in the Genomes of Eighteen Dothideomycetes Fungi. *PLoS Pathogens*, *8*(12), e1003037. <https://doi.org/10.1371/journal.ppat.1003037>
- Ohm, R. A., Riley, R., Salamov, A., Min, B., Choi, I. G., & Grigoriev, I. V. (2014). Genomics of wood-degrading fungi. *Fungal Genetics and Biology*, *72*, 82–90. <https://doi.org/10.1016/j.fgb.2014.05.001>
- Olombrada, M., Lázaro-Gorines, R., López-Rodríguez, J. C., Martínez-Del-Pozo, Á., Oñaderra, M., Maestro-López, M., Lacadena, J., Gavilanes, J. G., & García-Ortega, L. (2017). Fungal ribotoxins: A review of potential biotechnological applications. *Toxins*, *9*(2), 71. <https://doi.org/10.3390/toxins9020071>
- Olson, Å., Aerts, A., Asiغبu, F., Belbahri, L., Bouzid, O., Broberg, A., Canbäck, B., Coutinho, P. M., Cullen, D., Dalman, K., Deflorio, G., van Diepen, L. T. A., Dunand, C., Duplessis, S., Durling, M., Gonthier, P., Grimwood, J., Fossdal, C. G., Hansson, D., ... Stenlid, J. (2012). Insight into trade-off between wood decay and parasitism from the genome of a fungal forest pathogen. *New Phytologist*, *194*(4), 1001–1013. <https://doi.org/10.1111/j.1469-8137.2012.04128.x>
- Orford, K., Kharchenko, P., Lai, W., Dao, M. C., Worhunsky, D. J., Ferro, A., Janzen, V., Park, P. J., & Scadden, D. T. (2008). Differential H3K4 Methylation Identifies Developmentally Poised Hematopoietic Genes. *Developmental Cell*, *14*(5), 798–809. <https://doi.org/10.1016/j.devcel.2008.04.002>
- Parag, Y., & Raper, J. R. (1960). Genetic recombination in a common-B cross of *Schizophyllum commune*. *Nature*, *188*(4752), 765–766. <https://doi.org/10.1038/188765a0>
- Park, J., Park, J., Jang, S., Kim, S., Kong, S., Choi, J., Ahn, K., Kim, J., Lee, S., Kim, S., Park, B., Jung, K., Kim, S., Kang, S., & Lee, Y. H. (2008). FTFD: An informatics pipeline supporting phylogenomic analysis of fungal transcription factors. *Bioinformatics*, *24*(7), 1024–1025. <https://doi.org/10.1093/bioinformatics/btn058>
- Park, Y. J., Baek, J. H., Lee, S., Kim, C., Rhee, H., Kim, H., Seo, J. S., Park, H. R., Yoon, D. E., Nam, J. Y., Kim, H. II, Kim, J. G., Yoon, H., Kang, H. W., Cho, J. Y., Song, E. S., Sung, G. H., Yoo, Y. B., Lee, C. S., ... Kong, W. S. (2014). Whole genome and global gene expression analyses of the model mushroom *Flammulina velutipes* reveal a high capacity for lignocellulose degradation. *PLoS ONE*, *9*(4), e93560. <https://doi.org/10.1371/journal.pone.0093560>
- Park, Y. J., Lee, C. S., & Kong, W. S. (2019). Genomic insights into the fungal lignocellulolytic machinery of *Flammulina*

- rossica. *Microorganisms*, 7(10), 421. <https://doi.org/10.3390/microorganisms7100421>
- Parniske, M. (2008). Arbuscular mycorrhiza: The mother of plant root endosymbioses. *Nature Reviews Microbiology*, 6(10), 763–775. Nature Publishing Group. <https://doi.org/10.1038/nrmicro1987>
- Pascon, R. C., & Miller, B. L. (2000). Morphogenesis in *Aspergillus nidulans* requires Dopey (DopA), a member of a novel family of leucine zipper-like proteins conserved from yeast to humans. *Molecular Microbiology*, 36(6), 1250–1264. <https://doi.org/10.1046/j.1365-2958.2000.01950.x>
- Passmore, S., Elble, R., & Tye, B. K. (1989). A protein involved in minichromosome maintenance in yeast binds a transcriptional enhancer conserved in eukaryotes. *Genes & Development*, 3(7), 921–935. <https://doi.org/10.1101/gad.3.7.921>
- Patel, S., & Goyal, A. (2012). Recent developments in mushrooms as anti-cancer therapeutics: a review. *3 Biotech*, 2(1), 1–15. <https://doi.org/10.1007/s13205-011-0036-2>
- Pearson, J. C., Lemons, D., & McGinnis, W. (2005). Modulating Hox gene functions during animal body patterning. *Nature Reviews Genetics*, 6(12), 893–904. <https://doi.org/10.1038/nrg1726>
- Pekowska, A., Benoukraf, T., Ferrier, P., & Spicuglia, S. (2010). A unique H3K4me2 profile marks tissue-specific gene regulation. *Genome Research*, 20(11), 1493–1502. <https://doi.org/10.1101/gr.109389.110>
- Pelkmans, J. F., Patil, M. B., Gehrmann, T., Reinders, M. J. T., Wösten, H. A. B., & Lugones, L. G. (2017). Transcription factors of schizophyllum commune involved in mushroom formation and modulation of vegetative growth. *Scientific Reports*, 7(1), 1–11. <https://doi.org/10.1038/s41598-017-00483-3>
- Pelkmans, J. F., Vos, A. M., Scholtmeijer, K., Hendrix, E., Baars, J. J. P., Gehrmann, T., Reinders, M. J. T., Lugones, L. G., & Wösten, H. A. B. (2016). The transcriptional regulator c2h2 accelerates mushroom formation in *Agaricus bisporus*. *Applied Microbiology and Biotechnology*, 100(16), 7151–7159. <https://doi.org/10.1007/s00253-016-7574-9>
- Pellegrin, C., Morin, E., Martin, F. M., & Veneault-Fourrey, C. (2015). Comparative analysis of secretomes from ectomycorrhizal fungi with an emphasis on small-secreted proteins. *Frontiers in Microbiology*, 6, 1278. <https://doi.org/10.3389/fmicb.2015.01278>
- Peñalva, M. A., Tilburn, J., Bignell, E., & Arst, H. N. (2008). Ambient pH gene regulation in fungi: making connections. *Trends in Microbiology*, 16(6), 291–300. <https://doi.org/10.1016/j.TIM.2008.03.006>
- Peraro, M. D., & van der Goot, F. G. (2016). Pore-forming toxins: Ancient, but never really out of fashion. *Nature Reviews Microbiology*, 14(2), 77–92. <https://doi.org/10.1038/nrmicro.2015.3>
- Perkins, J. H. (1969). Morphogenesis in *Schizophyllum commune*. I. Effects of white light. *Plant Physiology*, 44(12), 1706–1711. <https://doi.org/10.1104/pp.44.12.1706>
- Peter, M., Kohler, A., Ohm, R. A., Kuo, A., Krützmann, J., Morin, E., Arend, M., Barry, K. W., Binder, M., Choi, C., Clum, A., Copeland, A., Grisel, N., Haridas, S., Kipfer, T., Labutti, K., Lindquist, E., Lipzen, A., Maire, R., ... Martin, F. M. (2016). Ectomycorrhizal ecology is imprinted in the genome of the dominant symbiotic fungus *Cenococcum geophilum*. *Nature Communications*, 7(1), 1-15. <https://doi.org/10.1038/ncomms12662>
- Petersen, T. N., Brunak, S., Von Heijne, G., & Nielsen, H. (2011). SignalP 4.0: Discriminating signal peptides from transmembrane regions. *Nature Methods*, 8(10), 785–786. <https://doi.org/10.1038/nmeth.1701>
- Plaza, D. F., Lin, C. W., van der Velden, N. S. J., Aebi, M., & Künzler, M. (2014). Comparative transcriptomics of the model mushroom *Coprinopsis cinerea* reveals tissue-specific armories and a conserved circuitry for sexual development. *BMC Genomics*, 15(1), 492. <https://doi.org/10.1186/1471-2164-15-492>
- Pohl, C., Kiel, J. A. K. W., Driessen, A. J. M., Bovenberg, R. A. L., & Nygård, Y. (2016). CRISPR/Cas9 Based Genome Editing of *Penicillium chrysogenum*. *ACS Synthetic Biology*, 5(7), 754–764. <https://doi.org/10.1021/acssynbio.6b00082>
- Pohl, C., Mózsik, L., Driessen, A. J. M., Bovenberg, R. A. L., & Nygård, Y. I. (2018). Genome editing in *penicillium chrysogenum* using cas9 ribonucleoprotein particles. In *Synthetic Biology. Methods in Molecular Biology* (Vol. 1772, pp. 213–232). Humana Press, New York, NY. https://doi.org/10.1007/978-1-4939-7795-6_12
- Pohleven, J., Brzin, J., Vrabec, L., Leonardi, A., Čokl, A., Štrukelj, B., Kos, J., & Sabotič, J. (2011). Basidiomycete *Clitocybe nebularis* is rich in lectins with insecticidal activities. *Applied Microbiology and Biotechnology*, 91(4), 1141–1148. <https://doi.org/10.1007/s00253-011-3236-0>
- Pokholok, D. K., Harbison, C. T., Levine, S., Cole, M., Hannett, N. M., Tong, I. L., Bell, G. W., Walker, K., Rolfe, P. A., Herbolzheimer, E., Zeitlinger, J., Lewitter, F., Gifford, D. K., & Young, R. A. (2005). Genome-wide map of nucleosome acetylation and methylation in yeast. *Cell*, 122(4), 517–527. <https://doi.org/10.1016/j.cell.2005.06.026>
- Portnoy, T., Margeot, A., Linke, R., Atanasova, L., Fekete, E., Sándor, E., Hartl, L., Karaffa, L., Druzhinina, I. S., Seiboth, B., Le Crom, S., & Kubicek, C. P. (2011). The CRE1 carbon catabolite repressor of the fungus *Trichoderma reesei*: A master regulator of carbon assimilation. *BMC Genomics*, 12(1), 1–12. <https://doi.org/10.1186/1471-2164-12-269>
- Prade, R. A., & Timberlake, W. E. (1993). The *Aspergillus nidulans* brIA regulatory locus consists of overlapping transcription units that are individually required for conidiophore development. *EMBO Journal*, 12(6),



- 2439–2447. <https://doi.org/10.1002/j.1460-2075.1993.tb05898.x>
- Pramila, T., Miles, S., GuhaThakurta, D., Jemiolo, D., & Breeden, L. L. (2002). Conserved homeodomain proteins interact with MADS box protein Mcm1 to restrict ECB-dependent transcription to the M/G1 phase of the cell cycle. *Genes and Development*, *16*(23), 3034–3045. <https://doi.org/10.1101/gad.1034302>
- Price, A. L., Jones, N. C., & Pevzner, P. A. (2005). De novo identification of repeat families in large genomes. *Bioinformatics*, *21*(suppl_1). <https://doi.org/10.1093/bioinformatics/bti1018>
- Price, M. N., Dehal, P. S., & Arkin, A. P. (2010). FastTree 2 - Approximately maximum-likelihood trees for large alignments. *PLoS ONE*, *5*(3), e9490. <https://doi.org/10.1371/journal.pone.0009490>
- Qi, Y., Chen, H., Zhang, M., Wen, Q., Qiu, L., & Shen, J. (2019). Identification and expression analysis of Pofst3 suggests a role during *Pleurotus ostreatus* primordia formation. *Fungal Biology*, *123*(3), 200–208. <https://doi.org/10.1016/j.funbio.2018.12.008>
- Qi, Y., Sun, X., Ma, L., Wen, Q., Qiu, L., & Shen, J. (2020). Identification of two *Pleurotus ostreatus* blue light receptor genes (PoWC-1 and PoWC-2) and in vivo confirmation of complex PoWC-12 formation through yeast two hybrid system. *Fungal Biology*, *124*(1), 8–14. <https://doi.org/10.1016/j.funbio.2019.10.004>
- Qin, H., Xiao, H., Zou, G., Zhou, Z., & Zhong, J. J. (2017). CRISPR-Cas9 assisted gene disruption in the higher fungus *Ganoderma* species. *Process Biochemistry*, *56*, 57–61. <https://doi.org/10.1016/j.procbio.2017.02.012>
- Raper, J. R., San Antonio, J. P., & Miles, P. G. (1958). The expression of mutations in common-A heterokaryons of *Schizophyllum commune*. *Zeitschrift Für Vererbungslehre*, *89*(4), 540–558. <https://doi.org/10.1007/BF00889087>
- Raudaskoski, M., & Kothe, E. (2010). Basidiomycete mating type genes and pheromone signaling. *Eukaryotic Cell*, *9*(6), 847–859. <https://doi.org/10.1128/EC.00319-09>
- Raudaskoski, M., & Viitanen, H. (1982). Effect of aeration and light on fruit body induction in *Schizophyllum commune*. *Transactions of the British Mycological Society*, *78*(1), 89–96. [https://doi.org/10.1016/s0007-1536\(82\)80080-6](https://doi.org/10.1016/s0007-1536(82)80080-6)
- Rawlings, N. D., Barrett, A. J., & Bateman, A. (2012). MEROPS: The database of proteolytic enzymes, their substrates and inhibitors. *Nucleic Acids Research*, *40*(D1), D503–D509. <https://doi.org/10.1093/nar/gkr987>
- Riley, R., Haridas, S., Wolfe, K. H., Lopes, M. R., Hittinger, C. T., Göker, M., Salamov, A. A., Wisecaver, J. H., Long, T. M., Calvey, C. H., Aerts, A. L., Barry, K. W., Choi, C., Clum, A., Coughlan, A. Y., Deshpande, S., Douglass, A. P., Hanson, S. J., Klenk, H. P., ... Jeffries, T. W. (2016). Comparative genomics of biotechnologically important yeasts. *Proceedings of the National Academy of Sciences of the United States of America*, *113*(35), 9882–9887. <https://doi.org/10.1073/pnas.1603941113>
- Riley, R., Salamov, A. A., Brown, D. W., Nagy, L. G., Floudas, D., Held, B. W., Levasseur, A., Lombard, V., Morin, E., Otiillar, R., Lindquist, E. A., Sun, H., LaButti, K. M., Schmutz, J., Jabbour, D., Luo, H., Baker, S. E., Pisabarro, A. G., Walton, J. D., ... Grigoriev, I. V. (2014). Extensive sampling of basidiomycete genomes demonstrates inadequacy of the white-rot/brown-rot paradigm for wood decay fungi. *Proceedings of the National Academy of Sciences of the United States of America*, *111*(27), 9923–9928. <https://doi.org/10.1073/pnas.1400592111>
- Roberts, A., Trapnell, C., Donaghey, J., Rinn, J. L., & Pachter, L. (2011). Improving RNA-Seq expression estimates by correcting for fragment bias. *Genome Biology*, *12*(3), 1–14. <https://doi.org/10.1186/gb-2011-12-3-r22>
- Robertson, C. I., Bartholomew, K. A., Novotny, C. P., & Ulrich, R. C. (1996). Deletion of the *Schizophyllum commune* Aα locus: The roles of Aα Y and Z mating-type genes. *Genetics*, *144*(4), 1437–1444. <https://doi.org/10.1093/genetics/144.4.1437>
- Ronda, C., Maury, J., Jakočiunas, T., Baall Jacobsen, S. A., Germann, S. M., Harrison, S. J., Borodina, I., Keasling, J. D., Jensen, M. K., & Nielsen, A. T. (2015). CrEdit: CRISPR mediated multi-loci gene integration in *Saccharomyces cerevisiae*. *Microbial Cell Factories*, *14*(1), 1–11. <https://doi.org/10.1186/s12934-015-0288-3>
- Rouxel, T., Grandaubert, J., Hane, J. K., Hoede, C., van de Wouw, A. P., Couloux, A., Dominguez, V., Anthouard, V., Bally, P., Bourras, S., Cozijnsen, A. J., Ciuffetti, L. M., Degrave, A., Dilmaghani, A., Duret, L., Fudal, I., Goodwin, S. B., Gout, L., Glaser, N., ... Howlett, B. J. (2011). Effector diversification within compartments of the *Leptosphaeria maculans* genome affected by repeat-induced mutations. *Nature Communications*, *2*(1), 1–10. <https://doi.org/10.1038/ncomms1189>
- Royse, D. J., Baars, J., & Tan, Q. (2017). Current Overview of Mushroom Production in the World. In *Edible and Medicinal Mushrooms* (pp. 5–13). John Wiley & Sons, Ltd. <https://doi.org/10.1002/9781119149446.ch2>
- Ruán-Soto, F., Garibay-Orijel, R., & Cifuentes, J. (2006). Process and dynamics of traditional selling wild edible mushrooms in tropical Mexico. *Journal of Ethnobiology and Ethnomedicine*, *2*(1), 1–13. <https://doi.org/10.1186/1746-4269-2-3>
- Ryan, O. W., Poddar, S., & Cate, J. H. D. (2016). Crispr-cas9 genome engineering in *Saccharomyces cerevisiae* cells. *Cold Spring Harbor Protocols*, *2016*(6), 525–533. <https://doi.org/10.1101/pdb.prot086827>
- Sakamoto, Y. (2018). Influences of environmental factors on fruiting body induction, development and maturation in mushroom-forming fungi. *Fungal Biology Reviews*, *32*(4), 236–248. Elsevier Ltd. [154](https://doi.org/10.1016/j.</p></div><div data-bbox=)

- fbr.2018.02.003
- Sakamoto, Y., Irie, T., & Sato, T. (2005). Isolation and characterization of a fruiting body-specific $\text{exo-}\beta\text{-1,3-glucanase}$ -encoding gene, *exg1*, from *Lentinula edodes*. *Current Genetics*, *47*(4), 244–252. <https://doi.org/10.1007/s00294-005-0563-7>
- Sakamoto, Y., Minato, K. I., Nagai, M., Mizuno, M., & Sato, T. (2005). Characterization of the *Lentinula edodes* *exg2* gene encoding a lentinan-degrading $\text{exo-}\beta\text{-1,3-glucanase}$. *Current Genetics*, *48*(3), 195–203. <https://doi.org/10.1007/s00294-005-0002-9>
- Sakamoto, Y., Nakade, K., & Konno, N. (2011). Endo- $\beta\text{-1,3-Glucanase}$ GLU1, from the fruiting body of *Lentinula edodes*, belongs to a new glycoside hydrolase family. *Applied and Environmental Microbiology*, *77*(23), 8350–8354. <https://doi.org/10.1128/AEM.05581-11>
- Sakamoto, Y., Watanabe, H., Nagai, M., Nakade, K., Takahashi, M., & Sato, T. (2006). *Lentinula edodes* *tlg1* encodes a thaumatin-like protein that is involved in lentinan degradation and fruiting body senescence. *Plant Physiology*, *141*(2), 793–801. <https://doi.org/10.1104/pp.106.076679>
- Salame, T. M., Knop, D., Tal, D., Levinson, D., Yarden, O., & Hadar, Y. (2012). Predominance of a versatile-peroxidase-encoding gene, *mnp4*, as demonstrated by gene replacement via a gene targeting system for *Pleurotus ostreatus*. *Applied and Environmental Microbiology*, *78*(15), 5341–5352. <https://doi.org/10.1128/AEM.01234-12>
- Salamov, A. A., & Solovyev, V. V. (2000). Ab initio gene finding in *Drosophila* genomic DNA. *Genome Research*, *10*(4), 516–522. <https://doi.org/10.1101/gr.10.4.516>
- Sammer, D., Krause, K., Gube, M., Wagner, K., & Kothe, E. (2016). Hydrophobins in the life cycle of the ectomycorrhizal basidiomycete *Tricholoma vaccinum*. *PLoS ONE*, *11*(12), e0167773. <https://doi.org/10.1371/journal.pone.0167773>
- Sánchez-García, M., Ryberg, M., Khan, F. K., Varga, T., Nagy, L. G., & Hibbett, D. S. (2020). Fruiting body form, not nutritional mode, is the major driver of diversification in mushroom-forming fungi. *Proceedings of the National Academy of Sciences of the United States of America*, *117*(51), 32528–32534. <https://doi.org/10.1073/pnas.1922539117>
- Sano, H., Kaneko, S., Sakamoto, Y., Sato, T., & Shishido, K. (2009). The basidiomycetous mushroom *Lentinula edodes* white collar-2 homolog PHRB, a partner of putative blue-light photoreceptor PHRA, binds to a specific site in the promoter region of the *L. edodes* tyrosinase gene. *Fungal Genetics and Biology*, *46*(4), 333–341. <https://doi.org/10.1016/j.fgb.2009.01.001>
- Sano, H., Narikiyo, T., Kaneko, S., Yamazaki, T., & Shishido, K. (2007). Sequence analysis and expression of a blue-light photoreceptor gene, *Le.phrA* from the basidiomycetous mushroom *Lentinula edodes*. *Bioscience, Biotechnology and Biochemistry*, *71*(9), 2206–2213. <https://doi.org/10.1271/bbb.70170>
- Sarkar, N., Ghosh, S. K., Bannerjee, S., & Aikat, K. (2012). Bioethanol production from agricultural wastes: An overview. *Renewable Energy*, *37*(1), 19–27. <https://doi.org/10.1016/j.renene.2011.06.045>
- Schmidt, O., & Liese, W. (1980). Variability of Wood Degrading Enzymes of *Schizophyllum commune*. *Holzforschung*, *34*(2), 67–72. <https://doi.org/10.1515/hfsg.1980.34.2.67>
- Scholtmeijer, K., Cankar, K., Beekwilder, J., Wösten, H. A. B., Lugones, L. G., & Bosch, D. (2014). Production of (+)-valencene in the mushroom-forming fungus *S. commune*. *Applied Microbiology and Biotechnology*, *98*(11), 5059–5068. <https://doi.org/10.1007/s00253-014-5581-2>
- Scholtmeijer, K., de Vocht, M. L., Rink, R., Robillard, G. T., & Wösten, H. A. B. (2009). Assembly of the fungal SC3 hydrophobin into functional amyloid fibrils depends on its concentration and is promoted by cell wall polysaccharides. *Journal of Biological Chemistry*, *284*(39), 26309–26314. <https://doi.org/10.1074/jbc.M109.005553>
- Schotanus, K., Soyer, J. L., Connolly, L. R., Grandaubert, J., Happel, P., Smith, K. M., Freitag, M., & Stukenbrock, E. H. (2015). Histone modifications rather than the novel regional centromeres of *Zygozooporia tritici* distinguish core and accessory chromosomes. *Epigenetics and Chromatin*, *8*(1), 1–18. <https://doi.org/10.1186/s13072-015-0033-5>
- Schubert, D., Raudaskoski, M., Knabe, N., & Kothe, E. (2006). Ras GTPase-activating protein Gap1 of the homobasidiomycete *Schizophyllum commune* regulates hyphal growth orientation and sexual development. *Eukaryotic Cell*, *5*(4), 683–695. <https://doi.org/10.1128/EC.5.4.683-695.2006>
- Schuren, F. H. J. (1999). Atypical interactions between thn and wild-type mycelia of *Schizophyllum commune*. *Mycological Research*, *103*(12), 1540–1544. <https://doi.org/10.1017/S095375629900893X>
- Schuren, F. H. J., & Wessels, J. G. H. (1994). Highly-efficient transformation of the homobasidiomycete *Schizophyllum commune* to phleomycin resistance. *Current Genetics*, *26*(2), 179–183. <https://doi.org/10.1007/BF00313808>
- Seppy, M., Manni, M., & Zdobnov, E. M. (2019). BUSCO: Assessing genome assembly and annotation completeness. In *Methods in Molecular Biology* (pp. 227–245). Humana, New York, NY. https://doi.org/10.1007/978-1-4939-9173-0_14



- Shaner, N. C., Campbell, R. E., Steinbach, P. A., Giepmans, B. N. G., Palmer, A. E., & Tsien, R. Y. (2004). Improved monomeric red, orange and yellow fluorescent proteins derived from *Discosoma* sp. red fluorescent protein. *Nature Biotechnology*, *22*(12), 1567–1572. <https://doi.org/10.1038/nbt1037>
- Shelest, E. (2017). Transcription factors in fungi: TFome dynamics, three major families, and dual-specificity TFs. *Frontiers in Genetics*, *8*, 53. <https://doi.org/10.3389/fgene.2017.00053>
- Shi, L., Zhang, T., Xu, C., Ren, A., Jiang, A., Yu, H., & Zhao, M. (2017). Development of a dual promoter-mediated gene silencing system in *Flammulina velutipes*. *Mycoscience*, *58*(3), 181–187. <https://doi.org/10.1016/j.myc.2017.01.003>
- Sikhakolli, U. R., López-Giráldez, F., Li, N., Common, R., Townsend, J. P., & Trail, F. (2012). Transcriptome analyses during fruiting body formation in *Fusarium graminearum* and *Fusarium verticillioides* reflect species life history and ecology. *Fungal Genetics and Biology*, *49*(8), 663–673. <https://doi.org/10.1016/j.fgb.2012.05.009>
- Simão, F. A., Waterhouse, R. M., Ioannidis, P., Kriventseva, E. V., & Zdobnov, E. M. (2015). BUSCO: Assessing genome assembly and annotation completeness with single-copy orthologs. *Bioinformatics*, *31*(19), 3210–3212. <https://doi.org/10.1093/bioinformatics/btv351>
- Sipos, G., Prasanna, A. N., Walter, M. C., O'Connor, E., Bálint, B., Krizsán, K., Kiss, B., Hess, J., Varga, T., Slot, J., Riley, R., Bóka, B., Rigling, D., Barry, K., Lee, J., Mihaltcheva, S., LaButti, K., Lipzen, A., Waldron, R., ... Nagy, L. G. (2017). Genome expansion and lineage-specific genetic innovations in the forest pathogenic fungi *Armillaria*. *Nature ecology & evolution*, *1*(12), 1931–1941. <https://doi.org/10.1038/s41559-017-0347-8>
- Skrzypek, M. S., Binkley, J., Binkley, G., Miyasato, S. R., Simison, M., & Sherlock, G. (2017). The *Candida* Genome Database (CGD): Incorporation of Assembly 22, systematic identifiers and visualization of high throughput sequencing data. *Nucleic Acids Research*, *45*(D1), D592–D596. <https://doi.org/10.1093/nar/gkw924>
- Šmid, I., Rotter, A., Gruden, K., Brzin, J., Buh Gašparič, M., Kos, J., Žel, J., & Sabotič, J. (2015). Clitocyprin, a fungal cysteine protease inhibitor, exerts its insecticidal effect on Colorado potato beetle larvae by inhibiting their digestive cysteine proteases. *Pesticide Biochemistry and Physiology*, *122*, 59–66. <https://doi.org/10.1016/j.pestbp.2014.12.022>
- Smit, A. F., Hubley, R., & Green, P. (2013). *RepeatMasker Open-4.0* (p. <<http://www.repeatmasker.org>>).
- Smith, K. M., Phatale, P. A., Sullivan, C. M., Pomraning, K. R., & Freitag, M. (2011). Heterochromatin Is Required for Normal Distribution of *Neurospora crassa* CenH3. *Molecular and Cellular Biology*, *31*(12), 2528–2542. <https://doi.org/10.1128/mcb.01285-10>
- Smith, S. E., & Smith, F. A. (2011). Roles of arbuscular mycorrhizas in plant nutrition and growth: New paradigms from cellular to ecosystem scales. *Annual Review of Plant Biology*, *62*, 227–250. <https://doi.org/10.1146/annurev-arplant-042110-103846>
- Song, H. Y., Kim, D. H., & Kim, J. M. (2018). Comparative transcriptome analysis of dikaryotic mycelia and mature fruiting bodies in the edible mushroom *Lentinula edodes*. *Scientific Reports*, *8*(1), 1–15. <https://doi.org/10.1038/s41598-018-27318-z>
- Song, L., Ouedraogo, J. P., Kolbusz, M., Nguyen, T. T. M., & Tsang, A. (2018). Efficient genome editing using tRNA promoter-driven CRISPR/Cas9 gRNA in *Aspergillus Niger*. *PLoS ONE*, *13*(8), e0202868. <https://doi.org/10.1371/journal.pone.0202868>
- Soyer, J. L., Möller, M., Schotanus, K., Connolly, L. R., Galazka, J. M., Freitag, M., & Stukenbrock, E. H. (2015). Chromatin analyses of *Zygomycetia tritici*: Methods for chromatin immunoprecipitation followed by high-throughput sequencing (ChIP-seq). *Fungal Genetics and Biology*, *79*, 63–70. <https://doi.org/10.1016/j.fgb.2015.03.006>
- Specht, C. A. (1995). Isolation of the B α and B β mating-type loci of *Schizophyllum commune*. *Current Genetics*, *28*(4), 374–379. <https://doi.org/10.1007/BF00326436>
- Spiteller, P. (2008). Chemical defence strategies of higher fungi. *Chemistry - A European Journal*, *14*(30), 9100–9110. <https://doi.org/10.1002/chem.200800292>
- Stadler, M., & Hoffmeister, D. (2015). Fungal natural products-the mushroom perspective. *Frontiers in Microbiology*, *6*, 127. <https://doi.org/10.3389/fmicb.2015.00127>
- Stahl, U., & Esser, K. (1976). Genetics of fruit body production in higher basidiomycetes - I. Monokaryotic fruiting and its correlation with dikaryotic fruiting in *Polyporus ciliatus*. *MGG Molecular & General Genetics*, *148*(2), 183–197. <https://doi.org/10.1007/BF00268384>
- Stajich, J. E., Wilke, S. K., Ahrán, D., Au, C. H., Birren, B. W., Borodovsky, M., Burns, C., Canbäck, B., Casselton, L. A., Cheng, C. K., Deng, J., Dietrich, F. S., Fargo, D. C., Farman, M. L., Gathman, A. C., Goldberg, J., Guigó, R., Hoegger, P. J., Hooker, J. B., ... Pukkila, P. J. (2010). Insights into evolution of multicellular fungi from the assembled chromosomes of the mushroom *Coprinopsis cinerea* (*Coprinus cinereus*). *Proceedings of the National Academy of Sciences of the United States of America*, *107*(26), 11889–11894. <https://doi.org/10.1073/pnas.1003391107>
- Stark, R., & Brown, G. (2011). *DiffBind: differential binding analysis of ChIP-Seq peak data*. <http://Bioconductor>.

- Org/Packages/Release/Bioc/Html/DiffBind.Html.
- Steffens, E. K., Becker, K., Krevet, S., Teichert, I., & Kück, U. (2016). Transcription factor PRO1 targets genes encoding conserved components of fungal developmental signaling pathways. *Molecular Microbiology*, *102*(5), 792–809. <https://doi.org/10.1111/mmi.13491>
- Stemmer, M., Thumberger, T., Del Sol Keyer, M., Wittbrodt, J., & Mateo, J. L. (2015). CCTop: An intuitive, flexible and reliable CRISPR/Cas9 target prediction tool. *PLoS ONE*, *10*(4), e0124633. <https://doi.org/10.1371/journal.pone.0124633>
- Strauss, J., Horvath, H. K., Abdallah, B. M., Kindermann, J., Mach, R. L., & Kubicek, C. P. (1999). The function of CreA, the carbon catabolite repressor of *Aspergillus nidulans*, is regulated at the transcriptional and post-transcriptional level. *Molecular Microbiology*, *32*(1), 169–178. <https://doi.org/10.1046/j.1365-2958.1999.01341.x>
- Stricker, A. R., Grosstessner-Hain, K., Würleitner, E., & Mach, R. L. (2006). Xyr1 (Xylanase Regulator 1) regulates both the hydrolytic enzyme system and D-xylose metabolism in *Hypocrea jecorina*. *Eukaryotic Cell*, *5*(12), 2128–2137. <https://doi.org/10.1128/EC.00211-06>
- Stricker, A. R., Mach, R. L., & de Graaff, L. H. (2008). Regulation of transcription of cellulases- and hemicellulases-encoding genes in *Aspergillus niger* and *Hypocrea jecorina* (*Trichoderma reesei*). *Applied Microbiology and Biotechnology*, *78*(2), 211–220. Springer. <https://doi.org/10.1007/s00253-007-1322-0>
- Stutz, K., Kaech, A., Aebi, M., Künzler, M., & Hengartner, M. O. (2015). Disruption of the *C. elegans* intestinal brush border by the fungal lectin CCL2 phenocopies dietary lectin toxicity in mammals. *PLoS ONE*, *10*(6), e0129381. <https://doi.org/10.1371/journal.pone.0129381>
- Sudbery, P. E. (2011). Growth of *Candida albicans* hyphae. *Nature Reviews Microbiology*, *9*(10), 737–748. <https://doi.org/10.1038/nrmicro2636>
- Sugano, S. S., Suzuki, H., Shimokita, E., Chiba, H., Noji, S., Osakabe, Y., & Osakabe, K. (2017). Genome editing in the mushroom-forming basidiomycete *Coprinopsis cinerea*, optimized by a high-throughput transformation system. *Scientific Reports*, *7*(1), 1–9. <https://doi.org/10.1038/s41598-017-00883-5>
- Talavera, G., & Castresana, J. (2007). Improvement of phylogenies after removing divergent and ambiguously aligned blocks from protein sequence alignments. *Systematic Biology*, *56*(4), 564–577. <https://doi.org/10.1080/10635150701472164>
- Tao, Y., Chen, R., Yan, J., Long, Y., Tong, Z., Song, H., & Xie, B. (2019). A hydrophobin gene, *Hyd9*, plays an important role in the formation of aerial hyphae and primordia in *Flammulina filiformis*. *Gene*, *706*, 84–90. <https://doi.org/10.1016/j.gene.2019.04.067>
- Tayrov, A., Stanley, C. E., Azevedo, S., & Künzler, M. (2019). Combining microfluidics and RNA-sequencing to assess the inducible defenseome of a mushroom against nematodes. *BMC Genomics*, *20*(1), 1–13. <https://doi.org/10.1186/s12864-019-5607-3>
- Tedersoo, L., Bahram, M., Pöhlme, S., Kõljalg, U., Yorou, N. S., Wijesundera, R., Ruiz, L. V., Vasco-Palacios, A. M., Thu, P. Q., Suijia, A., Smith, M. E., Sharp, C., Saluveer, E., Saitta, A., Rosas, M., Riit, T., Ratkowsky, D., Pritsch, K., Põldmaa, K., ... Abarenkov, K. (2014). Global diversity and geography of soil fungi. *Science*, *346*(6213), 1256688. <https://doi.org/10.1126/science.1256688>
- Ter-Hovhannisyanyan, V., Lomsadze, A., Chernoff, Y. O., & Borodovsky, M. (2008). Gene prediction in novel fungal genomes using an ab initio algorithm with unsupervised training. *Genome Research*, *18*(12), 1979–1990. <https://doi.org/10.1101/gr.081612.108>
- Terashima, K., Yuki, K., Muraguchi, H., Akiyama, M., & Kamada, T. (2005). The *dst1* gene involved in mushroom photomorphogenesis of *Coprinus cinereus* encodes a putative photoreceptor for blue light. *Genetics*, *171*(1), 101–108. <https://doi.org/10.1534/genetics.104.040048>
- Tobert, J. A. (2003). Lovastatin and beyond: The history of the HMG-CoA reductase inhibitors. *Nature Reviews Drug Discovery*, *2*(7), 517–526. <https://doi.org/10.1038/nrd1112>
- Todd, R. B., Zhou, M., Ohm, R. A., Leeggangers, H. A. C. F., Visser, L., & de Vries, R. P. (2014). Prevalence of transcription factors in ascomycete and basidiomycete fungi. *BMC Genomics*, *15*(1), 214. <https://doi.org/10.1186/1471-2164-15-214>
- Toome, M., Ohm, R. A., Riley, R. W., James, T. Y., Lazarus, K. L., Henrissat, B., Albu, S., Boyd, A., Chow, J., Clum, A., Heller, G., Lipzen, A., Nolan, M., Sandor, L., Zvenigorodsky, N., Grigoriev, I. V., Spatafora, J. W., & Aime, M. C. (2014). Genome sequencing provides insight into the reproductive biology, nutritional mode and ploidy of the fern pathogen *Mixia osmundae*. *New Phytologist*, *202*(2), 554–564. <https://doi.org/10.1111/nph.12653>
- Trapnell, C., Williams, B. A., Pertea, G., Mortazavi, A., Kwan, G., van Baren, M. J., Salzberg, S. L., Wold, B. J., & Pachter, L. (2010). Transcript assembly and quantification by RNA-Seq reveals unannotated transcripts and isoform switching during cell differentiation. *Nature Biotechnology*, *28*(5), 511–515. <https://doi.org/10.1038/nbt.1621>
- Traven, A., Jelacic, B., & Sopta, M. (2006). Yeast Gal4: A transcriptional paradigm revisited. *EMBO Reports*, *7*(5), 496–499. <https://doi.org/10.1038/sj.embor.7400679>

- Tullis, P. (2021). How ecstasy and psilocybin are shaking up psychiatry. *Nature*, 589(7843), 506–509. <https://doi.org/10.1038/d41586-021-00187-9>
- Vallim, M. A., Miller, K. Y., & Miller, B. L. (2000). Aspergillus SteA (Sterile12-like) is a homeodomain-C2/H2-Zn2 finger transcription factor required for sexual reproduction. *Molecular Microbiology*, 36(2), 290–301. <https://doi.org/10.1046/j.1365-2958.2000.01874.x>
- van den Berg, M. A., Albang, R., Albermann, K., Badger, J. H., Daran, J. M., M Driessen, A. J., Garcia-Estrada, C., Fedorova, N. D., Harris, D. M., Heijne, W. H. M., Joardar, V., W Kiel, J. A. K., Kovalchuk, A., Martín, J. F., Nierman, W. C., Nijland, J. G., Pronk, J. T., Roubos, J. A., van der Klei, I. J., ... Bovenberg, R. A. L. (2008). Genome sequencing and analysis of the filamentous fungus *Penicillium chrysogenum*. *Nature Biotechnology*, 26(10), 1161–1168. <https://doi.org/10.1038/nbt.1498>
- van der Vegt, W., van der Mei, H. C., Wosten, H. A. B., Wessels, J. G. H., & Busscher, H. J. (1996). A comparison of the surface activity of the fungal hydrophobin SC3p with those of other proteins. *Biophysical Chemistry*, 57(2–3), 253–260. [https://doi.org/10.1016/0301-4622\(95\)00059-7](https://doi.org/10.1016/0301-4622(95)00059-7)
- van Dijk, H., Onguene, N. A., & Kuyper, T. W. (2003). Knowledge and utilization of edible mushrooms by local populations of the rain forest of South Cameroon. *Ambio*, 32(1), 19–23. <https://doi.org/10.1579/0044-7447-32.1.19>
- van Leeuwe, T. M., Arentshorst, M., Ernst, T., Alazi, E., Punt, P. J., & Ram, A. F. J. (2019). Efficient marker free CRISPR/Cas9 genome editing for functional analysis of gene families in filamentous fungi. *Fungal Biology and Biotechnology*, 6(1), 1–13. <https://doi.org/10.1186/s40694-019-0076-7>
- van Nimwegen, E. (2003). Scaling laws in the functional content of genomes. *Trends in Genetics*, 19(9), 479–484. [https://doi.org/10.1016/S0168-9525\(03\)00203-8](https://doi.org/10.1016/S0168-9525(03)00203-8)
- van Peer, A. F., de Bekker, C., Vinck, A., Wösten, H. A. B., & Lugones, L. G. (2009). Phleomycin increases transformation efficiency and promotes single integrations in schizophyllum commune. *Applied and Environmental Microbiology*, 75(5), 1243–1247. <https://doi.org/10.1128/AEM.02162-08>
- van Peer, A. F., Wang, F., van Driel, K. G. A., de Jong, J. F., van Donselaar, E. G., Müller, W. H., Boekhout, T., Lugones, L. G., & Wösten, H. A. B. (2010). The septal pore cap is an organelle that functions in vegetative growth and mushroom formation of the wood-rot fungus *Schizophyllum commune*. *Environmental Microbiology*, 12(4), 833–844. <https://doi.org/10.1111/j.1462-2920.2009.02122.x>
- van Peij, N. N. M. E., Gielkens, M. M. C., de Vries, R. P., Visser, J., & de graaff, L. H. (1998). The transcriptional activator XlnR regulates both xylanolytic and endoglucanase gene expression in *Aspergillus niger*. *Applied and Environmental Microbiology*, 64(10), 3615–3619. <https://doi.org/10.1128/aem.64.10.3615-3619.1998>
- van Peij, N. N. M. E., Visser, J., & de Graaff, L. H. (1998). Isolation and analysis of xlnR, encoding a transcriptional activator co-ordinating xylanolytic expression in *Aspergillus niger*. *Molecular Microbiology*, 27(1), 131–142. <https://doi.org/10.1046/j.1365-2958.1998.00666.x>
- van Wetter, M. A., Schuren, F. H. J., Schuurs, T. A., & Wessels, J. G. H. (2006). Targeted mutation of the SC3 hydrophobin gene of *Schizophyllum commune* affects formation of aerial hyphae. *FEMS Microbiology Letters*, 140(2–3), 265–269. <https://doi.org/10.1111/j.1574-6968.1996.tb08347.x>
- van Wetter, M. A., Wösten, H. A. B., & Wessels, J. G. H. (2000). SC3 and SC4 hydrophobins have distinct roles in formation of aerial structures in dikaryons of *Schizophyllum commune*. *Molecular Microbiology*, 36(1), 201–210. <https://doi.org/10.1046/j.1365-2958.2000.01848.x>
- Varga, T., Földi, C., Bense, V., & Nagy, L. G. (2021). Developmental innovations promote species diversification in mushroom-forming fungi. *BioRxiv*. <https://doi.org/10.1101/2021.03.10.434564>
- Varga, T., Krizsán, K., Földi, C., Dima, B., Sánchez-García, M., Sánchez-Ramírez, S., Szöllősi, G. J., Szarkándi, J. G., Papp, V., Albert, L., Andreopoulos, W., Angelini, C., Antonín, V., Barry, K. W., Bougher, N. L., Buchanan, P., Buyck, B., Bense, V., Catcheside, P., ... Nagy, L. G. (2019). Megaphylogeny resolves global patterns of mushroom evolution. *Nature Ecology and Evolution*, 3(4), 668–678. <https://doi.org/10.1038/s41559-019-0834-1>
- Veerappan, C. S., Avramova, Z., & Moriyama, E. N. (2008). Evolution of SET-domain protein families in the unicellular and multicellular Ascomycota fungi. *BMC Evolutionary Biology*, 8(1), 1–20. <https://doi.org/10.1186/1471-2148-8-190>
- Vienken, K., & Fischer, R. (2006). The Zn(II)2Cys6 putative transcription factor NosA controls fruiting body formation in *Aspergillus nidulans*. *Molecular Microbiology*, 61(2), 544–554. <https://doi.org/10.1111/j.1365-2958.2006.05257.x>
- Vienken, K., Scherer, M., & Fischer, R. (2005). The Zn(II)2Cys6 putative *Aspergillus nidulans* transcription factor repressor of sexual development inhibits sexual development under low-carbon conditions and in submersed culture. *Genetics*, 169(2), 619–630. <https://doi.org/10.1534/genetics.104.030767>
- Villares, A., Moreau, C., Bennati-Granier, C., Garajova, S., Foucat, L., Falourd, X., Saake, B., Berrin, J. G., & Cathala, B. (2017). Lytic polysaccharide monoxygenases disrupt the cellulose fibers structure. *Scientific Reports*, 7(1), 1–9. <https://doi.org/10.1038/srep40262>

- Vonk, P. J., Escobar, N., Wösten, H. A. B., Lugones, L. G., & Ohm, R. A. (2019). High-throughput targeted gene deletion in the model mushroom *Schizophyllum commune* using pre-assembled Cas9 ribonucleoproteins. *Scientific Reports*, *9*(1), 1-8. <https://doi.org/10.1038/s41598-019-44133-2>
- Vonk, P. J., & Ohm, R. A. (2018). The role of homeodomain transcription factors in fungal development. *Fungal Biology Reviews*, *32*(4), 219–230. <https://doi.org/10.1016/j.fbr.2018.04.002>
- Vonk, P. J., & Ohm, R. A. (2021). H3K4me2 ChIP-Seq reveals the epigenetic landscape during mushroom formation and novel developmental regulators of *Schizophyllum commune*. *Scientific Reports*, *11*(1), 1-15. <https://doi.org/10.1038/s41598-021-87635-8>
- Walser, P. J., Kües, U., Aebi, M., & Künzler, M. (2005). Ligand interactions of the Coprinopsis cinerea galectins. *Fungal Genetics and Biology*, *42*(4), 293–305. <https://doi.org/10.1016/j.fgb.2004.12.004>
- Walton, J. (2018). Ecology and Evolution of the Amanita Cyclic Peptide Toxins. In *The Cyclic Peptide Toxins of Amanita and Other Poisonous Mushrooms* (pp. 167–204). Springer, Cham. https://doi.org/10.1007/978-3-319-76822-9_6
- Wang, R., Ma, P., Li, C., Xiao, L., Liang, Z., & Dong, J. (2019). Combining transcriptomics and metabolomics to reveal the underlying molecular mechanism of ergosterol biosynthesis during the fruiting process of *Flammulina velutipes*. *BMC Genomics*, *20*(1), 1–12. <https://doi.org/10.1186/s12864-019-6370-1>
- Wang, Y., Li, X., & Hu, H. (2014). H3K4me2 reliably defines transcription factor binding regions in different cells. *Genomics*, *103*(2–3), 222–228. <https://doi.org/10.1016/j.ygeno.2014.02.002>
- Wang, Y., Wei, D., Zhu, X., Pan, J., Zhang, P., Huo, L., & Zhu, X. (2016). A “suicide” CRISPR-Cas9 system to promote gene deletion and restoration by electroporation in *Cryptococcus neoformans*. *Scientific Reports*, *6*(1), 1-13. <https://doi.org/10.1038/srep31145>
- Wang, Z., Lopez-Giraldez, F., Lehr, N., Farré, M., Common, R., Trail, F., & Townsend, J. P. (2014). Global gene expression and focused knockout analysis reveals genes associated with fungal fruiting body development in *Neurospora crassa*. *Eukaryotic Cell*, *13*(1), 154–169. <https://doi.org/10.1128/EC.00248-13>
- Waterborg, J. H. (2012). Evolution of histone H3: Emergence of variants and conservation of post-translational modification sites. *Biochemistry and Cell Biology*, *90*(1), 79–95. <https://doi.org/10.1139/o11-036>
- Wessels, J. G. H. (1965). MORPHOGENESIS AND BIOCHEMICAL PROCESSES IN SCHIZOPHYLLUM COMMUNE FR. *Wentia*, *13*, 1–113. <https://doi.org/10.1111/j.1438-8677.1965.tb00016.x>
- Wessels, J. G. H. (1986). Cell Wall Synthesis in Apical Hyphal Growth. *International Review of Cytology*, *104*, 37–79. [https://doi.org/10.1016/S0074-7696\(08\)61923-3](https://doi.org/10.1016/S0074-7696(08)61923-3)
- Wessels, J. G. H., de Vries, O. M. H., Asgeirsdottir, S. A., & Springer, J. (1991). The thn mutation of *Schizophyllum commune*, which suppresses formation of aerial hyphae, affects expression of the Sc3 hydrophobin gene. *Journal of General Microbiology*, *137*(10), 2439–2445. <https://doi.org/10.1099/00221287-137-10-2439>
- Wessels, J. G. H. (1990). Role of Cell Wall Architecture in Fungal Tip Growth Generation. In *Tip Growth In Plant and Fungal Cells* (pp. 1–29). Elsevier. <https://doi.org/10.1016/b978-0-12-335845-5.50004-5>
- Wessels, J. G. H. (1993). Fruiting in the Higher Fungi. *Advances in Microbial Physiology*, *34*, 147–202. [https://doi.org/10.1016/S0065-2911\(08\)60029-6](https://doi.org/10.1016/S0065-2911(08)60029-6)
- Wiemann, P., Sieber, C. M. K., von Bargen, K. W., Studt, L., Niehaus, E. M., Espino, J. J., Huß, K., Michielse, C. B., Albermann, S., Wagner, D., Bergner, S. V., Connolly, L. R., Fischer, A., Reuter, G., Kleigrewe, K., Bald, T., Wingfield, B. D., Ophir, R., Freeman, S., ... Tudzynski, B. (2013). Deciphering the Cryptic Genome: Genome-wide Analyses of the Rice Pathogen *Fusarium fujikuroi* Reveal Complex Regulation of Secondary Metabolism and Novel Metabolites. *PLoS Pathogens*, *9*(6). <https://doi.org/10.1371/journal.ppat.1003475>
- Wirth, S., Kunert, M., Ahrens, L.-M., Krause, K., Broska, S., Paetz, C., Kniemeyer, O., Jung, E.-M., Boland, W., & Kothe, E. (2018). The regulator of G-protein signalling Thn1 links pheromone response to volatile production in *Schizophyllum commune*. *Environmental Microbiology*, *20*(10), 3684–3699. <https://doi.org/10.1111/1462-2920.14369>
- Woo, J. W., Kim, J., Kwon, S. Il, Corvalán, C., Cho, S. W., Kim, H., Kim, S. G., Kim, S. T., Choe, S., & Kim, J. S. (2015). DNA-free genome editing in plants with preassembled CRISPR-Cas9 ribonucleoproteins. *Nature Biotechnology*, *33*(11), 1162–1164. <https://doi.org/10.1038/nbt.3389>
- Wood, V., Gwilliam, R., Rajandream, M. A., Lyne, M., Lyne, R., Stewart, A., Sgouros, J., Peat, N., Hayles, J., Baker, S., Basham, D., Bowman, S., Brooks, K., Brown, D., Brown, S., Chillingworth, T., Churcher, C., Collins, M., Connor, R., ... Nurse, P. (2002). The genome sequence of *Schizosaccharomyces pombe*. *Nature*, *415*(6874), 871–880. <https://doi.org/10.1038/nature724>
- Wood, W. F., Clark, T. J., Bradshaw, D. E., Foy, B. D., Largent, D. L., & Thompson, B. L. (2004). Clitoclactone: A Banana Slug Antifeedant from *Clitocybe flaccida*. *Mycologia*, *96*(1), 23. <https://doi.org/10.2307/3761983>
- Wosten, H. A. B., Asgeirsdottir, S. A., Krook, J. H., Drenth, J. H. H., & Wessels, J. G. H. (1994). The fungal hydrophobin Sc3p self-assembles at the surface of aerial hyphae as a protein membrane constituting the hydrophobic rodlet layer. *European Journal of Cell Biology*, *63*(1), 122–129.
- Wösten, H. A. B., & Wessels, J. G. H. (2006). The Emergence of Fruiting Bodies in Basidiomycetes. In *Growth*,

- Differentiation and Sexuality* (pp. 393–414). Springer-Verlag. https://doi.org/10.1007/3-540-28135-5_19
- Wösten, H. A. B. (2001). Hydrophobins: Multipurpose Proteins. *Annual Review of Microbiology*, 55(1), 625–646. <https://doi.org/10.1146/annurev.micro.55.1.625>
- Wösten, H. A. B., & Scholtmeijer, K. (2015). Applications of hydrophobins: current state and perspectives. *Applied Microbiology and Biotechnology*, 99(4), 1587–1597. <https://doi.org/10.1007/s00253-014-6319-x>
- Wösten, H. A. B., van Wetter, M. A., Lugones, L. G., van der Mei, H. C., Busscher, H. J., & Wessels, J. G. H. (1999). How a fungus escapes the water to grow into the air. *Current Biology*, 9(2), 85–88. [https://doi.org/10.1016/S0960-9822\(99\)80019-0](https://doi.org/10.1016/S0960-9822(99)80019-0)
- Wu, B., Xu, Z., Knudson, A., Carlson, A., Chen, N., Kovaka, S., LaButti, K., Lipzen, A., Pennachio, C., Riley, R., Schakwitz, W., Umezawa, K., Ohm, R. A., Grigoriev, I. V., Nagy, L. G., Gibbons, J., & Hobbitt, D. (2018). Genomics and development of *Lentinus tigrinus*: A white-rot wood-decaying mushroom with dimorphic fruiting bodies. *Genome Biology and Evolution*, 10(12), 3250–3261. <https://doi.org/10.1093/gbe/evy246>
- Wu, F. L., Zhang, G., Ren, A., Dang, Z. H., Shi, L., Jiang, A. L., Zhao, M. W. (2016). The pH-responsive transcription factor PacC regulates mycelial growth, fruiting body development, and ganoderic acid biosynthesis in *Ganoderma lucidum*. *Mycologia*, 108(6), 1104–1113. <https://doi.org/10.3852/16-079>
- Wu, J., & Miller, B. L. (1997). *Aspergillus* asexual reproduction and sexual reproduction are differentially affected by transcriptional and translational mechanisms regulating stunted gene expression. *Molecular and Cellular Biology*, 17(10), 6191–6201. <https://doi.org/10.1128/mcb.17.10.6191>
- Wu, T., Hu, C., Xie, B., Wei, S., Zhang, L., Zhu, Z., Zhang, Z., & Li, S. (2020). A putative transcription factor LFC1 negatively regulates development and yield of winter mushroom. *Applied Microbiology and Biotechnology*, 104(13), 5827–5844. <https://doi.org/10.1007/s00253-020-10642-8>
- Wu, T., Zhang, Z., Hu, C., Zhang, L., Wei, S., & Li, S. (2020). A WD40 Protein Encoding Gene *Fvcpc2* Positively Regulates Mushroom Development and Yield in *Flammulina velutipes*. *Frontiers in Microbiology*, 11, 498. <https://doi.org/10.3389/fmicb.2020.00498>
- Xiao, Z., Storms, R., & Tsang, A. (2004). Microplate-based filter paper assay to measure total cellulase activity. *Biotechnology and Bioengineering*, 88(7), 832–837. <https://doi.org/10.1002/bit.20286>
- Xu, J., Saunders, C. W., Hu, P., Grant, R. A., Boekhout, T., Kuramae, E. E., Kronstad, J. W., DeAngelis, Y. M., Reeder, N. L., Johnstone, K. R., Leland, M., Fieno, A. M., Begley, W. M., Sun, Y., Lacey, M. P., Chaudhary, T., Keough, T., Chu, L., Sears, R., ... Dawson, T. L. (2007). Dandruff-associated *Malassezia* genomes reveal convergent and divergent virulence traits shared with plant and human fungal pathogens. *Proceedings of the National Academy of Sciences of the United States of America*, 104(47), 18730–18735. <https://doi.org/10.1073/pnas.0706756104>
- Yamagishi, K., Kimura, T., Suzuki, M., & Shinmoto, H. (2002). Suppression of fruit-body formation by constitutively active G-protein α -subunits ScGP-A and ScGP-C in the homobasidiomycete *Schizophyllum commune*. *Microbiology*, 148(9), 2797–2809. <https://doi.org/10.1099/00221287-148-9-2797>
- Yamagishi, K., Kimura, T., Suzuki, M., Shinmoto, H., & Yamaki, K. J. (2004). Elevation of intracellular cAMP levels by dominant active heterotrimeric G protein α subunits ScGP-A and ScGP-C in homobasidiomycete, *Schizophyllum commune*. *Bioscience, Biotechnology and Biochemistry*, 68(5), 1017–1026. <https://doi.org/10.1271/bbb.68.1017>
- Yan, J. J., Tong, Z. J., Liu, Y. Y., Li, Y. N., Zhao, C., Mukhtar, I., Tao, Y. X., Chen, B. Z., Deng, Y. J., & Xie, B. G. (2019). Comparative transcriptomics of *Flammulina filiformis* suggests a high CO₂ concentration inhibits early pileus expansion by decreasing cell division control pathways. *International Journal of Molecular Sciences*, 20(23), 5923. <https://doi.org/10.3390/ijms20235923>
- Yli-Mattila, T., Ruiters, M. H. J., Wessels, J. G. H., & Raudaskoski, M. (1989). Effect of inbreeding and light on monokaryotic and dikaryotic fruiting in the homobasidiomycete *Schizophyllum commune*. *Mycological Research*, 93(4), 535–542. [https://doi.org/10.1016/S0953-7562\(89\)80049-8](https://doi.org/10.1016/S0953-7562(89)80049-8)
- Yoav, S., Salame, T. M., Feldman, D., Levinson, D., Ioelovich, M., Morag, E., Yarden, O., Bayer, E. A., & Hadar, Y. (2018). Effects of cre1 modification in the white-rot fungus *Pleurotus ostreatus* PC9: Altering substrate preference during biological pretreatment. *Biotechnology for Biofuels*, 11(1), 1–16. <https://doi.org/10.1186/s13068-018-1209-6>
- Yu, G., Wang, L. G., & He, Q. Y. (2015). ChIPseeker: An R/Bioconductor package for ChIP peak annotation, comparison and visualization. *Bioinformatics*, 31(14), 2382–2383. <https://doi.org/10.1093/bioinformatics/btv145>
- Yu, Z., & Fischer, R. (2019). Light sensing and responses in fungi. *Nature Reviews Microbiology*, 17(1), 25–36. <https://doi.org/10.1038/s41579-018-0109-x>
- Zerbino, D. R., & Birney, E. (2008). Velvet: Algorithms for de novo short read assembly using de Bruijn graphs. *Genome Research*, 18(5), 821–829. <https://doi.org/10.1101/gr.074492.107>
- Zhang, H., Yohe, T., Huang, L., Entwistle, S., Wu, P., Yang, Z., Busk, P. K., Xu, Y., & Yin, Y. (2018). DbCAN2: A meta server for automated carbohydrate-active enzyme annotation. *Nucleic Acids Research*, 46(W1), W95–W101. <https://doi.org/10.1093/nar/gky418>

- Zhang, J., Parvin, J., & Huang, K. (2012). Redistribution of H3K4me2 on neural tissue specific genes during mouse brain development. *BMC Genomics*, *13*(8), 1-10. <https://doi.org/10.1186/1471-2164-13-s8-s5>
- Zhang, J., Hao, H., Liu, H., Wang, Q., Chen, M., Feng, Z., & Chen, H. (2021). Genetic and functional analysis of the Zn(II)2Cys6 transcription factor HADA-1 in *Hypsizygus marmoreus*. *Applied Microbiology and Biotechnology*, *105*(7), 2815–2829. <https://doi.org/10.1007/s00253-021-11175-4>
- Zhang, J., Ren, A., Chen, H., Zhao, M., Shi, L., Chen, M., Wang, H., & Feng, Z. (2015). Transcriptome analysis and its application in identifying genes associated with fruiting body development in basidiomycete *Hypsizygus marmoreus*. *PLoS ONE*, *10*(4), e0123025. <https://doi.org/10.1371/journal.pone.0123025>
- Zhang, J., Silverstein, K. A. T., Castaño, J. D., Figueroa, M., & Schilling, J. S. (2019). Gene regulation shifts shed light on fungal adaption in plant biomass decomposers. *MBio*, *10*(6), e02176-19. <https://doi.org/10.1128/mBio.02176-19>
- Zhao, Y., & Garcia, B. A. (2015). Comprehensive catalog of currently documented histone modifications. *Cold Spring Harbor Perspectives in Biology*, *7*(9), a025064. <https://doi.org/10.1101/cshperspect.a025064>
- Zhu, N., Liu, J., Yang, J., Lin, Y., Yang, Y., Ji, L., Li, M., & Yuan, H. (2016). Comparative analysis of the secretomes of *Schizophyllum commune* and other wood-decay basidiomycetes during solid-state fermentation reveals its unique lignocellulose-degrading enzyme system. *Biotechnology for Biofuels*, *9*(1), 42. <https://doi.org/10.1186/s13068-016-0461-x>
- Zuris, J. A., Thompson, D. B., Shu, Y., Guiling, J. P., Bessen, J. L., Hu, J. H., Maeder, M. L., Joung, J. K., Chen, Z. Y., & Liu, D. R. (2015). Cationic lipid-mediated delivery of proteins enables efficient protein-based genome editing in vitro and in vivo. *Nature Biotechnology*, *33*(1), 73–80. <https://doi.org/10.1038/nbt.3081>



Nederlandse samenvatting

Schimmels zijn eukaryote micro-organismen. Ze kunnen groeien als eencellige gisten of als meercellige filamenteuze schimmels die hyfen vormen. Een netwerk van hyfen wordt een mycelium genoemd. In de natuur vervullen ze functies als mutualist of ziekteverwekker in interacties met andere organismen en als onderdeel van de koolstofkringloop door het afbreken van dood organisch materiaal. Schimmels worden veelvuldig door de mens gebruikt. Bekende voorbeelden zijn het rijzen van deeg en het brouwen van alcohol door de bakkersgist *Saccharomyces cerevisiae*. Ze produceren echter ook veel andere chemische verbindingen, zoals organische zuren. In de medische wereld zijn schimmels erg belangrijk voor de productie van medicijnen, zoals antibiotica en cholesterolverlagende statines. Daarnaast zijn er veel ziekteverwekkende schimmels die voor infecties in mensen, dieren, planten en andere schimmels zorgen. De paddenstoelen van sommige schimmels zijn een belangrijke voedselbron met veel eiwitten, vezels, vitaminen en mineralen. In Nederland wordt vooral de champignon *Agaricus bisporus* gegeten, maar ook de shiitake *Lentinula edodes* en de oesterzwam *Pleurotus ostreatus* zijn populair. Recentelijk is er veel aandacht voor nieuwe toepassingen van schimmels, zoals het verbeteren van de groei van planten door symbiotische schimmels. Ook de afbraak van de complexe suikers in lignocellulose, de belangrijkste bouwsteen van planten, wordt veelvuldig onderzocht, omdat de simpele suikers die daarbij vrijkomen gebruikt kunnen worden voor de productie van chemicaliën. Een voorbeeld hiervan is het produceren van bio-ethanol als brandstof.

Hoewel schimmels veel belangrijke toepassingen hebben, is er weinig bekend over de ontwikkeling van schimmels. Dit is met name het geval bij de paddenstoelvormende schimmels, omdat deze erg moeilijk in het lab zijn te kweken. Wereldwijd bestaat 85% van de industrieel geproduceerde paddenstoelen uit slechts vijf soorten, omdat het kweken van veel soorten niet mogelijk is. Door het proces van paddenstoelvorming beter te begrijpen kunnen meer soorten industrieel gekweekt worden en kan de productie verhoogd worden. Ook zijn schimmels die paddenstoelen maken erg efficiënt in het afbreken van lignocellulose, in vergelijking met andere schimmels. Hoe deze afbraak in paddenstoelvormende schimmels gereguleerd wordt is echter niet bekend. Omdat paddenstoelvormende schimmels moeilijk in het lab groeien, zijn ze moeilijk te onderzoeken. Daarom is de meeste kennis over de genetica van deze soorten afkomstig van twee modelorganismen. Dit zijn het waaiertje *Schizophyllum commune* en de inktzwam *Coprinopsis cinerea*. Deze schimmels kunnen genetisch gemodificeerd worden en ze vormen in korte tijd paddenstoelen in het lab.

Vooraf over de genetica van *S. commune* is relatief veel bekend. Deze schimmel, die in het wild op dood hout groeit, kan in het lab binnen 10 dagen paddenstoelen vormen en wordt gebruikt als model voor paddenstoelvorming. Ontkiemende basidiosporen van *S. commune* groeien uit tot een monokaryotisch (iedere cel heeft één haploïde kern) mycelium. Dit mycelium kan fuseren met een partner met een verschillend mating type. De mating type wordt bepaald door twee mating type loci en reguleren de vorming van een vruchtbaar dikaryotisch mycelium, waarin iedere cel twee haploïde kernen heeft. Het vruchtbare mycelium kan vervolgens onder de juiste omstandigheden paddenstoelen vormen. Onder andere licht en de CO₂ concentratie spelen hierbij een belangrijke rol. Wanneer *S. commune* als monokaryon groeit, is de kolonie symmetrisch rond en wit. Als er een dikaryon gevormd

wordt en de condities goed zijn voor paddenstoelvorming, groeit *S. commune* asymmetrisch. Na een paar dagen vormen zich kleine aggregaten van hyfen die vervolgens uit kunnen groeien tot paddenstoelen die seksuele basidiosporen produceren.

In dit proefschrift wordt de regulatie van paddenstoelvorming en afbraak van hout in *S. commune* onderzocht. Hiervoor zijn genetische analyses gebruikt, nieuwe moleculaire genetische technieken ontwikkeld en transcriptiefactoren onderzocht die een rol spelen in paddenstoelvorming.

Genoomanalyse van homeodomein transcriptiefactoren in schimmels

Er zijn in de afgelopen jaren meer dan duizend genomen van schimmels gepubliceerd, waaronder veel paddenstoelvormende schimmels. In **Hoofdstuk 2** worden 222 genomen gebruikt om te analyseren wat de rol is van homeodomain transcriptiefactoren tijdens de ontwikkeling van schimmels. Deze transcriptiefactoren zijn erg belangrijk tijdens de ontwikkeling van dieren en planten, maar ook van schimmels. Eén van de mating type loci van paddenstoelvormende schimmels bestaat uit homeodomain transcriptiefactoren. Daarnaast is het belang van deze transcriptiefactoren in het verleden al aangetoond in *S. commune*. Zo zorgt het inactiveren van *hom1* ervoor dat een dikaryon van *S. commune* meer, maar kleinere paddenstoelen maakt. *Hom2* speelt ook een rol in paddenstoelvorming en dikaryons waarin *hom2* is geïnactiveerd vormen geen paddenstoelen. Een analyse van homeodomain transcriptiefactoren laat zien dat ze te verdelen zijn in 12 verschillende groepen. Vooral paddenstoelvormende schimmels hebben veel verschillende groepen van deze transcriptiefactoren. *S. commune* heeft 18 verschillende van deze genen, waarvan acht onderdeel zijn van de mating type loci. De andere tien zijn verdeeld over acht verschillende groepen. De hoge variatie suggereert dat ze een rol hebben in processen die uniek zijn voor paddenstoelvormende schimmels. Meer onderzoek naar de functie van de homeodomain transcriptiefactoren kan daarom nieuwe kennis over bijvoorbeeld paddenstoelvorming opleveren.

Moleculair genetische technieken

S. commune is één van de weinige paddenstoelvormende schimmels waarin het mogelijk is om gericht genen uit te schakelen met behulp van homologe recombinatie. Hierbij wordt een stuk DNA vervangen door een antibiotica resistentie gen. Dit is een belangrijke techniek om de functie van genen te bestuderen. De efficiëntie van deze techniek is echter relatief laag in paddenstoelvormende schimmels, door een lage activiteit van homologe recombinatie. In **Hoofdstuk 3** wordt een nieuwe techniek beschreven, waarbij CRISPR-Cas9 wordt gebruikt om de incidentie van homologe recombinatie te verhogen. CRISPR-Cas9 is een nieuwe techniek, waarmee gericht dubbelstrengs DNA breken worden gemaakt die de kans op homologe recombinatie verhogen. Hierdoor verhoogt CRISPR-Cas9 ook de incidentie van gendeletie, waardoor het makkelijker is om de functie van genen te bestuderen. Voor deze techniek werden Cas9 eiwitten in *S. commune* geïntroduceerd, omdat de expressie van een bacterieel eiwit als Cas9 erg lastig is in paddenstoelvormende schimmels. Door het gebruik van CRISPR-Cas9 werd de efficiëntie van het inactiveren van genen sterk verhoogd. In hoofdstuk **4-7** is deze techniek vervolgens toegepast om de functie van transcriptiefactoren te onderzoeken.



Een andere techniek die in dit proefschrift beschreven wordt, is chromatine immunoprecipitatie-sequencing (ChIP-Seq). Met deze techniek kunnen de interacties tussen eiwitten en genomisch DNA bepaald worden. Tijdens verschillende stadia van ontwikkeling in schimmels vinden er grote veranderingen plaats in de bereikbaarheid van het genomische DNA. Enerzijds door de modificatie van histonen die samen met DNA het chromatine vormen en de bereikbaarheid van het chromatine verhogen of verlagen. Anderzijds door de binding van transcriptiefactoren die de transcriptie van genen stimuleren of remmen. Om dit beter in kaart te brengen is in **Hoofdstuk 4** een ChIP-Seq techniek ontwikkeld om de locatie van DNA-bindende eiwitten op het genomische DNA te bepalen. Deze techniek is gebruikt om de verdeling van de histon-modificatie H3K4me₂, waarbij histon 3 op lysine 4 wordt gedimethyleerd, te bepalen. Deze modificatie is sterk geassocieerd met actieve genen. Door een vergelijking te maken van de verdeling van H3K4me₂ tijdens monokaryotische en dikaryotische groei van *S. commune*, kan bepaald worden hoe het genoom verandert tussen deze twee stadia. Dezelfde techniek wordt ook gebruikt in **Hoofdstuk 5**, om te bepalen waar een regulator van cellulase expressie, Roc1, het genomisch DNA bindt. Zo kunnen de genen die door Roc1 gereguleerd worden, worden geïdentificeerd.

Als laatste wordt er een techniek beschreven waarmee genen op een vaste plek in het genoom geïntegreerd kunnen worden. In deze thesis zijn veel geïnactiveerde genen teruggeplaatst in *S. commune* om de rol van een gen te bevestigen (**Hoofdstuk 4-6**). Ook is een gemuteerde versie van *roc1* in *S. commune* geïntroduceerd met een hemaglutinine epitootag. Deze tag is gebruikt om met ChIP-Seq te identificeren waar in het genoom Roc1 bindt (**Hoofdstuk 5**). Voor al deze transformaties is ectopische integratie gebruikt, waarbij een gen op een willekeurige plek in het genoom integreert. Dit kan resulteren in een sterk variërende expressie van het geïntegreerde gen, omdat transcriptie deels afhankelijk is van de structuur van het chromatine (open of dicht) en een gen bovendien meerdere keren kan integreren. Daarom moeten meerdere mutanten gescreend worden om een correcte mutant te identificeren. Als alternatief kan een gen altijd op dezelfde plek worden geïntegreerd met homologe recombinatie. In **Hoofdstuk 7** wordt daarvoor een knock-in techniek beschreven waarbij het gen voor dTomato (een rood-fluorescent eiwit) op een specifieke plek in het genoom wordt geïntegreerd. Op de plek van integratie bevinden zich geen regulatoire elementen en de omliggende genen hebben stabiele expressie en H3K4me₂ tijdens verschillende ontwikkelingsstadia van paddenstoelvorming. Dit resulteerde in meer vergelijkbare rood-fluorescente stammen ten opzichte van ectopische integratie mutanten. Deze techniek kan dus worden gebruikt om genen in het genoom van *S. commune* te introduceren en zo de functie te onderzoeken.

Regulatie van transcriptie in *S. commune*

In deze thesis wordt de functie van 11 transcriptiefactoren onderzocht, die een interessant expressieprofiel hebben onder verschillende omstandigheden. Zo wordt in **Hoofdstuk 5** transcriptiefactor Roc1 bestudeert. Deze transcriptiefactor komt hoog tot expressie wanneer *S. commune* op hout of cellulose groeit, maar niet bij groei op glucose. Een deletiestam van Roc1 is niet in staat op cellulose te groeien en maakt geen enzymen aan die deze complexe suikerpolymeer kunnen afbreken. ChIP-Seq toont aan dat Roc1 direct op de promotoren van cellulases en lytische polysaccharide mono-oxygenasen (LPMOs) bindt en dus waarschijnlijk de expressie van deze genen reguleert. Op basis van de promotoren waar Roc1 bindt, is het motief bepaald dat Roc1 herkent. Dit motief (CGG-N-CGG) is in de promotor van de

LPMO *lpmA* gemuteerd en voor een dTomato rood-fluorescent gen geplaatst. Stammen met de gemuteerde promotor werden niet rood-fluorescent wanneer *S. commune* op cellulose groeide, terwijl stammen met de wildtype promotor dat wel werden.

In **Hoofdstuk 4** en **Hoofdstuk 6** worden deletiestammen beschreven van 11 transcriptiefactoren die mogelijk betrokken zijn bij paddenstoelvorming. Deletie van de genen *ftr3*, *ftr4*, *hth1*, *tea3* en *zfc5* heeft geen effect op paddenstoelvorming in homozygote dikaryons, ondanks dat deze genen anders tot expressie komen tijdens paddenstoelvorming (**Hoofdstuk 6**). Een dikaryon waarin *ftr1* is geïnactiveerd, is niet in staat om paddenstoelen te maken en vormt een symmetrische kolonie. Dit fenotype is eerder beschreven bij inactivatie van de transcriptiefactoren Hom2, Wc2 en Tea1. *Ftr1* lijkt daarom belangrijk te zijn bij het begin van paddenstoelvorming.

De transcriptiefactoren *Fst1*, *Zfc4* en *Zfc7* spelen een rol bij de latere ontwikkeling van paddenstoelen (**Hoofdstuk 4** en **6**). Het gen voor *fst1* codeert voor een transcriptiefactor met een Zn₂Cys₆ zink vinger DNA bindend domein en de genen die coderen voor *zfc4* en *zfc7* voor een transcriptiefactoren C2H2 zink vinger DNA bindend domein. Homozygote dikaryons waarin *fst1*, *zfc4* of *zfc7* zijn geïnactiveerd stoppen de ontwikkeling van paddenstoelen na het vormen van aggregaten. In sommige gevallen maakt een deletiestam van *Zfc4* wel paddenstoelen, maar deze paddenstoelen zijn misvormd en erg klein. Het lijkt er op dat deze drie transcriptiefactoren op een later moment een rol spelen dan *Ftr1*.

Homozygote dikaryons waarin *bzt1* is geïnactiveerd vormen juist meer, maar kleinere paddenstoelen. Dit gen codeert voor een transcriptiefactor met een bZip DNA bindend domein. Op basis van het fenotype lijkt het dat deze transcriptiefactor de productie van paddenstoelen remt, waardoor er meer ruimte is voor de vorming van volwassen paddenstoelen. Met deze transcriptiefactor kan *S. commune* mogelijk competitie tussen de paddenstoelen voorkomen.

Impact van het onderzoek

De technieken die beschreven zijn in dit proefschrift dragen bij aan het efficiënter onderzoeken van paddenstoelvorming. De functie van genen kan sneller onderzocht worden door een nieuwe techniek voor het inactiveren van genen. Daarnaast kan de functie van transcriptiefactoren, waarover al veel bekend is in *S. commune* beter bestudeerd worden door het gebruik van ChIP-Seq. Deze techniek was tot nu toe nog niet eerder gebruikt in een paddenstoelvormende schimmel. Omdat deze technieken waarschijnlijk ook toepasbaar zijn op andere paddenstoelvormende schimmels kan er ook makkelijker onderzoek gedaan worden naar soorten die commercieel gecultiveerd worden. Een beter inzicht in de regulatie van paddenstoelvorming kan bijdragen aan de optimalisatie of zelfs het mogelijk maken van commerciële productie van paddenstoelen.



Acknowledgements

En dan nog het laatste onderdeel van de thesis. Het waren vijf fantastische jaren, zo leuk zelfs dat ik besloten heb nog minimaal vier jaar langer te blijven. Vijf jaar werken aan een proefschrift is niet iets dat je alleen doet. Op allerlei vlakken, wetenschappelijk en niet-wetenschappelijk, hebben mensen bijgedragen aan dit boekje. En daar hoort natuurlijk een dankwoord bij.

Als eerste natuurlijk Robin, mijn co-promotor. Je gaf me de kans om dit promotieonderzoek te doen en nam alle tijd om me de details te leren. Ondanks dat ik pas je tweede PhD student was, was daar niets van te merken en voor mij was je de perfecte begeleider. Je gaf me de vrijheid om mijzelf te ontwikkelen en was altijd beschikbaar voor vragen en discussies. Een baas die nog meer van speciaalbier houdt dan ik was mooi meegenomen. Ik denk dat niemand smakelijkere borrels heeft dan Fungal Genomics.

Han, als promotor kan jij hier natuurlijk niet ontbreken. Veel wetenschappelijke discussies hebben we niet gehad, maar op de momenten dat we die hadden, wist je me altijd nieuwe inzichten te geven. Ik wil je ook erg bedanken voor de manier waar op je leiding geeft aan de Microbiologie. De groep is een fantastische, informele plek om onderzoek te doen en jij maakt dat mogelijk.

De verschillende collega's van de Fungal Genomics met wie ik nauw samenwerkte wil ik ook bedanken. Ioana and Natalia, both of you had a big impact on this thesis. Ioana, some people have described our endless bickering in the lab as that of a married couple. It was great having you as co-PhD on the same project and I hope you will finish your thesis soon! Natalia, first I was your student, then we were co-workers. I enjoyed the years we worked together and I am grateful for all that you have taught me. Ivan, the master of bioinformatics. Thanks for always making me laugh with your dry wit. En natuurlijk Erik en Marieke, de toekomst van Fungal Genomics. Jullie nieuwe ideeën voegen veel toe aan de groep.

Mijn kamergenoten in O404 bedankt, voor het lachen, het uiten van frustraties en de filosofische gesprekken. Freek, in onze competities wie de ander het hardst kon beledigen won jij altijd. Bedankt dat je er altijd was voor een bemoedigend woord als ik mezelf niet meer vertrouwde. Inge, de moeder van O404 en degene met wie ik over files kon klagen. Maarten, mijn partner in (bioinformatica) crime. Zonder jou R skills hadden de figuren in dit boekje een stuk minder mooi geweest. En Koen, de man die niet door woorden geraakt lijkt te kunnen worden, welkom alvast bij de Fungal Genomics!

In de afgelopen jaren hebben een hoop studenten bijgedragen aan dit onderzoek. Benny, Gijs, Esther, Emmeline, Jelle, Brandon en Ella; het was heel leuk en een eer om jullie te begeleiden. Bedankt voor jullie inzet! A special thanks also to Eva and Yuanyuan. Who came from abroad to work with me. I cannot think of a better compliment and loved working with both of you. Eva, you and I share the same sarcastic humor and working with you was sometimes like looking in a mirror. I hope we can share a beer again soon! Yuanyuan, it was not easy starting here just as corona started to spread across the Netherlands. But you persevered and I will forever remember our discussions about mushrooms.

Ook alle andere collega's van de Microbiologie groep wil ik bedanken. In het bijzonder Hans en Luis. Hans, bedankt dat je mij als begeleider hebt geïntroduceerd in de Microbiologie. Luis, onze discussies eindigden altijd met meer vragen dan antwoorden. Jouw kijk op de biologie is eindeloos inspirerend en ik hoop dat er nog veel discussies volgen. En natuurlijk alle andere collega's: Jordi, Wieke, Margot, Aurin, Jun, Juan, Xiaoyi, Maryam (thanks for the mug!), Jacq, Esther (best party-committee ever!!), Eline, Jesus (my favorite bacteria), David, Ria T., Ria K., Jan, Pauline, Brigit, Martin, Fleur, Robert-Jan, Jeroen en Antonio.

Mijn mede PhD-Council leden, Laura, Tom, Violeta, Nathalie, Sanne, Gilles, Lisa en Zhilei, thanks for making a difference together and keep it up!

Evert en Sebastiaan, al 17 jaar mijn goede vrienden en nu mijn paranimfen. Ik heb voor jullie beiden als getuige mogen optreden op jullie huwelijk. Een echt huwelijk komt er voor mij vast nog wel een keer. Tot die tijd ben ik heel blij dat jullie mij bijstaan in mijn verbintenis met de wetenschap. Ook bedankt voor alle mannenavonden waarbij het even niet over wetenschap hoefde te gaan.

Mijn zussen, Elze en Eva. Al 5 jaar proberen jullie te begrijpen wat ik in vredesnaam doe op mijn werk. Tot een gastcollege op zaterdagavond bij Elze op de bank aan toe. Bedankt voor alle interesse in mijn werk. Ik hoop dat de Nederlandse samenvatting een idee geeft van waar ik me nou allemaal mee bezig heb gehouden.

Pap en Mam. Jullie hebben me altijd mijn eigen pad laten kiezen. Ook als dat pad niet het makkelijkste was, zoals toen ik stopte met de studie Elektrotechniek. Bedankt voor al dat vertrouwen waardoor ik mijn passie heb gevonden. Ook bedankt dat jullie van mij zo'n nieuwsgierig persoon hebben gemaakt.

Lieve Nora, als laatste wil ik jou bedanken. Zonder jou waren de afgelopen jaren niet zo leuk geweest en was het misschien allemaal heel anders gelopen. De afgelopen 10 jaar heb je me altijd gesteund. Als het goed ging en als het slecht ging. Beiden hebben we de afgelopen jaren af en aan gestudeerd; Zijn we nu dan eindelijk echt klaar? Ik denk het eigenlijk niet, want wij zijn samen nooit echt klaar. Ik kan niet wachten om te ontdekken hoe we elkaar in de toekomst blijven uitdagen en samen de mooiste dingen beleven.

Liefs,

Peter Jan



Curriculum vitae

Peter Jan Vonk was born on June 17th, 1991 in Giessenburg, The Netherlands. He followed his secondary education at the Gymnasium Camphusianum in Gorinchem, The Netherlands and graduated in 2009 with a Gymnasium-level diploma. In September 2010 he started his Bachelor in Biomedical Sciences at Utrecht University, followed by a Master in Molecular and Cellular Life Sciences at Utrecht University. As part of his studies he did an internship at the Microbiology group of the Department of Biology at Utrecht University under the supervision of N. Escobar and H. de Cock, followed by a second internship at Corbion in Gorinchem under supervision of A.L. Cruz. Peter Jan obtained his MSc diploma in August 2016. In January 2017 he started his PhD within the Microbiology group of the Department of Biology at Utrecht University under the supervision of Dr. R.A. Ohm and Prof. Dr. H.A.B. Wösten. Research on functional genomics in *Schizophyllum commune* was financially supported during this period by the European Research Council and is described in this thesis. In January 2022 Peter Jan started working at the Microbiology group of the Department of Biology at Utrecht University, where he teaches, studies functional genomics in *Schizophyllum commune* and works on bioinformatics.

List of publications

Vonk, P. J. & Ohm, R. A. (2018). The role of homeodomain transcription factors in fungal development. *Fungal Biology Reviews*, 32(4), 219–230. <https://doi.org/10.1016/j.fbr.2018.04.002>

Vonk, P. J. Escobar, N. Wösten, H. A. B. Lugones, L. G. & Ohm, R. A. (2019). High-throughput targeted gene deletion in the model mushroom *Schizophyllum commune* using pre-assembled Cas9 ribonucleoproteins. *Scientific Reports*, 9(1), 1-8. <https://doi.org/10.1038/s41598-019-44133-2>

Vonk, P. J. & Ohm, R. A. (2021). H3K4me2 ChIP-Seq reveals the epigenetic landscape during mushroom formation and novel developmental regulators of *Schizophyllum commune*. *Scientific Reports*, 11(1), 1-15. <https://doi.org/10.1038/s41598-021-87635-8>

